Colorado Water Institute
Annual Technical Report
FY 2009

Introduction

Water research is more pertinent than ever in Colorado. Whether the research explores the effects of decentralized wastewater treatment systems on water quality, optimal irrigation scheduling, household conservation patterns, the effects of wastewater reuse on turfgrass, the economics of water transfers, or historical and optimal streamflows, water is a critical issue. In a headwaters state where downstream states have a claim on every drop of water not consumed in the state, the quality and quantity of water becomes essential to every discussion of any human activity.

The State of Colorado is engaged in long term water supply planning that requires information from the research community on water demands, non-consumptive needs, climate change, conservation savings and other supply options. CWI is engaged in research effects to help clarify some of these research needs. We continue to work closely with state agencies, water providers, and the state legislation to meet these needs.

The Colorado Water Institute serves to connect the water expertise in Colorado's institutions of higher education to the information needs of water managers and users by fostering water research, training students, publishing reports and newsletters and providing outreach to all water organizations and interested citizens in Colorado.

Research Program Introduction

Colorado Water Institute funded 18 faculty research projects, 9 student research projects, and 2 internships this fiscal year; one of these projects was designated to receive federal funding due to its relation to water supply issues. The Advisory Committee on Water Research Policy selected these projects based on the relevancy of their proposed research to current issues in Colorado.

Under Section 104(b) of the Water Resources Research Act, CWI is to plan, conduct, or otherwise arrange for competent research that fosters the entry of new scientists into water resources fields, the preliminary exploration of new ideas that address water problems or expand understanding of water and water-related phenomena, and disseminates research results to water managers and the public. The research program is open to faculty in any institution of higher education in Colorado that has demonstrated capabilities for research, information dissemination, and graduate training to resolve State and regional water and related land problems. We received 5 new proposals for consideration this year from 2 institutions of higher education in Colorado (Colorado State University and University of Colorado). The general criteria used for proposal evaluation included: (1) scientific merit; (2) responsiveness to RFP; (3) qualifications of investigators; (4) originality of approach; (5) budget; and (6) extent to which Colorado water managers and users are collaborating. A peer review process and ranking by the CWI Advisory Committee resulted in funding four new projects for FY09.

Active projects and investigators are listed below:

Faculty Research

1. Adaptive Management of Zebra and Quagga Mussels in Colorado, Craig Bond, Colorado State University, $35000
2. Adjoint Modeling to Quantify Stream Flow Changes Due to Aquifer Pumping, Roseanna Neupauer, University of Colorado, $117847
3. Agricultural Water Conservation Clearinghouse, Reagan Waskom, Colorado State University, $10000
4. Assessing the Relative Costs/Values of New Water Supply Options, Doug Kenney, University of Colorado, $35000
5. Characterizing Non-Beneficial Evaporative Upflux from Shallow Groundwater under Uncultivated Land in an Irrigated River Valley, Jeffrey Niemann, Colorado State University, $40000
6. Data Analysis and Final Report of the Nature and Implications of Irrigation Practices in Colorado's Lower Arkansas River Valley, Tim Gates, Colorado State University, $48477
7. Determination of Consumptive Water Use by Alfalfa in Arkansas Valley, Lee Sommers, Colorado State University, $300000
8. Development of a Correction Function for the 3-inch, Thin-Walled, Helley-Smith Sampler Deployed on Coarse Gravel Beds, Steven Abt, Colorado State University, $21416
9. Development of Oilseed Crops for Biodiesel Production under Colorado Limited Irrigation Conditions, Jerry Johnson, Colorado State University, $60233
10. Direct Determination of Crop Evapotranspiration in the Arkansas Valley with a Weighing Lysimeter, Abdel Berrada, Colorado State University, $49995
11. Estimating the Cost Effectiveness of Water Conservation Programs, Chris Goemans, Colorado State University, $35000
12. Evaluation of Engineered Treatment Units for the Removal of Endocrine Disrupting Compounds and Other Organic Wastewater Contaminants During Onsite Wastewater Treatment, Robert Siegrist, Colorado School of Mines, $49746
13. Hydrologic Analysis and Process-Based Modeling for the Upper Cache la Poudre Basin, Stephanie Kampf, Colorado State University, $25000

14. New Methods for Sago Pondweed Management, Scott Nissen, Colorado State University, $20000
15. Occurence and Fate of Steroid Hormones in Sewage Treatment Plant Effluent, Animal Feeding Operation Wastewater and the Cache la Poudre River of Colorado, Thomas Borch, Colorado State University, $49944
16. Studies Supporting Sustainable Use of the Denver Basin Aquifers in the Vicinity of Castle Rock, Tom Sale, Colorado State University, $25000
17. Water Reallocation and Bioenergy in the South Platte: A Regional Economic Evaluation, James Pritchett, Colorado State University, $32981
18. Willow Creek Water Quality Study, John Stednick, Colorado State University, $21010

Student Research

1. Bear Creek Watershed Project, Kim Gortz-Reaves (Chase), University of Colorado at Denver, $1400
2. Developing Barriers to the Upstream Migration of New Zealand mudsnail (Potamopyrgus antipodarum) Phase III, Scott Hoyer (Myrick), Colorado State University, $5000
3. Estimating Errors Associated With Calculated Sublimation From Seasonally Snow-Covered Environments, Doug Hultstrand (Fassnacht), Colorado State University, $5000
4. Flow Device to Assess Biological Water Quality in Colorado Surface Water, Travis Steiner (Goodridge), Colorado State University, $5000
5. High Resolution Soil Moisture Retrieval in the Platte River Watersheds, Chengmin Hsu (Johnson), University of Colorado at Denver, $5000
6. Impact of Limited Irrigation on Health of Four Common Shrub Species, Jason Smith (Klett), Colorado State University, $5000
7. Potential Changes in Groundwater Acquisition by Native Phreatophytes in Response to Climate Change, Julie Kray (Cooper), Colorado State University, $5000
8. Studies Supporting Sustainable Use of the Denver Basin Aquifers in the Vicinity of Castle Rock, Kim Lemonde (Sale), Colorado State University, $5000
9. Understanding the Hydrologic Factors Affecting the Growth of the nuisance diatom Didymosphenia Geminata in Rivers, James Cullis (McKnight), University of Colorado, $5000

Internships

1. GEOLEM Internship, Roland Viger, USDA, $20000
2. OMS Internship, Robert S. Regan, USDA, $30000

For more information on any of these projects, contact the PI or Reagan Waskom at CWI. Special appreciation is extended to the many individuals who provided peer reviews of the project proposals.

Water Reallocation and Bioenergy in the South Platte: A Regional Economic Evaluation

Basic Information

Title:	Water Reallocation and Bioenergy in the South Platte: A Regional Economic Evaluation
Project Number:	2008CO167B
Start Date:	3/1/2008
End Date:	7/31/2009
Funding Source:	104B
Congressional District:	4th
Research Category:	Not Applicable
Focus Category:	Economics, Models, Water Supply
Descriptors:	
Principal Investigators:	Reagan M. Waskom, James Pritchett

Publication

1. Pritchett, James, 2009, Water Reallocation and Bioenergy in the South Platte: A Regional Economic Evaluation, Colorado Water Institute Proposal,18 pages.

Title: Water Reallocation and Bioenergy in the South Platte: A Regional Economic Evaluation
Project Duration: 1/2008 through 7/2009
Funds Requested: $ 47,981

Principal Investigator: James Pritchett, Associate Professor
Campus Mail 1172, Colorado State University
James.Pritchett@ColoState.edu
970.491.5496 (phone) 970.491.2067 (fax)
Fort Collins, CO 80523-1172

Keywords: Regional economic analysis; bioenergy; water transfers

Abstract Bioenergy crop production and refining are key opportunities for revitalizing rural communities in Colorado. This optimism stems, in part, from growing urban areas in Colorado that demand clean burning and relatively inexpensive biofuels. Yet, the same urban areas are rivals for two important inputs in biocrop farming: water and agricultural land. Increased municipal demands heighten the competition for water in Colorado's over-appropriated river basins increasing the value of each acre foot. Thus, the potential gains from bioenergy cropping must be attractive enough to retain water in irrigated agriculture else water will flow to municipal consumption. If profits for bioenergy crop production are limited, then outside investment in bioenergy refining and infrastructure is likely to suffer.

The rural economic impacts of bioenergy cropping and increasing water resource demands stretch beyond the farm gate. Agribusinesses that rely on the sale of crop inputs (e.g., seed, chemical and fertilizer sales) and the use of farm products (e.g., ethanol plants, dairies, feedlots, sugar processors and meatpackers) will find their activities are substantially altered by bioenergy cropping and/or water transfers. If irrigated acres are permanently fallowed, input suppliers and agribusiness processors will face significant reductions in economic activity. As biocropping gains popularity, agribusinesses that compete with biorefining for farm products (diaries, feedlots, and sugar processing) will certainly need to adapt and perhaps relocate. The economic outcome is uncertain.

Farming and agribusiness represent an important base industry for rural communities, and with few alternatives to agricultural production, these communities will suffer as economic activity is reduced. For the leaders of these communities, it is important to gain information about how resources, including tax revenues, may be altered by the competing incentives of water resources and bioenergy cropping. Likewise, water stakeholders, agribusiness leaders and farm organizations seek to understand the tradeoffs in policy initiatives.

Can Colorado's agricultural producers meet the challenges of a burgeoning bioenergy industry while still supplying water to growing municipalities? What impacts will be felt by local agribusiness, both suppliers of inputs (e.g., local supply cooperatives) and those who rely on irrigated crops for their livelihood (e.g., sugar processors, dairies and feedlots)? This proposal's overall objective is to provide insights into these important questions. The research involves developing a computable general equilibrium model for the South Platte Basin. This economic model extends previous research regarding irrigated agriculture's contribution to rural economic activity. Yet, rather than a snapshot of the economy, the proposed model will trace flow of water resources in and out of the basin with water transfers, while suggesting how cropping patterns are altered with bioenergy adoption. Further, the proposed model focuses on the impact to agribusinesses that utilize and process farm products, an analysis that has been neglected. Proposal objectives also include plans for analyzing potential policy scenarios, dissemination of results and presentations to stakeholders.

Water Reallocation and Bioenergy in the South Platte: A Regional Economic Evaluation

Problem Statement: Bioenergy crop production is a potential engine for rural economic growth. Colorado farmers, and especially those in the South Platte River Basin, are well positioned as key energy stock producers for prospective commercial biorefining processes. Farmers in the South Platte Basin are among the most efficient and productive in the United States cropping more than one million irrigated acres.

Bioenergy's bright prospects are in part a result of Colorado's growing cities; however, municipal development is also a significant competitor for crop inputs, especially water and agricultural land. Rapid urban growth increases the competition for water, and agriculture is the primary supplier for increased water demands. Thus, the potential gains from bioenergy cropping must be attractive enough to retain water in irrigated agriculture else the resource will flow to municipal consumption. If profits for bioenergy crop production are limited, then outside investment in bioenergy refining is likely to suffer.

Demand for water is increasing, but supplies in Colorado's South Platte Basin are over-appropriated, meaning that owned rights to water use exceed the actual amount of water in the basin. The Colorado Water Conservation Board's Statewide Water Supply Initiative (SWSI) predicts the South Platte Basin will experience a 61.9 percent increase in water demand by 2030 that will cause an approximately 180,000 irrigated acres to be permanently fallowed. The plans for nearly all South Platte water providers include significant agricultural water right transfers (CWCB, 2004).

Water transfers are likely to reduce the size of the local economic base because fewer irrigated acres are cropped, fewer irrigated crops are sold and fewer crop inputs are purchased. Without other viable, local base industries to generate revenues and provide employment, a reduction in the revenue generated in the agricultural sector will have adverse economic impacts throughout the regional economy. Impacts will be felt by input suppliers and by local governments whose property and sales tax base is eroded. Moreover, downstream users of irrigated crops (e.g., dairies, feedlots, meat packers, cheese manufacturers, sugar processors and ethanol plants) will be forced to seek more costly crops from distant locations.

In contrast, bioenergy crop production may generate many positive economic spillovers for communities; not only through additional crop sales, but also by generating economic activity for local input suppliers (e.g., crop chemical wholesalers) and by downstream users of the crops (e.g., ethanol production facilities). Value-added investment in bioenergy processing is likely to add to a rural community's infrastructure and local supply of labor.

How should community leaders and stakeholders proceed when caught between two rivals – water transfers and bioenergy cropping? Clearly, it is important to weigh the potential economic impact of a growing bioenergy crop industry with increased demands for water resources. Water stakeholders will benefit from a detailed basin level study examining the direct and indirect economic impacts of these rivals, as well as disaggregating these impacts among different industries in the region. This information will be valuable to many water stakeholders including farmers, businesses, water supply administrators, and regional leaders charged with economic development.

Aims/objectives: Can Colorado's agricultural producers meet the challenges of a burgeoning bioenergy industry while still supplying water to growing municipalities? What impacts will be felt by local agribusiness, both suppliers of inputs (e.g., local supply cooperatives) and those who rely on irrigated crops for their livelihood (e.g., sugar processors, dairies and feedlots)? This proposal's overall objective is to provide insights into these important questions. More specifically, the purposes of this study are to:

1. Describe the capacity of South Platte farms to supply bioenergy crops even as the demand for water resources increases. In the context of this study, the South Platte Basin will include farms in Adams, Boulder, Larimer, Logan, Morgan, Sedgwick and Weld counties.

2. Map the existing infrastructure and resources available for bioenergy production in South Platte Basin communities, so that gaps in infrastructure (water, transportation, land, labor) may be identified.

3. Measure the profitability of biofuel crops (e.g., corn for grain) against the profitability of traditional crops (e.g., corn silage, alfalfa, sugar beets) to better understand the farm level tradeoffs of supplying a bioenergy crop to a local purchaser vis a vis a crop designated for local, downstream agribusiness. Likewise, compare the returns from selling water off of the farm to maintaining irrigated agricultural production.

4. Perform extensive in-person interviews with agribusiness managers/owners in the South Platte Basin. The purpose of the interviews will be to collect the managers' assessment of water transfers and returns to bioenergy cropping, a description of the firm's current purchasing behavior with an emphasis on local vs. purchases outside the region, and the proportion of sales that are exported versus those held within the region.

5. Using data collected and validated in Objective 4, along with existing secondary data, create a social accounting matrix (SAM) for the South Platte Basin. The SAM captures the current financial interaction of sectors within an economy including activities, commodities, transactions costs, household income, taxes and government expenditures. The SAM is a baseline against which other economic scenarios might be measured.

6. Create a South Platte Basin computable general equilibrium model (CGE) from the SAM. While the SAM is a snapshot of the current activity within a region, a CGE model explains all of the transactions in the SAM and indicates how important variables (e.g., the price of water, price of land, size of the workforce, capital investment) are altered when resources such as water flow in and out of an economy.

7. Assess the potential regional economic impacts of bioenergy crop production and water transfers to rural economies when measured against a backdrop of current production. Economic scenarios will include incremental bioenergy crop adoption and reduction in irrigated crop acreage. The aforementioned SAM and CGE model will be used to quantify and measure these effects.

8. Interpret and deliver the study's results via meetings with water stakeholders including the South Platte Forum, the Lower South Platte Forum, the Colorado Water Congress, the basin roundtables, etc. Prepare CWRRI completion reports as appropriate and write short study summaries for the CWRRI newsletter.

The proposal's objectives are tightly aligned with the FY 2008 Priority Research Topics identified by the CWRRI Advisory Committee. Specifically, this proposal seeks to answer the question "What are the direct and indirect water related impacts and needs surrounding bioenergy production in Colorado?" To the authors' knowledge, no study has considered both the regional economic impacts of bioenergy crops and expected water transfers on Colorado's rural communities. This research proposal extends previous work on the economic activity generated by irrigated agriculture in Colorado, but now considers the impact of biofuels and biorefining on irrigated cropping profits and rural economic vitality.

Rationale, Significance and Project Benefits:

Without question, a growing population will lead to increased demand for M&I water use. The South Platte and Arkansas Basins represent about 80% of the total projected increase in Colorado's future gross M&I demands. Table 1 indicates the Statewide Water Supply Initiative (SWSI) projections of M&I water use in the year 2000 and for the year 2030.

Table 1. Projected Growth in Municipal and Industrial Water Demand Basins*

Basin	2000 Gross Water Demand (AFY)	2030 proj. Gross Water Demand (AFY)	Projected Increase (AFY)
Arkansas	256,900	373,500	98,000
Rio Grande	17,400	23,100	43,000
South Platte	772,400	1,250,800	409,700

In Colorado, a 68,000 acre foot shortfall exists between projected demands from Table 1 and identified water supplies. Shortfalls are greatest in the South Platte and Arkansas Basins, which supply most growing Front Range communities with water (Table 2). History indicates M&I providers will find avenues to meet customers' needs, and in these basins increasing pressure will be placed on agriculture to urban water transfers

Table 2. Shortfall Between Projected M&I Demands and Firm Supplies in 2030*

Basin	Supply Needed (AFY)	Supply Identified (%)	Shortfall (%)
Arkansas	98,000	82%	18%
Rio Grande	4,300	99%	1%
South Platte	409,700	78%	22%

Agriculture represents approximately 91 percent of water used in Colorado and SWSI projections indicate that it will make up 86 percent of the water use in 2030 (Lower South Platte Forum: Valuing your Water, *Colorado Water, Colorado State University,* April 2005). As population grows, increased M&I demands are met with transfers from irrigated agriculture. Clearly, irrigated agriculture will shrink in Colorado, and SWSI forecasts these reductions as summarized in Table 3.

Table 3. Shortfall Between Project M&I and Firm Supplies in 2030*

Basin	Projected Reduction In Irrigated Acres by 2030
Arkansas	↓23,000-72,000 acres
Rio Grande	↓60,000-100,000 acres
South Platte	↓133,000-226,000 acres

Economic activity is reduced in rural communities as irrigated crop acres are permanently fallowed. The direct and indirect economic activity generated by irrigated cropping has been quantified to a limited extent by Thorvaldson and Pritchett (2006). As indicated in Table 4, irrigated agriculture's economic activity is substantial in the South Platte Basin generating $690 per acre, which includes the direct activity from crop sales; the indirect activity of farm input suppliers; and the induced activity of wages spent by employees.

Table 4. Economic Activity of Irrigated Agriculture in Colorado Basins

Basin	Farm Gate Receipts Relative to Regional Sales	Economic Activity Generated per Acre of Irrigated Cropland
Arkansas	31 %	$ 428
Rio Grande	48 %	$1,127
South Platte	2 %	$ 690

The research by Thorvaldson and Pritchett (Pritchett is PI on this proposal) is an important first step; however, their analysis has several limitations. First, Thorvaldson and Pritchett completed their study prior to recent expansion of bioenergy cropping and the subsequent increased demand for crop inputs. Second, the authors limited their economic activity assessment to irrigated farms and input suppliers, while neglecting downstream agribusiness firms such as sugar processors, dairies, feedlots, and ethanol facilities. As a result, the economic activity generated by these firms is omitted. Finally, the input-output model used in Thorvaldson and Pritchett's research is merely a snapshot of current economic activity. In contrast, the proposed CGE model is dynamic and will trace the flow of resources (e.g., water and land) and their prices as the regional economy responds to increased bioenergy cropping and large scale transfers of water rights. The proposed research is a forecast of likely outcomes rather than a description of existing activity. It should be noted that *the proposed CGE model will be available for future economic analysis of policy change, so the research objectives an important step in building future capacity for answering water related, regional economic questions.*

Importantly, the Thorvaldson and Pritchett effort resulted in more than fifty presentations to stakeholder groups, eight additional requests for impact analysis, a related study focusing on the changing property tax base, two CWRRI completion reports, four articles in popular press, three academic poster presentations and a pair of academic working papers. It is expected that the proposed CGE model will have a similar outreach impact. Stakeholders have asked for, and continue to ask for, information about how agribusiness will be impacted by increasing demands for water resources and the growth of bioenergy cropping. Unfortunately, these questions have yet to be answered concretely.

Bioenergy has the potential to become an important base industry in Colorado. However, the industry's success depends importantly on a local supply of energy crops grown by irrigated agriculture. The number of acres devoted to irrigated agriculture is likely to decrease in the next

twenty-five years as water is transferred to M&I use. Will bioenergy crops alter the flow of water resources from rural regional economies? Will a sufficient number of irrigated crop acres be available to support the energy industry? As irrigated agriculture evolves, how will the size and number of irrigated farms change? Moreover, how will the downstream businesses, including feedlots, dairies, meat packers and cheese processors be impacted? This study seeks to provide tools to water resource and community stakeholders confronting these challenges. In particular, a basin level CGE model will be used to generate information for stakeholders. The following section describes the proposed research model.

Methodology and Previous/Related Research:

A computable general equilibrium (CGE) model captures the interactions of economic agents as resources are allocated. As illustrated in Figure 1, our South Platte Basin model will first capture the economic interaction of agents in the basin, and then examine how economic activity is altered with additional bioenergy cropping and water transfers. Important players in the upstream portion of the model include retailers that supply farm inputs (e.g., fertilizer, seed, and petroleum products), wholesalers, service providers (crop consultants, real estate services, and banking) and water suppliers. In the next stage of the model, irrigated agriculture represents a production unit that combines factor inputs from upstream businesses to generate products (irrigated crops) that are used by downstream industries. Important downstream industries include animal agriculture (e.g., feedlots, dairies), agricultural energy (ethanol), further processing and fabrication (cheese manufacturers and slaughter plants). Goods are used locally or may be shipped outside the region to the rest of the world (ROW). Likewise inputs may be purchased locally or from abroad. The CGE model will also capture the changing prices of resources as they are reallocated.

In order to construct a CGE model a Social Accounting Matrix (SAM) must be constructed first. A SAM is an all-inclusive, economy-wide data framework, typically representing the economy of a regional unit (e.g., a county or river basin). In practice, the social accounting matrix is a square matrix in which each account is represented by a row and a column. Each cell shows the payment from the account (economic sector) of its column to the account (economic sector) of its row. Thus, the incomes (sales) of an account appear along its row and its expenditures (demand) along its column. The underlying principle of double-entry accounting requires that, for each account in the SAM, total revenue (row total) equals total expenditure (column total). Data in the SAM are expressed in monetary terms.
The variables that will be in the SAM are grouped into the following sectors:

- Activities: The activities sector includes the following sub-sectors: large scale irrigated agriculture, small scale irrigated agriculture, dryland agriculture, industry, transportation, and other services such as utilities, wholesale, and housing
- Commodities: Commodities include crops, farm inputs, processed foods, industrial or manufacturing goods, transportation, and other services' commodities
- Transaction costs: Transaction costs include costs from domestic sales, imports and exports
- Factors: Primary inputs in the production process including water, land, labor and financial capital.
- Household income: households' income and wages in the regional economy, and
- Other institutions: This includes government, taxes, and an agglomerated rest of world.

Figure 1. Illustration of a Computable General Equilibrium Model

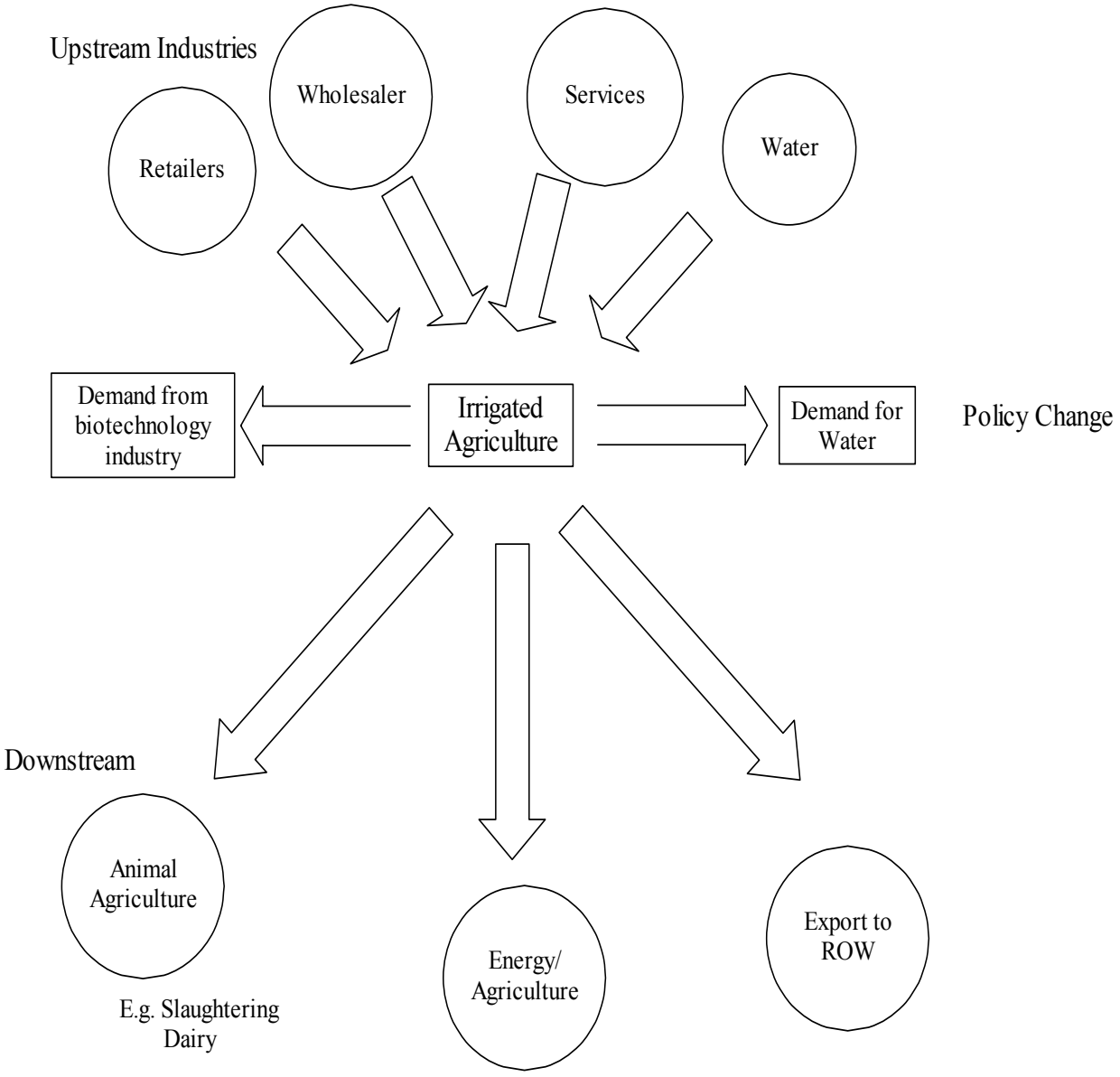

An advantage of a SAM is that the researcher can segment important or relevant sectors into different sub-sectors in order to thoroughly describe the impacts of external shocks. As an example, the proposed SAM splits the cropping sector into dryland and irrigated farm subsectors, and then further separates the farm subsector in those that sell water rights and those that retain water rights.

The Social Accounting Matrix is constructed in Microsoft Excel and is the base data that will be used in the Computable General Equilibrium (CGE) model. The CGE model will be constructed within the General Algebraic Modeling System (GAMS) program, and the SAM data will be imported into the model. GAMS is the mathematical optimization software that is typically used to perform CGE simulations.

Since the SAM data is exclusively monetary transactions, other values such as the number of farmers or the number of households have to be added to the SAM to construct the CGE model. The standard CGE model explains all of the payments recorded in the SAM. The model therefore follows the SAM disaggregation of factors, activities, commodities, and institutions. It is written as a set of simultaneous equations, many of which are nonlinear. The equations define the behavior of the different sectors. In part, this behavior follows simple rules captured by fixed coefficients (for example, ad valorem tax rates). Production and consumption decisions are driven by the maximization of profits and utility, respectively. The equations also include a set of constraints that have to be satisfied by the system as a whole but are not necessarily considered by any individual sector. These constraints cover markets (for factors and commodities) and macroeconomic aggregates.

CGE models have been used to assess the interaction of water resources and regional economics in other studies. Chapter 2 of Phil Scott Watson's dissertation "Of Golf and Grains: Three essays of resource use in the new American West (2006) focuses on the effects of increased population growth on water demand in agricultural and urban sectors using a CGE model. The CGE model proposed in this study will use the same methodology as Watson, but will instead represent the South Platte Basin and focus more intently on downstream agribusiness and irrigated cropping.

Goodman's examination of a proposed Pueblo reservoir expansion and temporary water transfers in the Arkansas basin suggest how a CGE model may be used to examine the impacts of water reallocation. Like Goodman, the proposed research considers water transfers, but will also consider the rivalry for resources represented by bioenergy, as well as a more extensive look at downstream agribusiness. In addition, published drought research (Horridge, Madden and Witwer) and a CGE model of agriculture (Adelman and Robinson) are important foundational literature describing the method of creating SAM's and CGE models.

Expected outcomes: A number of deliverable outputs are associated with the project. These outputs include:

- A social accounting matrix that accurately chronicles the economic activity of the South Platte Basin and is calibrated to the latest economic data.
- A computable general equilibrium model capable of examining water resource and bioenergy cropping questions for the South Platte Basin region.
- Presentations to stakeholder groups including the Colorado Water Congress, the South Platte Forum, the Lower South Platte Forum, the Agricultural Water Forum, the Northeastern Colorado Association of Local Governments annual meeting, the annual meeting of Colorado Soil and Water Conservation Districts, basin roundtables, and others.
- CWRRI completion reports and newsletter articles.
- Academic journal articles.

Timeline: Proposed project activities begin on January 1, 2008 and will be completed on July 1, 2009. A PhD candidate, Leonard Gwanmesia, has been identified for the project and has completed all of his academic coursework. The proposed research represents a significant portion of his PhD dissertation. Specific mileposts in the research include:

January 1, 2008 through March 1, 2008

Create the SAM model using secondary data.

March 1, 2008 through June 1, 2008

Validate the SAM model with in-person interview of agribusiness and the Colorado Department of Local Affairs.

June 1, 2008 through September 1, 2008

Create and validate the CGE model. Financial information and flows will be liberated form the SAM, but allocation of water and the flow of crops to bioenergy facilities must be added to the model. Use the CGE model to establish a benchmark of economic activity for the South Platte Basin.

September 1, 2008 through January 1, 2009

Design scenarios to be considered with the CGE model.

January 1, 2009 through March 1, 2009

Simulate scenarios and compile results from the CGE model.

March 1, 2009 through July 1, 2009.

Draft, edit and complete a CWRRI completion report, newsletter article and present results.

Training Potential A PhD graduate student will be trained in regional economic analysis and CGE models in this study. While the student (Leonard Gwanmesia) has completed extensive coursework in regional economics, he has had few opportunities to apply these tools.

Congressional District: Research activities will take place in the 4th Congressional District.

References

Adelman, I and S. Robinson, 1986. U.S. Agriculture in a General Equilibrium Framework: Analysis with a Social Accounting Matrix. American Journal of Agricultural Economics, 68 (5), 1196-1207.

Colorado Water Conservation Board. 2004. Statewide Water Supply Initiative. Available at http://cwcb.state.co.us

Goodman, D.J., 2000. More reservoir or transfer? A Computable
General Equilibrium Analysis of Projected Water Shortages in the Arkansas River Basin. Journal of Agricultural and Resource Economics, 25 (2), 698–713

Horridge, M., J. Madden, G. Wittwer, 2005. The impact of the 2002–2003 drought on Australia. Journal of Policy Modeling, 27, 285–308.

Thorvaldson, J. and J. Pritchett. "Economic Impact Analysis of Irrigated Acreage in Four River Basins in Colorado." Colorado Water Resources Research Institute Completion Report # 207. December 2006. Fort Collins, CO.

Watson, P., 2006. Golf and Grains: Three essays of resource use in the new American West. Dissertation, Department of Agricultural and Resource Economics, Colorado State University.

Budget

Project Title: **Water Reallocation and Bioenergy in the South Platte: A Regional Economic Evaluation**

	Cost Category	Year 1		Year 2		Total
1	GRAs					
	PhD GRA	$23,328.00		$12,131.00		$35,459.00
	Tuition (continuous registration)	$ 300.00		$ 158.00		$ 458.00
	Total Salary and Wages	**$23,628.00**		**$12,289.00**		**$35,917.00**
2	Fringe Benefits GRA @ 4.2%	$ 980.00		$ 510.00		$ 1,490.00
3	Supplies	$ 3,140.00		$ -		$ 3,140.00
4	Equipment					$ -
5	Services and Consultants					$ -
6	Travel	$ 1,847.00		$ 1,225.00		$ 3,072.00
7	Other Direct Costs					$ -
8	Total Direct Costs	$29,595.00		$14,024.00		$43,619.00
9	Indirect Costs	$ 2,960.00		$ 1,402.00		$ 4,362.00
10	**Total Project Costs**	**$32,555.00**		**$15,426.00**		**$47,981.00**

Budget Justification

Project Title: Water Reallocation and Bioenergy in the South Platte: A Regional Economic Evaluation

Salaries and Wages: Salary has been allocated for a PhD student, Leonard Gwanmesia, to work on this project as part of his dissertation. Mr. Gwanmssia has completed his coursework in agricultural economics as well as his preliminary doctoral examination, but must complete his field examination (January 2008). His stipend is calculated at $1,944 per month (3/4 time) for 12 months in year 1. The stipend increases at 4% for Year 2 in which he is funded 6 months.

Tuition: Continuous registration tuition (1 credit) is calculated for Mr. Gwanmesia at $150 per semester, 2 semesters in Year 1. Tuition increases 4% in Year 2, but is calculated for 1 semester.

Fringe Benefits: Fringe is 4.2% for GRA in both years 1 and 2.

Supplies:

Year 1 laptop computer @ $2,500
Year 1 GAMS software @ $640.

Extensive computer modeling is part of the project methods. Mr. Gwanmesia will travel throughout the South Plate River Basin in order to collect data, and a laptop computer is important for onsite data collection, entry and validation. Moreover, Mr. Gwanmesia will travel to the Basin, the Colorado Division of Natural Resources (State Engineers Office) and the Colorado Department of Local Affairs in Denver to validate data with experts. Lastly, the laptop will be used to present results at Water Congress meetings, the American Association of Agricultural Economics Meetings and to other stakeholder groups. The GAMS software is a necessary component for computable general equilibrium models and is not available as part of typical laptop computer software packages.

Equipment: N/A

Services or Consultants: N/A

Travel: Two distinct phases exist for travel: data collection/validation and results presentation. In Year 1, Mr. Gwanmesia will travel to seven South Platte counties to gather agribusiness data via in-person interview. The total travel costs are budgeted at $1,700. Two trips are planned in total with 897 miles per trip @ $0.39 per mile, 5 nights hotel per trip @ $61 per night on average, and per diem of $39 per day. Mr. Gwanmesia will travel to the Colorado Department of Local Affairs and the Colorado Division of Natural Resources (State Engineer) to validate data. Three trips for data validation have been budgeted with 125 miles roundtrip, $0.39 per mile.

Budget Justification (continued)

Project Title: **Water Reallocation and Bioenergy in the South Platte: A Regional Economic Evaluation**

Travel (cont.)

Year 2 travel includes registration and mileage to the Colorado Water Congress Annual Meeting ($259) and the American Agricultural Economics Association (AAEA) Meetings to present results ($966). Travel to the AAEA meetings includes airfare @ $450, three nights lodging at @ $96 per night, per diem, parking, tolls and mileage. Total is adjusted for 4% expected inflation in Year 2.

Other Direct Costs: N/A

Indirect Costs: 10% of total direct costs.

Grant No. 08HQGR0142 Development of a Correction Function for the 3-Inch, Thin-Walled, Helley-Smith Sampler Deployed on Coarse Gravel Beds

Basic Information

Title:	Grant No. 08HQGR0142 Development of a Correction Function for the 3-Inch, Thin-Walled, Helley-Smith Sampler Deployed on Coarse Gravel Beds
Project Number:	2008CO199S
Start Date:	7/1/2008
End Date:	7/31/2009
Funding Source:	Supplemental
Congressional District:	4th
Research Category:	Engineering
Focus Category:	Hydrology, Sediments, None
Descriptors:	
Principal Investigators:	Steven R. Abt, Kristin Bunte

Publication

1. Bunte, Kristin; Steven R. Abt, 2009, Transport Relationships Between Bedload Traps and a 3-Inch Helley-Smith Sampler in Coarse Gravel-Bed Streams and Development of Adjustment Functions, Completion Report 218, Colorado Water Institute, Colorado State University, Fort Collins, CO, 140 pgs.

Transport Relationships Between Bedload Traps and a 3-Inch Helley-Smith Sampler in Coarse Gravel-Bed Streams and Development of Adjustment Functions

Kristin Bunte
Steven R. Abt

December 2009

Completion Report No. 218

Colorado State University

This report was financed in part by the U.S. Department of the Interior, Geological Survey, through the Colorado Water Institute. The views and conclusions contained in this document are those of the authors and should not be interpreted as necessarily representing the official policies, either expressed or implied, of the U.S. Government.

Additional copies of this report can be obtained from the Colorado Water Institute, E102 Engineering Building, Colorado State University, Fort Collins, CO 80523-1033 970-491-6308 or email: cwi@colostate.edu, or downloaded as a PDF file from http://www.cwi.colostate.edu.

Transport relationships between bedload traps and a 3-inch Helley-Smith sampler in coarse gravel-bed streams and development of adjustment functions

Report submitted to the

Federal Interagency Sedimentation Project

3909 Halls Ferry Rd.
Vicksburg, MS 39180

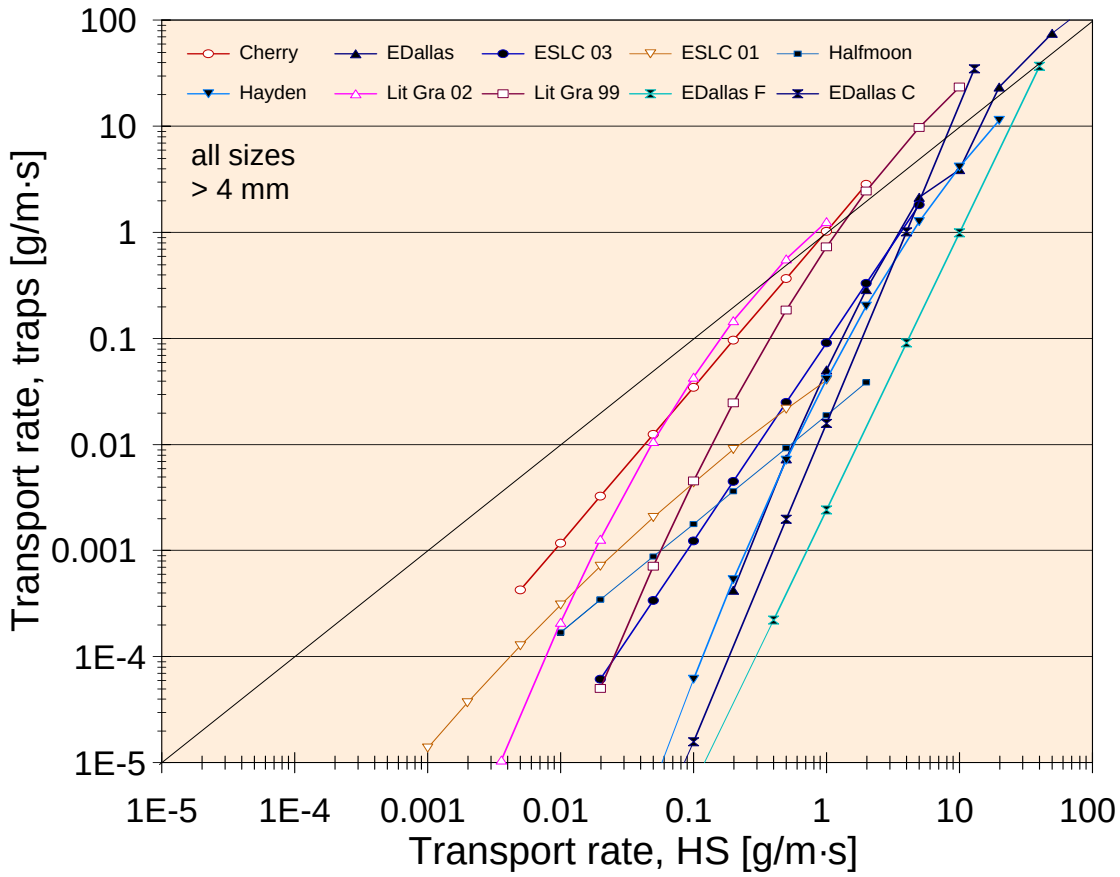

Kristin Bunte and Steven R. Abt

Engineering Research Center
Colorado State University
Fort Collins, CO

December 2009

Executive Summary

Sampling results obtained from a Helley-Smith (HS) sampler have been found to differ from those collected with other samplers, particularly those that are not restricted by a small opening size, a small sampler bag, short sampling times, and direct contact with the bed. The ability to convert HS sampling results to those obtained from a sampler without those restrictions, such as bedload traps, might be beneficial because HS samplers are frequently used in field studies due to their widespread availably and ease of use.

This study compared sampling results from bedload traps with those collected by a 3-inch, thin-walled, wide-flared HS sampler over a wide range of transport rates at nine coarse-bedded mountain stream study sites. Ratios of transport rates collected with both samplers are not constant but change over the range of sampled transport rates. Inter-sampler transport relationships are quantifiable by regression functions that can be used to convert HS transport rates to those that might have been measured with bedload traps.

Inter-sampler transport relationships were established for all gravel size fractions as well as for total gravel transport rates for all study sites. Inter-sampler transport relationships generally follow a similar pattern: they approach or intersect the line of perfect agreement (1:1 line) at high transport rates. At lower transport rates, relationships diverge below the 1:1 line, indicating that transport rates from the HS sampler exceed those from bedload traps by several orders of magnitude. This pattern shifts slightly among particle sizes but is notably variable among streams.

Two approaches were used for the comparison of HS sampling results to those of bedload traps: 1) The rating curve approach fits power functions rating curves to the relationship of bedload transport rates versus discharge that are measured with both samplers and then creates data pairs from transport rates predicted for each sampler at specific discharges. 2) The paired data approach establishes data pairs from transport rates measured almost concurrently with both samplers. Both, the rating curve and the paired data approach clearly suggested a segregation of inter-sampler transport relationships into two groups (termed “red” and “blue”), and both approaches resulted in almost the same classification of streams into the groups. Study streams of the “red” and “blue” group differed significantly with respect to bedload transport conditions. In comparison to “blue” streams, “red” streams have steeper rating and flow competence curves, smaller transport rates and smaller bedload D_{max} particle sizes at 50% Q_{bkf} , and larger bedload D_{max} at Q_b = 1g/m·s. Threshold values for these attributes are provided to differentiate between stream groups.

Inter-sampler transport relationships for all approaches were averaged over the streams within each group. For “blue” streams, the group-average trendlines were quite similar among approaches but less so for “red” streams. Averaging over all approaches yielded an adjustment function for each stream group that serves to convert HS sampling results to those that might have been measured with bedload traps.

While both approaches—rating curve and paired data—have advantages and disadvantages, this study favors the paired data approach. The paired data approach omits the error prone and time-consuming step of fitting rating curves and allows operators to make informed decisions about data trends. Another advantage is that results from the paired data approach offer the possibility to predict stream-specific inter-sampler transport ratios based on a stream's sediment supply and flow competence.

From the various inter-sampler transport relationships identified for the nine study streams using two study approaches, the study distilled two numerical correction functions for HS sampling results. They are meant for gravel transport in coarse-bedded mountain streams depending on threshold values of their characteristics of bedmaterial and bedload transport. Compared to their wide variability among streams, correction functions vary generally much less among size fractions, and this may be ignored for now. More studies are needed to validate conversion functions and to extend the range of stream conditions for which conversion functions are available.

Table of contents

1. Introduction

1.1 Study overview

Several studies have shown that sampling results measured with a 3-inch Helley-Smith sampler (HS) differ from those measured with other samplers. There are known problems of over-sampling and undersampling by the HS sampler in gravel-bed streams depending on the conditions of the channel bed and on bedload transport characteristics. Bedload traps are relatively new sampling devices that were designed to overcome the HS-typical sampling challenges in gravel-bed streams; on these grounds sampling results from bedload traps are assumed to be more encompassing than those from a HS sampler. However, the HS sampler is the most frequently used sampling device due to its widespread availability and ease of use, and a large number of HS data exist. It would be beneficial if HS-measured transport rates could be aligned to those measured with bedload traps. The objective of this study is to provide adjustment functions with which to align transport rates measured by a HS sampler to those measured with bedload traps.

The study will demonstrate that bedload sampling results differ among samplers, particularly those not affected by the design and operational properties of a Helley-Smith sampler. Direct contact with the channel bed appears to be the most influential factor among several HS-typical attributes causing sampling differences. Preliminary analyses of bedload trap and HS sampling results indicate that ratios of HS to bedload trap sampling results vary with bedload transport rates, and the data suggest that these ratios may vary with bedload particle sizes, as well as among streams. These findings suggest that conversion of HS sampling results is not a matter of applying one simple factor. Rather, conversion functions are dependent on transport rates and likely vary among bedload particle sizes, as well as among streams due to differences in bedmaterial conditions and characteristics of bedload transport.

To compute conversion functions, the analyses will utilize an existing body of bedload transport rates that were measured with bedload traps and the HS sampler over snowmelt highflow seasons at nine sites in mountain gravel-bed streams. Two approaches were used to illustrate the relationships between transport rates measured with a HS sampler and bedload traps at the study streams. 1) The rating curve approach employs gravel bedload rating curves established for both samplers and, in a second step, matches transport rates predicted from both rating curves to establish an inter-sampler transport relationship. Inter-sampler transport relationships are quantified via fitted power functions in the general form of $Q_{B\,traps} = a\,Q_{B\,HS}{}^{b}$, and the parameters a and b are used to convert a HS-measured transport rate $Q_{B\,HS}$. 2) The paired data approach uses transport rates measured concurrently with both samplers and fits power functions as well as polynomial functions to the plotted data to characterize inter-sampler transport relationships.

Both comparison approaches indicate that inter-sampler transport relationships vary moderately among particle-size classes, but widely among streams. Inter-sampler relationships for total gravel transport appear to be segmented into two groups that differ mostly for high transport rates in the rating curve approach. In the paired data approach, the two groups differ primarily for low transport rates and appear to converge when transport is high. The study provides a grouping of bedload transport parameters from which a user can estimate into which group a study stream may fall, and subsequently select the appropriate function for adjusting HS sampling results. For

the paired data approach, the study also provides relationships with which a user can determine the adjusted transport rates for selected HS-measured transport rates based on bedmaterial properties and bedload transport characteristics of the study stream.

1.2 Sampling results deviate among various bedload samplers

HS-type samplers are widely used for collecting bedload in gravel-bed streams. HS-type samplers (including the BL-84, the 3-inch and 6-inch HS samplers, the 8 by 4 inch Elwha sampler, and the 12 by 8 inch Toutle River II sampler) differ not only in the size of the sampler opening but also in the shape of the sampler body, as well as the capacity and mesh size of the sampler bag. Several studies show that Helley-Smith-type samplers of different sizes, shapes, and sampler bags collect different transport rates (e.g., Johnson et al. 1977, Beschta 1981, O'Leary and Beschta 1981, Pitlick 1988, Gray et al. 1991; Gaudet et al. 1994, Childers 1991, 1999; Ryan and Troendle 1997; Ryan and Porth 1999, Ryan 2005; Vericat et al. 2006). Sampling results differ not only among HS-type samplers but also from those obtained by bedload samplers that do not have the HS-typical restrictions of small opening sizes, small collection bags, short sampling times, and direct interaction with bedmaterial. For example, when compared to unweighable pit traps excavated into a natural channel bed, the HS sampler (deployed for hours at a time) oversampled sand in near-bed suspension and under-sampled sand and gravel that passed beneath the sampler perched on cobbles (Sterling and Church 2002). The passage of sand under a HS perched on a cobble bed was also observed on flume experiments by O'Brien (1987). Compared to weighable pit traps in a large flume study, the Helley-Smith-type samplers over-sampled sand and gravel bedload (Hubbell et al. 1985, 1987), and the degree of oversampling varied among various HS samplers, albeit that a reanalysis of these data by Thomas and Lewis (1993) suggests less difference. Compared to bedload traps, gravel transport rates (> 4 mm) measured with the 3-inch HS sampler were orders of magnitude higher during low transport at nine study sites. With increasing transport rates, results from both samplers converged, and fitted rating curves intersected on average near 130% Q_{bkf} (or near 125% if the two samplers' transport relationships are multiplied by the Ferguson (1986, 1987) bias correction factor). At higher flows, the HS sampler under-sampled transport rates because coarse gravel and cobbles cannot enter the HS opening (Bunte et al. 2004, 2008) (this is illustrated in Figure A1 in the Appendix). This pattern was exhibited at all study sites where bedload traps and a HS sampler were deployed together. However, details in the relationships between bedload trap and HS transport rates varied among streams: the difference in gravel transport rates between the two samplers measured at flows 50% Q_{bkf} extended over 1 to 4 orders of magnitude, and the intersection points of the rating curves from the two samplers ranged from 93 to 181% Q_{bkf} (illustrated in Figure A2).

1.2.1 Direct bed contact responsible for most differences in sampling results

Several pieces of evidence suggest that much of the difference in sampling results between the HS and other samplers is a result of direct contact between the HS sampler and the channel bed. In two of the nine study streams, the 3-inch, thin-walled HS sampler was deployed not only on the bed but also on the ground plates on which otherwise bedload traps were deployed (see Bunte and Swingle (2008) for study details). Setting the HS sampler onto ground plates greatly reduced transport rates compared to those measured with the HS set directly on the bed, particularly at

low flows. As a result, transport rates measured by the HS on plates approach those measured with bedload traps to within an order of magnitude or less (illustrated in Figure A3) (Bunte and Swingle 2008; Bunte et al. 2007b). The higher transport rates of the HS on the bed are ascribed to the following mechanism. Setting the HS sampler onto the channel bed exerts a slight pressure onto bed particles, dislocating a few particles near the sampler edge from their interlock with neighboring particles. Being slightly more exposed to flow, the hydraulic sampler efficiency of 1.5 from the wide-flared sampler opening can entrain dislocated particles into the sampler and collect gravel particles that are otherwise not in motion on the bed. Ground plates under the HS sampler prevent direct interaction with the gravel bed, and placement of a sampler onto plates avoids inadvertent particle dislocation and entrainment. Avoidance of direct contact with the bed is likely the main reason for collection of similar transport rates with a 3-inch HS placed on a concrete sill and the conveyor belt sampler (Emmett 1980, 1981, 1984).

A comparison of the bedload D_{max} particle sizes sampled by the HS deployed on the bed *vs*. those on grounds plates demonstrates that both sampler deployments collected similar transport rates and similar bedload D_{max} particle sizes during high transport. At low transport, however, the HS on the bed collected not only higher transport rates but also larger bedload D_{max} particle sizes than the HS on the plates (Figure A4). Collection of larger bedload D_{max} particles suggests that inadvertent particle displacement and entrainment is the mechanism that results in oversampling when a HS is placed directly on the bed.

Direct placement of the HS sampler on the bed may add an occasional particle per vertical. Nevertheless, the chance of including an extra particle into the sampler accumulates when the HS is deployed at 15-20 verticals per cross-section (Bunte et al. 2008). Collecting additional gravel particles can overestimate transport rates by orders of magnitude when transport is otherwise very low. When transport is high, an occasionally dislocated and entrained particle in the HS sampler contributes minor amounts in comparison to the large number of particles entering the sampler per time. HS-measured transport rates therefore approach those from bedload traps when transport is high, and the accuracy of the HS measurements likely improves with increasing gravel bedload transport rates. The potential for inadvertent particle dislodgement and entrainment by the HS sampler as well as for active particle "scooping" due to an unfavorable sampler position has been mentioned as a problem for the 3-inch HS sampler by several (Helley and Smith 1971; Beschta 1981; O'Leary and Beschta 1981; Ryan and Troendle 1997), and by Vericat et al. (2006) for the 6-inch HS.

The importance of deploying the HS to ensure good contact with the stream bottom in order to avoid over- or undersampling has been presented (Johnson et al. 1977; Emmett 1980, 1981, 1984; Beschta 1981; O'Brien 1987; Kuhnle 1992; Childers 1999, Sterling and Church 2002; Bunte et al. 2004, 2007b, 2009b). Data shown by Wilcox et al. (1996) indicate that a HS deployed directly on a coarse gravel bed collected more gravel and less sand than a HS deployed on a wooden sill nearby. Collecting less sand can be the result of loosing fine particles beneath the sampler perched on gravel, while collecting more gravel can result from inadvertently dislocating and entraining gravel particles by the sampler on the bed.

1.2.2 Other sampler characteristics contributing to differences in sampling results

Apart from particle dislocation and entrainment (Bunte et al. 2004, 2007b, 2008, Bunte and Swingle 2008), or pedestalling (O'Brien 1987; Childers 1999; Sterling and Church 2002) (Figure 1 a and b) due to direct bed contact, other attributes in the HS sampler design and deployment method contribute to differences in measured transport rates and bedload D_{max} particle sizes as well. For example, gravel transport relationships obtained from two samplers will not be the same if samplers have different sampling times (Bunte and Abt 2005) (Figure 1c), opening sizes (Thomas and Lewis 1993; Gaudet et al. 1994; Childers 1999; Vericat et al. 2006) (Figure 1d), and sampling efficiency (Druffel et al. 1976; Pitlick 1988; Gray et al. 1991; Childers 1991, 1999) (Figure 1 e). The sampler-specific differences in measured transport rates vary with flow and with transport rates. The combined effects caused the HS sampler to measure higher gravel transport rates than bedload traps at low flow and similar or higher transport rates at high flows.

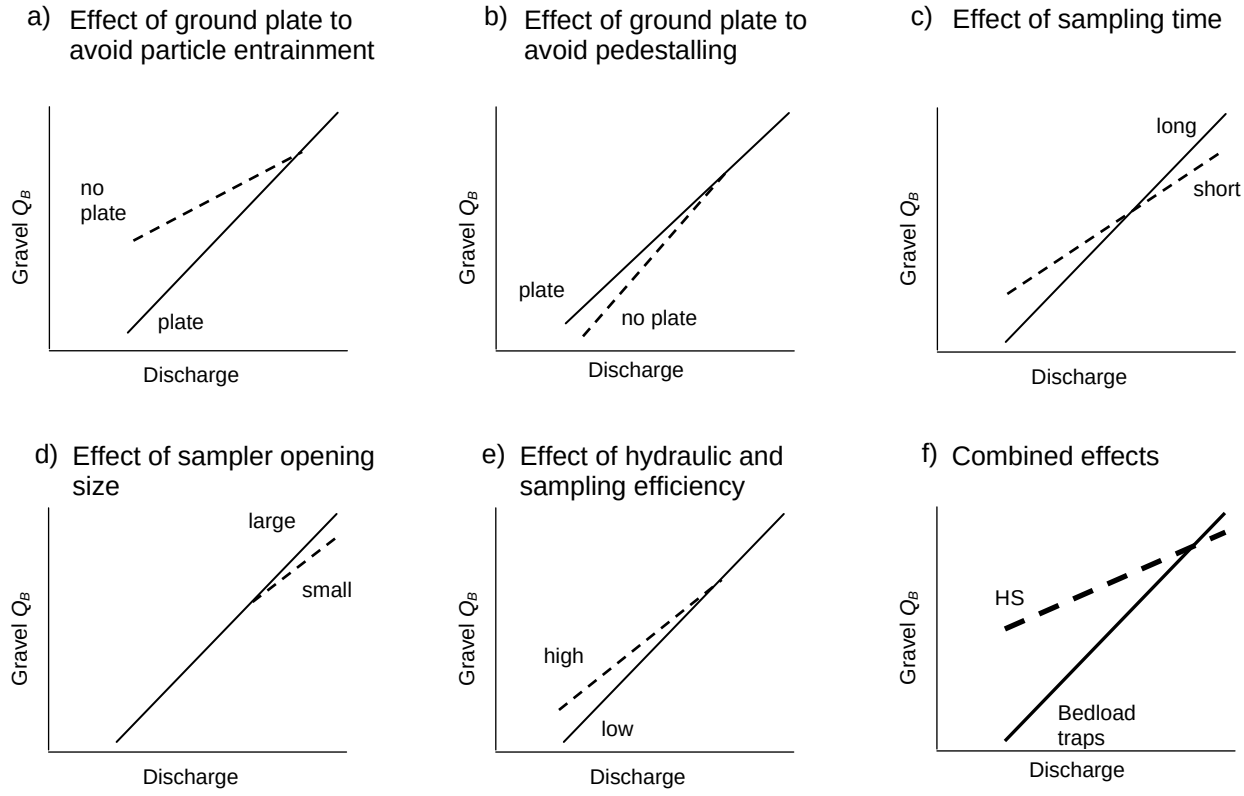

Figure 1: Effects of short sampling time, small opening size, high hydraulic and sampling efficiency, scooping, and pedestalling on sampled gravel transport rates in a coarse-bedded mountain gravel-bed stream over flows ranging from about 15 to 140% of bankfull (i.e., within the range of infrequent motion of pea gravel to frequent motion of coarse gravels including occasional cobbles).

The difference in sampling results among the 3-inch HS sampler and non-HS samplers makes determining adjustment functions to convert transport rates between samplers an important task. Without those functions, sampling results obtained by different samplers cannot be compared.

Once conversion functions are available to account for inter-sampler differences, the choice of bedload sampler for future studies can be guided by convenience or availability. The ability to account for inter-sampler differences may also allow the reanalyzing of old data or compiling them for meta studies.

1.3 Objectives of the study

The objective of the study is to develop conversion functions that can be applied to data collected with a wide-flared, thin-walled, 3-inch Helley-Smith sampler. The conversion functions are directly derived from relationships of transport rates measured with bedload traps to those measured at the same flow with the 3-inch, wide-flared, thin-walled Helley-Smith sampler placed directly on the bed. The study uses a large body of field-measured gravel transport rates that were collected with bedload traps and a 3-inch HS sampler deployed side by side in nine mountain gravel-bed streams during snowmelt runoff over a wide range of flow and transport rates (Bunte et al. 2008).

2. Transport relationships between bedload traps and the HS

2.1 Affecting parameters

Analyses prior to this study had indicated that the variability of bedload trap to HS transport ratios among streams may be influenced by factors such as bedload transport rates, bedload particle-size fractions, as well as bedmaterial characteristics of the study streams (Bunte and Swingle 2008).

Effects of HS-measured bedload transport rates

Results from the nine field studies indicate that the thin-walled HS sampler measured transport rates several orders of magnitude higher than those collected with bedload traps when flows and transport were low (Figure A1). With increasing flows and transport rates, transport rates collected by both samplers approach and may intersect. Based on these results, ratios of transport rates measured with bedload trap and the HS sampler (F_{HS}) at the same flow should be formulated as a function of the transport rate measured by the HS sampler in the basic form of

$$F_{HS} = q_{B,trap} = a \cdot q_{B,HS}{}^{b} \quad (1)$$

where $q_{B\,trap}$ and $q_{B\,HS}$ are the mass-based transport rate per unit stream width (g/m·s) measured with bedload traps and the HS sampler, respectively; a is a coefficient and b an exponent. The function describing how bedload trap-HS transport ratios changes with increasing transport rates is termed inter-sampler transport relationship in this study (Figure 2a).

Effects of bedload particle-size fractions

Fractional bedload rating curves fitted to bedload trap data and the HS sampler for the study sites differ from each other. For bedload traps, they are typically parallel and relatively close to each other. For the HS sampler, fractional rating curves are typically less parallel and further apart with higher transport rates for larger particles (Bunte et al. 2004). These differences will likely

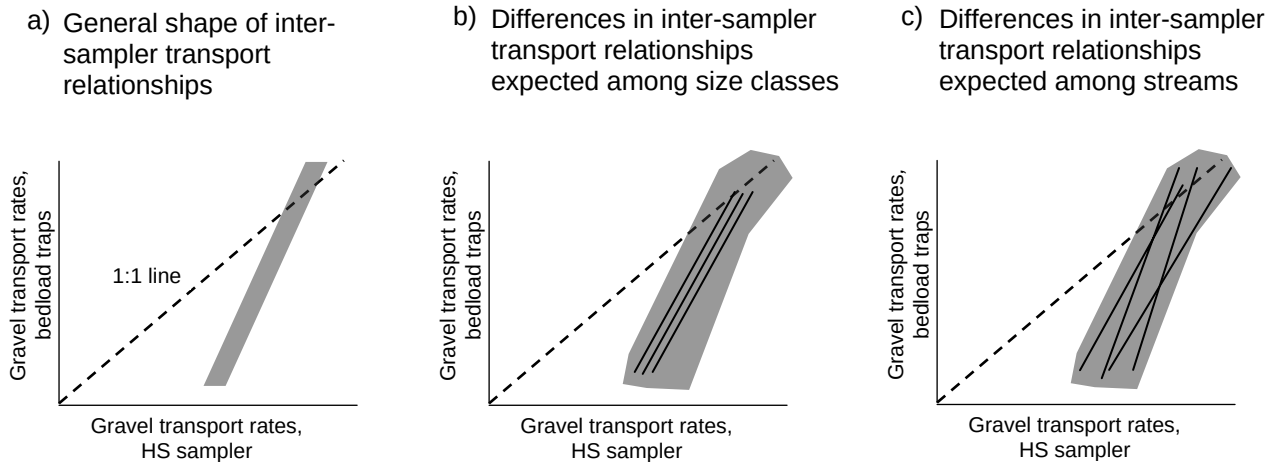

Figure 2: General shape of inter-sampler transport relationships plotted in log-log space (a) and expected differences among particle-size classes (b) and among streams (c).

cause the ratio of transport rates between the two samplers to vary among size fractions. Consequently, inter-sampler transport relationships (Eq. 1) may need to be formulated for individual size fractions (*i*) in the form of (Figure 2b):

$$F_{HS,i} = q_{B\ trap,i} = a_i \cdot q_{B\ HS,i}^{\ bi} \qquad (2)$$

Effects of stream sediment supply: subsurface sediment size and rating curve steepness
Studies have shown that the difference between bedload trap and HS gravel bedload rating curves differ among the study streams (see Figures A1 and A2 in the Appendix). It appears important to identify the parameters that differ among streams and that may cause systematic variability among streams (Figure 2c).

Studies by Bunte et al. (2006) have shown that bedload traps tend to have flatter transport relationships (i.e., lower exponents of fitted power function rating curves) in streams with large amounts of subsurface fines < 8 mm than in stream with fewer subsurface fines. Conversely, rating curve coefficients tend to increase with the percent subsurface fines (see Figure A5 a and b in the appendix as an illustration). High amounts of subsurface fines < 8 mm suggest a high supply of easily transportable sediment, and this causes the lower end of bedload trap rating curves to be elevated, and thus the rating curve slope to be rather flat. Rating curve exponents and coefficients obtained from HS samples differ much less with the amount of subsurface fines. If the difference in gravel rating curve steepness between the two samplers decreases with increasing amount of subsurface fines, the ratios of transport rates between bedload traps and the HS sampler should vary with the amount of subsurface fines as well, probably in a way that the ratio between HS and bedload trap transport rates becomes smaller in streams with high sediment supply. To test this assumption, the study should explore whether inter-sampler transport relationships vary among streams and whether they show similarities for streams that share commonalities of the shape of bedload rating curves as well as sediment supply.

Effects of bedload D_{max} particle size

Earlier study results suggested that the ratio of transport rates should be affected by the size of the largest particles in transport. Comparison of HS and bedload trap sampling results between East Dallas and Hayden Creek shows that the HS sampler is most likely to collect transport rates similar to those from bedload traps when a large amount of small gravel particles that fit into the 3-inch opening are in motion per time. Thus, transport ratios between the two samplers at high flows should approach unity when transport is high and comprised of relatively small gravel. When a large amount of coarse gravel and cobbles are in transport, the HS transport rate should fall below that of bedload traps, as these large clasts cannot enter the 3-inch HS sampler. When small amounts of medium gravel are in motion, inadvertent particle dislocation and entrainment increases HS transport rates beyond those collected with bedload traps. Bedload trap-HS transport relationships should therefore be evaluated for variability within the transported bedload D_{max} particle size.

Accounting for the potential effects of subsurface fines, the rating curve steepness, and the bedload D_{max} particle sizes, inter-sampler transport relationships assume the general form of

$$F_{HS,,sed} = a_{,sed} \cdot q_{B\ HS,sed}{}^{b,sed} \tag{3}$$

where the subscript *sed* denotes the magnitude of rating curve steepness, subsurface fines, bedload D_{max} particle sizes, or a combination of some or all of these factors.

2.2 Effects of sampler behavior

Attributes of sampler design and deployment method affect the differences in rating curves measured by bedload traps and the HS sampler (Figure 1), causing either oversampling or undersampling compared to transport rates collected in a sampler (e.g., bedload traps) that is neither deployed directly in the bed nor shares other design attributes of a 3-inch, thin-walled, wide-flared HS sampler. Figure 3 illustrates how the various sampling behaviors "plot out" in inter-sampler transport relationship graphed in a diagram of bedload trap versus HS transport rates.

Oversampling occurs as the HS sampler:

a) Inadvertently dislocates particles at the sampler entrance when set on the bed. Without support from neighboring particles, dislocated particles are easily entrainable by flow and aided by the sampler's high hydraulic efficiency, these particles are likely to enter the sampler: → oversampling gravel
   The effects of particle dislocation and entrainment increase with the number of verticals per cross-section and the brevity of sampling time.
b) Is not set flatly on the bed and inadvertently scoops an easily entrainable particle as the HS is set on the bed: → oversampling gravel
c) Has a high hydraulic efficiency: → oversampling sand and pea gravel.
d) Is set onto the bed: Particles dislocation and subsequent entrainment, as well as particle scooping and a hydraulic efficiency → oversampling particularly when transport rates are otherwise very low.

Undersampling occurs when the HS sampler

1. is perched on cobbles or coarse gravel in a coarse bed: → undersampling small particles that pass beneath the sampler,
2. is not on the bed sufficiently long to capture infrequently moving (large) particle sizes: → undersampling large particles
3. when particles in transport exceed the sampler opening size: → undersampling large particles
4. when a large particle lodged in front of the sampler blocks the sampler opening: → undersampling any particle size in a specific sample.

Each of these processes individually affects transport relationships between a HS sampler that is deployed directly on the bed (x) and bedload traps (y). Several of these processes may occur in combination during an individual sample or while a sequence of samples is collected over the cross-section. This causes variability in the inter-sampler transport relationship in response to changing conditions of bedload transport and bedmaterial at the time of sampling.

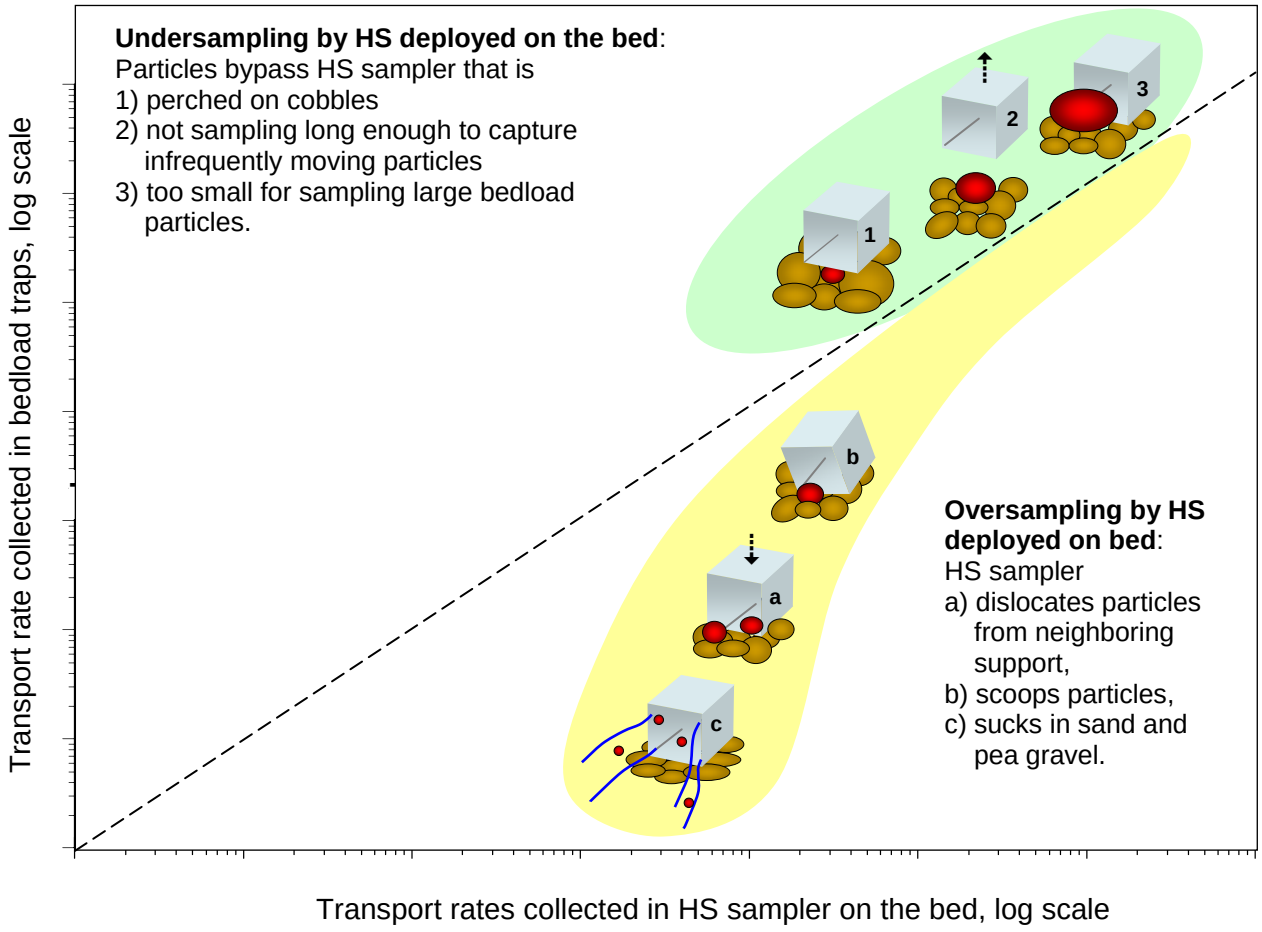

Figure 3: Sampling behaviors of a HS sampler (shown here only with its cube-shaped entry part) and their expected effects on the ratio of transport rates between bedload traps and a HS deployed directly on the channel bed.

3. Methods

3.1 Data collection

Field data were collected at nine study sites in mountain streams with armored, coarse gravel and small cobble beds (Table 1). The sites were located on National Forest land in the northern and central Rocky Mountains (USA) in subalpine and montane zones at altitudes between 2,000 to 3,000 m above sea level. Most of the stream basins experienced some logging, mining and road building several decades ago, but today the basins are comparatively undisturbed and mostly forested. Valley floors are mainly open and vegetated by meadows with shrubs or willow thickets. All sampled streams have a snowmelt highflow regime in which runoff typically

Table 1: Characteristics of the streams near the study sites.

Parameters / Stream; Year sampled	Predo-minant lithology	Basin area (km^2)	Bank-full flow (m^3/s)	Bank-full width (m)	Meas'd range of flow (%Q_{bkf})	Water surface slope (m/m)	Surface		Subsurface % fines		Sub-surface D_{50} (mm)	Predominant stream type
							D_{50} (mm)	D_{84} (mm)	< 2 mm	< 8 mm		
St. Louis Cr., '98	Granite	34	3.99	6.5	26 - 65	0.017	76	163	9	24	41	plane-bed, forced pool-riffle
Little Granite Cr., nr. confluence '99	Sediment-ary	55	5.66	14.3	61 - 131	0.017	59	133	8	16	42	plane-bed, forced pool-riffle
Cherry Cr., '99	Volcanic	41	3.09	9.5	49 - 145	0.025	49	140	11	27	30	plane-bed, forced pool-riffle
E. St. Louis Cr., '01	Granite	8	0.76	3.7	26 - 71	0.093	108	258	6	17	54	step-pool
Little Granite Cr., abv. Boulder Cr. '02	Sediment-ary	19	2.83	6.3	37 - 102	0.012	67	138	10	25	34	plane-bed, forced pool-riffle
E. St. Louis Cr., '03	Granite	8	0.76	3.7	44 - 144	0.093	108	258	6	17	54	step-pool
Halfmoon Cr., '04	Granite	61	6.23	8.6	17 - 77	0.014	49	119	13	29	26	plane-bed, forced pool-riffle
Hayden Cr., '05	Sediment-ary	39	1.92	6.5	28 - 149	0.038	63	164	13	26	36	step-pool, plane-bed, mixed
East Dallas Cr., 07	Volcanic	34	3.7	8.0	10 - 113	0.017	58	128	12	31	21	plane-bed, forced pool-riffle

increases from 10-20 % of bankfull discharge (Q_{bkf}) in early to mid May to 80 - 140% Q_{bkf} between late May and mid June, depending on the annual snowpack and spring weather conditions. Daily fluctuations of flow can be pronounced, varying by up to 50% between daily low flows in the early afternoon and daily peak flows in the early to late evening. The streams are typically incised into glacial or glacio-fluvial deposits. At most sites, the streambed is entrenched into a floodplain such that highflows of l40% Q_{bkf} cause little overbank flooding.

3.1.1 Bedload trap data

At all study sites, gravel bedload was sampled using bedload traps that consist of an aluminum frame 0.3 by 0.2 m in size. Bedload is collected in an attached net 0.9 – 1.6 m long and with a mesh width just below 4 mm. Bedload traps are mounted onto ground plates 0.43 by 0.37 m in size that are anchored on the stream bottom with metal stakes. This deployment set-up not only permits long sampling times but also avoids direct contact of bedload traps with the channel bed.

Four to six bedload traps were installed across each of the study streams spaced 1-2 m apart, typically in a locally wide cross-section. All traps sampled simultaneously, typically for 1 hour per sample, but sampling time was reduced to 30 or even 10 minutes when transport rates were high in order to avoid overfilling the sampler net (Bunte et al. 2008). Four to nine samples of gravel bedload were collected back-to-back on almost all days of the snowmelt highflow seasons that extended over 4 to 7 weeks. Therefore, 2l-196 samples were collected per site with an average number of 92 samples. Sampled flows ranged from low flows of 16% to highflows of 140% of bankfull discharge, but only 5 of the nine study streams exhibited this range.

3.1.2 Helley Smith data

Bedload was sampled at all study sites using a 76 by 76 mm opening, thinwalled Helley-Smith sampler with a 3.22 opening ratio and a 0.25 mm mesh bag. Sampling locations were spaced in 0.4-1.0 m increments across the stream, yielding 12 to 18 verticals that were sampled for 2 minutes each, completing one traverse. At several sites, HS samples were collected in the same cross-section as the bedload traps, and the HS verticals were placed into spaces between the traps. This arrangement permitted simultaneous sampling with bedload traps and a HS sampler, however, individual verticals were not all evenly spaced. At other sites, HS samples were collected in a cross-section about 1.8 m downstream from the traps by an operator standing on a low footbridge (decking height 0.4 – 0.7 m above the water surface). This permitted an even spacing of the HS verticals but required that bedload traps were removed from the ground plates while the HS samplers were collected. One set of HS samples was typically collected in the morning before bedload traps were fastened on the ground plates and one in the evening after the bedload traps were removed. Depending on the length of the field season, about 20 – 80 samples were collected with the HS sampler for each site per season. Most of the HS samples were paired with a bedload trap sample that was collected either immediately before or after the HS sample. Flows were quite similar for the two paired samples in the morning, but could vary by up to 20% for some of the evening samples when flows increased. Transport relationships computed from HS samples in this study usually aligned with HS samples that the USDA Forest Service had obtained at or close to sites in this study in earlier years (mainly between 1993 and 2002, see data sets in Ryan et al. 2002, 2005).

3.2 Data analysis

Two approaches were considered when comparing transport rates collected with bedload traps and the HS sampler. The rating curve approach compares transport rates predicted for each of the two samplers for a specified flow from a fitted rating curve. The paired data approach compares transport rates measured sequentially by the two samplers at a similar flow. Both approaches are applied to data from all study streams.

3.2.1 Rating curve approach

The rating curve approach uses all non-zero gravel transport rates collected at a study site to compute bedload transport rating curves for total and individual size fractions (total and fractional rating curves). Several computational steps are required to predict transport rates for specific flows from both samplers and to establish inter-sampler transport relationships. These steps are explained and repeated at each study stream.

3.2.1.1 Establishing total and fractional transport relationships

a) Plot total gravel and fractional gravel transport rates for each 0.5 phi size class versus discharge for both samplers.

b) Establish rating curves by fitting power function regressions to the total and all fractional transport relationship for both samplers. Power functions were selected because they are frequently used for gravel transport (e.g., Barry et al. 2004, King et al. 2004, Bunte et al. 2008) and are convenient for subsequent computations.

$$q_{B\,trap,i} = g_i \cdot Q^{hi} \tag{4}$$

$$q_{BHS,i} = c_i \cdot Q^{di} \tag{5}$$

where $q_{B\,trap,i}$ and $q_{BHS,i}$ are either the total gravel or fractional gravel transport rates predicted for the i^{th} size class (g/m·s), Q is discharge (m^3/s), g_i and c_i are coefficients, and h_i and d_i are exponents for bedload traps and the HS sampler, respectively.

c) Compute and evaluate the *p*-value[1] for the fitted total and fractional rating curves. *p*-values smaller than 0.05 are typically considered to indicate statistical validity of a fitted relationship. For streams in which many size fractions were in transport, most of the bedload trap rating curves for individual size fractions as well as total gravel transport had *p*-values << 0.05. However, for the one or two largest size classes transported within a given highflow year, small sample sizes and narrow ranges of flow result in rather flat transport relationships for both samplers, and *p*-values were typically >> 0.05, i.e., statistically not significant, and not suitable for comparison of fractional transport rates between the two samplers. For HS samples, *p*-values were generally higher (i.e., somewhat less significant) than for bedload traps because HS samples tended to have larger data scatter and sometimes a slightly smaller range of sampled flows. In order not to exclude several of the HS fractional rating curves from further analysis, *p*-values within the range 0.05 – 0.1 were considered valid. Many of the sites at which HS samples were collected in this

[1] All *p*-values in this report are two-tailed.

study had been sampled by Ryan et al (2002, 2005) a few years earlier when flows reached higher peaks[2] and transport rates extended over wider ranges. However, transport relationships measured in both studies fall within a common envelope, and fitted gravel transport rating curves are similar between both studies. It may be reasoned that many of the HS fractional transport relationships fitted in this studies would have been statistically significant with $p < 0.05$ had there been an opportunity to sample over a larger range of flows.

d) Plot the computed total and fractional transport relationships over the range of flow for which transport of a specified size fraction was observed. The power functions fitted to the fractional transport relationships streams are shown for all study streams in Figure 4**Error! Reference source not found.**. The parameters of the fitted power functions are listed in Table 10 in the Appendix.

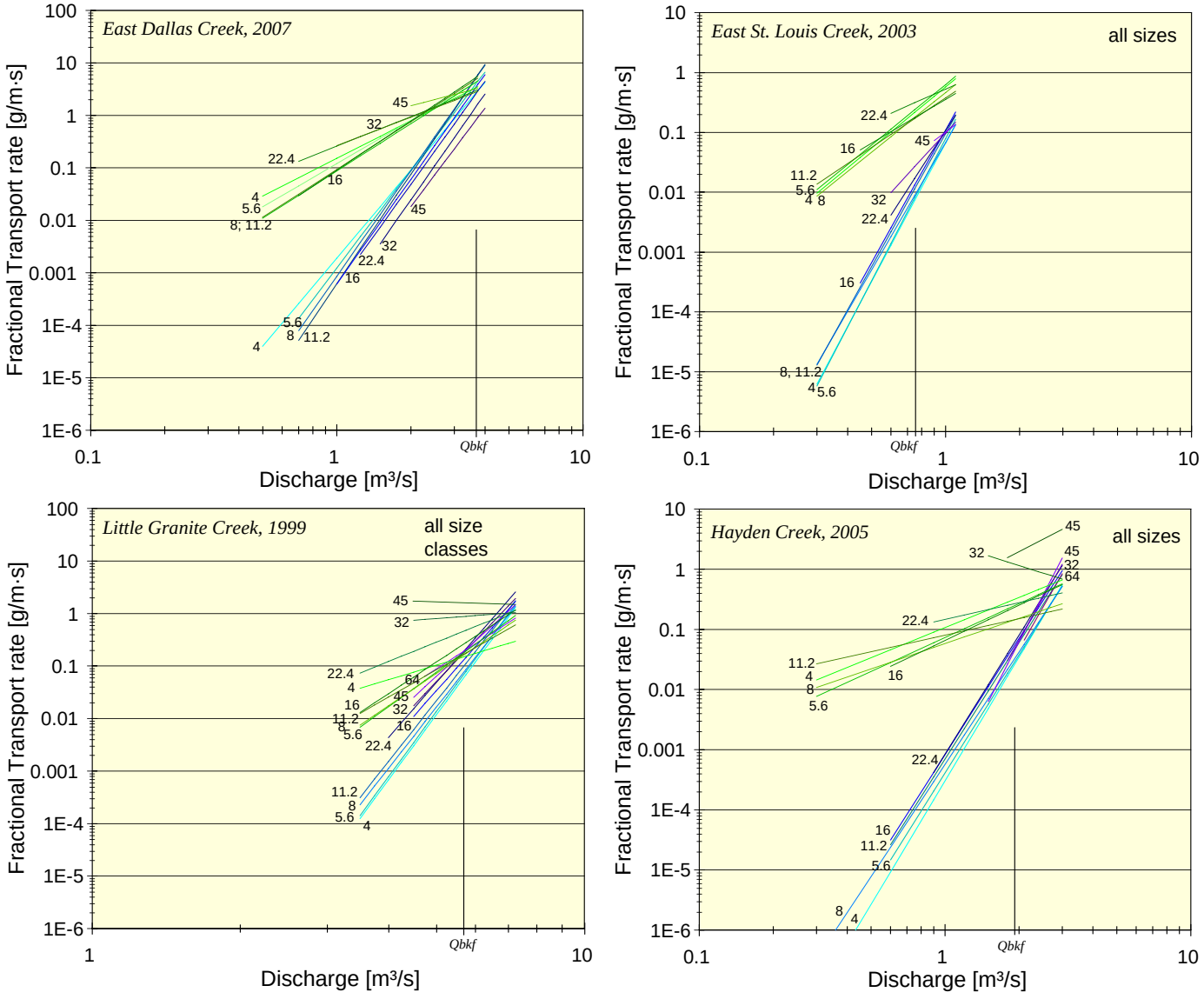

[2] The years 1995, 1996, 1997, and 1999 reached peak flows of 130 - 170% of bankfull. Data for the study presented here were collected between 1998 and 2007; flows peaked within 80 - 100% Q_{bkf} in 1998, 2001, 2002, and 2004.

Fig. 4, cont'd next page

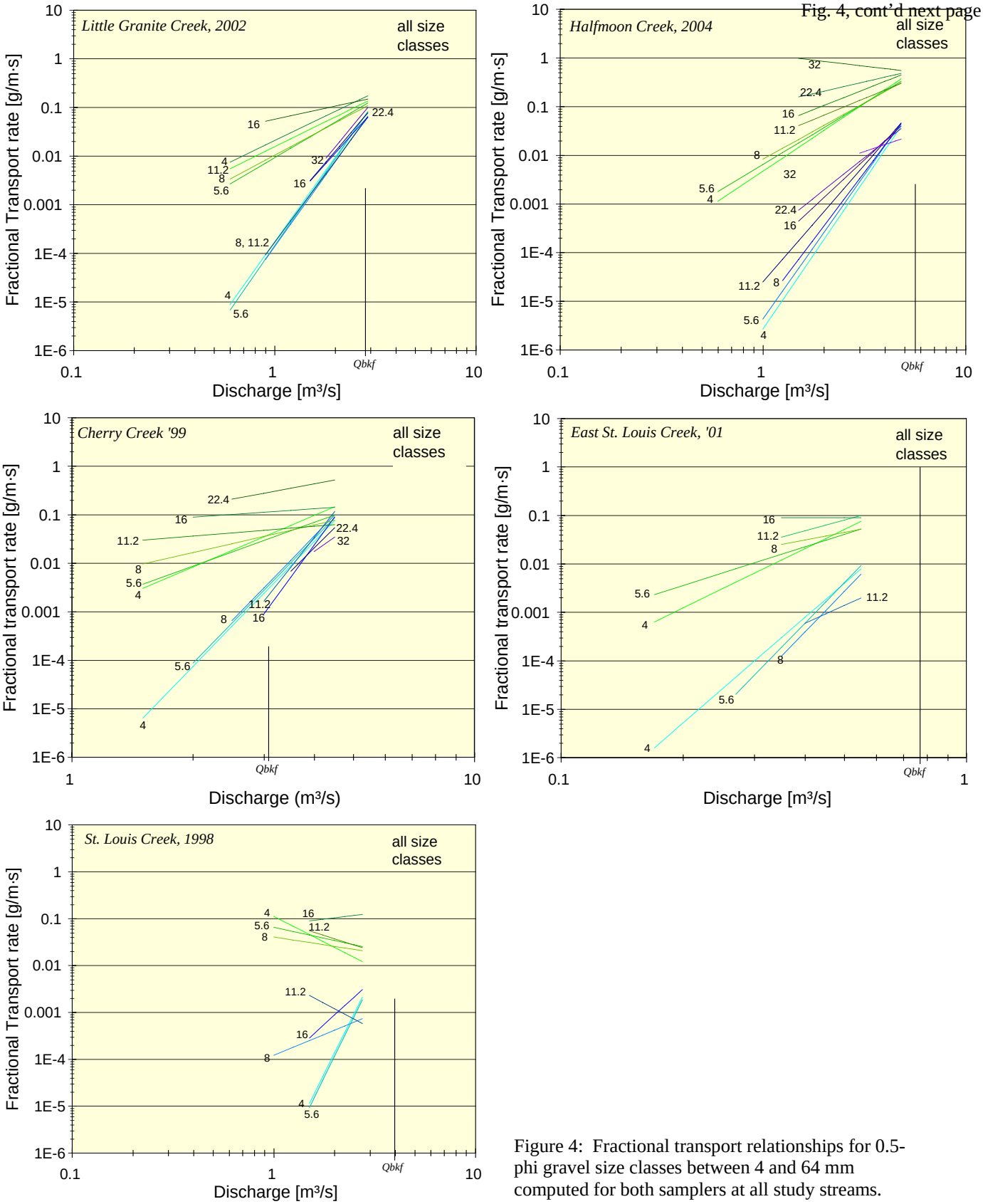

Figure 4: Fractional transport relationships for 0.5-phi gravel size classes between 4 and 64 mm computed for both samplers at all study streams.

3.2.1.2 Bias correction factors

Any prediction of a *y*-estimate from a value of *x* in a power function relationship fitted to data that exhibit scatter suffers an inherent underestimation in the *y*-estimate. The underestimation is zero for perfectly correlated data and increases—typically to a factor of 1.5-5 for the study streams—with the amount of data scatter that is quantified by the standard error of the *y*-estimate. To adjust for the underestimation, the computed *y*-estimate needs to be multiplied by a bias correction factor (*CF*). Several factors are available, e.g., Ferguson (1986, 1987), Duan (1983), and Koch and Smilie (1986). This study used Ferguson's correction factor for the rating curve approach based on Hirsch et al. (1993) who consider Ferguson's correction factor very suitable if the standard error of the *y*-estimate (s_y) is < 0.5 and if sample size (n) is > 30. The corrections factor CF_{Ferg} is computed as

$$CF_{Ferg} = \exp (2.651 \cdot s_y^2) \tag{6a}$$

if the logarithm to the base of 10 (i.e., log) is used for the log-transformation of the *x*- and *y*-data (as was done in this study); s_y is typically provided in a spreadsheet regression table. For log transformations using the natural logarithm,

$$CF_{Ferg} = \exp (s_y^2/2). \tag{6b}$$

Values for CF_{Ferg} typically range between 1 and 3 for fractional transport rates from the HS sampler, and values up to 4 for total bedload transport rates. Values of CF_{Ferg} are somewhat lower for bedload trap data because transport rates collected with bedload traps tend to have less scatter in their relationship with flow than HS samples. In cases when s_y exceeds 0.5 and n drops below 30, Ferguson's bias correction function overcorrects and creates a bias in the opposite direction. To prevent this overcorrection, Hirsch et al. (1993) suggest using the nonparametric smearing function by Duan (1983) for bias correction (CF_{Duan}) which is computed from

$$CF_{Duan} = \frac{\sum_{i=1}^{n} 10\text{^}(e_i)}{n} \tag{7a}$$

when power function regressions are fitted log-transformed data based on decadal logarithms. e_i are the residuals of the predicted *y*-estimate (i.e., the difference between the measured and the predicted *y*-values) that are exponentiated, summed, and divided by the sample size n. For natural logarithms, Duan's correction factor is computed from

$$CF_{Duan} = \frac{\sum_{i=1}^{n} \exp(e_i)}{n} \tag{7b}$$

CF_{Duan} yielded higher values than CF_{Ferg} when the standard error s_y took values of up to 0.6, but the sample size was much larger than 30. In these cases (i.e., when only one of the conditions

described by Hirsch et al. (1993) was fulfilled) the CF_{Ferg} bias correction factor was applied. Transport rates for bedload traps and the HS sampler for specified discharges are then predicted from the power function fitted to fractional transport relationships and multiplied by a correction factor.

$$q_{B\,trap,i} = CF \cdot g_i \cdot Q^{hi} \tag{8}$$

$$q_{BHS,i} = CF \cdot c_i \cdot Q^{di} \tag{9}$$

where g_i is the power function coefficient for the i^{th} size class and h_i is the power function exponent for bedload trap transport relationships. CF is either Ferguson's or Duan's correction factor. c_i and d_i are the power function coefficient and exponents for the i^{th} size class for HS sampler transport relationships. The value of the bias correction factor affects the coefficient, but not the exponent of the predictive function. Similarly, the bias correction factor affects the coefficient of the ratio between bedload trap and HS fractional transport rates.

3.2.1.3 Creating and plotting data pairs

Transport rates are predicted for discharges from the fractional rating curves fitted to HS and bedload trap samples (Eqs. 8 and 9) and paired with each other. The matches include the smallest and the largest flows to which fractional transport rates for both samplers extend, as well as a few flows within the extremes. These data paired values are plotted against each other with $q_{B\,traps,i}$ on the *y*-axis and $q_{B\,HS,i}$ on the *x*-axis (Figure 5). All plotted transport ratios necessarily assume a straight line (in log-log space) that describes the inter-sampler transport relationships between bedload traps and the HS sampler for each size fraction.

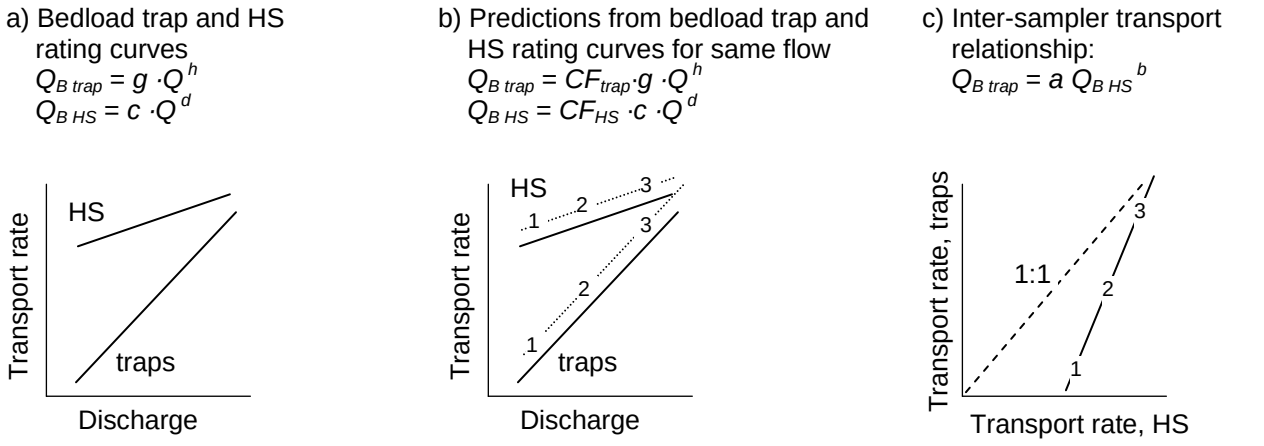

Figure 5: Computation of inter-sampler transport relationship using the rating curve approach: a) Bedload rating curves for bedload trap and HS sampler; b) 1, 2, and 3 are bias-corrected, predicted transport rates from the bedload trap and HS rating curves at the same flows. c) The paired transport rates are plotted versus each other. The fitted power function describes the inter-sampler transport relationship.

3.2.1.4 Formulating inter-sampler transport relationships

To numerically describe fractional inter-sampler transport relationships ($F_{HS,i}$), power function regressions are fitted to two arbitrarily selected data pairs of predicted, log-transformed fractional transport rates for both samplers. Size fractions for which the fitted fractional rating curves for both samplers obtained *p*-values > 0.05 were flagged (some exceptions for $0.05 > p < 0.1$ were allowed). Multiplication by a bias correction factor is not necessary in this step because the power function regression functions fitted to two data pairs have no scatter ($r^2 = 1$).

$$F_{HS,i} = q_{B\,traps,i} = a_i \cdot q_{B\,HS,i}^{\,bi} \tag{10}$$

where a_i and b_i are the power coefficients and exponents for the *i*th size class or the total transport rate. The resulting power functions (F_{HSi}) represent the average ratio of transport rates measured with the two samplers for different particle size fractions and different flows. These functions could be used for adjusting transport rates from a thinwalled, 3-inch HS sampler deployed in mountain gravel-bed streams to transport rates measured with bedload traps.

3.2.1.5 Analyzing inter-sampler transport relationships

Inter-sampler transport relationships are analyzed in various ways. Of interest to this study are analyses of how inter-sampler transport relationships differ among size classes and among study sites. The possibility of systematic differences among streams is assessed by comparing the exponents and coefficients of power functions fitted to inter-sampler transport relationships with parameters describing channel morphology as well as to characteristics of the bedload trap and HS rating curves.

3.2.2 Paired data approach

As an alternative to the rating curve approach, the paired data approach is used to directly compare data pairs of total and fractional transport rates measured with bedload traps and the HS sampler. In this approach, transport rates measured with bedload traps ($q_{B\,trap}$) (*y*-axis) are plotted against those measured with the HS sampler ($q_{B\,HS}$) (*x*-axis) at nearly the same time and the same flow. Regression functions are fitted to the plotted data to describe the inter-sampler transport relationships for all particle sizes and all study streams. To predict an appropriate function for converting HS sampling results to those that would have been measured with bedload traps, parameters of the regression functions are related to parameters of bedmaterial conditions as well as bedload transport characteristics observed in the study streams.

The paired data approach made use of an additional two data sets that were not included in the rating curve approach: samples collected at East Dallas Creek at individual stream locations with particularly fine and coarse beds (i.e., not across the entire stream bed). One bedload trap was deployed at the coarse and the fine bed, and HS samples were collected at two verticals (for 2 min each) in front of the traps after they had been removed (see Bunte and Swingle (2008) for study details). Because bedload was measured locally, while discharge was measured over the cross-section, these data were not suitable for the rating curve approach.

3.2.2.1 Identification of measured data pairs

From all bedload data collected at a specified site, those collected with the HS sampler and bedload traps either concurrently or immediately following each other were identified. When a bedload trap sample was collected both just before and just after the HS sample, these two samples were averaged before being paired with the HS sample. At Little Granite Creek 2002, the number of data sets could be extended by using not only 1-hour samples, but also 10-min bedload trap samples when a HS sample was collected in close temporal proximity. The number of paired data sets when total gravel transport were > 0 for both samplers ranged from 15 to 74 with a mean of 37 for all the study sites. The number of data pairs decreases with increasing particle size such that for the coarsest 1 – 3 particle-size classes mobile in a specified stream there are only five or fewer data pairs.

Data pairs are plotted against each other with bedload trap transport rates ($q_{B\,traps}$) on the *y*-axis and HS-measured transport rates ($q_{B\,HS}$) on the *x*-axis. Values of zero-transport rates for any of the samplers are assigned a transport rate of 1E-6 g/m·s and plotted along the axes (Figure 6 a and b). For a specific size fraction, transport ratios between the two samplers scatter over 1 – 2 orders of magnitude. The scatter decreases towards large transport rates.

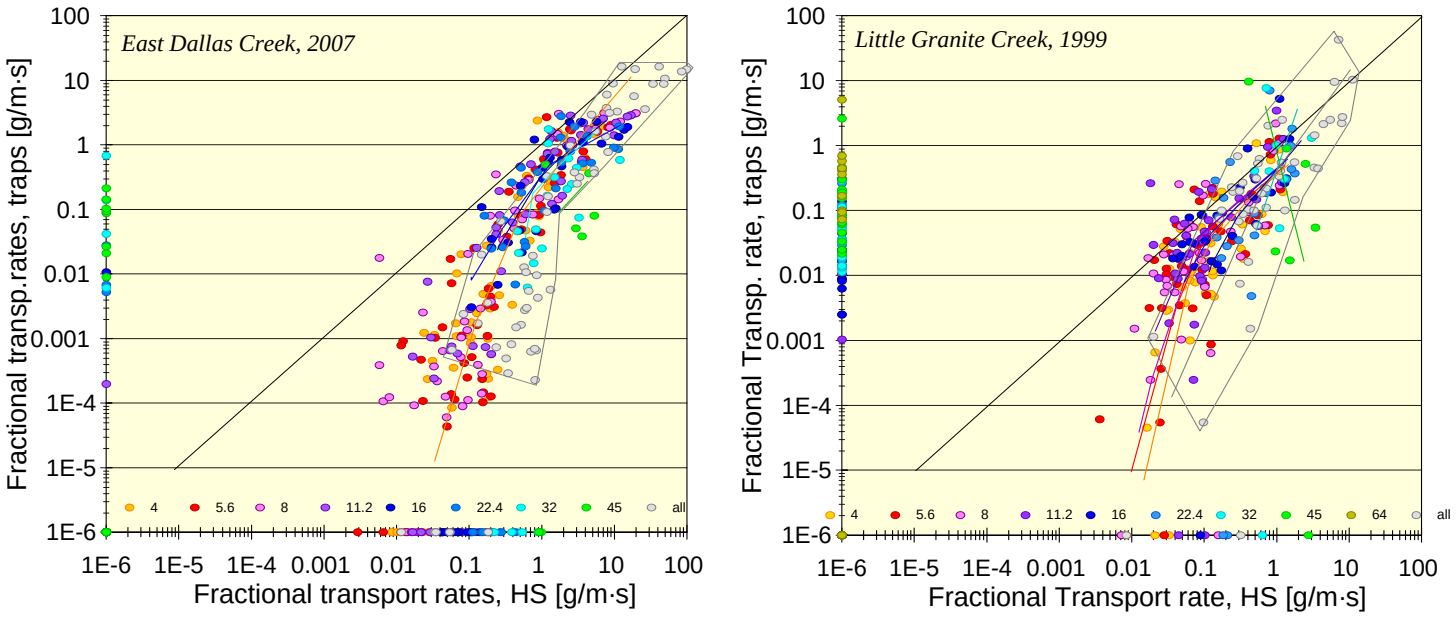

Fig. 6, continued on next page

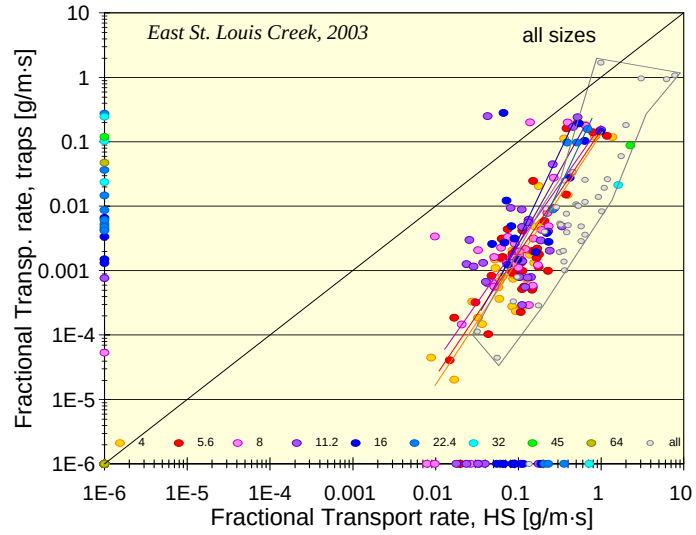

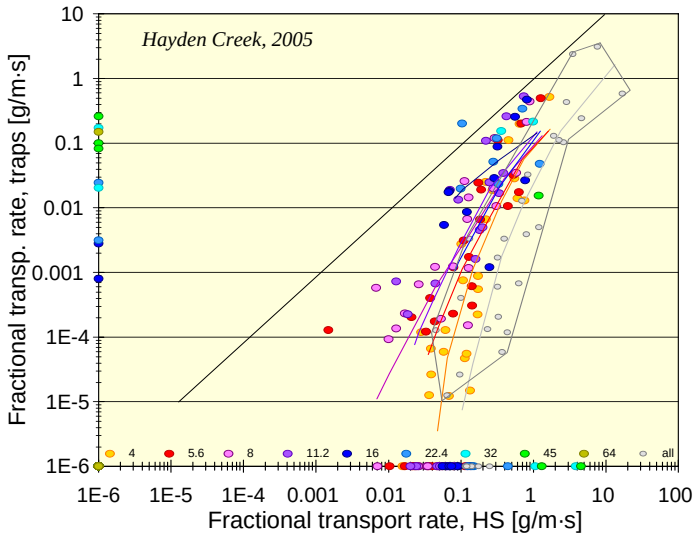

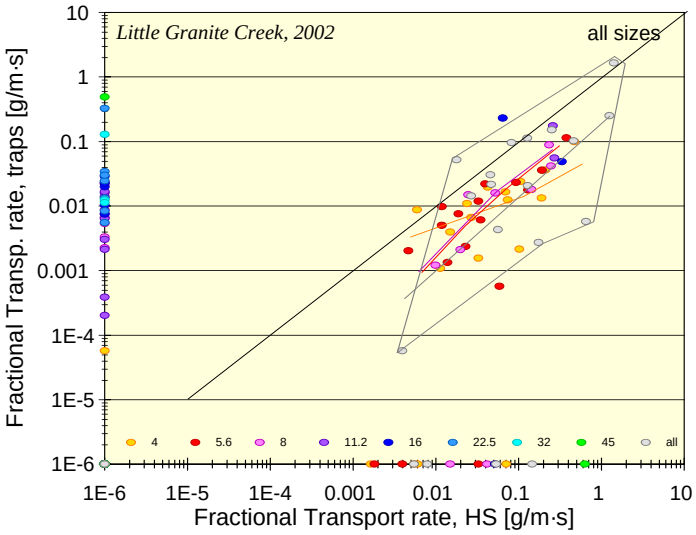

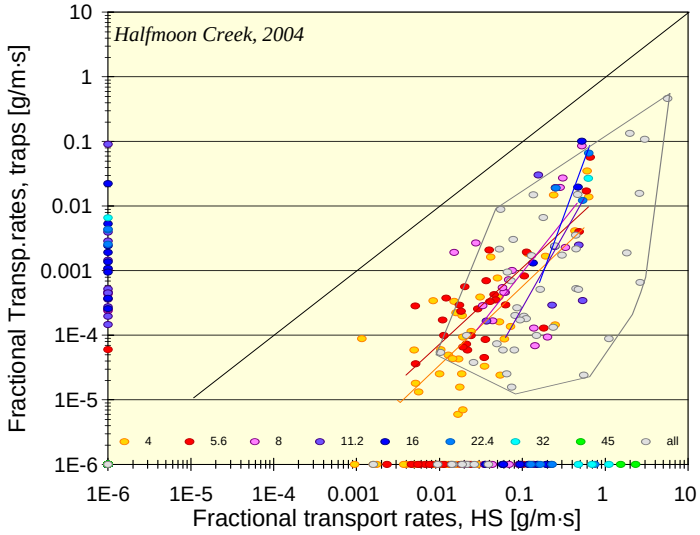

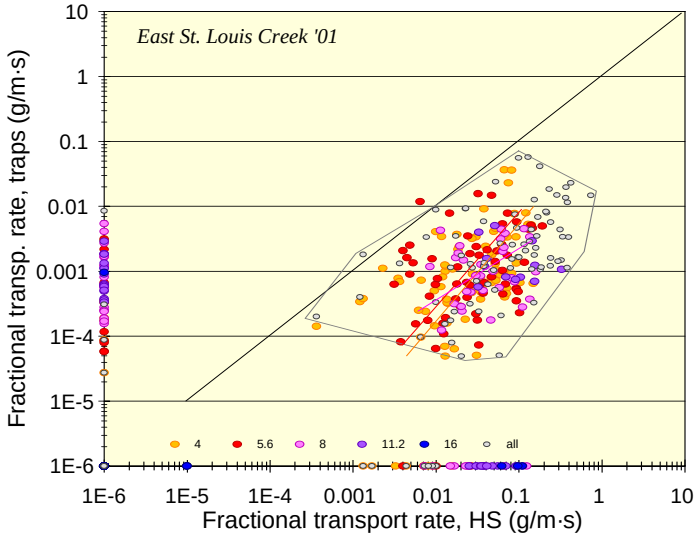

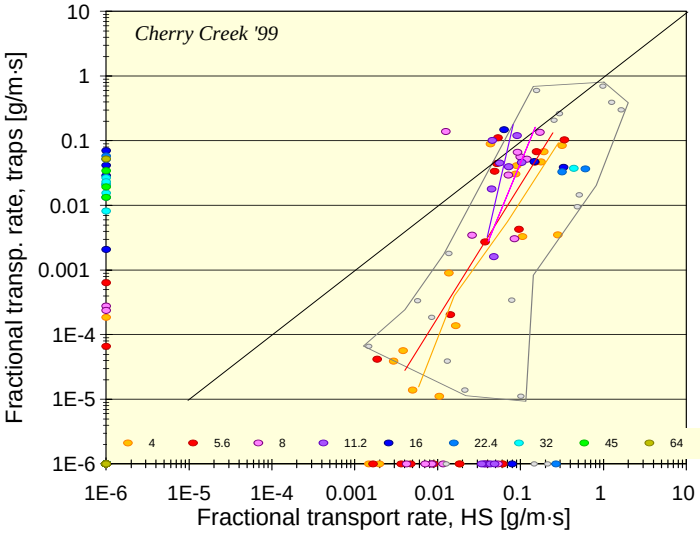

Fig. 6, continued on next page

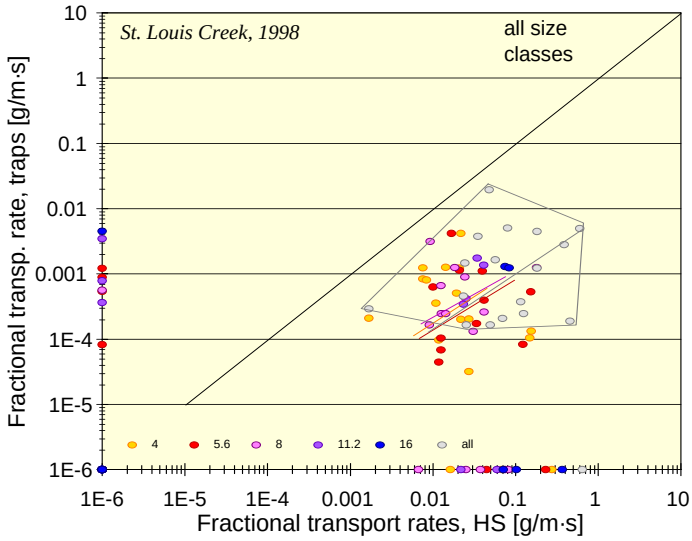

Figure 6a: Paired data approach: measured pairs of total and fractional transport rates collected concurrently with bedload traps and the HS sampler at the nine study sites. Inter-sampler transport relationships shown here are sketched only.

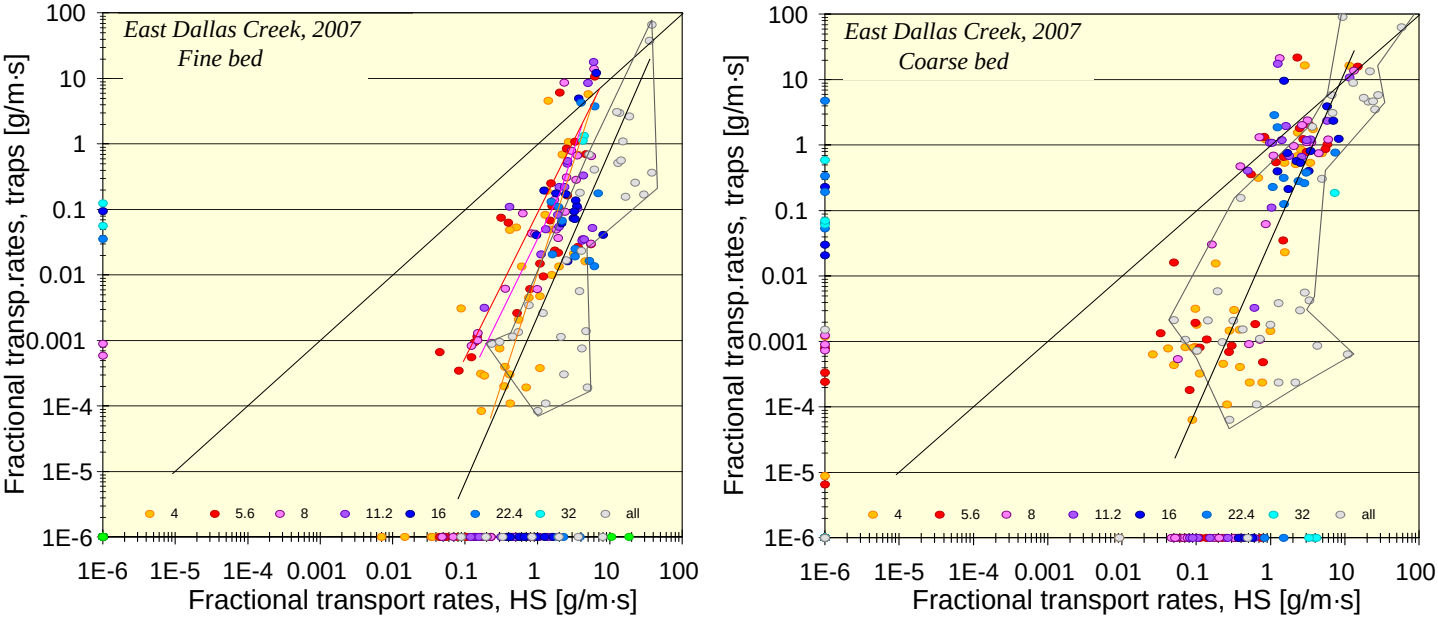

Figure 6b: Paired data approach: measured pairs of total and fractional transport rates collected concurrently with bedload traps and the HS sampler at the two additional stream locations with fine and coarse beds at East Dallas Creek. Inter-sampler transport relationships shown here are sketched only.

3.2.2.2 Identification of patterns in plotted data trends

Stream sites that yielded a large number of data pairs over a large range of transport rates with both samplers show a recurring pattern in the plotted data. Generally, data points for small gravel sizes (4, 5.6, and 8 mm) follow a convex-upward trend. At the lower end, data scatter widely[3], but the data field narrows as the inter-sampler transport ratios approach the 1:1 line or a line parallel to it, creating a data field that has the outline of a downward-facing cornucopia as presented in Figure 7.

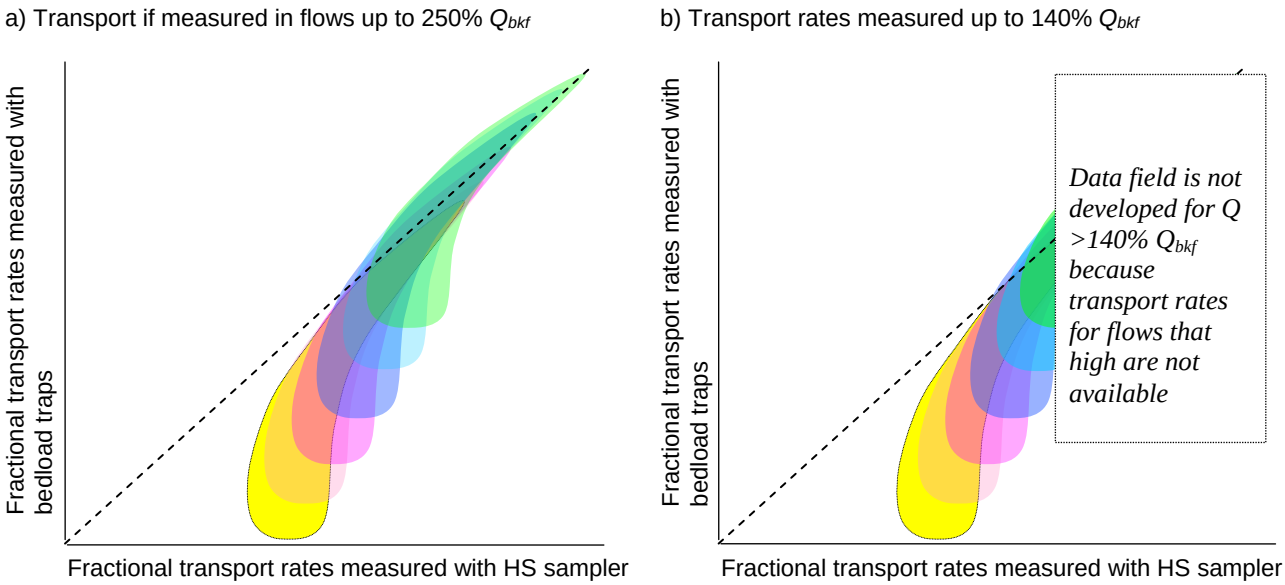

Figure 7: Data fields for inter-sampler fractional transport relationships take the shape of a downward-facing cornucopia. Particle-size classes increase with color spectrum from yellow (small gravel) via red and blue to green (coarse gravel). The trends would likely continue if transport rates were measured up to very high flows (left). Data fields are cropped at the upper portion when sampling is restricted to highflows up to 140% Q_{bkf} (right).

The pattern repeats, shifting upward and towards the right for increasing bedload particle sizes. The trend likely continues up to the 45-64 mm size class, the largest size to fit into the HS opening, if flows reach approximately 250% of bankfull and facilitate collection of 45-64 mm particles over a wide range of transport rates. Flows in the study streams did not exceed 140% of bankfull, thus 45-64 mm particles were just beginning to be collected in both samplers. Consequently, data pairs for the largest particle sizes in motion are scarce, and the upper-right part of the otherwise cornucopia-shaped data field remains undeveloped. A regression function fitted to the "cropped" data field suggests either an overly steep trend for the largest particle size in motion for a given stream, or one that is overly flat.

[3] The plotted data pairs are particularly scattered at Halfmoon Creek where the transport relationships measured with both samplers are already scattered. This is attributed to the multi-peaked hydrograph of the 2004 highflow season that peaked at about 76% of bankfull flow. In a coarse gravel-bed stream where pea gravel is supplied from low lying gravel bars and other instream deposits, this kind of flow patterns leads to hysteresis effects and large differences in transport rates for a specified flow, particularly at low and moderate flows (Thompson 2008).

The problem of undeveloped data fields was not limited to large gravel, but also occurred for smaller gravel when sampled flows did not exceed 80% Q_{bkf}. When only the lower portion of the potential data field exists, the full trend of the data from low to high flows is not developed. A fitted regression is then limited to the low-flow data that plot within a rounded or elongated field. The result is a fitted regression function that is too flat.

3.2.2.3 Fitting regression functions

To determine inter-sampler transport relationships, power functions and polynomial functions were fitted to data pairs from each size fraction as well as to total transport rates. All zero values (i.e., when transport rates for either the HS or the bedload trap or both were zero) were excluded from the data before fitting regressions. The remaining data were log-transformed.

a) **Power function regressions**

When the data field appeared to follow a straight-line shape, power function regressions were fitted to transport rates for each size class (i.e., linear functions fitted to log-transformed data).

$$q_{B\,traps,i} = a_i \cdot q_{B\,HS,i}^{\,bi} \tag{11a}$$

The regression functions are typically statistically significant (p-values << 0.05) for the smaller gravel sizes. Because the analysis is limited to non-zero transport rates for both samplers, the number of data pairs becomes small for the largest size classes in motion at a specific stream. As a result, p-values exceed 0.05, and this limits the possibility to formulate inter-sampler transport relationships for these particle sizes.

In order to formulate an inter-sampler transport relationship with which to adjust measured HS transport rates (F_{HSi}), the fitted power function (Eq. 11) needs to be multiplied by a bias correction factor CF

$$F_{HS,i} = q_{B\,traps,i} = a_i \cdot q_{B\,HS,i}^{\,bi} \cdot CF \tag{11b}$$

The Duan (1983) smearing function (CF_{Duan}) (Eq. 7) is used for the paired data sets because the standard errors s_y of the fitted power functions typically range between 0.6 and 0.8 which makes the Ferguson (1986, 1987) correction factor unsuitable.

b) **Polynomial functions**

In study streams where transport rates were measured with both samplers over a wide range of flows (up to 140% Q_{bkf}), plotted log-transformed data pairs take the shape of a downward-facing cornucopia (Figure 6 and Figure 7). Power functions poorly represent that data, and residuals obtained from a power function fit are not homoscedastically distributed. To better represent the curved, convex upward trend of the plotted data, second order polynomial functions in the form

$$y = ax^2 + bx + c \tag{12}$$

were fitted to the log-transformed data of transport rates from bedload traps (y) and the HS sampler (x). However, obtaining a visually satisfying fit was not straightforward.

In some cases, the data scatter for low values of *x* and *y* caused best-fit polynomial functions to have a concave upward instead of a convex upward trendline (Figure 8A). In another case, a wide *y*-range caused a maximum in the trend near the upper end of the *x*-data range (Figure 8B). Neither of the two features represents the trend of the plotted data. To yield a visually more satisfactory fit to the plotted data, auxiliary data points were generated, one at the lower and one at the upper end of the *x*-range, and in some cases one in the center of the *x*-range. Each auxiliary point was entered approximately10 times to the pool of data to which the polynomial function is fitted. Together with setting a visually determined best-fit *y*-intercept, these measures of guiding the polynomial function improved the visual fit to the plotted data (Figure 8C).

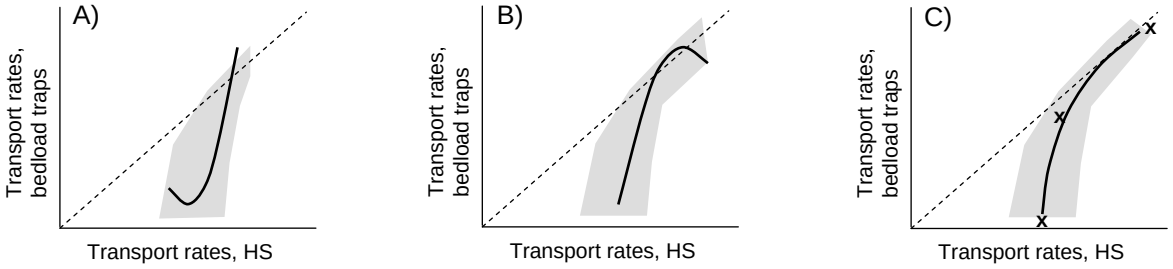

Figure 8: Shapes of second-order polynomial functions obtained by curve-fitting program. The gray-shaded area indicates the plotted field of data. **x** indicates auxiliary data points used to guide the fit.

Guiding the polynomial function did not achieve as much of an asymptotic approach of the fitted function to the 1:1 line (or a parallel to it) as desired. Thus, the fitted polynomial functions should not be extrapolated beyond the range of measured *x*-values (i.e., measured HS transport rates).

Polynomial functions fitted to log-transformed data cannot be easily back-transformed to linear units. Instead, the fitted function is used to predict log *y* for specified log *x*. The values of log *x* and the predicted values for log *y* values are then backtransformed (exponentiated). These predictions also require a bias correction similar to the bias correction required for *y*-values predicted from power functions fitted to log-transformed data in Section 3.2.2.3.a. However, computing the Duan smearing estimate from residuals of the fitted polynomial function was considered invalid because several data points had been added to guide the fit. Also, the correction factor to be applied to the guided polynomial function should be smaller than the one obtained from the power function because the guided polynomial functions had a visually better fit than the fitted power functions. Based on these considerations, Duan's smearing functions computed for the fitted power functions was used as bias correction for the polynomial functions but the computed value was reduced by 20% (= 0.8 CF_{Duan}). The inter-sampler transport relationships for polynomial functions were thus computed from

$$q_{bi\ traps} = (10\ \hat{}(a \log(q_{bi\ HS})^2 + b \log(q_{bi\ HS}) + c)) \cdot 0.8\ CF_{Duan} \quad (13)$$

Fitting polynomial functions was a workable solution. Nevertheless, a curve type that asymptotically approaches the 1:1 line or one of its parallels while facilitating a steep increase for small transport rates would have better represented the plotted data. Several alternatives may be explored in a mathematically more advanced data analysis. Those include hyperbolic functions, a LOWESS fit, and a breakpoint analysis[4].

3.2.2.4 Analyzing inter-sampler transport relationships

Similar to the rating curve approach, inter-sampler transport relationships for fractional and total transport rates were plotted in two different ways: 1) for individual study sites to analyze the difference among size classes and 2) over all sites to analyze the difference among study streams. To assess systematic differences following stream or transport characteristics, exponents and coefficients of the inter-sampler transport relationships were compared to parameters describing channel morphology as well as to exponents and coefficients of the bedload trap and HS rating curves.

4. Results

Results of the data analysis are shown and discussed separately for the rating curve as well as the paired data approach. For each approach, variability of inter-sampler transport relationships is analyzed among size fractions, and particularly among study streams. Different methods are applied to predict a HS adjustment function that best fit a specified study stream.

4.1 Rating curve approach

Fractional inter-sampler transport relationships computed are shown for all study streams (Figure 9). Parameters of the best-fit power functions for fractional the inter-sampler transport relationships are listed in Table 2. Data from St. Louis Creek ’98 are not included in the curve-fitting analysis because sample size and the range of measured flows are too small to show meaningful trends in fractional inter-sampler transport relationships. Fractional inter-sampler transport relationships for the other study streams generally have positive slopes. They intersect the line of perfect agreement (=1:1 line) at high transport rates and fall (mostly) far below the 1:1 line at low transport rates. These results show that the HS sampler collects transport rates several orders of magnitude higher than bedload traps when transport is low and that both samplers collect similar rates when transport is high. The plots in Figure 9 show that the pattern also holds for individual size fractions.

---

[4] A hyperbolic function can better represent data that asymptotically approach some axes than a parabolic function. However, fitting hyperbolic functions in which the axis of symmetry is not parallel to the *x*- or *y*-axes was mathematically too involved to be performed in this study.

Curved log-log relationships between paired transport data from the two samplers might be presented by a LOWESS fit, an iterative procedure called *locally weighted scatter-plot smoothing*. A LOWESS fit is computationally intensive and not suitable for a spreadsheet analysis. Besides, while providing the possibility for a visually pleasing trendline, the LOWESS fit does not yield a simple function to describe the data.

The ratio of transport rates measured with the two samplers might be describable with a breakpoint approach that finds the two least-square linear equations that can be fitted to a curved data set (in this case log-transformed transport data).

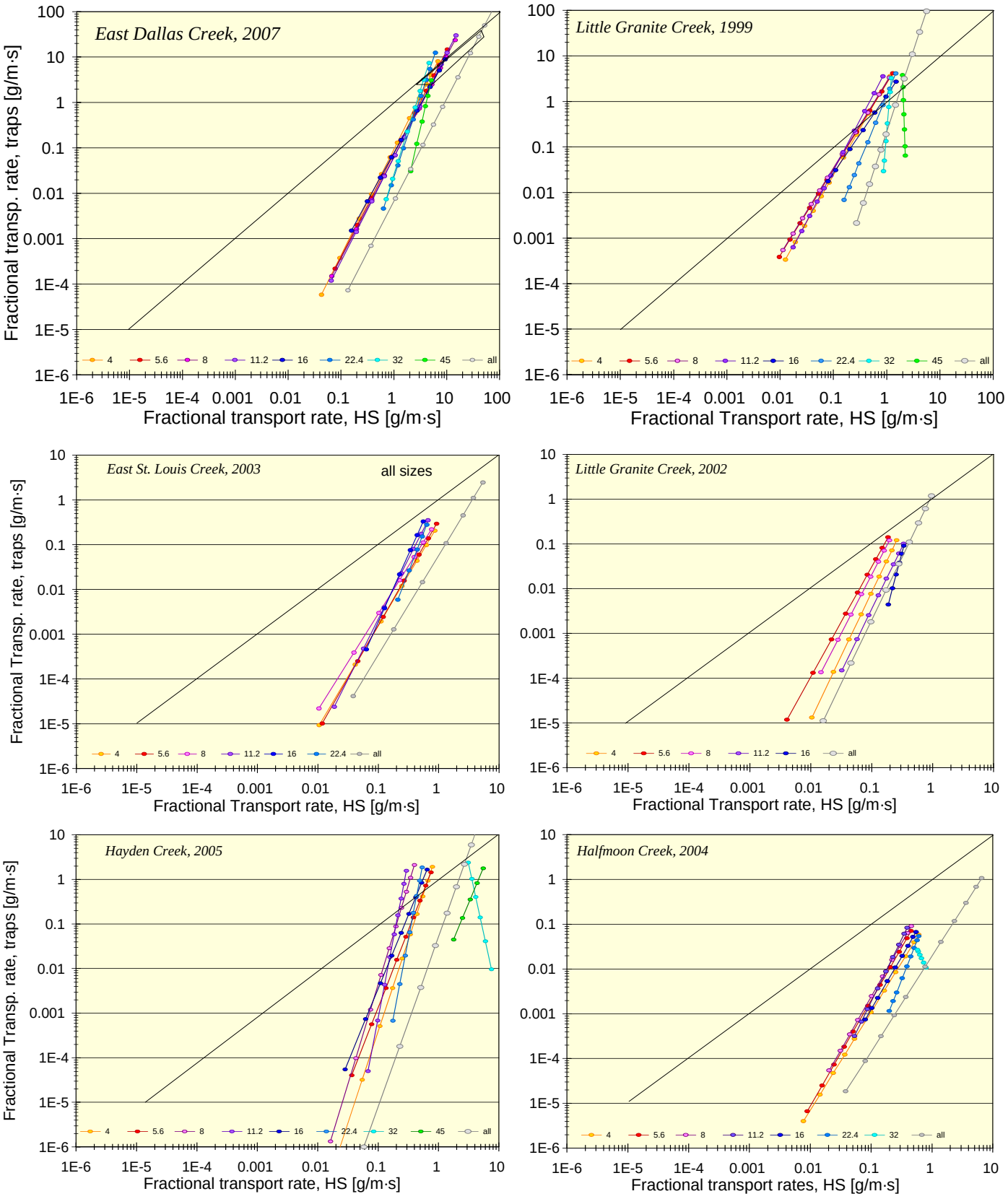

Fig. 9, continued on next page

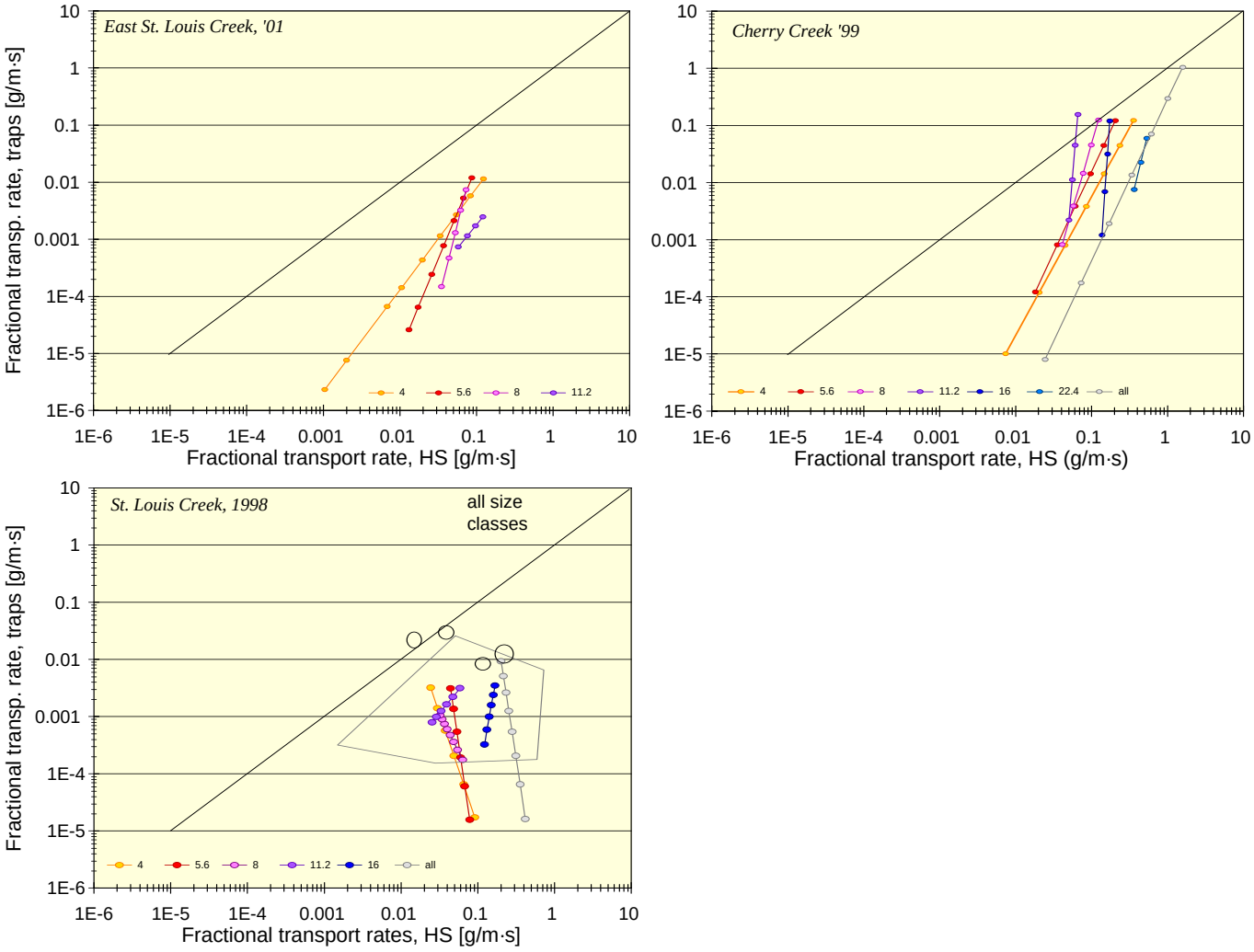

Figure 9: Rating curve approach: fitted inter-sampler transport relationships for individual gravel sizes classes as well as total gravel transport rates at all study streams.

Table 2: Parameters of best-fit power functions describing inter-sampler transport relationships for individual 0.5 phi particle-size fractions.

	4 - 5.6 mm		5.6 – 8 mm		8 - 11.2 mm		11.2 - 16 mm	
Study stream	*a*	*b*	*a*	*b*	*a*	*b*	*a*	*B*
East Dallas Creek	0.0911	2.33	0.0730	2.27	0.0616	2.23	0.0608	2.29
Halfmoon Creek	0.170	2.19	0.449	2.36	0.580	2.39	1.12	2.79
East St. Louis Cr. '03	0.283	2.27	0.351	2.35	0.390	2.14	1.04	2.69
East St. Louis Cr. '01	0.471	1.78	32.3	3.24	8911	5.36	-	-
Cherry Creek	1.48	2.42	10.8	2.84	1611	4.54	5.2E+17	15.7
Little Granite Cr. '99	2.68	2.05	2.49	1.89	2.66	1.89	5.05	2.22
Hayden Creek	4.82	4.11	3.88	3.48	124	4.46	8945	7.08
Little Granite Cr. '02	5.67	2.84	8.58	2.45	8.61	2.62	2.15	2.79

Table 2, continued on next page

Table 2, cont'd.

	16 – 22.4 mm		22.4 - 32 mm		32 – 45 mm		45 - 64 mm	
Study stream	*a*	*b*	*a*	*b*	*a*	*b*	*a*	*b*
East Dallas Creek	0.0760	2.12	0.0224	3.49	0.0249	3.71	7.26E-04	5.10
Halfmoon Creek	0.273	2.34	0.295	3.45	0.00573	-2.87	-	-
East St. Louis Cr. '03	1.94	3.03	1.35	3.50	-	-	-	-
East St. Louis Cr. '01	-	-	-	-	-	-	-	-
Cherry Creek	7.2E+13	19.5	1.61	5.30	-	-	-	-
Little Granite Cr. '99	1.35	1.71	1.31	2.85	0.194	13.9	-	-
Hayden Creek	6.89	3.30	151	7.09	-	-	-	-
Little Granite Cr. '02	24.6	5.16	-	-	-	-	-	-

$r^2 = 1$, and a bias correction factor *CF* is unnecessary (see also Sect. 3.2.1.4). Numbers printed in gray indicate that the fitted regression functions have *p*-values > 0.05, either for samples from bedload traps or, more likely, from the HS sampler (see Table 10, Appendix). Shading in red and blue marks streams classified as the "red" or "blue" groups (see explanation in Section 4.1.3.1).

4.1.1 Variability among bedload particle-size classes

Parallel trends for small gravel

Fractional inter-sampler transport relationships plot approximately parallel, at least for the smaller gravel sizes that are transportable and measurable in both samplers (Figure 9). In four of the study streams (East Dallas Creek, East St. Louis Creek '03, Little Granite Creek '99, and Halfmoon Creek), fractional inter-sampler transport relationships are nearly aligned. This indicates that sampling differences between traps and the HS sampler are similar, at least for the smaller gravel size classes (Figure 9). In the other four streams, transport relationships are "stacked" above each other, separated by a factor of 2-4 for increasingly coarser size classes (Hayden Creek, Little Granite Creek 02, and Cherry Creek). In these streams, the HS sampler collects more fine gravel than bedload traps.

Deviation from parallel trend for coarse gravel: sampling artifact

Inter-sampler transport relationships for the coarsest gravel size-classes that are mobile in a specified stream (typically size classes larger than 16, 22.4, or 32 mm depending on the highflow magnitude) deviate from the parallel trend and become steeper for increasingly larger particles. The slope may become negative. This pattern is most likely a computational artifact occurring when both samplers collected transport rates over a small range. If samples could have been collected in flows up to 250% of bankfull (which in high-elevation Rocky Mountain gravel-bed streams represents approximately the 50-year flood), transport relationships for the largest gravel particles would likely have been flatter and possibly attained slopes similar to or just slightly steeper than those for smaller gravel sizes (see also discussion in Section 3.2.2.2), however only up to the gravel size that fits into the HS opening.

4.1.2 Variability among streams

Inter-sampler transport relationships plotted for individual gravel size classes (Figure 10) as well as total gravel transport rates are combined for all study streams (Figure 11) and show the variability among streams. Analyses of variability among streams were limited to total gravel

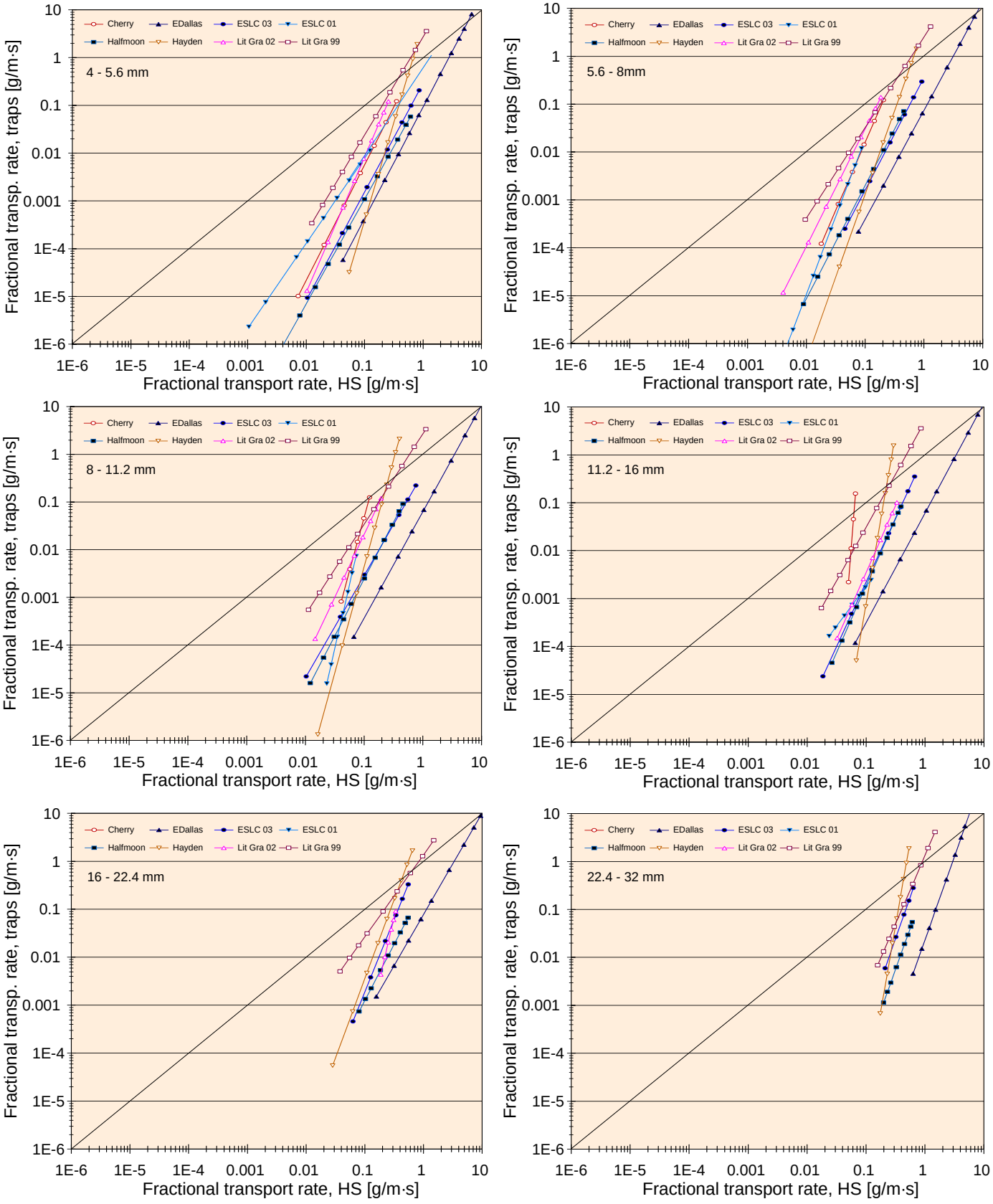

Fig. 10, continued on next page

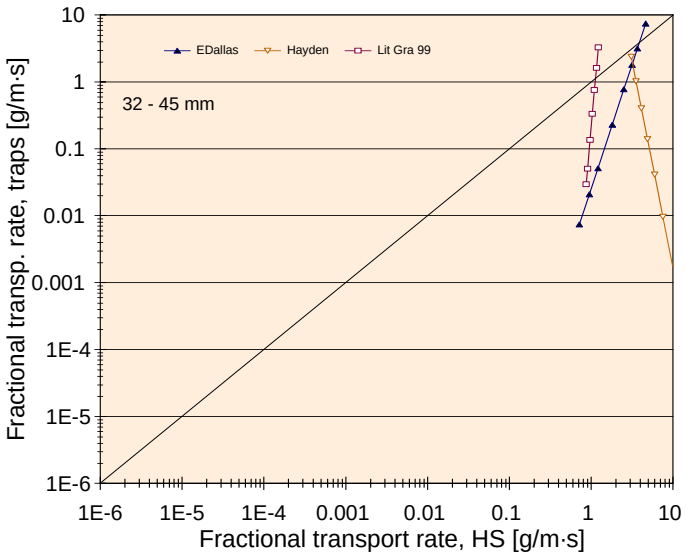

Figure 10: Rating curve approach: fitted inter-sampler transport relationships for individual gravel fractions combined for all study streams. Streams falling into the "red" group are indicated by reddish line colors and open symbols, streams in the "blue" group by bluish line colors and closed symbols (see Section 4.1.3.1 for explanations).

transport rates. The similarity of pattern observed for total transport rates with those for the smallest gravel size classes suggests that analyses could be extended to inter-sampler transport relationships of individual size classes, at least for smaller, well-sampled, gravels.

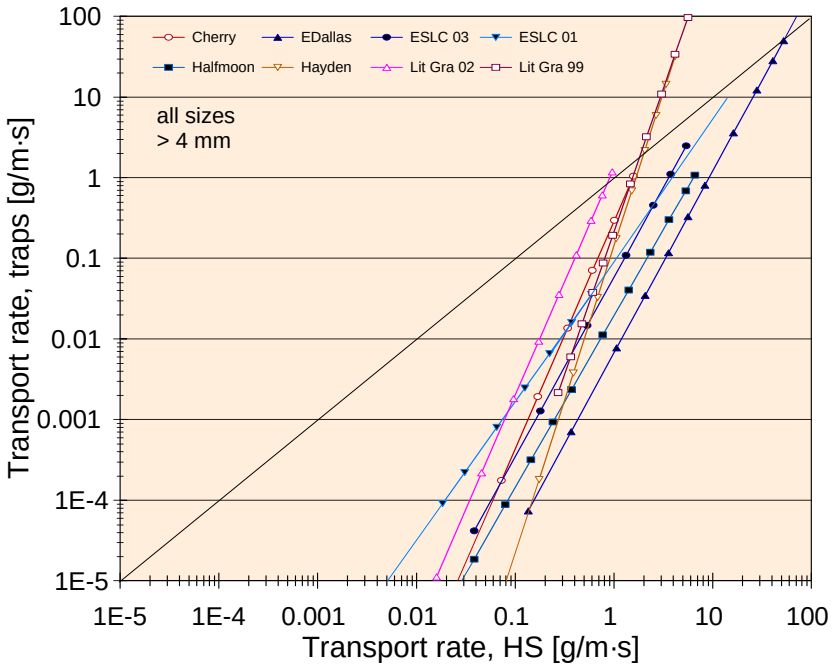

Figure 11: Inter-sampler transport relationships for total gravel transport obtained from rating curve approach plotted for all study streams. Streams within the "red" group have reddish line colors and open symbols, streams in the "blue" group have bluish line colors and closed symbols.

Trendlines for all the inter-sampler relationships of total gravel transport measured at low flows appear to originate within the range of 1E-5 to 1E-4 g/m·s for bedload traps and 0.01 – 0.1 g/m·s for the HS sampler (Figure 11). From this common starting point, inter-sampler transport relationships disperse for individual streams, assuming different steepness (*b*-exponents), different *a*-coefficients, and different intersections with the 1:1 line (Table 3). Several variables describing channel and bedmaterial characteristics as well as bedload transport were tried to predict the steepness, coefficients, and intersections with the 1:1 line of the inter-sampler transport relationships.

Table 3: Parameters of best-fit power functions as well as intersection with 1:1 line of inter-sampler transport relationships for total gravel transport rates and of inter-sampler bedload D_{max} relationships.

	Total gravel transport			Bedload D_{max} size			
Study stream	*a*	*b*	*1:1 line*	*a*	*b*	*1:1 line*	
East Dallas Creek	0.00659	2.26	54.5	1.97	0.0364	29.9	
Halfmoon Creek	0.0191	2.13	33.1	1.37	0.280	32.1	blue group
East St. Louis Cr. '03	0.0573	2.22	10.4	1.85	0.160	14.1	
East St. Louis Cr. '01	0.0870	1.72	29.7	1.18	0.739	5.52	
Cherry Creek	0.285	2.82	1.99	3.22	0.00417	11.9	
Little Granite Cr. '99	0.210	3.55	1.85	2.17	0.0489	13.2	red group
Hayden Creek	0.0498	3.81	2.91	2.27	0.0182	23.6	
Little Granite Cr. '02	1.30	2.82	0.87	8.65E-5	5.15	4.53	

$r^2 = 1$, and a bias correction factor *CF* is unnecessary (see also Sect. 3.2.1.4). All bedload rating curves from which inter-sampler transport relationships were derived have *p*-values >> 0.05 (see Table 10, Appendix). Shading in red and blue marks streams classified as the "red" or "blue" group (see explanation in the text below).

4.1.2.1 Channel and bedmaterial characteristics

The channel and bedmaterial characteristics such as bankfull flow, basin area, bankfull stream width, stream gradient, surface D_{50} and D_{84} sizes, the percent surface and subsurface sediment < 2 and < 8 mm, as well as the subsurface D_{50} and D_{84} sizes did not show a statistically significant correlation with the exponents or coefficients of power functions describing inter-sampler relationships for total gravel transport rates. However, the steepness of these fitted power functions was found to decrease for streams that are well armored[5] (Eq. 15). The correlation is statistically significant ($p < 0.05$) and suggests that exponents of the inter-sampler transport relationship (*b*) may be predictable from the extent of bed armoring (D_{50surf}/D_{50sub}).

[5] Armoring is the ratio D_{50surf}/D_{50sub}. In the study streams, a high degree of armoring was typically caused by high percentages of subsurface fines < 8 mm. Thus, armoring and the % subsurface fines < 8 mm are positively related. Size distributions of surface and subsurface sediment are affected by the methods used to sample bedmaterial, sample size, and methods of particle-size measurements (Bunte and Abt 2001; Bunte et al. 2009b). In this study, a sampling frame was used for pebble counts, and more than 400 particles were collected over the bankfull width of a reach; particle sizes were measured using a template; several large subsurface samples were collected per site using a plywood shield to shelter a 2 by 2 ft (0.36 m^2) area from flow.

$$b = 5.73\ (D_{50surf}/D_{50sub})^{-1.21} \quad (14)$$

with $r^2 = 0.69$, $n = 8$, $p = 0.0112$, $s_y = 0.071$

4.1.2.2 Effects of gravel transport characteristics

Conditions of gravel transport in a specified stream can be described by the steepness and coefficients of the gravel bedload rating and the flow competence curves measured with bedload traps. The study found that inter-sampler transport relationships are affected by a stream's transport and flow competence curves. Inter-sampler transport relationships intersect the 1:1 line at lower values in streams with steep bedload trap flow competence curves ($r^2 = 0.53$, $p = 0.041$), while inter-sampler transport relationships decrease in steepness with increasing rating curve coefficients in a marginal way ($r^2 = 0.39$, $p = 0.0971$) (Table 11, Appendix). Streams with steeper rating and flow competence curves tend to have relatively large differences between bedload trap and HS measurements, while in streams with less steep rating and flow competence curves both samplers measure more similar results.

4.1.2.3 Effects of HS sampling results

It would be beneficial if HS correction functions could be predicted directly from HS sampling results, without bedload trap measurements. However, none of the HS rating or flow competence curve parameters showed a relationship with *b*-exponents and *a*-coefficients of inter-sampler transport relationships, nor with intersections at the 1:1 line (Table 13, Appendix).

4.1.3 Segregation of inter-sampler transport relationships into groups

Section 4.1.2.3 indicated that steeper inter-sampler transport relationships and lower intersections with the 1:1 line occur in poorly armored streams. These streams also have steep bedload transport rating and flow competence curves (Bunte et al. 2006) (Figure A5, left). However, the relationships were not sufficiently defined to predict inter-sampler transport relationships for individual streams. The one exception was the parameter armoring that has a moderately well defined correlation ($r^2 = 0.69$, $p = 0.0112$, Eq. 15**Error! Reference source not found.**) but is laborious to measure in coarse-bedded streams. In order to simplify the prediction of inter-sampler transport relationships that are best suited for a specified stream, predictions were attempted for stream groups that share common characteristics, rather than for individual streams.

4.1.3.1 Visual segregation into two groups

Based on the steepness and the point of intersection with the 1:1 line, inter-sampler relationships for total gravel transport can be visually segregated into two groups: one group with relatively steep inter-sampler transport relationships (plotted in reddish colors and with a reddish shading in Figure 12: Cherry Creek, Hayden Creek Little Granite Creek '99, and Little Granite Creek '02) and one with flatter relationships (plotted in bluish colors and a bluish shading: East Dallas Creek, East St. Louis Creek '01, East St. Louis Creek '03, and Halfmoon Creek). Inter-sampler transport relationships of the steep (red) group have exponents of 2.8 – 3.8 and intersect the 1:1 line around 1 - 3 g/m·s, i.e., the two samplers obtain similar sampling results during moderate

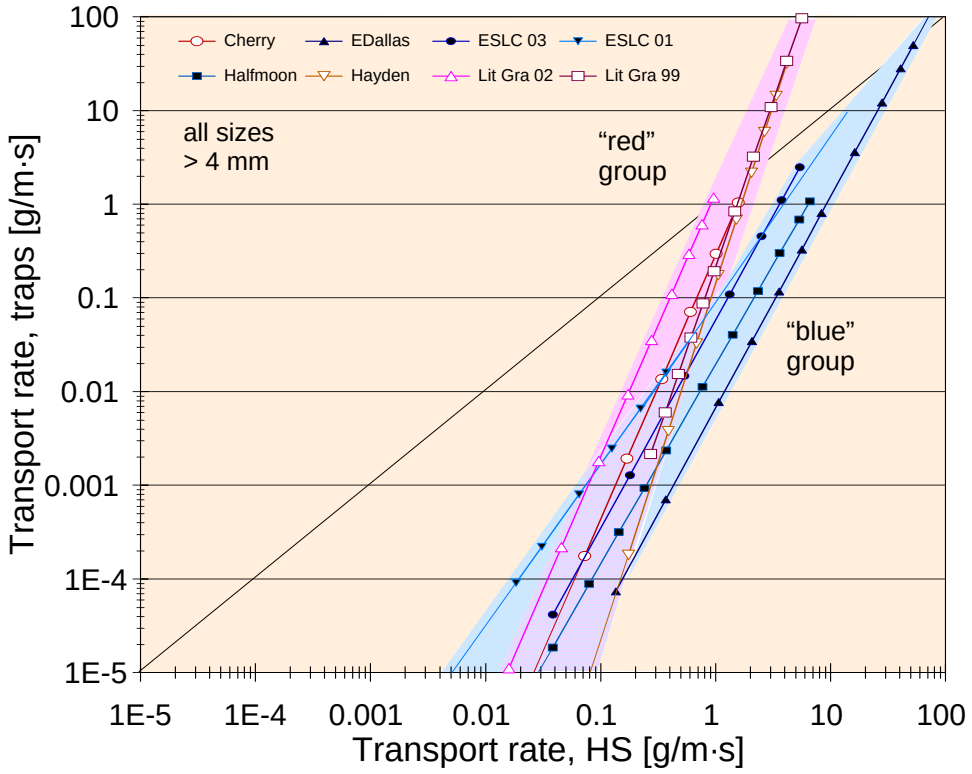

Figure 12: Inter-sampler transport relationships for total gravel transport obtained from rating curve approach plotted for all study streams. Streams falling into the "red" group are indicated by reddish line colors, open symbols, and red shading, streams in the "blue" group by bluish line colors, closed symbols, and blue shading.

transport (Table 3). Within the flat (blue) group, exponents range from 1.7 – 2.3 and intersections of the 1:1 line from 10 - 55 g/m·s, i.e., both samplers provide similar results when transport is high. A *t*-test with a 0.05 confidence level showed that the mean exponents, coefficients, and intersections with the 1:1 line computed for each of the two stream groups are significantly different among the two groups, and this supports the validity of the visual segregation. For fractional inter-sampler transport relationships, segregation into two groups is visually justifiable for the three (or four) smallest gravel size classes, but deviates for larger gravel sizes, most likely because inter-sampler transport relationships are not computed accurately when particle size classes are not sampled over a sufficiently wide range of transport rates.

4.1.3.2 Average inter-sampler transport relationships for both stream groups

Fractional and total gravel transport

To attain group-averaged inter-sampler transport relationships, the arithmetic means of the four exponents and the geometric means of the four coefficients were computed of the blue and red groups (Table 4) and plotted (Figure 13 a and b). Only inter-sampler transport relationships derived from rating curves with *p*-values < 0.05 (<0.1 in a few exceptions) were included in the

computation. These group-averages were computed for both fractional and total transport rates. Exponents and coefficients in Table 4 provide adjustment functions to convert fractional and total transport rates collected with a 3-inch, thin-walled, HS sampler to those collected with bedload traps in streams falling into the blue and red groups. The group-averaged inter-sampler transport relationship for total gravel transport rates are (Table 4):

$$F_{HS} = q_{B\,traps} = 0.249 \cdot q_{B\,HS}^{\,3.25} \quad \text{(red group: less armoring, less subsurface fines, Steeper rating and flow competence curves)} \tag{15}$$

and

$$F_{HS} = q_{B\,traps} = 0.0282 \cdot q_{B\,HS}^{\,2.08} \quad \text{(blue group: more armoring, more subsurface fines, flatter rating and flow competence curves)} \tag{16}$$

Table 4: Exponents and coefficients of inter-sampler transport relationship for individual size classes, total gravel transport rate, and the bedload D_{max} size averaged over the four streams falling into the "red" and "blue" stream groups.

		> 4 mm	>5.6 mm	>8 mm	>11.2 mm	>16 Mm	>22.4 mm	total gravel transport	D_{max} mm	Avg. for any 0.5 phi size class	
Geom. mean	a-coeff.	0.213	0.781	0.241	0.414	0.343	0.207	0.0282	0.168	**0.325**	"blue" stream group
Arith. mean	b-exp.	2.14	2.56	2.25	1.94	1.87	2.61	2.08	1.59	**2.23**	
CV(%)	a-coeff.	143	145	965	174	207	434	1789	334	**68.1**	
CV(%)	b-exp.	11.6	18.0	69.1	67.6	69.8	66.7	11.9	23.9	**13.7**	
Geom. mean	a-coeff.	3.23	5.48	46.2	-	-	-	0.249	0.00423	**9.35**	"red" stream group
Arith. mean	b-exp.	2.85	2.67	3.38	-	-	-	3.25	3.20	**2.97**	
CV(%)	a-coeff.	8.24	5.43	2.69	-	-	-	233	28574	**6.55**	
CV(%)	b-exp.	31.3	25.1	39.3	-	-	-	15.5	43.2	**12.5**	

Bedload D_{max} particle sizes

Inter-sampler bedload D_{max} relationships were combined for all study streams in Figure 14 (left). The exponents, coefficients, and intersections with the 1:1 line were checked for possible relatedness to exponents and coefficients of bedload rating and flow competence curves measured with both samplers (Table 12, Appendix). No statistically significant relationships were found with bedload trap measurements. However, *b*-exponents of the inter-sampler bedload D_{max} relationships at the study streams are negatively related to the HS-measured flow competence exponent ($r^2 = 0.64$; $p = 0.0176$), while the *a*-coefficients are positively related the HS-measured flow competence exponent ($r^2 = 0.77$; $p = 0.0044$) (Table 14, Appendix). HS sampling characteristics appear to affect the inter-sampler bedload D_{max} relationships.

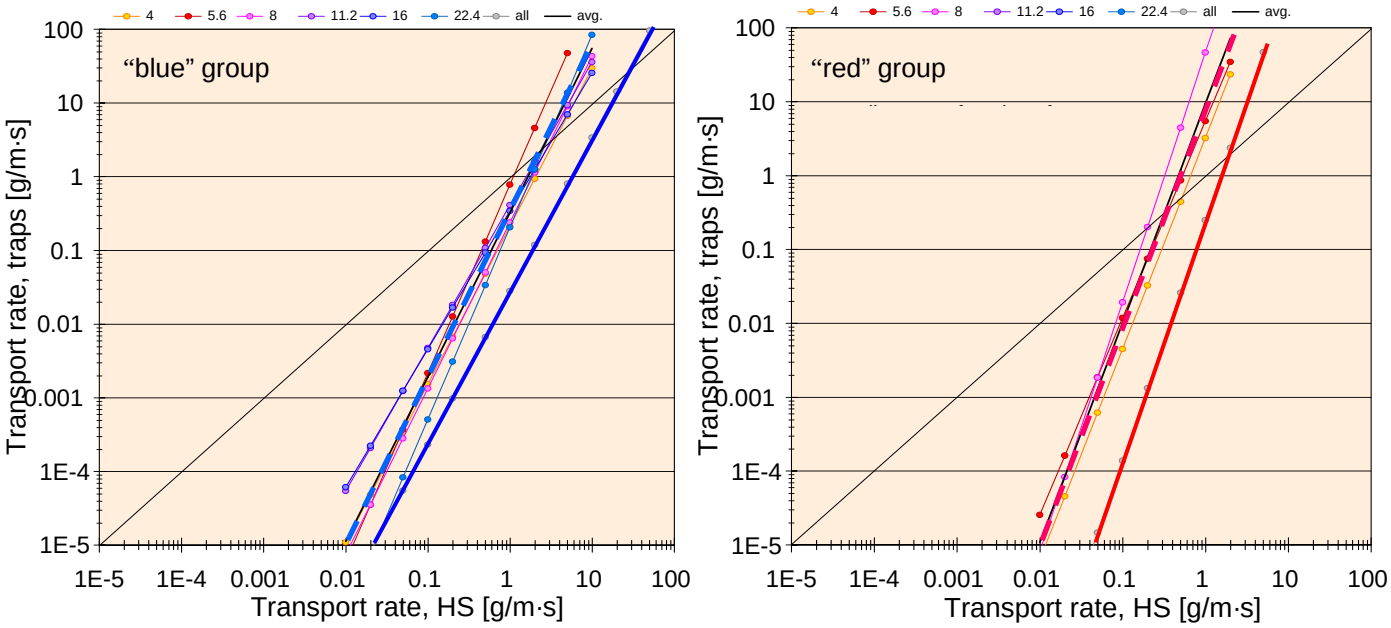

Figure 13: Fractional inter-sampler transport relationships averaged over the four "blue" (left) and "red" (right) streams. The color scheme used to mark individual size fractions follows the one used for size fractions throughout the study. The dashed thick blue and red lines indicate the average inter-sampler transport relationship applicable to any 0.5 phi gravel size fraction over the four "blue" and "red" streams. Solid thick blue and red lines show group-averaged inter-sampler transport relationships for total gravel transport.

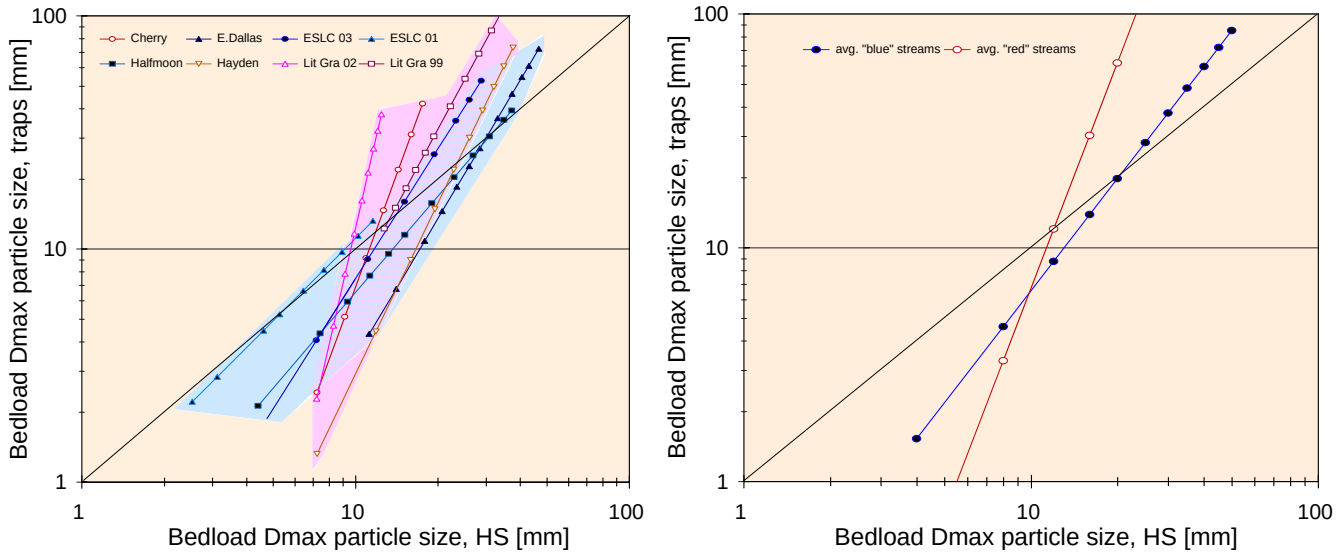

Figure 14: Inter-sampler relationships of bedload D_{max} particle sizes collected with bedload traps and the HS sampler at all study sites (left). Red and blue shading highlights streams of the "red" and "blue stream groups. Bedload D_{max} particle size relationships averaged over study streams within "red" and "blue" stream groups (right).

Segregation of inter-sampler bedload D_{max} relationships computed into two groups is less obvious than for inter-sampler transport relationships. However, a significant difference in *a*-coefficients as well as *b*-exponents between streams falling in the red and the blue groups suggests that a separation into two stream groups is appropriate (Figure 14, right). It is further supported that the streams falling into the "red" and "blue" groups are the same for inter-sampler relationships of both bedload D_{max} particle sizes and total gravel transport rates. Streams that have flatter inter-sampler relationships for bedload D_{max} particle sizes (blue group) have flatter inter-sampler transport relationships. By contrast, streams in the red group have steeper inter-sampler relationships for bedload D_{max} particle sizes and show steeper transport relationships (Table 4) (compare Figure 14 (left) with Figure 11).

Exponents of the inter-sampler relationships for bedload D_{max} sizes were averaged arithmetically over the two stream groups; coefficients were averaged geometrically. The averaged exponents and coefficients in Table 4 provide adjustment functions for the "red" and "blue" stream groups to convert D_{max} particle sizes collected with a 3-inch, thin-walled, HS sampler to those that might have been collected with bedload traps.

$$F_{HS} = D_{max,traps} = 0.00423 \cdot D_{max,HS}^{3.20} \qquad \text{(red group)} \qquad (17)$$

and

$$F_{HS} = D_{max,traps} = 0.168 \cdot D_{max,HS}^{1.59} \qquad \text{(blue group)} \qquad (18)$$

4.1.3.3 Averaging over all size classes within the two stream groups

Inter-sampler fractional transport relationships averaged over the two stream groups fell within a narrow band for all individual size classes (Figure 13), suggesting that within the two groups inter-sampler transport relationships are relatively similar for all 0.5 phi size fractions. The relative similarity suggests that exponents and coefficients of inter-sampler transport relationships may be averaged over all size fractions to attain an inter-sampler transport relationship applicable to any 0.5 size fraction, i.e., one relationship for the steep (red) stream group and one for the flat (blue) stream group (see Figure 13 and the last column in Table 4). The resulting correction functions for any 0.5 phi size class are:

$$F_{HS} = q_{B\,trap,f} = 9.35 \cdot q_{B\,HS,f}^{2.97} \qquad \text{(red group: less armoring, less subsurface fines, Steeper rating and flow competence curves)} \qquad (19)$$

and

$$F_{HS} = q_{B\,trap,f} = 0.325 \cdot q_{B\,HS,f}^{2.23} \qquad \text{(blue group: more armoring, more subsurface fines, flatter rating and flow competence curves)} \qquad (20)$$

These relationships may serve to convert fractional gravel transport rates of any 0.5 phi size class collected with the HS sampler to those that might have been collected with bedload traps for streams in the blue and red groups, respectively. The correction functions for a 0.5 size class (Eq. 19 and 20) differ by more than one order of magnitude from the group-averaged inter-sampler transport relationship for total gravel transport rates (Eqs. 15 and 16) (Figure 13).

4.1.3.4 Bedmaterial and bedload conditions in "red" and "blue" streams

Average values of bedmaterial parameters for the "blue" and "red" stream group were evaluated for statistical difference based on whether the 95% confidence interval around the group means overlapped. Mean values of bed armoring were statistically different between the two groups. Similarly, the arithmetic mean of exponents and the geometric mean of coefficients of bedload rating and flow competence curves measured with bedload traps are statistically different between the "red" and the "blue" stream groups. The midpoints between the means for the two stream groups were considered threshold values to indicate whether inter-sampler transport relationship of the "red" or "blue" group should be used for adjustment of HS-sampled transport rates. For HS samples, only the coefficients of the bedload rating and flow competence curves were statistically different between the red and blue stream groups.

The threshold values for bedmaterial and bedload conditions are compiled in Table 5 and may be used to categorize a study stream as either a "red" or "blue" stream. For example, for a coarse-bedded mountain stream with armoring of less than 1.96, and a HS-measured rating curve coefficient < 0.094, conversion functions obtained for the "red" stream group might be used to adjust HS sampling results. Threshold values in Table 5 are applicable in a strict sense only if the highest four values of any parameter fall into one group while the lowest ones fall into the other. Because this is rarely the case, each threshold has some variability. The user should therefore consider threshold values of several parameters before classifying a study stream.

If the characteristics of a study stream do not fall clearly into one of the stream groups, the user might compare the characteristics of the stream with those listed in Table 1. For conversion of HS sampling results, the inter-sampler transport relationships determined for a specific stream might then be used.

4.1.3.5 Using a correction function to adjust a HS rating curve

To arrive at an adjusted HS rating curve for the study streams, the exponent *b* and coefficient *a* of the respective inter-sampler transport relationships (i.e., correction function) is applied to the measured HS power function rating curve ($Q_{B\,HS} = c \cdot Q^{b}$) to yield

$$q_{B\,traps} = F_{HS} = a \cdot (c \cdot Q^{d})^{b} \tag{21}$$

The exponents and coefficient of the adjusted HS rating curve can then be computed analytically or be obtained via a curve-fitting analysis. Comparing adjusted HS rating curves with those measured using bedload traps shows that for three of the "blue" stream groups, adjusted HS rating curves deviate less than a factor of 2 from the measured bedload trap rating curve. The deviation was more than one order of magnitude for East St. Louis Creek '01, for which the

Table 5: Bedmaterial characteristics and conditions of bedload transport that determine the stream group and the respective inter-sampler relationships (rating curve approach).

	Streams in "red" group	Stream in "blue" group
<u>For bedmaterial conditions of:</u>		
Armoring ($D_{50\,surf}/D_{50\,sub}$)	< 2.0	> 2.0
<u>For bedload conditions measured with bedload trap:</u>		
Exponent of bedload rating curve	> 8.9	< 8.9
Coefficient of bedload rating curve	< 1.1E-4	> 1.1 E-4
Exponent of flow competence curve	> 1.9	< 1.9
Coefficient of flow competence curve	< 5.30	> 5.30
Bedload D_{max} (mm) at 50% Q_{bkf}	< 11	> 11
Gravel transport rate (g/m·s) at 50% Q_{bkf}	< 0.001*	> 0.001*
Bedl. D_{max} (mm) at gravel transp. rate of 1 g/m·s	> 40	< 40
<u>For bedload conditions measured with HS sampler:</u>		
Exponent of bedload rating curve	< 3.4*	> 3.4*
Coefficient of bedload rating curve	< 0.094	> 0.094
Exponent of flow competence curve	> 0.91*	< 0.91*
Coefficient of flow competence curve	< 9.7	> 9.7
Bedload D_{max} (mm) at 50% Q_{bkf}	< 13*	> 13*
Gravel transport rate (g/m·s) at 50% Q_{bkf}	< 0.15*	> 0.15*
Bedl. D_{max} (mm) at gravel transp. rate of 1 g/m·s	< 18*	> 18*
<u>Inter-sampler transport relationships that may be used to adjust HS measurements:</u>		
For any size 0.5 phi size fraction	Eq. 19: $q_{B\,traps,f} = 9.35\ q_{B\,HS,f}^{2.97}$	Eq. 20: $q_{B\,traps,f} = 0.325\ q_{B\,HS,f}^{2.23}$
For total gravel transport rates	Eq. 15: $Q_{B\,traps} = 0.249\ Q_{B\,HS}^{3.25}$	Eq. 16: $Q_{B\,traps} = 0.0282\ Q_{B\,HS}^{2.08}$
For bedload D_{max} particle size class	Eq. 17: $D_{max\,traps} = 0.00423\ D_{max\,HS}^{3.20}$	Eq. 18: $D_{max\,traps} = 0.168\ D_{max\,HS}^{1.59}$

* Difference between red and blue stream group not statistically significant. Red and blue shading refers to "red" and "blue" stream groups.

original HS rating curve was measured over a small range of flows. These results are encouraging but also emphasize the importance of using HS measurements that extend over a wide range of flow. A user must note that inter-sampler transport relationships presented in this study were obtained in mountain-gravel bed streams. The adjustment functions suggested for conversion of HS sampling results should therefore be applied to streams with similar characteristics as the study streams.

Summary for rating curve approach

Inter-sampler transport relationships were computed for all streams and for all particle size classes as well as for total transport rates and the bedload D_{max} sizes. The variability of fractional inter-sampler transport relationships among size classes is generally less than expected, although some streams indicate that the difference between the two samplers is greatest for the smallest gravel sizes.

Inter-sampler transport relationships vary among streams. The relationships are flatter in streams that are well armored and have high amounts of subsurface fines < 8 mm; the correlation with armoring is sufficient to serve as a prediction. Bedload transport characteristics as measured with bedload traps also affect inter-sampler transport relationships; the intersection with the 1:1 line decreases with the steepness of flow competence curves. For example, at Little Granite Creek (1999) with a flow competence curve exponent of 2.98, both samplers yield similar results at a relatively low transport of about 1 g/m·s, whereas at East Dallas Creek with a flow competence curve exponent of 1.32, similar results for both samplers are obtained at a transport rate of about 26 g/m·s. Similarly, inter-sampler transport relationships are steeper for streams with lower rating curve coefficients. At Little Granite Creek (1999) with a bedload trap rating curve coefficient of 7.3E-12, the inter-sampler transport relationship has an exponent of 3.5, while at East St. Louis Creek (2001) with a rating curve coefficient of 3.9, the exponent of the inter-sampler transport relationship was 2.1. Inter-sampler transport relationships were unrelated to transport measurements made with a HS sampler, making it very difficult to determine conversion functions based on HS measurements alone.

Inter-sampler transport relationships can be visually and statistically segregated into two groups: one with flatter trendlines that intersect the 1:1 line at high values (blue group) and one with steeper trendlines that intersect the 1:1 line at lower values (red group). This allows inter-sampler transport relationships to be reduced to two cases: those applicable to the “red” and those to the “blue” stream group. The similarity of fractional inter-sampler transport relationships among individual size classes and within each of the two stream groups suggests that one inter-sampler transport relationship may apply to any 0.5 phi gravel size fraction. This reduces the number of inter-sampler transport relationships needed to convert HS sampling results to those that might have been collected with bedload traps to six: one for fractional transport rates of any 0.5 size class, one for total gravel transport, and one for bedload D_{max} particle sizes for each the “red” or the “blue” stream group.

Several bedmaterial parameters as well as the exponents and coefficients of bedload rating and flow competence curves measured with bedload traps (and to some degree also measured with a HS sampler) were statistically different for streams falling in to the “red” and “blue” stream groups. The blue group occurs in streams with more armoring, higher amounts of subsurface fines < 8 mm, and steeper bedload rating and flow competence curves. This segregation opens the possibility of placing a study stream either into the “red” or the “blue” stream group. The respective inter-sampler transport relationship is then selected, and its coefficient and exponent are applied to the measured HS rating curve.

4.2 Paired data approach

Power and polynomial functions that were fitted to plotted data pairs (see Figure 6) describe the inter-sampler transport relationships for fractional and total transport rates obtained at each study stream from the paired data approach. At sites with relatively small sample sizes and narrow ranges of measured transport rates, power functions provided a visually acceptable fit to the plotted data (East St. Louis Creek '03, Cherry Creek, Little Granite Creek '02, and Halfmoon Creek). Polynomial functions were visually more satisfying at sites with larger sample sizes and a wider range of sampled transport rates (East St. Louis Creek '01, East Dallas Creek, Hayden Creek, and Little Granite Creek '99) (Figure 15).

Inter-sampler transport relationships obtained from the paired data approach or intersect the 1:1 line at moderate to high transport rates and fall below the 1:1 line when transport is low (Figure 15). Regression functions for data sets with low sample size or a narrow range of measured transport rates have flatter slopes (Little Granite Creek '02, East St. Louis Creek '01, and Halfmoon Creek) than other streams. There are two explanations for the flatness: one is that the data range was too narrow to reflect the well developed, steep trend otherwise seen in inter-sampler-transport relationships (see Figure 7). Another is that a fitted straight function tends to be overly flat in data sets that extend over a narrow x-range and have a lot of scatter.

Fitted power functions were statistically significant ($p < 0.05$) for the two smallest size classes (4 – 5.6 and 5.6 – 8 mm) as well as for total gravel transport rates, but not necessarily for the coarsest gravel sizes. The goodness-of-fit for the polynomial functions is difficult to assess because guiding the function (Section 3.2.2.3) makes statistical measures of fit such as r^2 and *p*-values meaningless. Inter-sampler transport relationships are formulated using the *a*- and *b*-parameters from fitted power functions and have the form $F_{HS} = Q_{B,traps} = a\ Q_{B,HS}^{\ b}$ (Table 6). For fitted polynomial functions (Eq. 13), the *a*-, *b*-, and *c*-coefficients in Table 6 need to be used with Eq. 14.

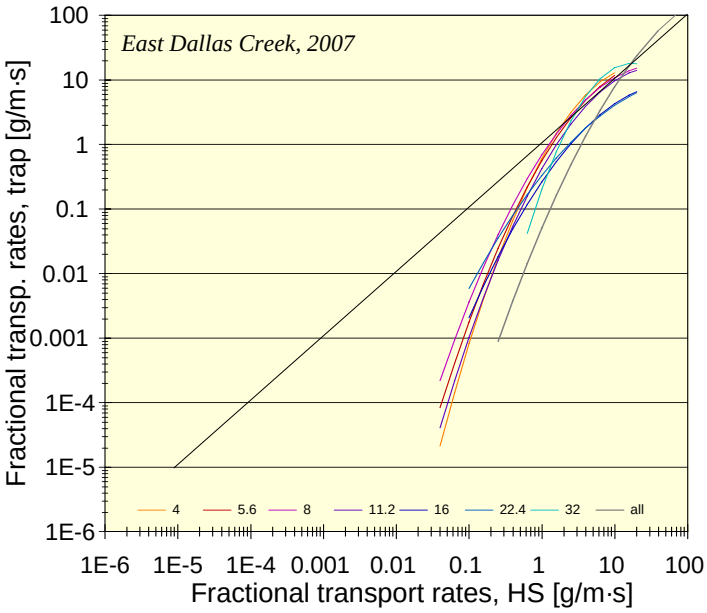

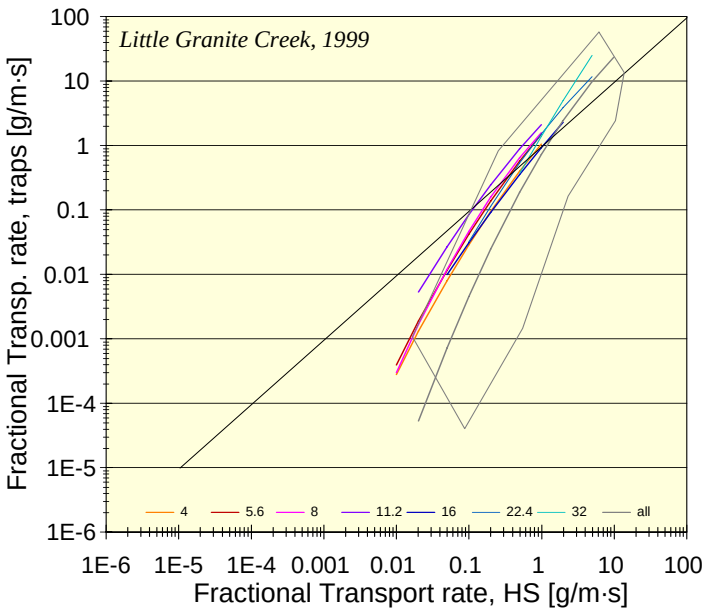

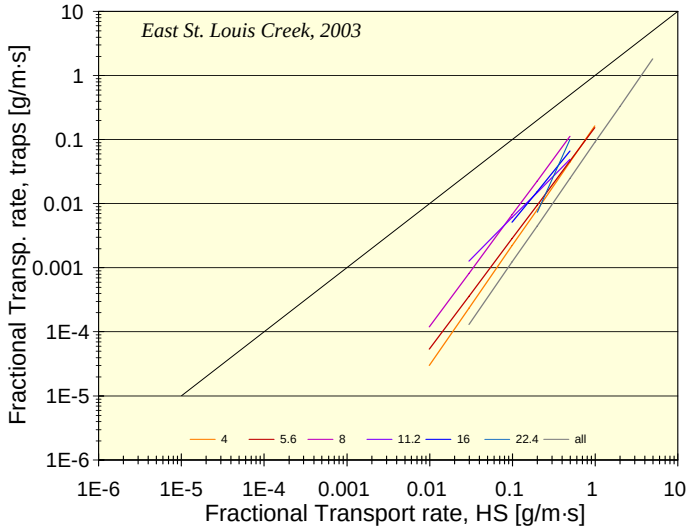

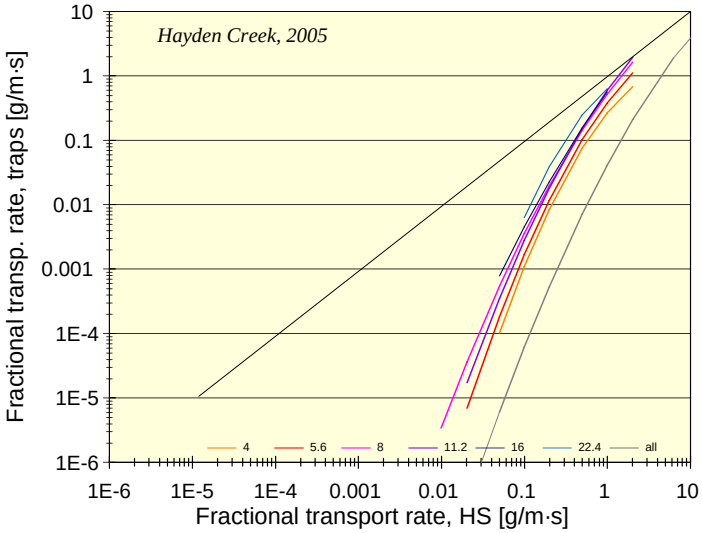

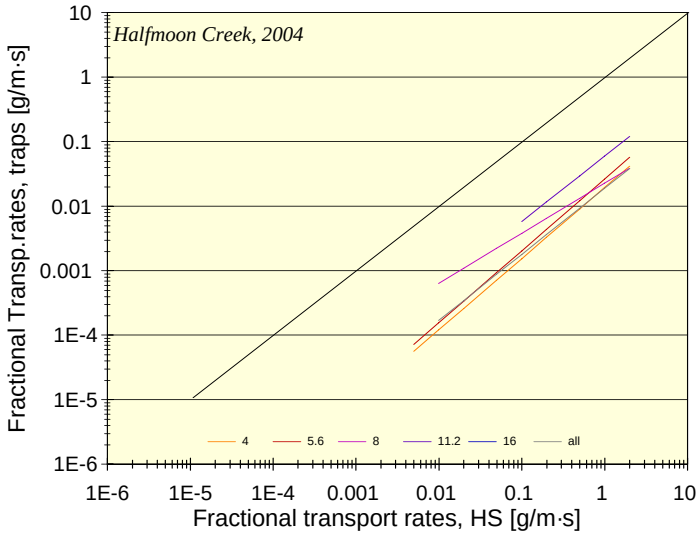

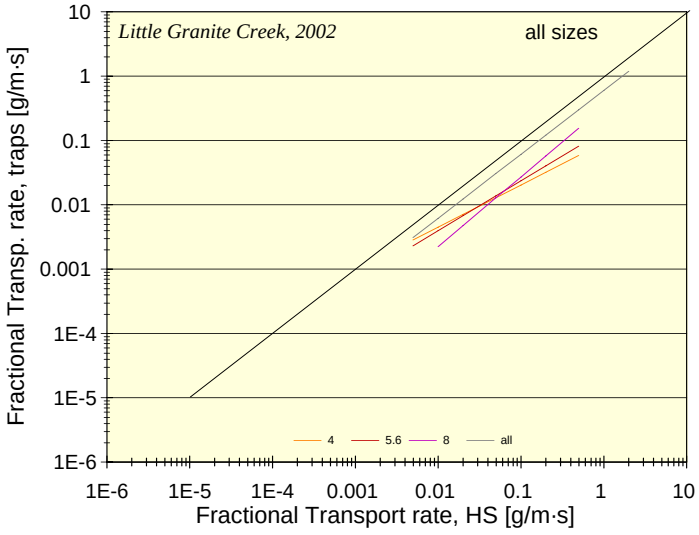

Fig. 15, continued on next page

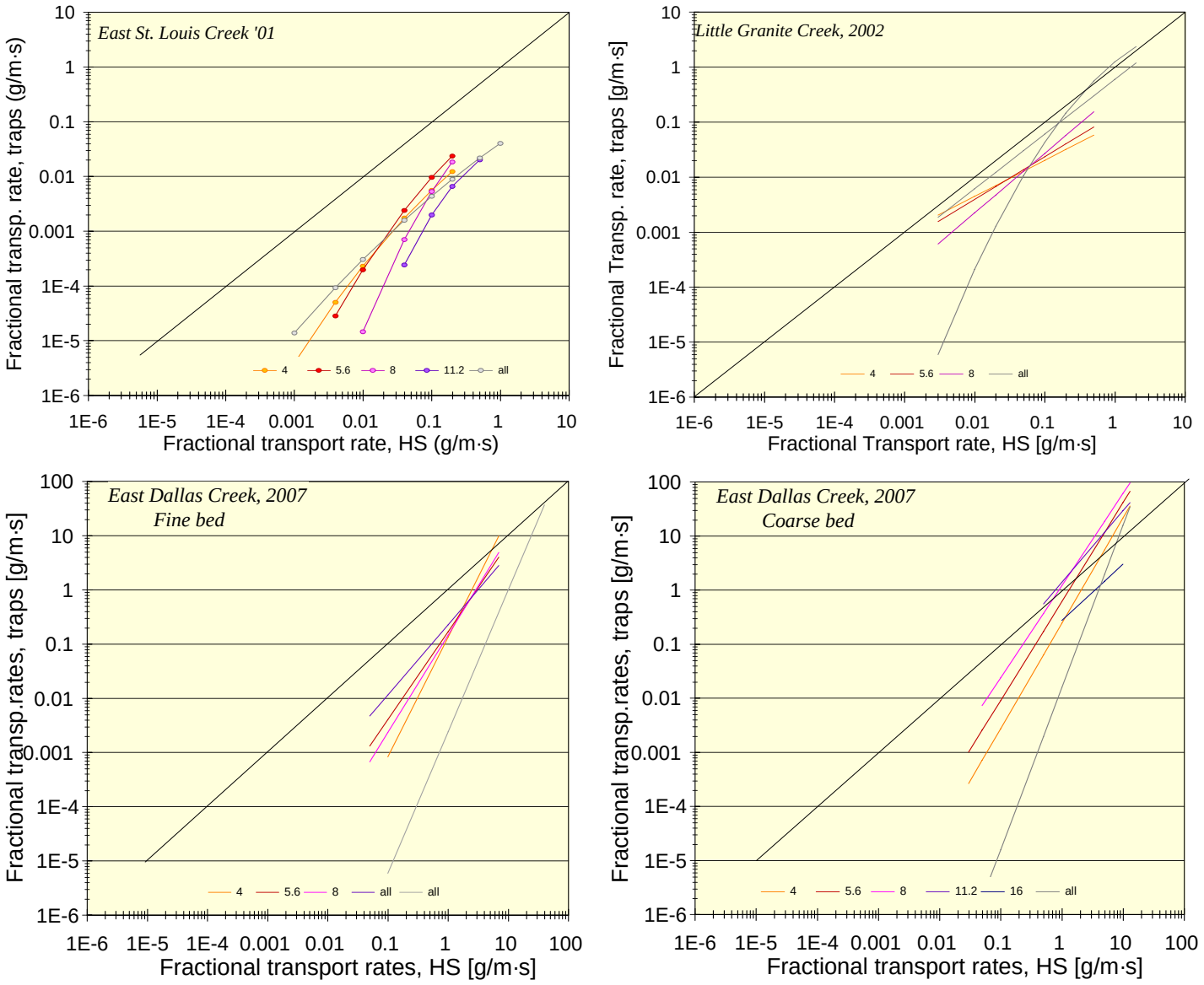

Figure 15: Paired data approach: fitted inter-sampler transport relationships for individual gravel sizes classes and total gravel transport at all study streams.

Table 6: Parameters of power functions (*a*-coefficient and *b*-exponent, no value for *c*) and polynomial functions (*a*-, *b*-, and *c*-coefficients) fitted to inter-sampler transport relationships for individual size fractions and total gravel transport rates using the paired data approach. Also given are number of non-zero samples (*n*), coefficient of variation (r^2), *p*-value (*p*), the standard error of the *y*-estimate (s_y), as well as bias correction factors after Ferguson (1986, 1987) (CF_F) and Duan (1983) (CF_D) obtained for fitted power functions.

		Streams in "blue" stream group						Streams in "red" stream group			
Size class (mm)	Para-meter	East Dallas Cr.	E. Dallas fine bed	E. Dallas coarse bed	Half-moon Cr.	E. St. Louis Cr. '03	Hayden Cr.	E. St. Louis Cr. '01	Cherry Cr.	Little Granite Cr. '99	Little Granite Cr. '02
4-5.6	*n*	53	30	34	35	38	24	72	14	40	14
	a	-0.772	0.0141	0.0533	0.00752	0.113	-0.809	-0.193	0.7	-0.226	0.066
	b	2.1	2.21	1.95	1.1	1.87	1.58	0.808	1.8	1.34	0.656
	c	-0.55	-	-	-	-	-0.91	-1.5	-	-0.2	-
	r^2	0.76	0.52	0.67	0.53	0.81	0.75	0.22	0.73	0.54	0.41
	p-value	<<	<<	<<	<<	<<	<<	<<	<<	<<	0.013
	s_y	0.69	0.96	0.96	0.66	0.39	0.73	0.56	0.8	0.59	0.43
	CF_F	3.47	11.2	11.2	3.13	1.5	4.17	2.27	5.57	2.53	1.65
	CF_D	2.7	9.58	4.58	2.58	1.45	2.72	2.22	3.99	2.09	1.4
5.6 - 8	*n*	53	24	23	28	37	19	60	10	41	14
	a	-0.59	0.0382	0.100	0.0146	0.08	-0.653	-0.304	1.26	-0.237	0.102
	b	1.91	1.62	1.83	1.11	1.73	1.7	0.776	1.64	1.32	0.775
	c	-0.65	-	-	-	-	-0.56	-1.2	-	-0.1	-
	r^2	0.76	0.63	0.65	0.6	0.64	0.79	0.08	0.75	0.53	0.44
	p-value	<<	<<	<<	<<	<<	<<	0.029	0.0012	<<	0.009
	s_y	0.77	0.78	0.99	0.52	0.51	0.53	0.57	0.64	0.67	0.48
	CF_F	4.72	4.92	13.3	2.06	2.01	2.08	2.35	2.95	3.34	1.83
	CF_D	3.14	4.47	6.15	1.8	1.91	1.75	2.3	2.31	2.36	1.38
8-11.2	*n*	49	22	17	19	31	19	31	8	39	7
	a	-0.544	0.0363	0.186	0.00804	0.132	-0.431	-0.6	0.0595	-0.331	0.269
	b	1.74	1.80	1.70	0.775	1.75	1.73	0.764	0.227	1.2	1.08
	c	-0.55	-	-	-	-	-0.5	-1	-	-0.05	-
	r^2	0.81	0.67	0.53	0.31	0.59	0.72	0.03	0.02	0.46	0.82
	p-value	<<	<<	<<	0.013	<<	<<	0.33	0.76	<<	<<
	s_y	0.73	0.70	0.99	0.72	0.53	0.63	0.44	0.7	0.63	0.31
	CF_F	4.17	3.70	13.4	3.95	2.09	2.86	1.68	3.64	2.83	1.29
	CF_D	3.08	4.10	6.52	2.81	2.86	2.07	1.55	1.97	2.22	1.22
11.2-16	*n*	39	17	14	13	25	14	11	7	36	2
	a	-0.627	0.0529	0.402	0.018	0.0567	-0.519	-0.765	5.57	-0.202	-
	b	1.99	1.29	1.32	1.01	1.3	1.81	0.445	1.87	1.2	-
	c	-0.6	-	-	-	-	-0.4	-1.5	-	0.0	-
	r^2	0.82	0.33	0.32	0.28	0.45	0.69	0.05	0.2	0.39	-
	p-value	<<	0.0156	0.0358	0.065	<<	<<	0.49	0.32	<<	-
	s_y	0.6	0.77	0.76	0.8	0.6	0.58	0.32	0.62	0.65	-
	CF_F	2.57	4.79	4.58	5.52	2.59	2.41	1.31	2.77	3.02	-
	CF_D	2.1	4.31	3.49	3.31	2.13	1.89	1.27	1.74	2.64	-
16 - 22.4	*n*	28	14	10	4	13	10	0	3	26	2
	a	-0.449	0.0496	0.239	-	0.125	-0.339	-	-	-0.125	-
	b	1.68	1.08	1.04	-	1.59	1.76	-	-	1.35	-
	c	-0.7	-	-	-	-	-0.4	-	-	-0.15	-
	r^2	0.7	0.11	0.59	-	0.69	0.36	-	-	0.62	-
	p-value	<<	0.238	0.00982	-	<<	0.068	-	-	<<	-
	s_y	0.46	0.77	0.26	-	0.46	0.66	-	-	0.42	-
	CF_F	1.75	4.76	1.19	-	1.74	3.14	-	-	1.61	-
	CF_D	1.66	4.78	1.15	-	1.6	1.78	-	-	1.63	-

Size class (mm)	Para-meter	East Dallas Cr.	E.Dallas fine bed	E. Dallas coarse bed	Half-moon Cr.	E. St. Louis Cr. '03	Hayden Cr.	E. St. Louis Cr. '01	Cherry Cr.	Little Granite Cr. '99	Little Granite Cr. '02
22.4 - 32	n	24	2	9	3	4	7	0	22	18	0
	a	-0.334	-	-	-	0.642	-0.916	-	-	-0.241	-
	b	1.42	-	-	-	2.86	1.09	-	-	1.43	-
	c	-0.6	-	-	-	-	-0.3	-	-	-0.2	-
	r^2	0.57	-	-	-	0.81	0.03	-	-	0.29	-
	p-value	<<	-	-	-	0.1	0.705	-	-	0.021	-
	s_y	0.48	-	-	-	0.3	0.5	-	-	0.68	-
	CF_F	1.65	-	-	-	1.14	1.59	-	-	3	-
	CF_D	1.86	-	-	-	1.27	1.96	-	-	3.35	-
32 - 45	n	16	0	1	1	1	2	0	2	8	0
	a	-1.28	-	-	-	-	-	-	-	-0.121	-
	b	3.16	-	-	-	-	-	-	-	1.88	-
	c	-1	-	-	-	-	-	-	-	-0.2	-
	r^2	0.35	-	-	-	-	-	-	-	0	-
	p-value	0.015	-	-	-	-	-	-	-	0.88	-
	s_y	0.6	-	-	-	-	-	-	-	0.68	-
	CF_F	2.6	-	-	-	-	-	-	-	3.43	-
	CF_D	2.52	-	-	-	-	-	-	-	2.75	-
All gravel size classes	n	53	32	33	39	38	25	74	16	41	15
	a	-0.459	1.39E-03*	0.0117[#]	0.00393	0.0339	-0.413	-0.0946	0.144	-0.348	-0.424
	b	2.65	2.09*	1.78[#]	1.02	1.87	2.41	0.871	1.47	1.86	1.040
	c	-1.70	-	-	-	-	-1.78	-1.70	-	-0.40	-0.10
	r^2	0.79	0.64	0.63	0.37	0.77	0.79	0.24	0.59	0.59	0.45
	p-value	<<	<<	<<	<<	<<	<<	<<	<<	<<	0.006
	s_y	0.75	1.01	1.19	0.88	0.5	0.74	0.62	1.19	0.7	0.8
	CF_F	4.36	15.1	43.9	7.65	1.94	4.25	2.75	42.1	3.66	5.39
	CF_D	3.17	4.42	10.7	4.81	2.67	3.08	2.54	7.08	2.28	2.58

<< indicates a value << 0.05; Gray print indicates *p*-values ≥ 0.1. Pale red and blue shading indicates classification as "red" or "blue" stream group (see explanation in the text). *A slight alteration of the *a*-coefficient to 5.50E-04, and the *b*-exponent to 2.61 improved the visual fit to the plotted data. [#]A slight alteration of the *a*-coefficient to 0.00316, and the *b*-exponent to 3.00 improved the visual fit to the plotted data.

4.2.1 Variability among particle size classes

Fractional inter-sampler transport relationships tend to shift upwards toward the 1:1 line for increasingly coarser particle-size classes. The "stacked" trend is best developed at sites where measurements extend over a wide range of transport rates and provide a large *n* for many size fractions. In this case, fractional inter-sampler transport relationships differ by a factor of up to 2 – 4 between neighboring size classes, and maximally by to a factor of 10 (Figure 15). These results suggest that HS sampling results exceed those from bedload traps to a higher degree for fine gravel than for coarse gravel. However, for the coarsest size classes (for which only a few data pairs exist), fractional inter-sampler transport relationships tend to cross or deviate in some other way from the otherwise parallel upward trend.

It is difficult at this point to pinpoint whether different trends for the coarsest particles is merely a computational artifact caused by a small and narrow range of measured transport rates, or whether inter-sampler transport relationships for coarse particles actually follow a different trend.

Based on results where a large number of samples had been collected over a wide range of flows and transport rates, it is expected that the trend displayed for the smallest gravel size classes would continue for the coarser size classes as well. However, as soon as the size of transported gravels approaches the size of the HS sampler opening, the trend would be expected to change.

4.2.2 Variability among streams

Inter-sampler transport relationships are combined over all study streams (Figure 16) to show variability among streams. The variability among streams for a specified gravel size fraction is notably larger than the variability among gravel fractions for a specified stream (Figure 15). Fine gravel as well as total gravel transport (last plot of Figure 16) show a similar pattern of variability among streams. Based on this similarity, and based on not knowing the true inter-sampler

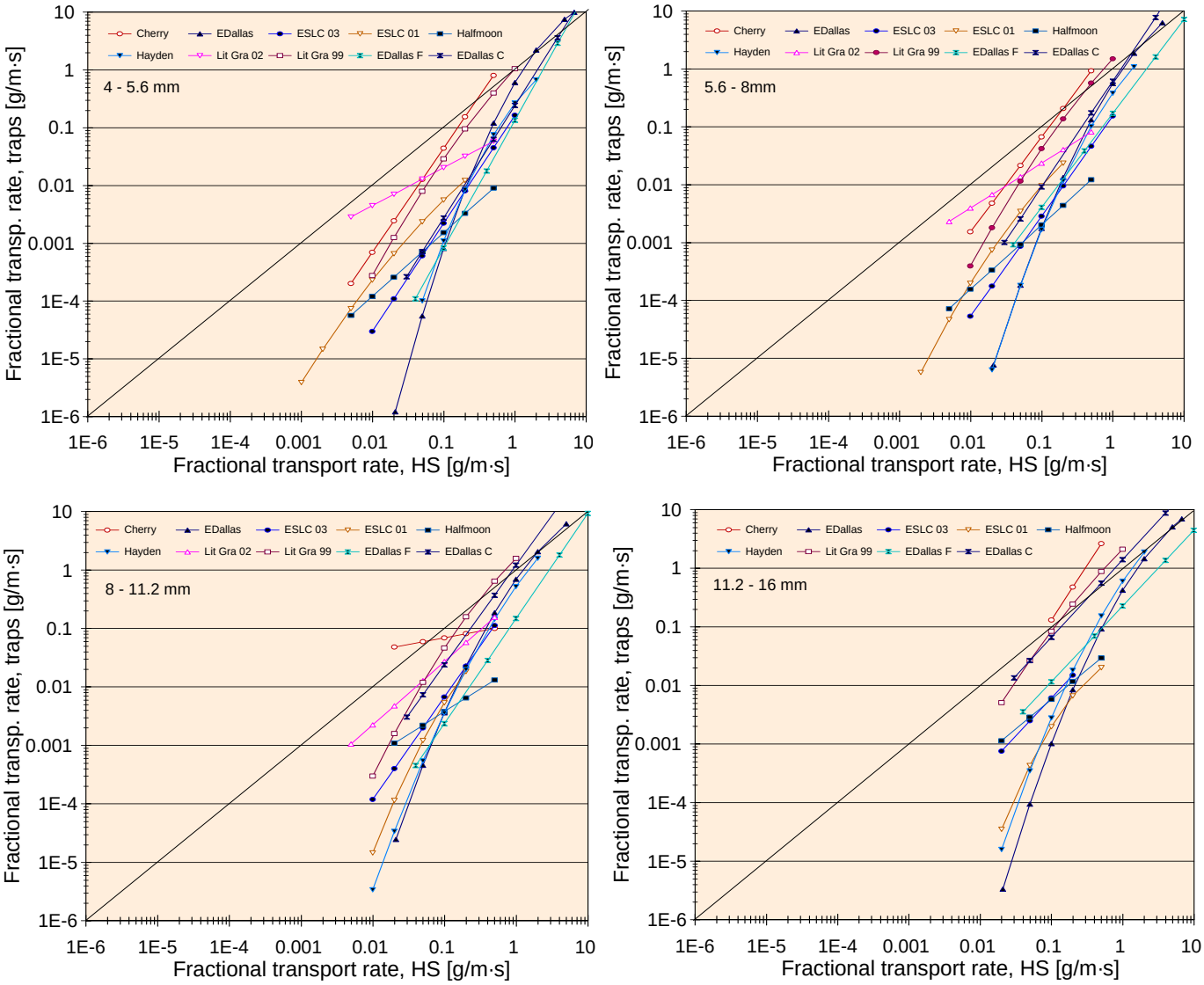

Figure 16 continued on next page

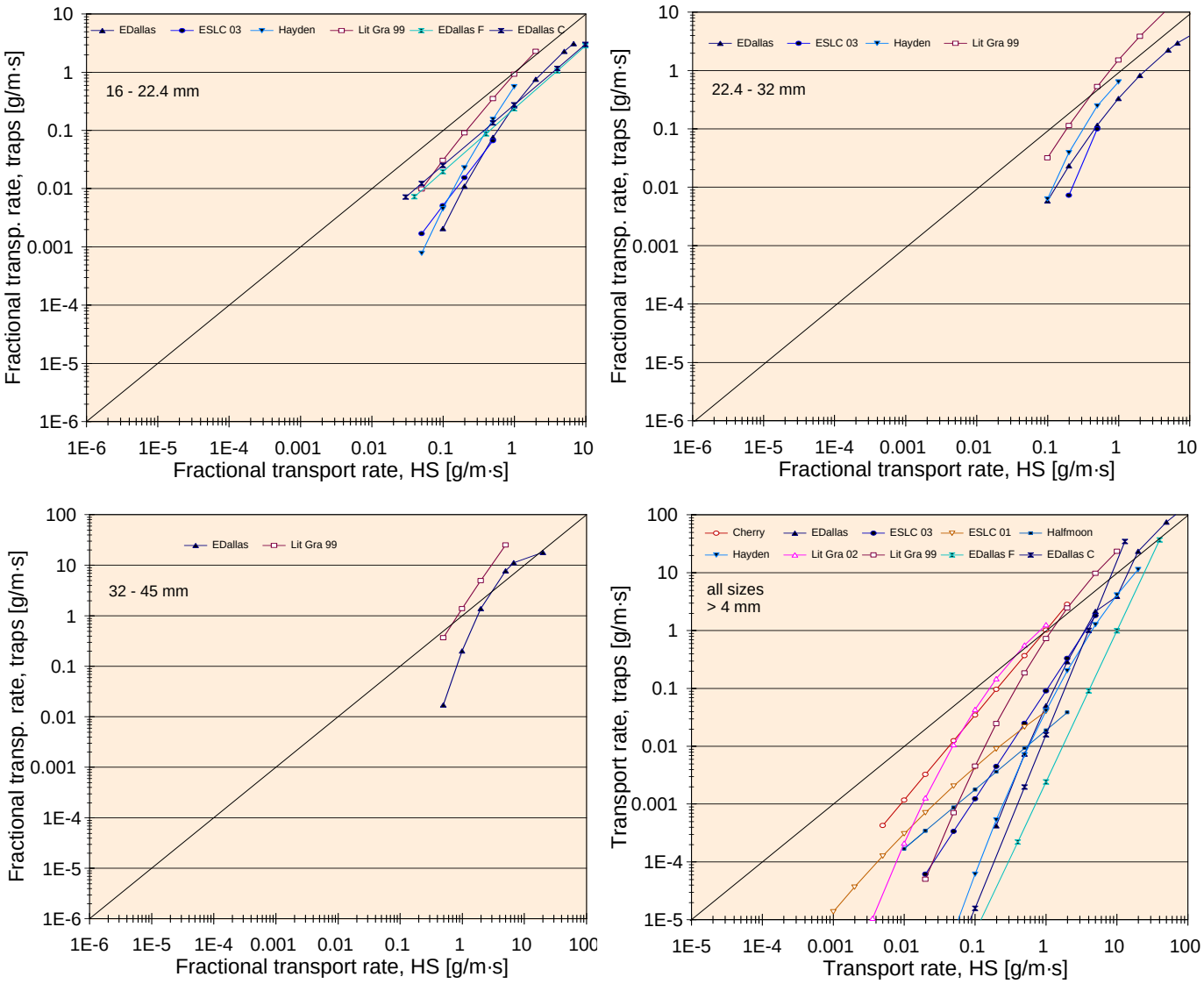

Figure 16: Paired-data approach: inter-sampler transport relationships for individual gravel size classes as well as total gravel transport rates (last plot) combined for all study streams. Streams classified as the "red" group are indicated by reddish line colors and open symbols; streams in the "blue" group by bluish line colors and closed symbols (see explanation in text).

transport relationships for the coarsest size classes, analyses of variability among streams were limited to total gravel transport rates in this study. Had all study streams provided a large number of samples collected over a wide range of transport rates (i.e., in flows up to 200% of bankfull), it is expected that trends displayed for the smallest size classes and for total transport rates would continue in a similar fashion for coarser size classes, until the sampling limitation imposed by the small HS opening size sets in.

Inter-sampler relationships for total gravel transport appear to have a common origin for all streams in the vicinity of the 1:1 line at about 100 g/m·s, i.e., when transport is high. There, transport relationships disperse for lower transport rates and take different courses for individual streams. Given the wide range of different inter-sampler transport relationships, a user should ideally be able to select an adjustment function suitable to a specific study stream. Two methods are considered: One approach assigns a group-average adjustment function to a stream that meets some general criteria of bedmaterial and transport characteristics (Section 4.2.2.1.ff). The other approach focuses on predicting individual adjustment factors to a study stream based on bedload characteristics measured with bedload traps and a HS sampler in that stream (Section 4.2.2.5).

4.2.2.1 Segregation into two stream groups

Inter-sampler transport relationships for total gravel transport visually fall into two groups (Figure 17). Inter-sampler transport relationships for the "red" group plot close to the 1:1 line and approach or intersect the 1:1 line at transport rates (around 1 – 2 g/m·s). Inter-sampler transport relationships from the "blue" group plot further away from the 1:1 line and intersect at 8 g/m·s and higher. Three of the four streams that had been categorized as "red" and "blue" groups in the rating curve approach (Section 4.1.3.1) remained in these groups in the paired data approach. The exceptions are East St. Louis Creek '01 that moved from the "red" group in the

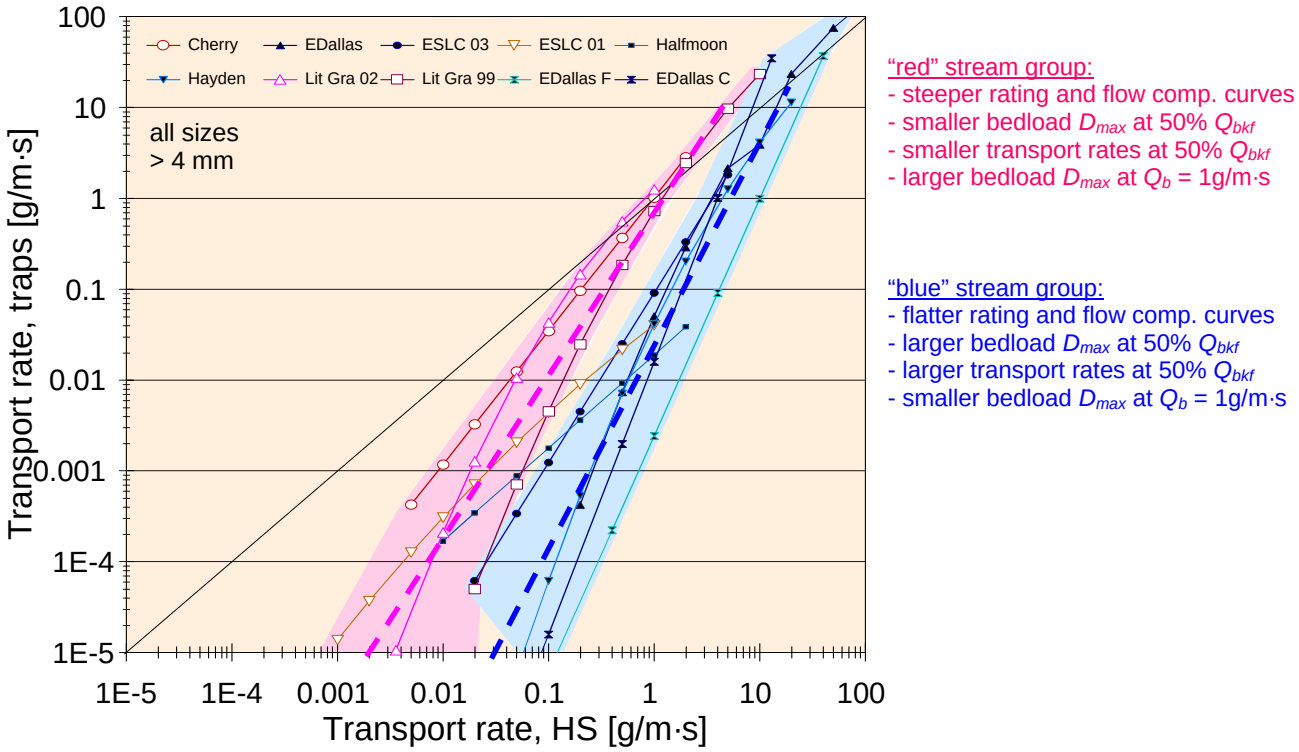

Figure 17: Paired-data approach: Inter-sampler transport relationships for total gravel transport combined for all study streams. Streams falling into the "red" group are indicated by open symbols and reddish line colors, streams in the "blue" group by closed symbols and bluish line colors. Thick dashed lines are functions that visually average over the trendlines of the "red" and "blue" stream groups.

rating curve approach to the "blue" group in the paired data approach, and Hayden Creek that moved from the "blue" to the "red" group. The "red" group of inter-sampler transport relationships is generally flatter than those in the "blue" group. The steepness of inter-sampler transport relationships in the "red" group is the main difference between the paired data and the rating curve approach ("red" group flatter than "blue" group in paired data approach but steeper than the "blue" group in the rating curve approach).

Inter-sampler transport relationships in the rating curve approach could be described by commonalities in their *a*-coefficients and *b*-exponents of the fitted power functions. This approach is not applicable when a combination of power and polynomial functions are used to describe inter-sampler transport relationships. Therefore, inter-sampler transport relationships in the paired data approach were quantified by the bedload trap transport rates associated with HS-measured transport rates of 0.1 and 1.0 g/m·s. (i.e., the intersections with vertical lines at HS-measured transport rates of x = 0.1 and x = 1 g/m·s). These two transport rates were selected because they were measured with the HS sampler for nearly all size fractions and streams (thus did not require extrapolation).

Inter-sampler relationships for total gravel transport from the "red" group intersect the line x = 0.1 g/m·s within the range of 0.004 – 0.06 g/m·s, indicating that HS sampler collected transport rates 0.5 – 1.5 orders of magnitude higher than those collected with bedload traps. At transport rates of 1 g/m·s, both samplers collect similar transport rates. In the "blue" group, sampling differences between the two samplers are larger for small transport rates (2-4 orders of magnitude of x = 0.1 g/m·s) but decrease during higher transport (1-2 orders of magnitude at x = 1 g/m·s) and approach near-unity at high transport (10 g/m·s) (Figure 17). The group-averaged bedload trap-measured transport rates at x = 0.1 g/m·s and x = 1.0 g/m·s are significantly different between the two stream groups, suggesting that inter-sampler transport relationships among the two stream groups are statistically different.

4.2.2.2 Bedmaterial and bedload conditions in "red" and "blue" streams

Streams categorized as "red" or "blue" can be distinguished based on whether the 95% confidence interval around the group mean values for parameters of bedmaterial and bedload transport overlap. When there was no overlap, the two stream groups were considered different with respect to a specified parameter, and the value equidistant to both group means served as a threshold to differentiate among groups. The computed threshold values[6] are presented in Table 7 and allow a user to classify a study stream as either "red" or "blue". Stream groups in the paired data approach did not differ in their bankfull flow (Q_{bkf}), bankfull width (w_{bkf}), stream gradient (S), the surface D_{50} and D_{84} sizes, the subsurface D_{50} size (D_{50sub}), the % surface and the % subsurface sediment < 2 and < 8 mm, or bed armoring. The same evaluation showed that several bedload transport characteristics were significantly (α = 0.05) different between the "red" and the "blue" stream groups. Bedload rating and flow competence curves measured with both samplers were generally less steep for "blue" streams and had higher coefficients than the "red" streams. In "blue" streams, both samplers collected significantly larger gravel transport rates and bedload D_{max} sizes at 50% of bankfull flow. A discharge of 50% Q_{bkf} was selected because it did

[6] Threshold values are associated with some variability except those printed in bold. The user should therefore consider threshold values for several parameters before classifying a stream.

not require extrapolating bedload rating and flow competence curves above the measured range in study streams where bankfull flows were not obtained. Also significantly different between stream groups was the bedload D_{max} particle size collected at a fixed transport rate of 1 g/m·s.

Table 7: Bedmaterial characteristics and conditions of bedload transport that determine the stream group and the respective inter-sampler relationships for the paired data approach.

	Streams in "red" group	Stream in "blue" group
<u>For bedload conditions measured with bedload trap:</u>		
Exponent of bedload rating curve	> 8.9	< 8.9
Coefficient of bedload rating curve	< 1.1E-4	> 1.1 E-4
Exponent of flow competence curve	> 1.9	< 1.9
Coefficient of flow competence curve	< 5.30	> 5.30
Bedload D_{max} at 50% Q_{bkf}	< 11 mm	> 11 mm
Gravel transport rate at 50% Q_{bkf}	< 0.001 g/m·s	> 0.001 g/m·s
Bedl. D_{max} at gravel transp. rate of 1 g/m·s	> 40 mm	< 40 mm
<u>For bedload conditions measured with HS sampler:</u>		
Exponent of bedload rating curve	< 3.4*	> 3.4*
Coefficient of bedload rating curve	< 0.094	> 0.094
Exponent of flow competence curve	> 0.91*	< 0.91*
Coefficient of flow competence curve	< 9.7	> 9.7
Bedload D_{max} at 50% Q_{bkf}	**< 13 mm**	**> 13 mm**
Gravel transport rate at 50% Q_{bkf}	**< 0.15 g/m·s**	**> 0.15 g/m·s**
Bedl. D_{max} at gravel transp. rate of 1 g/m·s	< 18 mm	> 18 mm
<u>Inter-sampler transport relationships (F_{HS}) that may be used to adjust HS measurements of total gravel transport:</u>		
Power functions visually fitted over all trendlines	Eq. 22: $Q_{B\,trap} = 0.635\ Q_{B\,HS}^{1.73}$	Eq. 23: $Q_{B\,trap} = 0.0305\ Q_{B\,HS}^{2.29}$
Power functions fitted to all individual data pairs	Eq. 24: $Q_{B\,traps} = 4.80^{\#} \cdot 0.120\ Q_{B\,HS}^{1.25}$	Eq. 25: $Q_{B\,traps} = 3.90^{\#} \cdot 0.0191 Q_{B\,HS}^{1.75}$
Power functions visually fitted to all individual data pairs	Eq. 26: $Q_{B\,traps} = 0.316\ Q_{B\,HS}^{1.50}$	Eq. 27: $Q_{B\,traps} = 0.0234\ Q_{B\,HS}^{2.25}$
Power function visually fitted to average over results from all approaches and submethods	Eq. 30 (avg. over Eqs. 22, 24, 26) $Q_{B\,traps} = 0.532\ Q_{B\,HS}^{1.58}$	Eq. 29 (avg. Eq.16, 23, 25, 27) $Q_{B\,traps} = 0.0235\ Q_{B\,HS}^{2.10}$

* and gray print: Difference between red and blue stream group not statistically significant; **Bold Print:** Threshold value between groups is considered precise; # Duan (1983) bias correction factor. Red and blue shadings refer to "red" and "blue" stream groups (see text for explanation).

4.2.2.3 Computation of group-average inter-sampler transport relationships

The inter-sampler transport relationships determined from the paired data approach cannot be easily mathematically averaged because the *a*-and *b*-parameters of the fitted power functions are not directly comparable to those from the fitted polynomials. To attain group-averaged inter-sampler transport relationships, three methods of integration were applied.

1) A straight-line (i.e., power function) was fitted to visually average the inter-sampler transport relationships for the "red" and for the "blue" stream group (Figure 17). This approach places approximately equal weight to the trendline of each stream within a group. Power functions subsequently fitted to the visually fitted straight lines yielded the equations

$$Q_{B\,trap} = F_{HS} = 0.635\ Q_{B\,HS}^{\ 1.73} \qquad \text{"red" streams} \qquad (22)$$

and

$$Q_{B\,trap} = F_{HS} = 0.0305\ Q_{B\,HS}^{\ 2.29} \qquad \text{"blue" streams} \qquad (23)$$

2) For a statistically more defensible approach, power functions were fitted to individual data pairs of measured transport ratios within the "red" and within the "blue" stream group (Figure 18). This approach places equal weight to each data measured pair. The power functions yielded the equations:

$$Q_{B\,trap} = F_{HS} = 0.1207\ Q_{B\,HS}^{\ 1.252} \qquad \text{"red" streams} \qquad (24)$$

with $n = 146$, $r^2 = 0.59$, $s_y = 0.87$, and $CF_{Duan} = 4.80$

and

$$Q_{B\,trap} = F_{HS} = 0.01913\ Q_{B\,HS}^{\ 1.745} \qquad \text{"blue" streams } \textit{(excluding East Dallas Creek, fine and coarse bed)} \qquad (25)$$

with $n = 155$, $r^2 = 0.76$, $s_y = 0.79$, and $CF_{Duan} = 3.90$

Predictions of inter-sampler transport relationships for streams falling into the "red" or "blue" groups based on Eqs. 24 and 25 need to be multiplied by the Duan (1983) smearing estimate (CF_{Duan}). Visually, Eqs. 24 and 25 do not fit the plotted data well.

3) As an alternative, straight lines that visually integrate over individual data pairs within the "red" and "blue" stream groups (Figure 18) are offered. They are described by the power function equations

$$Q_{B\,trap} = F_{HS} = 0.316\ Q_{B\,HS}^{\ 1.50} \qquad \text{"red" streams} \qquad (26)$$

$$Q_{B\,trap} = F_{HS} = 0.0234\ Q_{B\,HS}^{\ 2.25} \qquad \text{"blue" streams} \qquad (27)$$

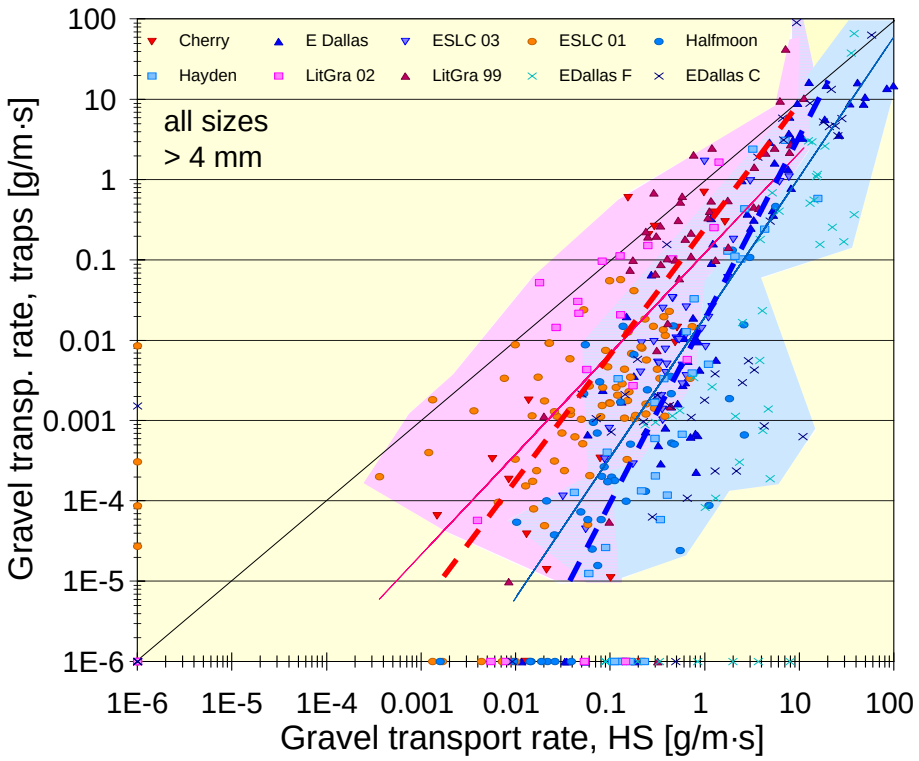

Figure 18: Ratios of total gravel transport rates measured with bedload traps *vs*. the HS for all study streams combined. Red and blue shading marks the field of data collected in "red" and "blue" streams. Thin red and blue lines indicate power functions fitted to data from all "red" and all "blue" streams (Eqs. 24 and 25). Dashed thick red and blue lines indicate functions that visually integrate over the "red" and "blue" stream groups (Eqs. 26 and 27).

The three functions are combined in Figure 19. The segregation of the two groups is maintained indicating that the variability between the two stream groups is larger than the variability among the three functions fitted to integrate over streams within a group. It is difficult to evaluate which of the three integrating methods provides the preferred inter-sampler transport relationship to be used for correction of HS samples.

4.2.2.4 Using the correction function to adjusted a HS rating curve

Equations 22 – 27 can be applied to adjust either individual HS measurements of gravel transport or a measured HS transport relationship after the study stream has been classified as a "red" or "blue" based on threshold values of bedload conditions (Table 7). To arrive at an adjusted HS rating curve for a study stream, transport rates are measured with a HS sampler over a range of flows, and a rating curve is fitted to the data. The exponent *b* and coefficient *a* of the respective inter-sampler transport relationships (i.e., one of Eqs. 22 – 27) are then applied to the study stream's power function rating curve ($Q_{B\,HS} = c{\cdot}Q^{d}$) and multiplied by a bias correction factor *CF* (to be computed from the data scatter of field measurements) to yield

$$q_{B\,traps} = F_{HS} = CF_{Duan}{}^{*} \cdot a \cdot (CF \cdot c{\cdot}Q^{d})^{b} \qquad (28)$$

where the asterisk * denotes that CF_{Duan} is to be applied if a user chooses to use regression Eqs. 24 and 25. The exponents and coefficient of the adjusted HS rating curve can be computed analytically or be obtained via a curve-fitting analysis using two data points.

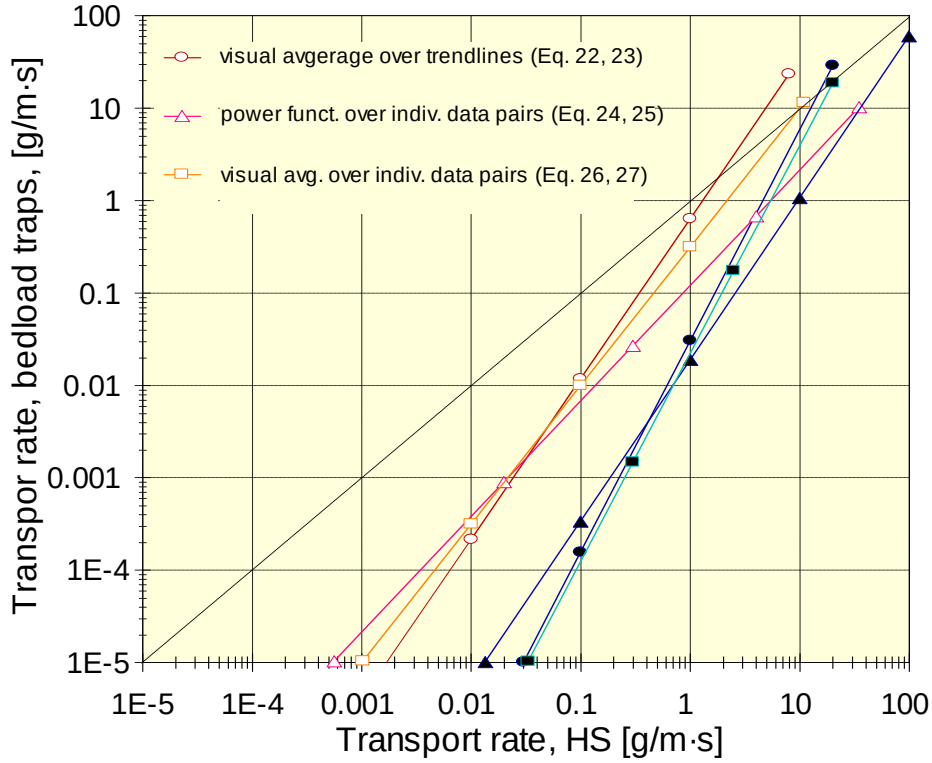

Figure 19: Inter-sampler transport relationships for total gravel transport (= HS correction functions) obtained from various methods of integrating over the "red" and "blue" groups in the paired data approach. Numbers on graphs refer to equation numbers. Inter-sampler transport relationships from the "red" stream group are plotted in reddish colors and those from the "blue" stream group in bluish colors.

4.2.2.5 Correction factors directly related to HS transport characteristics

This study also explored whether adjustment functions for individual streams (as opposed to stream groups) could be predicted from HS-measured transport characteristics. If a well-defined relationship existed between inter-sampler transport relationships and the bedload characteristics measured at a particular stream, a user could select a more representative HS correction function.

Parameters determining the magnitude of difference between HS and bedload traps

To explore the possibility of providing adjustment functions that are more closely matched to an individual stream, bedload trap transport rates associated with HS-measured transport rates of 0.01, 0.1 and 1 g/m·s were regressed against transport characteristics measured with bedload traps as well as the HS sampler in the study streams. The transport characteristics included exponents and coefficients of the bedload rating and flow competence curves as well as gravel transport rates and the bedload D_{max} particle sizes collected at 50% Q_{bkf}, and the bedload D_{max} particle sizes collected at a transport rate of 1 g/m·s. All except two of these parameters had been identified as

statistically different between the "red" and the "blue" stream groups (Table 7). Data from East Dallas Creek at the fine and coarse bed locations were included in these analyses. Power function regressions were used in all cases.

Effects of rating and flow competence curve characteristics

Bedload trap transport rates associated with HS-measured transport rates of 0.01, 0.1, and 1.0 g/m·s were not consistently correlated to parameters of the rating and flow competence curves measured with either bedload traps or the HS sampler. Statistically significant correlations were found only with the steepness of the bedload trap-measured flow competence curve as well as the coefficient of the HS-measured rating curve (Table 15 and Table 16, both in the Appendix) (r^2-values of 0.50 and 0.49, respectively).

Effects of transport rates and bedload D_{max} sizes collected at 50% Q_{bkf} and Q_b = 1 g/m·s

Bedload trap transport rates associated with HS-measured transport rates of 0.1, and 1.0 g/m·s were better correlated with transport rates and the bedload D_{max} particle size measured at a specific discharge. Values of r^2 were 0.57 and 0.60, respectively, for the negative correlation with the bedload trap transport rates collected at 50% Q_{bkf} (Figure 20, Table 9). Correlations were stronger with the HS-measured gravel transport rate at 50% Q_{bkf} (r^2-values of 0.67 and 0.81). Similarly, the bedload trap transport rates associated with HS-measured transport rates of 0.1, and 1.0 g/m·s decreased with the HS-measured D_{max} particle size at 50% Q_{bkf} (r^2-values of 0.69 and 0.55) and to a lesser degree with the bedload D_{max} particle sizes collected in bedload traps at 50% Q_{bkf} (r^2-values of 0.48 and 0.50). Bedload trap transport rates associated with HS-measured transport rates of 0.1, and 1.0 g/m·s were weakly correlated with the bedload trap D_{max} particle sizes collected at a transport rate of 1 g/m·s (Figure 21; Table 8), but not with the HS-measured D_{max} particle size at 1 g/m·s. The bedload trap transport rates associated with HS-measured transport rates of 0.01 g/m·s were not significantly related to any of the parameters discussed.

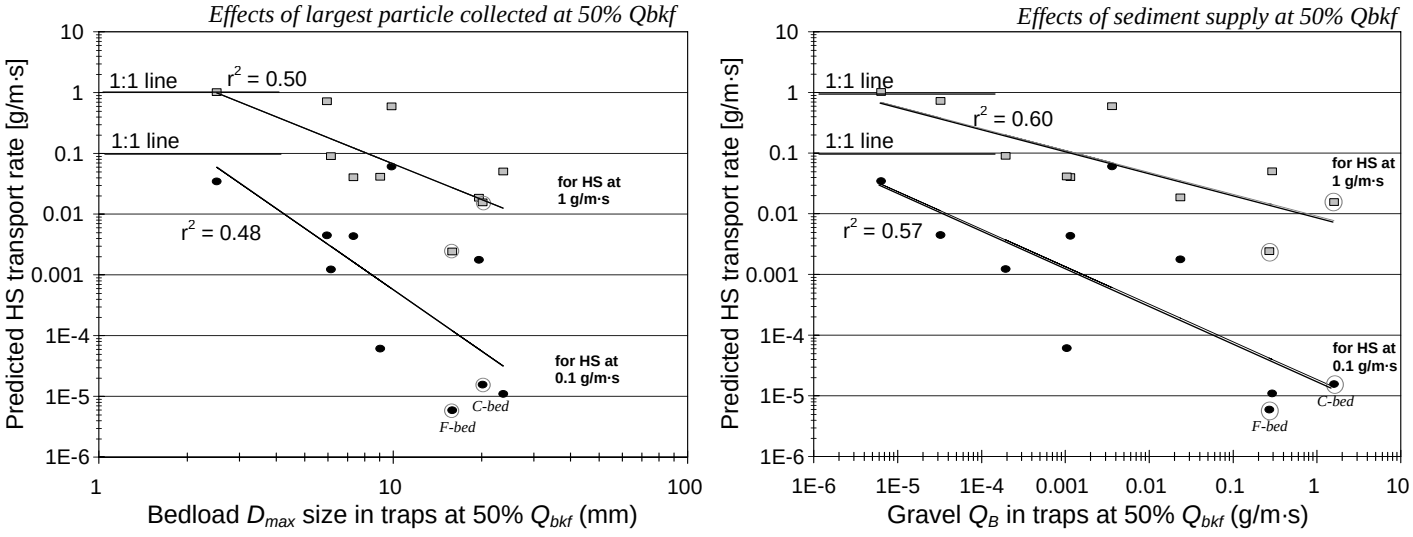

Figure 20 continued on next page

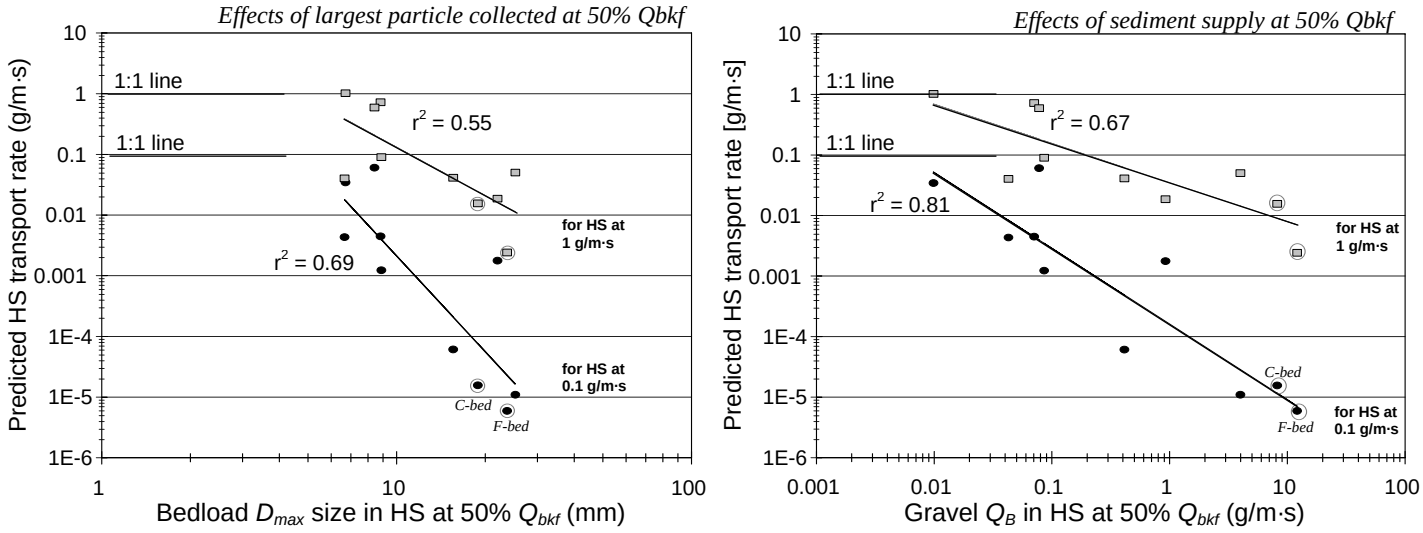

Figure 20: Effects of D_{max} bedload particle size and transport rates collected at 50% of bankfull flow with bedload traps (top plots) and the HS sampler (bottom plots) on transport rates predicted for the HS sampler from bedload trap measurements when HS collected transport rates of 0.1 and 1.0 g/m·s. Data points for sites with fine and coarse beds at East Dallas Creek are marked by dashed circles.

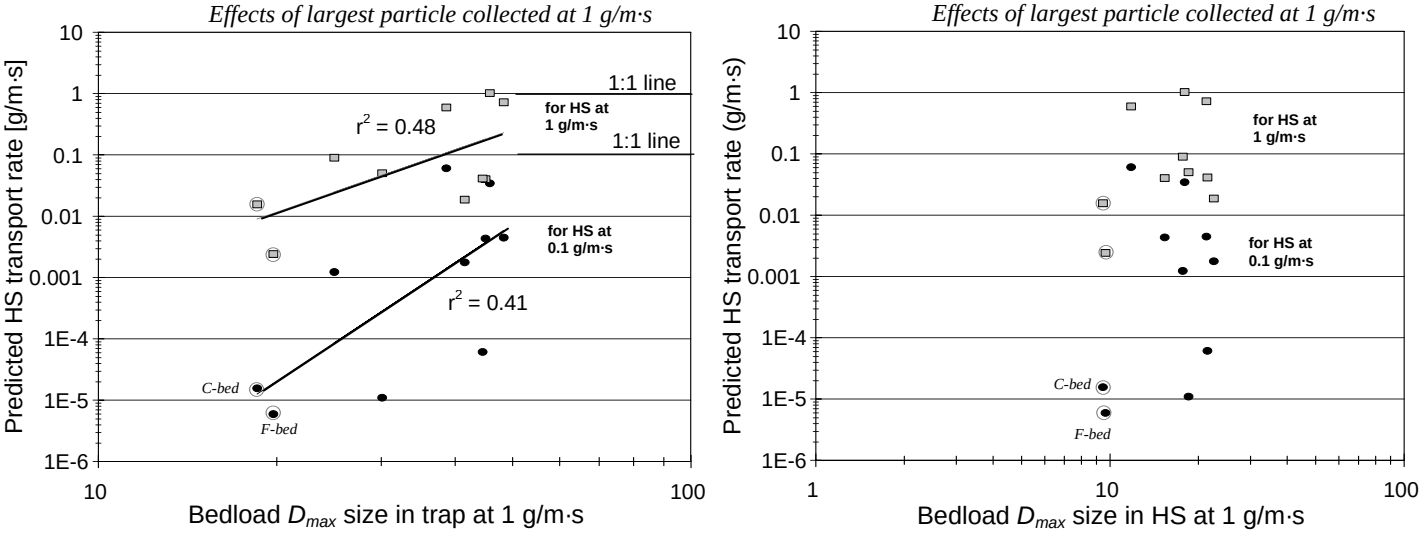

Figure 21: Effects of bedload D_{max} particle size and transport rates collected at 50% of bankfull flow with bedload traps (top plots) and the HS sampler (bottom plots) on transport rates predicted for the HS sampler from bedload trap measurements when HS collected transport rates of 0.1 and 1.0 g/m·s. Data points for sites with fine and coarse beds at East Dallas Creek are marked by dashed circles.

Table 8: HS transport rate predicted from inter-sampler transport relationships for transport rates of 0.01, 0.1, and 1.0 g/m·s.

		a-coefficient	*b*-exponent	r^2	*N*	*p-value*[#]	s_y	CF_{Duan}
Predicted from bedload trap measurements:								
for 0.01 g/m·s	*transp. rates* at 50% Q_{bkf}	7.78E-06	-0.363	0.11	8	0.423	1.68	
	bedload D_{max} at 50% Q_{bkf}	9.01E-03	-2.13	0.16	8	0.330	1.63	
for 0.1g/m·s	***transp. rates* at 50% Q_{bkf}**	**1.88E-05**	**-0.619**	**0.57**	**10**	**0.0121**	**1.03**	**11.6**
	bedload D_{max} at 50% Q_{bkf}	1.32	-3.36	0.48	10	0.0257	1.12	13.7
	D_{max} at 1g/m·s	9.36E-14	6.41	0.48	10	0.0275	1.13	7.03
for 1 g/m·s	***transp. rates* at 50% Q_{bkf}**	**9.20E-03**	**-0.361**	**0.60**	**10**	**0.0089**	**0.56**	**1.94**
	bedload D_{max} at 50% Q_{bkf}	6.01	-1.95	0.50	10	0.0214	0.62	2.10
	D_{max} at 1g/m·s	4.73E-07	3.38	0.41	10	0.0465	0.68	2.13
Predicted from HS measurements:								
for 0.01 g/m·s	*transp. rates* at 50% Q_{bkf}	8.02E-06	-1.32	0.44	8	0.0743	1.33	
	bedload D_{max} at 50% Q_{bkf}	5.53	-4.53	0.40	8	0.0931	1.38	
for 0.1g/m·s	***transp. rates* at 50% Q_{bkf}**	**1.63E-04**	**-1.25**	**0.81**	**10**	**0.0004**	**0.68**	**3.06**
	***bedload* D_{max} at 50% Q_{bkf}**	**370**	**-5.24**	**0.69**	**10**	**0.0027**	**0.86**	**6.83**
	D_{max} at 1g/m·s	1.02E-07	3.14	0.09	10	0.398	1.49	
for 1 g/m·s	***transp. rates* at 50% Q_{bkf}**	**3.52E-02**	**-0.647**	**0.67**	**10**	**0.0038**	**0.51**	**1.59**
	bedload D_{max} at 50% Q_{bkf}	58.2	-2.65	0.55	10	0.0140	0.59	1.76
	D_{max} at 1g/m·s	1.18E-04	2.31	0.15	10	0.265	0.82	

Values printed in gray have *p*-values > 0.05 and are statistically not (or only marginally) significant. Values printed in bold have *p*-values < 0.001 and indicate well-correlated relationships.

The correlations of transport rates measured by bedload traps when the HS sampler collected 1.0 and 0.1 g/m·s with transport characteristics provide two important results. 1) The relationship between bedload trap and HS transport measurements is affected by a stream's transport and bedload D_{max} characteristics (as measured with bedload traps). 2) The relatively well-defined correlations with HS measurements offer the opportunity of predicting inter-sampler transport relationships from HS measurements.

Similar results from correlation analyses and segregation into "red" and "blue" stream groups

Results from the correlation analyses are generally in line with those obtained from classifying streams into two groups. Figure 20 illustrates that HS and bedload trap measurements differ most at sites where bedload transport is well developed at 50% of bankfull flow and comprises medium or larger gravel as the D_{max} particle size. This is characteristic of "blue" streams. By contrast, HS and bedload trap measurements differ least at sites where at 50% of bankfull flow bedload transport is still poorly developed and comprises maximally pea gravel, attributes characteristic of "red" streams. Also, HS and bedload trap measurements differ most at sites where only medium gravel is mobile at a transport rate of 1 g/m·s ("blue" streams), and differ least where at a transport rate of 1 g/m·s coarse gravels are mobile ("red" streams) (Figure 21).

Computations of adjusted HS transport rates

The analyses offer conversion of two HS-sampled transport rates, at 0.1 and 1.0 g/m·s, to those collected with bedload traps. Based on a field-measured HS transport rates at 50% Q_{bkf}, the transport rate that bedload traps would have when the HS measured 0.1 and 1.0 g/m·s can be

computed from the functions provided under "predicted from HS measurements" in Table 8. For example, if a HS collected 0.3 g/m·s at 50% of bankfull flow, then the HS-measured transport rates of 0.1 and 1.0 g/m·s should be adjusted to 0.0007 and 0.08 g/m·s, respectively. Similarly, if a HS collected bedload D_{max} particles of 10 mm, HS-measured transport rates of 0.1 and 1.0 g/m·s should be adjusted to 0.002 and 0.13 g/m·s, respectively. Note that these results need to be multiplied by the Duan (1983) smearing estimate (i.e., by a factor of about 2 in most cases, but a factor of >10 in some cases, see last column of Table 8) to adjust for the inherent underprediction of *y* from *x* in power functions fitted to scattered data.

Figure 17 can be used for predictions of adjusted HS-transport rates over a wider transport rate. It is believed that if adjusted HS transport rates are predicted directly from bedmaterial and bedload characteristics observed in a study stream, results may be more representative of that stream than those obtained from applying one of the correction functions devised for streams categorized either as the "red" or "blue" stream group. Unfortunately, computation of adjusted HS transport rates using the proposed relationships in Table 8 do not provide continuous conversion functions (similar to those listed in Table 5) that can be applied to measured HS transport rates in order to yield the adjusted HS rating curve (Eq. 28). However, a user could devise a continuous function by regressing adjusted HS transport rates *vs*. measured HS transport rates of 0.1 and 1.0 g/m·s.

4.3 Comparison of rating curve and paired data approach

A variety of different inter-sampler transport relationships were computed for total gravel transport for each of the two stream groups (Table 5 and Table 7). The rating curve approach yielded one group-average inter-sampler relationship (Eqs. 15 and 16) per stream group. The paired data approach yielded three results per group depending on the method used to integrate over the streams within each group (Eqs. 22 – 27). All results are combined in Figure 22. The question arises how results vary among computational methods, whether correction functions from both approaches can be used interchangeably for adjusting HS sampling results to those obtained from bedload traps, and whether there is reason to believe that one approach and its results may be more desirable.

4.3.1 Similarities in results from both approaches

Segregation into two groups with similar streams per group

Both the rating curve and the paired data approach clearly suggest that inter-sampler transport relationships segregate into two groups. The lines along which stream groups split are similar for the two approaches. Three of the four streams that fell into the "red" or the "blue" stream group are the same between the two approaches, while two streams switched groups. The similarity among the approaches validates the segregation. While the mean group characteristics of bedload transport vary slightly between the two approaches, threshold values distinguishing between the two group averages are independent of grouping.

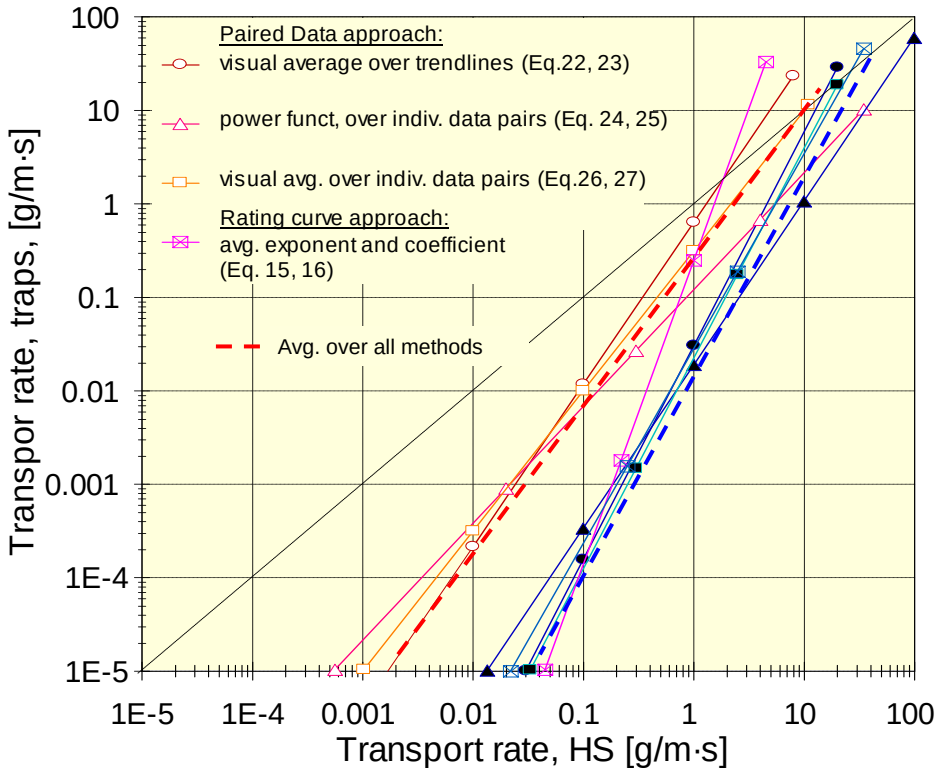

Figure 22: Comparison of inter-sampler transport relationships for total gravel transport (= HS correction functions) within the "red" and "blue" group obtained from various methods applied to the rating curve and paired data approaches. Numbers on graphs refer to equations. Inter-sampler transport relationships from the "red" stream group are plotted in reddish colors and those from the "blue" stream group in bluish colors. Thick dashed lines indicate group averages over all approaches.

Inter-sampler transport relationships differ little among size classes

Inter-sampler transport relationships were computed for individual size fractions for the rating curve and the paired data approach (Figure 9, Figure 10, and Figure 15). Both approaches indicate that inter-sampler differences tend to be slightly larger for small gravel particles compared to larger gravel. However, this trend is neither pronounced nor visible for all study streams. The general similarity among fractional inter-sampler transport relationships in the rating curve approach suggested that the same function may be applied for adjustment of all individual 0.5 phi size fractions (Figure 13).

Similar inter-sampler transport relationships for "blue" streams

Both the rating curve and the paired data approach indicated similar inter-sampler transport relationships for the "blue" stream group, suggesting that methodological differences are not critical when computing correction functions in streams characterized by relatively high transport rates of small to mid-sized gravel. Based on this finding, it appears reasonable to integrate all approaches and submethods (i.e., over Eqs. 15, 23, 25, and 27) and arrive at one inter-sampler

transport relationship to be used for adjustment of HS gravel transport rates for streams in the "blue" group (Figure 22):

$$Q_{B\,trap} = F_{HS} = 0.0235\, Q_{B\,HS}^{\,2.10} \qquad \text{"blue" streams} \qquad (29)$$

Eq. 28 can be used to apply Eq. 29 for correction of a HS-measured gravel bedload rating curve.

4.3.2 Differences in results from both approaches

Inter-sampler transport relationships computed from the rating curve and paired data approach showed several differences. Differences between the two approaches were largest for streams in the "red" group and when the range of transport rates available for analysis was narrow.

Variability among streams follows different patterns in the two approaches

The two approaches indicate a different pattern of variability among streams. In the rating curve approach, inter-sampler transport relationships for "red" and "blue" stream groups differ mostly at their upper ends, i.e., when transport rates are high. In the paired data approach, inter-sampler transport relationships for "red" and "blue" stream groups differ mostly at their lower ends, when transport rates are low. Field experience suggests similarity among samplers when transport is high and large differences (that vary in magnitude among streams) when transport is low. Results from the paired data approach align with field experience rather than the rating curve results.

Different computational response to narrow ranges of measured transport rates

The rating curve and paired data approaches lead to different inter-sampler transport relationships when data available for analysis are limited to a narrow range of transport rates. The rating curve approach creates overly steep inter-sampler transport relationships that may yield negative exponents. In the paired data approach, by contrast, overly flat inter-sampler transport relationships resulted from narrow data ranges. The two approaches differ less when samples used for analysis extend over a wide range of transport rates.

Inter-sampler transport relationships from rating curve approach appear overly steep, particularly for "red" streams

Inter-sampler transport relationships computed from the rating curve approach are straight and steep. By comparison, inter-sampler transport relationships from the paired data approach are either straight and less steep or steep during small transport rates and flatten to approach the 1:1 line when transport is high. For "blue" streams that transport relatively large amounts of small to mid-sized gravel, these differences cause only moderate disagreements in the inter-sampler transport relationships computed from the two approaches. However, the differences are pronounced for "red" streams that typically transport less, but coarser gravel. The "red" stream group is closer to the 1:1 line and intersects at lower transport rates than "blue" streams for both

approaches. However, in the rating curve approach, inter-sampler transport relationships of the "red" group are steeper than the "blue" group; in the paired data approach, the "red" stream group was flatter than the "blue" group.

The steep "red" inter-sampler transport relationships from the rating curve approach indicate that the HS sampler collects at least three orders of magnitude more gravel than bedload traps when transport is low (0.05 g/m·s), and the 1:1 line is intersected at relatively low transport rates of 2 g/m·s. Consequently at transport above 2 g/m·s, the rating curve approach indicates that the HS collects less gravel than bedload traps, up to an order of magnitude less when transport is high. Undersampling by the HS occurs when bedload contains many coarse particles that exceed the size of the HS opening, when sampling time is too short to representatively collect infrequently moving large gravel, or when the HS is perched on cobbles and fine gravel passes under the sampler (see Figure 3). However, the degree of undersampling of the HS computed by the rating curve approach appears to be exaggerated.

Based on the greatly differing results between the rating curve and paired data approach for streams in the "red" group, it is concluded that results from the two approaches cannot be used interchangeably for "red" streams. Together with the interpretation that the rating curve approach exaggerated the degree of undersampling by the HS sampler at high transport, it is not prudent to include the rating curve results when computing the HS correction function for the "red" stream group. Instead, the three correction functions obtained by integrating over the streams within the "red" group in the paired-data approach (Figure 22) (i.e., over Eqs. 22, 24, and 26) were visually averaged. The fitted grand-average correction function can be described as

$$Q_{B\,trap} = F_{HS} = 0.532\ Q_{B\,HS}^{\ 1.58} \qquad \text{"red" streams} \qquad (30)$$

Eq. 28 is used to apply Eq. 30 to a HS-measured rating curve.

5. Discussion

The discussion will address the evaluation of the rating and paired data approaches and include recommendations. Also, recommendations for future study needs will be presented.

5.1 Evaluation of the rating curve and paired data approaches

The rating and paired data approach both have advantages and disadvantages that are discussed below. The advantages and disadvantages are then weighed using a numerical comparison that highlights data requirements, the efforts and accuracy of preliminary computations, as well as the effort and accuracy of the resulting inter-sampler transport relationships (Table 9). The scores for each item ranged between -1 (negative attribute), -0.5 (somewhat negative), 0 (neutral), +0.5 (somewhat beneficial), and + 1 (beneficial attribute), offering five evaluation choices.

5.1.1 Rating curve approach

The major advantage of the rating curve approach is that the computation is straightforward and its results are statistically defensible. The rating curve approach involves all data collected with bedload traps and the HS sampler at a study stream. Using all samples increases the data range, but it may complicate the relationship between the two samplers if the relationship of transport rates versus discharge has scatter or hysteresis. Fitting rating curves to data sets is a laborious step. Another disadvantage in the rating curve approach is that inter-sampler transport relationships tend to become overly steep in "red" streams where transport is low at low flows and includes cobbles at high flows. Overly steep inter-sampler transport relationships also occur when sample size and/or the range of measured transport rates are small.

5.1.2 Paired data approach

The paired data approach requires concurrently measured data. Because hysteresis and other effects causing variability in the relationships between transport rates and flow have little if any effect on the paired data approach, limiting computations to measured data pairs ensures that data used to create data pairs are of high-quality. However, the number of pairs with non-zero transport rates from both samplers rapidly decreases for the coarsest size classes in motion, as the coarsest particle size in motion may not be simultaneously contained in the bedload trap or the HS sample, and scarcity of data pairs for the coarsest particles is of concern.

Transport relationships of data pairs from bedload traps *vs.* the HS sampler have a curved trend in some streams, and this feature requires a curvilinear function. A guided polynomial function, fitted curve segments, or a computationally involved LOWESS fit may be used. All of these procedures are time-consuming and result in functions more difficult to engage in subsequent computations than power functions. Visually fitted procedures are prone to some degree of operator variability. However, with plotted data extending over several log cycles, functions fitted by multiple operators should not vary by more than approximately half a log unit (i.e., a factor of about ±3.2) in *x* and *y*-direction. This degree of variability is often less than the error introduced by a statistical regression that is visually too flat or does not account for the proper curvature of the plotted data. Another argument that supports operator guidance is that the plotted data have a context, such as the relationship to neighboring size classes (that may have a wider range of sampled transport rates) or similarity with streams in which a wider range of transport rates and particle sizes was collected. Being aware of these relationships, an operator can often make a valid estimate of the data trend up to approximately half a log unit beyond the plotted data and use this information to guide the fit.

An advantage of the paired data approach is that its inter-sampler transport relationships align better with field observations. Transport rates and collected particle sizes differ among the two samplers when transport rates are small. Transport rates from the two samplers approach each other with increasing transport, and their ratios remain in the vicinity of the 1:1 line during high transport. The paired data approach is able to reflect this relationship.

The paired data approach offers the added possibility of using transport rates and the bedload D_{max} size collected in the HS sampler at 50% of bankfull flow to predict the bedload trap transport rate associated with the HS collected rate of 0.1 and 1.0 g/m·s. The ability to predict

correction factors for individual streams is likely to represent conditions in a study stream better than classification of a study stream into one of two stream groups and applying group-average correction functions.

Table 9: Evaluation and scoring of various attributes within the rating curve and the paired data approach.

Computational component		Rating curve approach	Score	Paired data approach	Score
Source data	Requirements	All bedload samples for which flow is known; but data quality may be hampered by hysteresis	+0.5	Only concurrently measured data pairs; results in fewer data but excludes hysteresis effects	0
	Effect of limitations	Rating curves may expand information beyond measured range (or introduce error).	0	Non-zero data pairs become scarce for infrequently transported large particles.	-1
Preliminary Computation	Time and effort	Fitting rating curves is an extra step.	-1	Compilation of data pairs not too laborious.	0
	Accuracy	Fitting rating curves can be error prone	-1	Little or no error involved in creating data pairs.	+0.5
Inter-sampler transport relationships:	Time and effort of computations	Simple computation	+1	For curved data trends: Visually fitting curves or guiding a polynomial fit is laborious.	-1
	Potential for operator guidance	Operator cannot guide the fit.	-1	Operator guidance justified because operators "knows" expected trends.	+1
	For large *n* and wide range of measured transport rates	Somewhat steep results.	-0.5	Somewhat flat results, but correctable by guiding the fit.	+0.5
	For small *n* or narrow range of measured transport rates	Overly steep and even negative results.	-1	Results too flat, but somewhat correctable by guiding the fit.	+0.5
	Statistical rigor	Statistically defensible.	+1	Guiding polynomial introduces some degree of operator variability.	-0.5
	Perceived accuracy of result	Potentially inaccurate, particularly when *n* and/or range of measured transport rates are small.	-1	A known, small degree of inaccuracy; but no major errors.	+0.5
	Applicability of results	User can differentiate among "red" and "blue" stream group and select a group-specific adjustment function. Adjustment functions cannot be determined based on HS sampling results alone.	0	User can differentiate among "red" and "blue" stream group and select a group-specific adjustment function; User can adjust HS transport rates based on measurements made with either traps or HS.	+1
Total score			-3.0		+1.5

Positive and negative evaluations are visually enhanced by light green and light purple shadings, respectively.

It is concluded that the paired data approach was more suitable for this study (see also scoring in Table 9). The relative small error introduced by operator variability when guiding or fitting inter-sampler transport relationships outweighs the potentially large error introduced by the rating curve approach that offers no operator guidance. However, the selection of the study approach may be influenced by the source data, particularly if concurrently measured data pairs are scarce. The rating curve approach can be improved by using functions with multiple segments or a curved function to optimize the rating curve fit. Both approaches yield poor results in streams that have a narrow range of measured transport rates as well as a large amount of data scatter, but a salient operator can salvage the data by guiding or handfitting functions.

5.2 Future study needs

Several topics for future work arise from the analyses in this study. They include 1) the need for more field data, 2) the need for more extensive computations (e.g., using curved or segmented regression functions and extending computations to individual size fractions), 3) the need for analyzing the effects and variability among computational methods, and 4) the need for validation of computed results. These points are discussed below.

More field data needed to improve accuracy of correction functions

Only 5 of the 9 study streams have a wide data range that extends from around 15% to 140% of bankfull flow, and one of these streams (Cherry Creek) has a small sample size. Inter-sampler transport relationships are not well developed when the range of sampled flows, and thus the range of measured transport rates, is narrow. The resulting inter-sampler transport relationships are overly steep in the rating curve approach and overly flat in the paired data approach. Consequently, the computed inter-sampler transport relationship may not be truly representative of the conditions of bedmaterial and bedload transport in that particular stream. When the measured range of transport rates is narrow, data are lacking particularly for medium and large gravel. Data sets collected over a wide range of transport rates are needed to establish accurate inter-sampler transport relationships for medium and coarse gravel, and to differentiate between differences due to computational artifacts and those due to transport mechanisms of coarse particles or the way that coarse particles are trapped in a sampler.

Formulate correction functions for individual particle-size fractions

Analyses of how inter-sampler transport relationships from both approaches were related to and predictable from parameters of bedmaterial and bedload transport were limited to total gravel transport. The study indicated that the variability among size fractions is comparatively low, and that some streams have somewhat larger inter-sampler transport ratios for smaller gravel. To improve correction of HS transport rates, the analyses should be extended to involve individual particle-size fractions in future studies. To include particle size fractions of medium and coarse gravel in these computations, more data sets are needed that extend over a wide range of flows and transport rates.

Cover stream types other than mountain gravel-bed streams

Results from this study pertain to armored coarse gravel and cobble beds typical of mountain gravel-bed streams. The wide variability of computed inter-sampler transport relationships

among these streams suggests that correction functions are stream-type specific, and that correction functions computed in this study should not be applied to streams other than the types analyzed in this study. To expand the applicability of correction functions, studies are needed in other kinds of streams, such as streams with fine gravel beds, cobble beds that transport mostly sand, and mixed sand-gravel beds. It could likewise be advisable to conduct studies where samples from a HS sampler are compared to those from samplers not affected by HS-typical restrictions other than bedload traps.

Select curved or segmented functions, if necessary, to improve the fit

The rating curve approach was based on power functions that were fitted to bedload rating curves. Fitting power functions is a common practice (e.g., Barry et al. 2004; King et al. 2004, Bunte et al. 2008), and they are convenient for subsequent computations. However, power functions (straight lines in log-log space) do not necessarily provide the best fit in all situations. If a HS sampler collects large amounts of fine gravel at low flow during otherwise very low transport rates, a knickpoint appears in the rating curve at flows less than half bankfull (not to be equated with the breakpoints observed in linear plots at around 80% of bankfull flow (Ryan et al. 2002, 2005)). A change in rating curve steepness can be addressed by fitting curved functions, such as polynomial functions, by using a LOWESS fit, or by fitting two (or more) power function segments. A better representation of the rating curve would improve inter-sampler transport relationships computed from the rating curve approach. However, using curved functions increases the computational effort and, in case of a LOWESS fit, exceeds spreadsheet capabilities. While straight rating curves fitted to the relationship of transport versus discharge necessarily result in straight inter-sampler transport relationships, curved rating curves result in curved inter-sampler transport relationships. Curved inter-sampler transport relationships represent the true trend of plotted data pairs better in some streams, as could be seen from the paired data approach.

Comparison of methods for computing group averages

In this study, group-averaged inter-sampler transport relationships were computed in several ways depending on the data source: 1) The rating curve approach suggested that arithmetic and geometric averaging over the exponents and coefficients, respectively, from fitted power functions was a suitable method. In the paired data approach, 2) fitted inter-sampler transport relationships were visually averaged over the streams within a stream group, 3) power function curves were fitted over all data within a group without regard to individual streams, and 4) functions fitted by eye to integrate over all data within a group without regard to individual streams. Computational differences within a stream group were less different than results between the two stream groups. Nevertheless, the consequences of selecting either one of these methods should be further explored.

Validate correction functions

The adjustment functions computed in this study have not been validated in streams that are not part of this study. To assess the accuracy of the proposed correction functions, they should be applied to data sets where HS samples can be paired either with bedload trap samples or with data from another sampler that is not subject to HS-typical restrictions, such as a vortex or pit sampler. However, care must be taken to ensure that bedload and bedmaterial conditions in a validation stream meet those of the study streams.

6. Summary

This study computed transport relationships between bedload traps and a HS sampler based on field data obtained from intensive sampling with both samplers in nine mountain gravel-bed study streams. The computed inter-sampler transport relationships generally display a similar pattern, with transport rates of the HS being orders of magnitude lower than those collected with bedload traps, but approaching or intersecting the 1:1 line at high transport. However, the computed inter-sampler transport relationships vary not only between the two computational approaches, but also among streams, and to a smaller degree among bedload particle-size fractions. Results from this study are limited to coarse-bedded, armored, mountain gravel-bed streams.

The rating and paired data approaches suggested that inter-sampler transport relationships computed for the study streams segregate into two groups. Inter-sampler transport relationships in the group called "red" in this report stayed relatively close to the 1:1 line and intersected at relatively low flows. The "blue" group remained further away from the 1:1 line (i.e., larger difference in transport rates between the two samplers when transport was low) and approached the 1:1 line at higher flows. Three of the four streams comprising each group were identical in the two approaches. Compared to "blue" streams, streams in the "red" group transported smaller amounts of fine gravel at low flows but coarser gravel at high flows. Such ("red") streams exhibit generally steep rating and flow competence curves, smaller bedload D_{max} particle sizes and transport rates at a moderate flow of 50% Q_{bkf}, but larger bedload D_{max} particles at a fixed transport rate of 1 g/m·s. Threshold values are provided to differentiate these parameters into the "red" and "blue" stream groups, and they permit a user to identify the appropriate group for a specific study stream.

The inter-sampler transport relationships identified for the "blue" stream group are relatively similar for the two approaches, as well as among the various submethods employed in the paired data approach used to average over the streams within the group. This suggested that any of the approaches may be used interchangeably and justified formulating one HS correction function for "blue" streams:

$$Q_{B\,trap} = F_{HS} = 0.0235\, Q_{B\,HS}^{\,2.10} \qquad \text{"blue" streams} \qquad (29)$$

The inter-sampler transport relationships computed within the "red" (steeper) stream group differ between the two approaches. In the rating curve approach, the "red" group had steeper inter-sampler transport relationships than the "blue" group; in the paired data approach, the "red" group of inter-sampler transport relationships was flatter than the "blue" group. The rating curve result averaged over the "red" stream group is considerably steeper than any of the three group-average results obtained by the paired data approach. The rating curve and the paired data approach cannot be used interchangeably for streams in the "red" group (i.e., when transport rates are low at low flows, and particles are coarse at high flow). Because the rating curve result deviated from the general trend of inter-sampler transport relationships obtained for the "red" group in the paired data approach, the rating curve result was excluded when formulating the average HS correction function for "red" streams which was given as

$$Q_{B\,trap} = F_{HS} = 0.532\, Q_{B\,HS}^{\,1.58} \qquad \text{"red" streams} \qquad (30)$$

Whether the rating curve or paired data approach should be selected for determining inter-sampler transport relationships, and therefore HS correction functions, depends on the kind of data available and conditions in a study stream. The rating curve approach is best applied when bedload transport-discharge relationships for both samplers can be accurately defined by a power function (always problematic for the coarsest size classes for which relatively few samples exist). If a fitted power function does not accurately reflect the rating curve over the entire range of measured flows, then the resulting inter-sampler transport relationship may not be accurate. Determining properly fitting rating curves can be challenging, requiring the use of polynomial functions, LOWESS fits, or function segments.

The paired data approach avoids the time-consuming and error-prone step of fitting rating curves and fits regression functions directly to pairs of bedload samples collected concurrently with bedload traps and HS, provided that data pairs exist in sufficient quantity. Ratios of bedload trap transport rates versus those collected with a HS sampler may assume either a straight trend (in log-log space), or a curved trend. Curve-fitting difficulties again arise for curved inter-sampler transport relationships, requiring either guided polynomial functions (as used in this study) or the computationally more involved methods of fitting function segments, or a LOWESS fit.

For the present study, the paired data approach appears to have yielded more accurate results, not least because it immediately made clear that curved functions (in log-log space) were needed to appropriately represent the trend of inter-sampler transport relationships. The advantage gained by presenting plotted data in a visually satisfying way outweighs inaccuracies introduced by the potential for operator subjectivity when guiding a polynomial fit and by the lack of statistical rigor.

Acknowledgements
Field work to collect the data used in this study could not have been accomplished without the efforts of Kurt Swingle. The field studies were funded by the USDA Forest Service Stream Systems Technology Center. We thank John Potyondy for encouragement and good advice.

The project described in this publication was supported by Grant/Cooperative Agreement Number 08HQGR0142 from the United States Geological Survey. Its contents are solely the responsibility of the authors and do not necessarily represent the official views of the USGS. The views and conclusions contained in this document are those of the authors and should not be interpreted as representing the opinions or policies of the U.S. Government. Mention of trade names or commercial product does not constitute their endorsement by the U.S. Government.

7. References

Barry, J. J., J. M. Buffington, and J. G. King, 2004. A general power equation for predicting bed load transport rates in gravel bed rivers, *Water Resources Research*, 40, W10401, doi:10.1029/2004WR003190.

Beschta, R.L., 1981. Increased bag size improves Helley-Smith bed load sampler for use in streams with high sand and organic matter transport. In: *Erosion and Sediment Transport Measurement.* IAHS Publ. no. 133: 17-25.

Bunte, K. and S.R. Abt, 2001. Sampling Surface and Subsurface Particle-Size Distributions in Wadable Gravel- and Cobble-Bed Streams for Analysis in Sediment Transport, Hydraulics, and Streambed Monitoring. USDA Forest Service, Rocky Mountain Research Station, Fort Collins, CO, *General Technical Report* RMRS-GTR-74, 428 pp. [Online] Available: http://www.fs.fed.us/rm/pubs/rmrs/gtr_74.html

Bunte, K. and S.R. Abt, 2005. Effect of sampling time on measured gravel bed load transport rates in a coarse-bedded stream. *Water Resources Research*, *41*, W11405, doi:10.1029/2004WR003880.

Bunte, K. and K.W. Swingle, 2008. Bedload traps and the Helley-Smith sampler deployed on the bed and on ground plates: Sampling results from East Dallas Creek, CO. Report submitted to Stream Systems Technology Center, USDA Forest Service, Rocky Mountain Research Station, Fort Collins, CO, 104 pp.

Bunte, K., S.R. Abt, and K.W. Swingle, 2006. Predictability of bedload rating and flow competence curves from bed armoring, stream width and basin area. Proceedings of the Eighth Federal Interagency Sedimentation Conference, April 2-6, 2006 in Reno, NV., Session 4A-2, 9 pp. [CD ROM] and [Online] Available: http://pubs.usgs.gov/misc_reports/FISC_1947-2006/html/pdf.html

Bunte, K., K. Swingle, and S.R. Abt, 2007a. Guidelines for using bedload traps in coarse-bedded mountain streams: Construction, installation, operation and sample processing. General Technical Report RMRS-GTR-191, Fort Collins, CO, U.S. Department of Agriculture, Forest Service, Rocky Mountain Research Station, 91 pp. [Online] Available: http://www.fs.fed.us/rm/pubs/rmrs_gtr191.pdf

Bunte, K., K.W. Swingle and S.R. Abt, 2007b. Adjustment Needed for Helley-Smith Bedload Samples Collected at low Transport Rates on Coarse Gravel Beds. Abstract. *Eos Trans. AGU*, 88(52), Fall Meet. Suppl., Abstract H41A-0132. [Online] Available: http://www.agu.org/meetings/fm07/waisfm07.html

Bunte, K., K.W. Swingle and S.R. Abt, 2009a. Necessity and difficulties of field calibration of signals from surrogate techniques in gravel-bed streams: possibilities for bedload trap samples. U.S. Geological Survey Scientific Investigations Report (*in press*).

Bunte, K., S.R. Abt, J.P. Potyondy, and S.E. Ryan, 2004. Measurement of coarse gravel and cobble transport using a portable bedload trap. *Journal of Hydraulic Engineering* 130(9): 879-893.

Bunte, K., S.R. Abt, J.P. Potyondy and K.W. Swingle, 2008. A comparison of coarse bedload transport measured with bedload traps and Helley-Smith samplers. *Geodinamica Acta* 21(1/2): 53-66 (supplement, Gravel-Bed Rivers VI Meeting)

Bunte, K., S.R. Abt, K.W. Swingle, and J.P. Potyondy, 2009b. Comparison of three pebble count protocols (EMAP, PIBO, and SFT) in two mountain gravel-bed streams. *Journal of the American Water Resources Association, in press.*

Childers, D., 1991. Sampling differences between the Helley-Smith and BL-84 bedload samplers. In: *Proceedings of the Fifth Federal Interagency Sedimentation Conference, March 18-21, 1991, Las Vegas, NV.,* Subcommittee of the Interagency Advisory Committee on Water Data, p. 6.31-6.38.

Childers, D., 1999. Field comparison of six-pressure-difference bedload samplers in high energy flow. U.S. Geological Survey, *Water Resources Investigations Report* 92-4068, Vancouver, WA, 59 pp.

Druffel, L., W.W. Emmett, V.R. Schneider, and J.V. Skinner, 1976. Laboratory hydraulic calibration of the Helley-Smith bedload sediment sampler. *U.S. Geological Survey Open-File Report* 76-752, 63 pp.

Duan, N., 1983. Smearing estimate: a nonparametric retransformation method. *Journal of the American Statistical Association* 87: 605-610.

Emmett, W.W., 1980. A Field Calibration of the Sediment Trapping Characteristics of the Helley-Smith Bedload Sampler. *Geological Survey Professional Paper* 1139, Washington, DC.

Emmett, W.W., 1981. Measurement of bed load in rivers. In: *Erosion and Sediment Transport Measurements*, IAHS Publ. no. 133: 3-15.

Emmett, W.W., 1984. Measurement of bedload in rivers. In: *Erosion and Sediment Yield: Some Methods of Measurement and Modelling.* R.F. Hadley and D.E. Walling (eds.), Geo Books, Norwich, Great Britain, p. 91-109.

Ferguson, R.I., 1986. River loads underestimated by rating curves. *Water Resources Research* 22(1): 74-76.

Ferguson, R.I., 1987. Accuracy and precision of methods for estimating river loads. *Earth Surface Processes and Landforms* 12: 95-104.

Gaudet, J.M., A.G. Roy and J.L. Best, 1994. Effects of orientation and size of Helley-Smith sampler on its efficiency. *Journal of Hydraulic Engineering* 120 (6): 758-766.

Gray, J.R., R.H. Webb and D.W. Hyndman, 1991. Low-flow sediment transport in the Colorado River. *Proceedings of the Fifth Federal Interagency Sedimentation Conference*, March 18-21, 1991, Las Vegas, Nev., Subcommittee on Sedimentation of the Interagency Advisory Committee on Water Data, p. 4.63-4.71.

Helley, E.J. and W. Smith, 1971. Development and calibration of a pressure-difference bedload sampler. USDI, Geological Survey, Water Resources Division, Open File Report, Menlo Park, California, 18pp.

Hirsch, R.M., D.R. Helsel, T.A. Cohn and E.J. Gilroy, 1993. Statistical analysis of hydrological data. In: *Handbook of Hydrology*, Maidment, D.R. (ed.) McGraw-Hill, New York.

Horowitz, A.J., 2003. An evaluation of sediment rating curves for estimating suspended sediment concentrations for subsequent flux calculations. *Hydrological Processes* 17: 3387–3409, DOI: 10.1002/hyp.1299.

Hubbell, D.W., H.H. Stevens, J.V. and J.P. Beverage, 1985. New approach to calibrating bed load samplers. *Journal of Hydraulic Engineering* 111(4): 677-694.

Hubbell, D.W., H.H. Stevens Jr., J.V. Skinner, and J.P. Beverage, 1987. Laboratory Data on Coarse-Sediment Transport for Bedload-Sampler Calibrations. *U.S. Geological Survey Water-Supply Paper* 2299*:* 1-31. http://pubs.er.usgs.gov/pubs/wsp/wsp2299/

Johnson, C.W., R.L. Engleman, J.P. Smith and C.L. Hansen, 1977. Helley-Smith bed load samplers. *Journal of the Hydraulics Division, ASCE,* 103 (HY10): 1217-1221.

King, J.G., W.W. Emmett, P.J. Whiting, R.P. Kenworthy and J.J. Barry, 2004. *Sediment transport data and related Information for Selected Coarse-Bed Streams and Rivers in Idaho*. USDA Forest Service, Rocky Mountain Research Station, General Technical Report RMRS-GTR 131, 26 pp. [Online] Available: http://www.fs.fed.us/rm/pubs/rmrs_gtr131.html

Koch, R.W. and G.M. Smillie, 1986. Bias in hydrologic prediction using log-transformed prediction models. *Water Resources Bulletin* 22(5): 717-723.

Kuhnle, R.A., 1992. Fractional transport rates of bedload on Goodwin Creek. In: *Dynamics of Gravel Bed Rivers*. P. Billi, R.D. Hey, C.R. Thorne and P. Tacconi (eds.), John Wiley, Chichester, p.141-155.

O'Brien, J.S., 1987. A case study of minimum streamflow for fishery habitat in the Yampa River. In: *Sediment Transport in Gravel-Bed Rivers*. C.R. Thorne, J.C. Bathurst and R.D. Hey (eds.), John Wily and Son, Chichester, UK, p. 921-948.

O'Leary, S.J. and R.L. Beschta, 1981. Bed load transport in an Oregon Coast Range stream. *Water Resources Bulletin* 17(5): 886-894.

Pitlick, J.C., 1988. Variability of bed load measurement. *Water Resources Research* 24(1): 173-177.

Ryan, S.E., 2005. The use of pressure-difference samplers in measuring bedload transport in small, coarse-grained alluvial channels, in: Proc. Federal Interagency Sediment Monitoring Instrument and Analysis Workshop**,** September 9-11, 2003, Flagstaff, Arizona, J.R. Gray, ed.: *U.S. Geological Survey Circular* 1276, 78 p. available on the Web, accessed August 21, 2008, at http://water.usgs.gov/osw/techniques/sediment/sedsurrogate2003workshop/listofpapers.html

Ryan, S.E. and L.S. Porth, 1999. A field comparison of three pressure-difference bedload samplers. *Geomorphology* 30: 307-322.

Ryan, S.E. and C.A. Troendle, 1997. Measuring bedload in coarse-grained mountain channels: procedures, problems, and recommendations. In: *Water Resources Education, Training, and Practice: Opportunities for the Next Century*. American Water Resources Association Conference, June 29-July 3, Keystone, CO, p. 949-958.

Ryan, S.E., L.S. Porth and C.A. Troendle, 2002. Defining phases of bedload transport using piecewise regression. *Earth Surface Processes and Landforms*, 27(9): 971-990.

Ryan, S.E., L.S. Porth and C.A. Troendle, 2005. Coarse sediment transport in mountain streams in Colorado and Wyoming, USA. *Earth Surface Processes and Landforms* 30: 269–288. DOI: 10.1002/esp.1128

Sterling, S.M. and M. Church, 2002. Sediment trapping characteristics of a pit trap and the Helley-Smith sampler in a cobble gravel-bed river. *Water Resources Research* 38(6), 10.1029/2000WR000052, 2002.

Thomas, R.B. and J. Lewis, 1993. A new model for bed load sampler calibration to replace the probability-matching method. *Water Resources Research* 29 (3): 583-597.

Thompson, D.M., 2008. The influence of lee sediment behind large bed elements on bedload transport rates in supply-limited channels. *Geomorphology* 99: 420–432

Vericat, D., M. Church and R.J.Batalla, 2006. Bed load bias: Comparison of measurements obtained from using two (76 and 152 mm) Helley-Smith samplers in a gravel bed river. *Water Resources Research* 42, W01402, doi:10.1029/2005WR004025.

Wilcox, M.S., C.A. Troendle and J.M. Nankervis, 1996. Bedload transported in gravelbed streams in Wyoming. Proceedings of the Sixth Federal Interagency Sedimentation

Conference, March 10-14, Las Vegas, Nevada. Interagency Advisory on Water Data, Subcommittee on Sedimentation, Vol. 2: VI.28-VI.33.

Appendices

A. Figures provided for illustration of information in Section 1

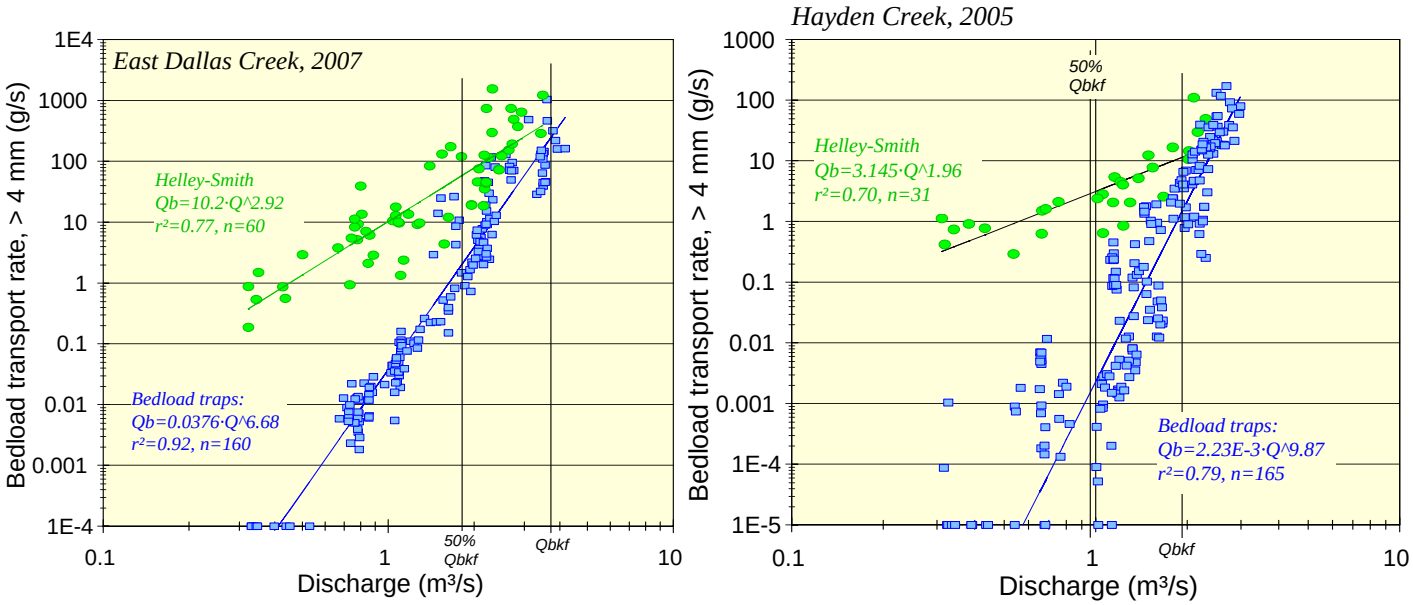

Figure A1: Sampling results from bedload traps and the HS sampler deployed directly on the bed. Examples from East Dallas Creek (left) and Hayden Creek (right).

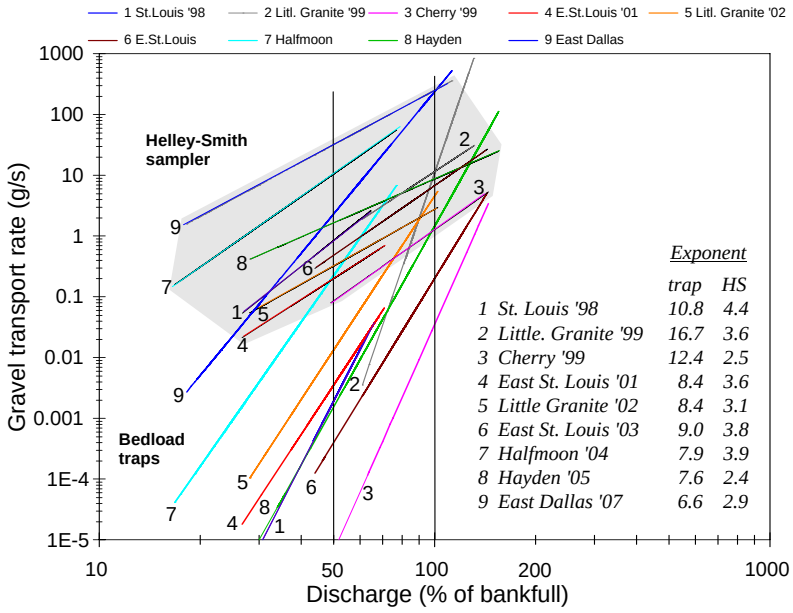

Figure A2: Gravel transport rates plotted versus percent of bankfull flow for bedload traps and the HS sampler at all study streams. Transport relationships measured with the HS sampler are within the gray-shaded area.

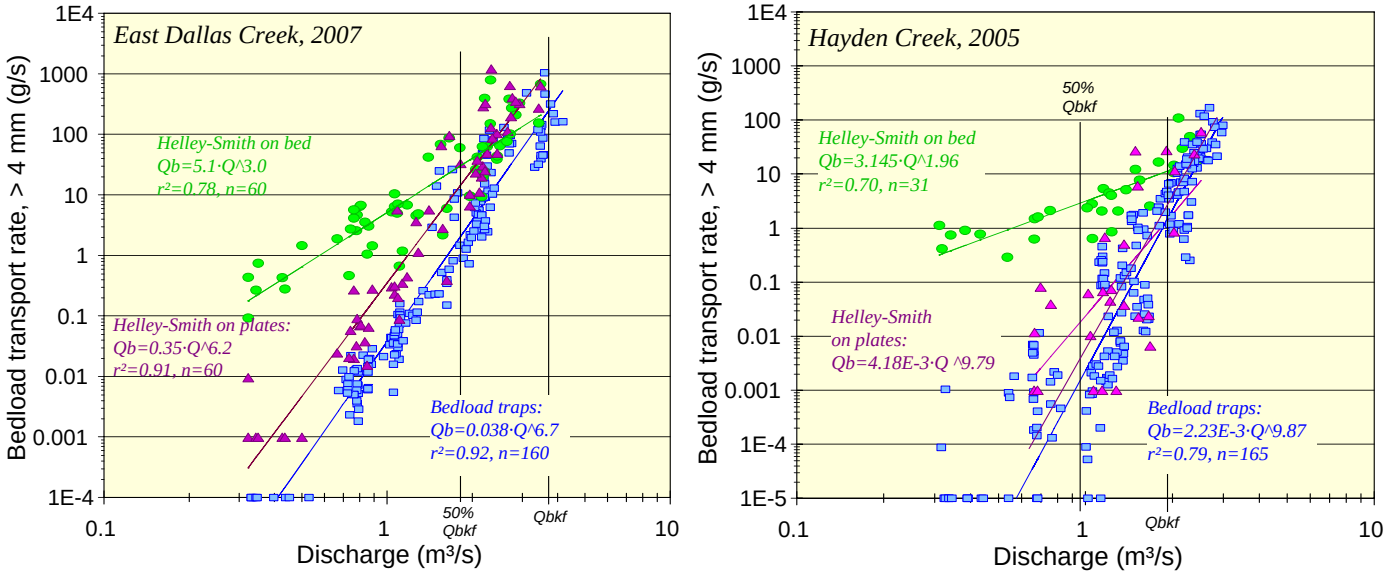

Figure A3: Sampling results from bedload traps (blue symbols) and the HS sampler deployed directly on the bed (green symbols) and on ground plates (magenta symbols). Examples from East Dallas Creek (left) and Hayden Creek (right) (from Bunte and Swingle 2008; Bunte et al. 2007b).

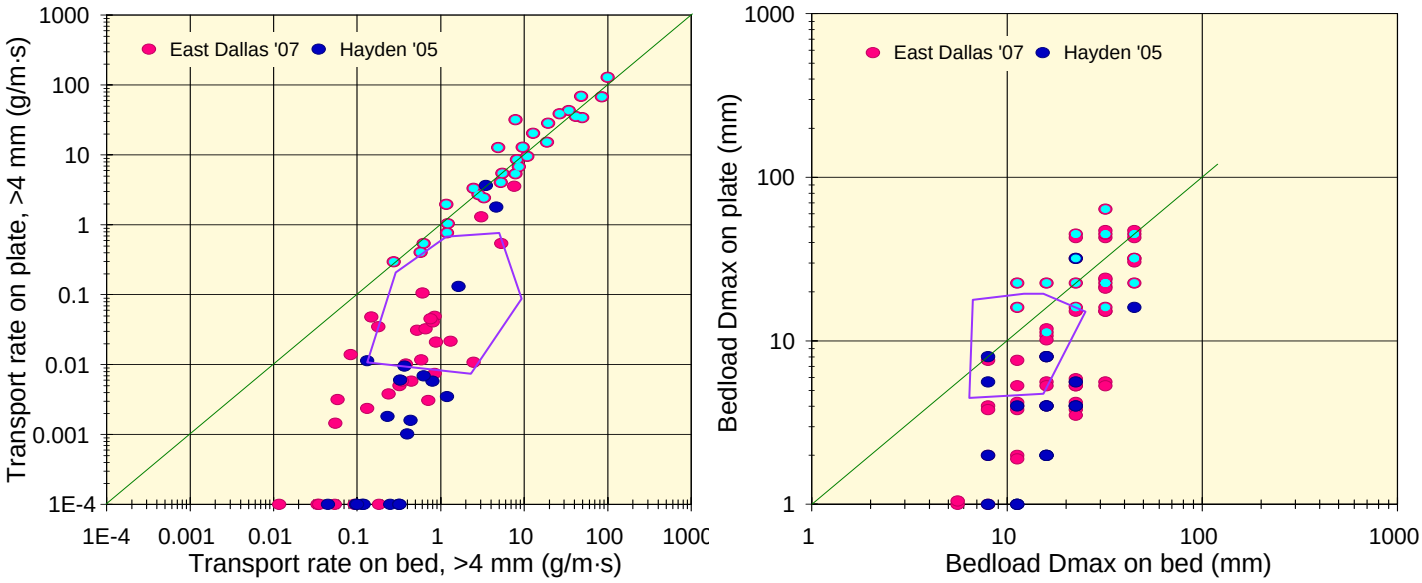

Figure A4: Relationship of sampling results obtained for HS samples collected on ground plates and on the bed: bedload transport rates (left) and bedload D_{max} particle sizes (right). For data that would otherwise plot on top of each other, data points are slightly shifted to visualize all samples. The light-blue overlay symbols are applied to the same group of samples in both plots. When transport is high, samples with similar transport rates for both HS deployments tend to have similar D_{max} particle sizes. When transport is low, on-bed samples with larger transport rates also tend to have larger D_{max} particles.

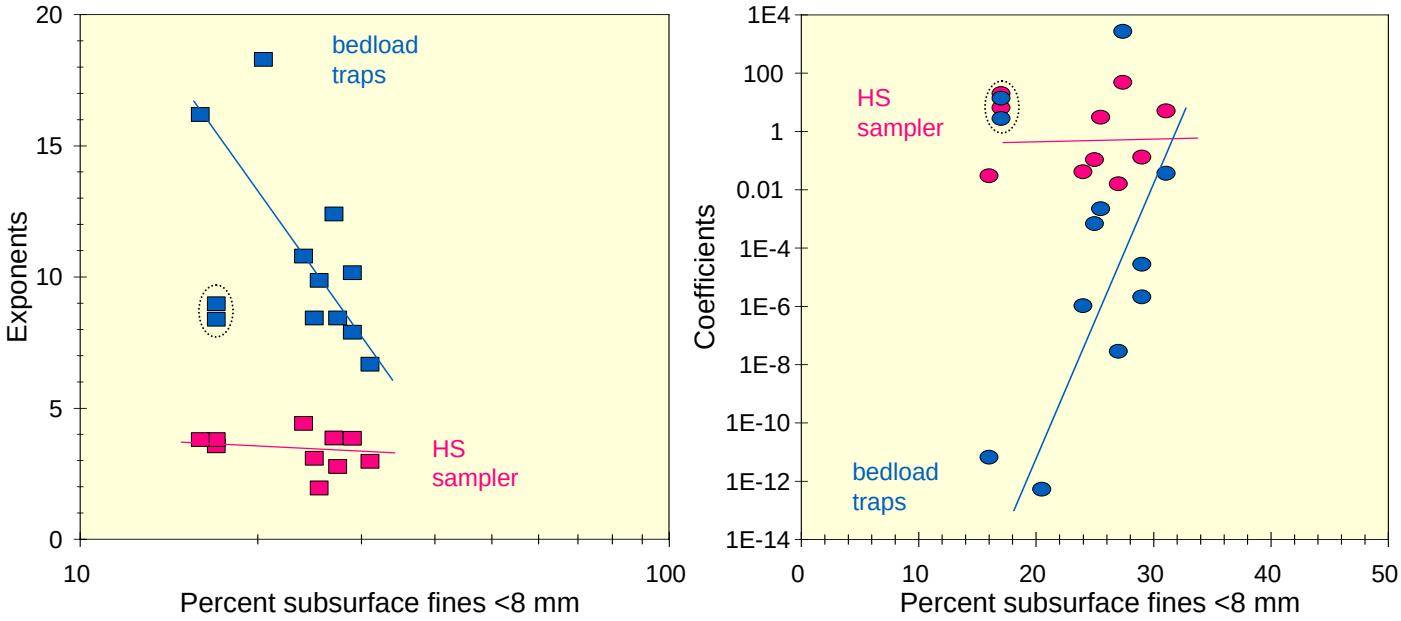

Figure A5: Relationships of exponents (left) and coefficients (right) of gravel bedload rating curves fitted to gravel transport rates collected with bedload traps and the HS sampler with the percent subsurface fines < 8 mm. While there is hardly any trend for HS gravel rating curves, the trend is moderately well developed for gravel bedload rating curves measured using bedload traps. One step-pool stream (circled data points), however, appears to deviate from the general trends observed for bedload traps.

B. Tables 11 to 17

Table 10: Parameters of power function regressions fitted to data of transport rates (g/m·s) versus discharge (m^3/s) for individual size classes (mm) (= fractional transport relationships) and for all gravel size classes combined (=total gravel transport relationships), as well as for data of bedload D_{max} particle sizes (mm) versus discharge (m^3/s) (=flow competence curves). Table 11 is presented in two parts for each study site, once for measurements made with bedload traps and once for the HS sampler.

Cherry Creek	Bedload particle-size classes								
Bedload traps	4 - 5.6 mm	5.6 - 8 mm	8 - 11.2 mm	11.2 - 16 mm	16 - 22.4 mm	22.4 - 32 mm	32 - 45 mm	all gravel sizes	D_{max} (mm)
constant	-6.70	-6.62	-6.58	-7.78	-8.46	-6.64	-5.26	-7.21	-0.09
a-coefficient	2.00E-07	2.41E-07	2.60E-07	1.66E-08	3.46E-09	2.29E-07	5.50E-06	6.10E-08	8.15E-01
Std. err of y	0.54	0.44	0.38	0.42	0.51	0.22	0.28	0.59	0.13
$CF_{(Ferg)}$	2.15	1.69	1.48	1.60	1.98	1.14	1.23	2.55	1.04
$CF_{(Duan)}$	1.59	1.39	1.25	1.34	1.33	1.10	1.16	1.72	1.04
r^2	0.87	0.88	0.87	0.64	0.59	0.45	0.15	0.89	0.92
n	17	14	12	9	9	8	7	18	18
b-exponent	8.55	8.51	8.55	10.48	11.36	8.23	5.82	10.71	2.60
p-values	<<0.05	<<0.05	<<0.05	<<0.05	0.0157	0.0698	0.383	<<0.05	<<0.05

Cherry Creek	Bedload particle-size classes								
Helley-Smith	4 - 5.6 mm	5.6 - 8 mm	8 - 11.2 mm	11.2 - 16 mm	16 - 22.4 mm	22.4 - 32 mm	32 - 45 mm	all gravel sizes	D_{max} (mm)
constant	-3.14	-2.96	-2.34	-1.64	-1.22	-1.30		-2.72	0.68
a-coefficient	7.28E-04	1.10E-03	4.52E-03	2.31E-02	5.98E-02	5.06E-02		1.91E-03	4.73
Std. err of y	0.59	0.52	0.40	0.16	0.38	0.17		0.68	0.20
$CF_{(Ferg)}$	2.55	2.07	1.54	1.07	1.47	1.08		3.44	1.12
$CF_{(Duan)}$	2.43	2.07	1.62	1.06	1.21	1.03		2.77	1.10
r^2	0.46	0.46	0.38	0.31	0.070	0.57		0.43	0.28
n	20	18	17	12	4	3		21	21
b-exponent	3.53	2.99	1.88	0.666	0.583	1.55		3.79	0.81
p-values	<<0.05	0.00191	0.00793	0.0606	0.735	0.457		0.00134	0.385

East Dallas Creek	Bedload particle-size classes								
Bedload traps	4 - 5.6 mm	5.6 - 8 mm	8 - 11.2 mm	11.2 - 16 mm	16 - 22.4 mm	22.4 - 32 mm	32 - 45 mm	all gravel sizes	D_{max} (mm)
constant	-2.72	-2.91	-3.07	-3.21	-3.21	-3.28	-3.63	-2.33	1.02
a-coefficient	1.90E-03	1.24E-03	8.61E-04	6.20E-04	6.10E-04	5.27E-04	2.34E-04	4.71E-03	10.47
Std. err of y	0.38	0.43	0.49	0.56	0.59	0.52	0.53	0.43	0.11
$CF_{(Ferg)}$	1.46	1.62	1.89	2.30	2.49	2.04	2.09	1.64	1.03
$CF_{(Duan)}$	1.53	1.93	2.60	3.13	2.65	2.05	3.37	1.97	1.03
r^2	0.91	0.91	0.90	0.84	0.70	0.67	0.66	0.92	0.87
n	157	157	148	121	90	76	56	160	160
b-exponent	5.57	6.20	6.68	6.94	6.63	6.53	6.71	6.71	1.32
p-values	<<0.05	<<0.05	<<0.05	<<0.05	<<0.05	<<0.05	<<0.05	<<0.05	<<0.05

East Dallas Creek			Bedload particle-size classes
Bedload traps	45 - 64 mm	64 - 90 mm	
constant	-3.61	-2.29	
a-coefficient	2.48E-04	5.07E-03	
Std. err of y	0.44	0.45	
$CF_{(Ferg)}$	1.67	1.71	
$CF_{(Duan)}$	1.73	1.50	
r^2	0.66	0.31	
n	36	9	
b-exponent	6.22	3.93	
p-values	<<0.05	0.118	

East Dallas Creek				Bedload particle-size classes				
Helley-Smith	4 - 5.6 mm	5.6 - 8 mm	8 - 11.2 mm	11.2 - 16 mm	16 - 22.4 mm	22.4 - 32 mm	32 - 45 mm	all gravel sizes	D_{max} (mm)
constant	-0.82	-0.92	-1.06	-1.03	-1.04	-0.59	-0.58	-0.19	1.22
a-coefficient	0.152	0.121	0.087	0.094	0.090	0.259	0.265	0.64	16.73
Std. err of y	0.38	0.45	0.55	0.53	0.46	0.43	0.32	0.44	0.16
$CF_{(Ferg)}$	1.47	1.70	2.25	2.08	1.76	1.61	1.31	1.68	1.07
$CF_{(Duan)}$	1.51	1.66	1.99	1.96	1.75	1.63	1.28	1.62	1.06
r^2	0.76	0.75	0.66	0.65	0.63	0.49	0.39	0.78	0.59
n	60	60	57	50	40	34	20	60	60
b-exponent	2.39	2.73	2.99	3.03	3.12	1.87	1.81	2.97	0.670
p-values	<<0.05	<<0.05	<<0.05	<<0.05	<<0.05	<<0.05	0.00302	<<0.05	<<0.05

East Dallas Creek		Bedload particle-size classes
Helley-Smith	45 - 64 mm	
constant	-0.18	
a-coefficient	0.658	
Std. err of y	0.34	
$CF_{(Ferg)}$	1.36	
$CF_{(Duan)}$	1.22	
r^2	0.10	
n	7	
b-exponent	1.22	
p-values	0.479	

East St. Louis Cr.'01				Bedload particle-size classes					
Bedload traps	4 - 5.6 mm	5.6 - 8 mm	8 - 11.2 mm	11.2 - 16 mm	16 - 22.4 mm	22.4 - 32 mm	32 - 45 mm	all gravel sizes	D_{max} (mm)
constant	-0.22	0.21	0.03	-1.72				0.59	1.50
a-coefficient	0.601	1.60	1.08	1.92E-02				3.86	31.97
Std. err of y	0.37	0.31	0.26	0.28				0.35	0.10
$CF_{(Ferg)}$	1.45	1.29	1.19	1.24				1.38	1.03
$CF_{(Duan)}$									
r^2	0.69	0.76	0.69	0.21				0.78	0.60
n	77	73	50	27				79	79
b-exponent	7.24	8.62	8.64	3.79				8.39	1.52
p-values	<<0.05	<<0.05	<<0.05	0.0158				<<0.05	<<0.05

East St. Louis Cr. '01	Bedload particle-size classes								
Helley-Smith	4 - 5.6 mm	5.6 - 8 mm	8 - 11.2 mm	11.2 - 16 mm	16 - 22.4 mm	22.4 - 32 mm	32 - 45 mm	all gravel sizes	D_{max} (mm)
constant	-0.07	-0.59	-0.86	-0.40	-1.12			0.68	1.37
a-coefficient	0.860	0.258	0.137	0.394	0.077			4.80	23.27
Std. err of y	0.43	0.44	0.36	0.27	0.18			0.56	0.17
$CF_{(Ferg)}$	1.64	1.66	1.41	1.21	1.09			2.28	1.08
$CF_{(Duan)}$									
r^2	0.38	0.17	0.05	0.13	0.01			0.39	0.45
n	80	64	41	26	3			81	91
b-exponent	4.07	2.66	1.61	2.29	-0.15			4.88	1.29
p-values	<<0.05	<<0.05	0.167	0.0708	0.923			<<0.05	<<0.05

East St. Louis Cr.'03	Bedload particle-size classes								
Bedload traps	4 - 5.6 mm	5.6 - 8 mm	8 - 11.2 mm	11.2 - 16 mm	16 - 22.4 mm	22.4 - 32 mm	32 - 45 mm	all gravel sizes	D_{max} (mm)
constant	-1.18	-1.10	-1.17	-1.02	-0.96	-0.97	-1.01	-0.16	1.62
a-coefficient	6.63E-02	7.87E-02	6.78E-02	9.54E-02	1.09E-01	1.07E-01	9.75E-02	6.99E-01	41.45
Std. err of y	0.39	0.46	0.44	0.48	0.39	0.37	0.36	0.42	0.14
$CF_{(Ferg)}$	1.49	1.76	1.66	1.84	1.50	1.43	1.42	1.58	1.06
$CF_{(Duan)}$									
r^2	0.80	0.74	0.69	0.63	0.70	0.64	0.41	0.81	0.68
n	131	131	122	103	86	57	24	131	133
b-exponent	7.70	7.90	7.09	7.39	7.36	6.36	4.47	8.47	1.97
p-values	<<0.05	<<0.05	<<0.05	<<0.05	<<0.05	<<0.05	<<0.05	<<0.05	<<0.05

East St. Louis Cr.'03	Bedload particle-size classes
Bedload traps	45 - 64 mm
constant	-0.99
a-coefficient	1.02E-01
Std. err of y	0.31
$CF_{(Ferg)}$	1.28
$CF_{(Duan)}$	
r^2	0.11
n	6
b-exponent	3.10
p-values	0.523

East St. Louis Cr. '03	Bedload particle-size classes								
Helley-Smith	4 - 5.6 mm	5.6 - 8 mm	8 - 11.2 mm	11.2 - 16 mm	16 - 22.4 mm	22.4 - 32 mm	32 - 45 mm	all gravel sizes	D_{max} (mm)
constant	-0.24	-0.20	-0.33	-0.42	-0.45	-0.28		0.54	1.40
a-coefficient	0.58	0.63	0.46	0.38	0.36	0.53		3.44	24.99
Std. err of y	0.18	0.16	0.27	0.34	0.28	0.07		0.19	0.12
$CF_{(Ferg)}$	1.09	1.07	1.21	1.36	1.24	1.01		1.10	1.04
$CF_{(Duan)}$									
r^2	0.83	0.86	0.65	0.39	0.44	0.89		0.85	0.50
n	40	40	39	34	23	7		40	40
b-exponent	3.39	3.36	3.31	2.75	2.43	1.82		3.81	1.07
p-values	<<0.05	<<0.05	<<0.05	<<0.05	0.00247	0.00164		<<0.05	<<0.05

Halfmoon Cr.			Bedload particle-size classes						
Bedload traps	4 - 5.6 mm	5.6 - 8 mm	8 - 11.2 mm	11.2 - 16 mm	16 - 22.4 mm	22.4 - 32 mm	32 - 45 mm	all gravel sizes	D_{max} (mm)
constant	-2.33	-2.19	-2.08	-1.69	-1.47	-0.97	0.08	-1.65	0.84
a-coefficient	4.72E-03	6.52E-03	8.32E-03	2.03E-02	0.034	0.11	1.20	2.23E-02	6.86
Std. err of y	0.43	0.35	0.38	0.32	0.27	0.30	0.14	0.46	0.17
$CF_{(Ferg)}$	1.65	1.38	1.48	1.31	1.22	1.27	1.05	1.73	1.08
$CF_{(Duan)}$									
r^2	0.61	0.66	0.51	0.42	0.40	0.19	0.47	0.66	0.59
n	49	46	37	29	13	7	4	49	49
b-exponent	2.78	2.51	2.31	1.72	1.65	0.96	-0.49	3.28	1.03
p-values	<<0.05	<<0.05	<<0.05	<<0.05	0.0185	0.323	0.310	<<0.05	<<0.05

Halfmoon Cr.			Bedload particle-size classes						
Helley-Smith	4 - 5.6 mm	5.6 - 8 mm	8 - 11.2 mm	11.2 - 16 mm	16 - 22.4 mm	22.4 - 32 mm	32 - 45 mm	all gravel sizes	D_{max} (mm)
constant	-2.33	-2.19	-2.08	-1.69	-1.47	-0.97	0.08	-1.65	0.84
a-coefficient	4.72E-03	6.52E-03	8.32E-03	2.03E-02	0.034	0.11	1.20	2.23E-02	6.86
Std. err of y	0.43	0.35	0.38	0.32	0.27	0.30	0.14	0.46	0.17
$CF_{(Ferg)}$	1.65	1.38	1.48	1.31	1.22	1.27	1.05	1.73	1.08
$CF_{(Duan)}$									
r^2	0.61	0.66	0.51	0.42	0.40	0.19	0.47	0.66	0.59
n	49	46	37	29	13	7	4	49	49
b-exponent	2.78	2.51	2.31	1.72	1.65	0.96	-0.49	3.28	1.03
p-values	<<0.05	<<0.05	<<0.05	<<0.05	0.0185	0.323	0.310	<<0.05	<<0.05

Hayden Cr.			Bedload particle-size classes						
Bedload traps	4 - 5.6 mm	5.6 - 8 mm	8 - 11.2 mm	11.2 - 16 mm	16 - 22.4 mm	22.4 - 32 mm	32 - 45 mm	all gravel sizes	D_{max} (mm)
constant	-3.52	-3.39	-3.24	-3.15	-3.08	-3.08	-3.60	-2.85	1.01
a-coefficient	3.03E-04	4.11E-04	5.71E-04	7.02E-04	8.31E-04	8.39E-04	2.52E-04	1.41E-03	10.27
Std. err of y	0.78	0.76	0.73	0.59	0.51	0.66	0.47	0.86	0.20
$CF_{(Ferg)}$	4.99	4.57	4.14	2.55	2.01	3.13	1.79	7.16	1.11
$CF_{(Duan)}$	3.48	2.74	4.07	1.91	1.75	1.62	1.55	5.91	1.11
r^2	0.73	0.69	0.68	0.70	0.73	0.67	0.66	0.75	0.71
n	172	159	151	125	113	94	75	177	177
b-exponent	6.83	6.51	6.20	6.42	6.41	6.58	7.93	7.50	1.62
p-values	<<0.05	<<0.05	<<0.05	<<0.05	<<0.05	<<0.05	<<0.05	<<0.05	<<0.05

Hayden Cr.			Bedload particle-size classes
Bedload traps	45 - 64 mm	64 – 90 mm	
constant	-3.34	-3.48	
a-coefficient	4.52E-04	3.33E-04	
Std. err of y	0.37	0.36	
$CF_{(Ferg)}$	1.43	1.41	
$CF_{(Duan)}$	1.46	1.65	
r^2	0.53	0.36	
n	50	22	
b-exponent	7.18	7.13	
p-values	<<0.05	0.00316	

Hayden Cr.			Bedload particle-size classes						
Helley-	4 - 5.6	5.6 - 8	8 - 11.2	11.2 - 16	16 - 22.4	22.4 - 32	32 - 45	all gravel	D_{max}
Smith	mm	mm	mm	mm	mm	mm	mm	sizes	(mm)
constant	-0.97	-1.13	-1.24	-1.10	-1.18	-0.83	0.45	-0.35	1.20
a-coefficient	0.107	0.073	0.058	0.080	0.066	0.147	2.815	0.45	16.03
Std. err of y	0.28	0.37	0.45	0.40	0.27	0.36	0.49	0.36	0.16
$CF_{(Ferg)}$	1.23	1.44	1.73	1.52	1.21	1.40	1.90	1.42	1.07
$CF_{(Duan)}$	1.20	1.31	1.50	1.36	1.17	1.32	4.54	1.40	1.07
r^2	0.74	0.66	0.40	0.26	0.59	0.10	0.09	0.70	0.60
n	31	31	30	25	18	11	4	31	31
b-exponent	1.66	1.87	1.39	0.91	1.94	0.93	-1.28	1.97	0.72
p-values	<<0.05	<<0.05	<<0.05	<<0.05	<<0.05	0.337	0.690	<<0.05	<<0.05

Little Granite Cr. '02			Bedload particle-size classes						
Bedload	4 - 5.6	5.6 - 8	8 - 11.2	11.2 - 16	16 - 22.4	22.4 - 32	32 - 45	all gravel	D_{max}
traps	mm	mm	mm	mm	mm	mm	mm	sizes	(mm)
constant	-3.76	-3.84	-3.86	-3.78	-3.32	-3.36	-3.32	-3.55	0.73
a-coefficient	1.73E-04	1.43E-04	1.39E-04	1.68E-04	4.78E-04	4.36E-04	4.79E-04	2.81E-04	5.31
Std. err of y	0.38	0.45	0.47	0.42	0.37	0.34	0.29	0.44	0.16
$CF_{(Ferg)}$	1.48	1.72	1.81	1.60	1.43	1.37	1.26	1.69	1.07
$CF_{(Duan)}$									
r^2	0.81	0.71	0.55	0.59	0.48	0.57	0.68	0.84	0.71
n	52	48	38	37	21	16	6	52	52
b-exponent	5.79	5.96	5.80	5.57	4.60	4.86	5.02	7.35	1.78
p-values	<<0.05	<<0.05	<<0.05	<<0.05	<<0.05	<<0.05	0.0409	<<0.05	<<0.05

Little Granite Cr. '02			Bedload particle-size classes						
Helley-	4 - 5.6	5.6 - 8	8 - 11.2	11.2 - 16	16 - 22.4	22.4 - 32	32 - 45	all gravel	D_{max}
Smith	mm	mm	mm	mm	mm	mm	mm	sizes	(mm)
constant	-1.81	-2.03	-1.98	-1.68	-1.24			-1.50	0.87
a-coefficient	0.016	0.009	0.010	0.021	0.058			0.032	7.46
Std. err of y	0.49	0.39	0.47	0.50	0.56			0.50	0.23
$CF_{(Ferg)}$	1.90	1.51	1.79	1.92	2.27			1.92	1.15
$CF_{(Duan)}$									
r^2	0.40	0.57	0.43	0.66	0.21			0.53	0.08
n	20	19	11	4	3			21	21
b-exponent	2.04	2.43	2.21	1.99	0.89			2.60	0.35
p-values	<<0.05	<<0.05	0.0271	0.190	0.696			<<0.05	0.202

Little Granite Cr. '99			Bedload particle-size classes						
Bedload	4 - 5.6	5.6 - 8	8 - 11.2	11.2 - 16	16 - 22.4	22.4 - 32	32 - 45	all gravel	D_{max}
traps	mm	mm	mm	mm	mm	mm	mm	sizes	(mm)
constant	-10.83	-10.78	-10.16	-9.96	-8.86	-8.83	-8.20	-11.13	-0.57
a-coefficient	1.49E-11	1.66E-11	6.98E-11	1.10E-10	1.37E-09	1.47E-09	6.26E-09	7.35E-12	0.27
Std. err of y	0.62	0.62	0.58	0.52	0.42	0.42	0.44	0.64	0.18
$CF_{(Ferg)}$	2.75	2.75	2.43	2.03	1.61	1.59	1.68	2.94	1.09
$CF_{(Duan)}$									
r^2	0.70	0.72	0.69	0.74	0.73	0.76	0.69	0.76	0.62
n	53	54	51	52	47	46	40	54	54
b-exponent	12.7	12.7	12.0	11.9	10.6	10.8	9.87	14.7	2.98
p-values	<<0.05	<<0.05	<<0.05	<<0.05	<<0.05	<<0.05	<<0.05	<<0.05	<<0.05

Little Granite Cr. '99		Bedload particle-size classes	
Bedload traps	45 - 64 mm	64 - 90 mm	90 – 128 mm
constant	-7.16	-5.26	-6.53
a-coefficient	6.97E-08	5.44E-06	2.93E-07
Std. err of y	0.59	0.61	0.61
$CF_{(Ferg)}$	2.56	2.70	2.70
$CF_{(Duan)}$			
r^2	0.48	0.20	0.28
n	31	19	5
b-exponent	8.52	6.02	7.83
p-values	<<0.05	0.0594	0.358

Little Granite Cr. '99				Bedload particle-size classes				
Helley-Smith	4 - 5.6 mm	5.6 - 8 mm	8 - 11.2 mm	11.2 - 16 mm	16 - 22.4 mm	22.4 - 32 mm	32 - 45 mm	all gravel sizes	D_{max} (mm)
constant	-5.39	-5.83	-5.56	-4.80	-5.25	-3.18	-0.590	-3.02	0.33
a-coefficient	4.10E-06	1.46E-06	2.74E-06	1.57E-05	5.64E-06	6.54E-04	0.257	0.001	2.12
Std. err of y	0.31	0.36	0.39	0.36	0.31	0.31	0.24	0.42	0.17
$CF_{(Ferg)}$	1.29	1.42	1.51	1.40	1.28	1.30	1.17	1.61	1.08
$CF_{(Duan)}$									
r^2	0.63	0.59	0.51	0.49	0.65	0.43	0.04	0.59	0.51
n	42	42	41	38	27	20	9	43	43
b-exponent	6.21	6.74	6.32	5.33	6.18	3.77	0.71	4.14	1.37
p-values	<<0.05	<<0.05	<<0.05	<<0.05	<<0.05	0.00192	0.624	<<0.05	<<0.05

Little Granite Cr. '99		Bedload particle-size classes
Helley-Smith	45 - 64 mm	
constant	0.373	
a-coefficient	2.360	
Std. err of y	0.35	
$CF_{(Ferg)}$	1.37	
$CF_{(Duan)}$		
r^2	0.00	
n	7	
b-exponent	-0.24	
p-values	0.898	

Table 11: Parameters of best-fit power functions relating the *b*-exponent, *a*-coefficient, and intersection with 1:1 line of inter-sampler transport relationships to exponents and coefficients of rating and flow competence curves measured with bedload traps.

	coefficient	exponent	r^2	*n*	*p-value*[#]	s_y
Correlations of inter-sampler transport relationships' *b*-exponent with:						
rating curve exponent	0.12	0.430	0.18	8	-*	0.108
rating curve coefficient	2.17	-0.019	0.39	8	0.0971	0.099
flow comp. exponent	1.83	0.559	0.35	8	-	0.102
flow comp. coefficient	3.02	-0.094	0.36	8	-	0.101
Correlation of inter-sampler transport relationships' *a*-coefficient with:						
rating curve exponent	2.2E-04	2.77	0.20	8	-	0.691
rating curve coefficient	0.049	-0.058	0.10	8	-	0.733
flow comp. exponent	0.010	3.47	0.37	8	0.110	0.613
flow comp. coefficient	0.151	-0.354	0.14	8	-	0.716
Correlations of inter-sampler transport relationships' intersection with 1:1 line with:						
rating curve exponent	3653	-2.920	0.24	8	-	0.645
rating curve coefficient	15.9	0.091	0.26	8	-	0.636
flow comp. exponent	**79.3**	**-3.986**	**0.53**	**8**	**0.041**	**0.507**
flow comp. coefficient	3.06	0.489	0.29	8	-	0.625

[#] two-tailed; * No values indicate $p >> 0.05$

Table 12: Parameters of best-fit power functions relating the *b*-exponent, *a*-coefficient, and intersection with 1:1 line of inter-sampler **bedload D_{max}** relationships to exponents and coefficients of rating and flow competence curves measured with bedload traps.

	coefficient	exponent	r^2	*n*	*p-value*[#]	s_y
Correlations of inter-sampler transport relationships' *b*-exponent with:						
rating curve exponent	1.51	0.168	0.01	8	-	0.218
rating curve coefficient	1.86	-0.017	0.10	8	-	0.208
flow comp. exponent	1.47	0.635	0.15	8	-	0.202
flow comp. coefficient	2.55	-0.099	0.13	8	-	0.204
Correlation of inter-sampler transport relationships' *a*-coefficient with:						
rating curve exponent	0.011	0.418	0.00	8	-	1.32
rating curve coefficient	0.052	0.073	0.05	8	-	1.28
flow comp. exponent	0.120	-2.45	0.06	8	-	1.28
flow comp. coefficient	0.012	0.469	0.08	8	-	1.26
Correlations of inter-sampler transport relationships' intersection with 1:1 line with:						
rating curve exponent	94.3	-0.855	0.14	8	-	0.262
rating curve coefficient	13.7	-0.011	0.02	8	-	0.279
flow comp. exponent	23.0	-0.695	0.11	8	-	0.267
flow comp. coefficient	15.8	-0.027	0.01	8	-	0.282

Table 13: Parameters of best-fit power functions relating the *b*-exponent, *a*-coefficient, and intersection with 1:1 line of inter-sampler transport relationships to exponents and coefficients of rating and flow competence curves measured with a HS sampler.

	coefficient	exponent	r^2	*n*	*p-value*[#]	s_y
Correlations of inter-sampler transport relationships' *b*-exponent with:						
rating curve exponent	4.83	-0.523	0.31	8	-*	0.105
rating curve coefficient	2.32	-0.046	0.31	8	-	0.105
flow comp. exponent	2.52	-0.150	0.06	8	-	0.123
flow comp. coefficient	3.79	-0.168	0.29	8	-	0.107
Correlations of inter-sampler transport relationships' *a*-coefficient with:						
rating curve exponent	0.052	0.396	0.00	8	-	0.769
rating curve coefficient	0.049	-0.226	0.20	8	-	0.690
flow comp. exponent	0.068	-1.25	0.12	8	-	0.725
flow comp. coefficient	0.478	-0.765	0.16	8	-	0.706
Correlations of inter-sampler transport relationships' intersection with 1:1 line with:						
rating curve exponent	1.13	1.506	0.08	8	-	0.710
rating curve coefficient	13.4	0.280	0.33	8	0.1334	0.603
flow comp. exponent	8.74	1.407	0.16	8	-	0.678
flow comp. coefficient	0.70	1.005	0.30	8	-	0.616

[#] two-tailed; * No values indicate $p >> 0.05$

Table 14: Parameters of best-fit power functions relating the *b*-exponent, *a*-coefficient, and intersection with 1:1 line of inter-sampler bedload D_{max} relationships to exponents and coefficients of rating and flow competence curves measured with the HS sampler.

	coefficient	exponent	r^2	*n*	*p-value*[#]	s_y
Correlations of inter-sampler bedload D_{max} relationships' *b*-exponent with:						
rating curve exponent	5.19	-0.730	0.20	8	-	0.196
rating curve coefficient	1.85	-0.066	0.21	8	-	0.194
flow comp. exponent	**1.88**	**-0.836**	**0.64**	**8**	**0.0176**	**0.132**
flow comp. coefficient	3.44	-0.204	0.14	8	-	0.203
Correlations of inter-sampler bedload D_{max} relationships' *a*-coefficient with:						
rating curve exponent	6.73E-05	4.99	0.26	8	-	1.13
rating curve coefficient	0.060	0.342	0.16	8	-	1.21
flow comp. exponent	**0.067**	**5.53**	**0.77**	**8**	**0.0044**	**0.64**
flow comp. coefficient	2.68E-03	1.01	0.10	8	-	1.25
Correlations of inter-sampler bedload D_{max} relationships' intersection with 1:1 line with:						
rating curve exponent	59.5	-1.147	0.30	8	-	0.237
rating curve coefficient	14.5	-0.016	0.01	8	-	0.282
flow comp. exponent	14.7	-0.125	0.01	8	-	0.281
flow comp. coefficient	15.8	-0.020	0.00	8	-	0.283

[#] two-tailed; * No values indicate $p >> 0.05$

Table 15: Correlations of HS transport rates predicted for x = 0.1 and x = 1.0 g/m•s from the inter-sampler transport relationships for total gravel transport at all study streams to exponents and coefficients of rating and flow competence curves measured with bedload traps.

	coefficient	exponent	r^2	*n*	*p-value*[#]	s_y
HS transport rates for x = 0.1 g/m·s with:						
rating curve exponent	6.88E-06	2.05	0.02	10	-	1.54
rating curve coefficient	1.83E-04	-0.138	0.10	10	-	1.48
flow comp. exponent	1.36E-05	6.37	0.24	10	-	1.36
flow comp. coefficient	1.93E-03	-0.689	0.10	10	-	1.48
HS transport rates for x = 1.0 g/m·s with:						
rating curve exponent	2.82E-04	2.52	0.10	10	-	0.84
rating curve coefficient	2.30E-02	-0.128	0.27	10	-	0.76
flow comp. exponent	**3.05E-03**	**5.25**	**0.50**	**10**	**0.0222**	**0.63**
flow comp. coefficient	2.06E-01	-0.642	0.26	10	-	0.76

[#] two-tailed; * No values indicate $p >> 0.05$

Table 16: Correlations of HS transport rates predicted for x = 0.1 and x = 1.0 g/m·s from the inter-sampler transport relationships for total gravel transport at all study streams to exponents and coefficients of rating and flow competence curves measured with the HS sampler.

	coefficient	exponent	r^2	*n*	*p-value*[#]	s_y
HS transport rates for x = 0.1 g/m·s with:						
rating curve exponent	9.66E-06	3.42	0.07	10	-	1.51
rating curve coefficient	1.84E-04	-0.634	0.33	10	0.0830	1.28
flow comp. exponent	4.76E-04	-2.32	0.08	10	-	1.49
flow comp. coefficient	2.92E-02	-1.70	0.15	10	-	1.44
HS transport rates for x = 1.0 g/m·s with:						
rating curve exponent	0.0345	0.575	0.01	10	-	0.88
rating curve coefficient	**0.0306**	**-0.438**	**0.49**	**10**	**0.0249**	**0.63**
flow comp. exponent	0.0577	-1.82	0.16	10	-	0.81
flow comp. coefficient	1.26	-1.27	0.26	10	-	0.76

[#] two-tailed; * No values indicate $p >> 0.05$

C. Example computations of HS adjustment functions

Depending on three cases of data availability, example computations provide step-by-step guidance for the computations of HS adjustment functions:

1) Data of gravel transport rates and discharge exist at a site for a HS sampler and a non-HS sampler such as bedload traps, but the data were not necessarily collected side-by-side or immediately following each other. However, it is assumed that the relationship between bedload transport and discharge remained unchanged between measurements made with both samplers.

2) Data pairs of gravel transport rates are available that were measured almost concurrently with both samplers.

3) Gravel transport rates were measured only with a HS sampler.

Each of the three cases requires a different approach for the computation of HS adjustment functions.

1. Rating curve method

The rating curve method is employed when the two samplers were deployed at a site but not necessarily concurrently.

1. Data compilation and plotting

A) Compile data of gravel transport rates and discharges for the HS sampler (Table 17) and the non-HS sampler, such as bedload traps (Table 18). Gravel transport rates (>4 mm) collected at Little Granite Creek, 2002, were used for the example computations. The tables provided below can be copied and pasted into a spreadsheet program.

Table 17: Gravel transport rates (> 4 mm) collected with 3-inch HS sampler at Little Granite Creek, 2002.

Date	Time	Q (m^3/s)	$Q_{B\,HS}$ (g/m·s)	Date	Time	Q (m^3/s)	$Q_{B\,HS}$ (g/m·s)
May 9	17:54	0.272	1E-6	May 25	16:13	0.828	0.00398
May 15	15:43	0.627	0.00790	May 28	20:17	1.304	0.176
May 16	13:58	0.596	0.00547	May 29	20:14	1.882	0.463
May 17	12:52	0.693	0.0705	May 30	17:59	2.422	1.26
May 18	12:01	0.828	1E-6	May 31	18:29	2.840	1.41
May 18	17:36	1.192	0.146	June 1	18:24	2.171	0.252
May 19	12:20	1.060	0.0536	June 3	15:34	1.669	0.129
May 19	16:21	1.576	0.652	June 4	15:37	1.481	0.0268
May 20	16:58	2.282	0.0825	June 5	14:27	1.384	0.0567
May 20	20:53	2.364	0.167	June 5	17:50	1.579	0.0179
May 21	15:50	1.862	0.0457	June 6	16:26	1.741	0.0467
				June 6	18:44	1.900	0.127

Table 18: Gravel transport rates (> 4 mm) collected with bedload traps at Little Granite Creek, 2002.

Date	Time	Q (m^3/s)	$Q_{B,\ traps}$ (g/m·s)
May 9	15:22	0.272	1E-6
May 15	13:27	0.596	1E-6
May 15	13:54	0.596	1E-6
May 15	14:44	0.596	1E-6
May 16	11:21	0.627	1E-6
May 18	11:05	0.836	1E-6
May 18	16:34	1.112	1E-6
May 19	11:19	1.043	1E-6
May 19	13:45	1.147	0.000287
May 19	15:17	1.372	0.000324
May 19	17:05	1.740	0.00578
May 19	17:38	1.854	0.00656
May 19	18:11	1.877	0.0140
May 20	12:55	1.778	0.00235
May 20	13:47	1.945	0.0134
May 20	14:54	2.131	0.0308
May 20	16:00	2.286	0.0967
May 21	13:27	1.924	0.0150
May 21	16:49	1.797	0.0143
May 21	17:26	1.769	0.00774
May 23	14:21	1.078	0.000560
May 23	15:29	1.070	0.000461
May 23	16:33	1.074	0.000731
May 23	17:46	1.095	0.000999
May 24	13:45	0.900	0.000133
May 24	15:16	0.899	8.26E-05
May 25	13:56	0.799	1E-6
May 25	15:25	0.811	5.74E-05
May 26	14:29	0.793	1E-6
May 26	15:35	0.816	0.000103
May 28	11:42	0.960	8.289E-05
May 28	16:30	1.123	0.000228
May 28	18:04	1.245	0.00387
May 29	14:24	1.511	0.00289
May 29	16:01	1.823	0.0684
May 29	17:50	1.954	0.130
May 29	20:17	1.879	0.103
May 30	13:37	1.892	0.00548
May 30	15:23	2.065	0.0428
May 30	17:10	2.342	0.253
May 30	20:58	2.562	0.774
May 31	14:06	2.324	0.0405
May 31	16:36	2.670	0.564
May 31	20:57	2.881	0.435
June 1	14:35	2.233	0.0803
June 1	16:26	2.231	0.138
June 1	19:36	2.235	0.152
June 3	11:50	1.596	0.00369
June 3	14:04	1.610	0.0138
June 3	17:28	1.699	0.0660
June 3	19:44	1.680	0.171
June 4	12:31	1.458	0.00713
June 4	14:45	1.487	0.0145
June 4	17:58	1.517	0.0340
June 5	12:44	1.354	0.00514
June 5	16:17	1.473	0.00814
June 5	18:41	1.598	0.0525
June 6	14:58	1.586	0.00810
June 6	17:50	1.845	0.0313
June 6	20:18	1.931	0.119
June 7	20:52	1.703	0.00958
June 9	12:51	1.140	0.000688

B) Plot both data sets in log-log space.

2) Regression analysis

A) Fit power function regressions in the form of $Q_B = c\ Q^d$ to the transport relationship of each sampler (i.e., a linear regression function to log-transformed data of transport rates *vs*. discharge. Zero-values were assigned a value of 1E-6 for plotting and were excluded from the analysis, but might be included at the user's discretion.

B) Print a regression table (Table 19).

Table 19: Parameters of power function rating curves fitted to gravel transport rates collected with a HS sampler and bedload traps at Little Granite Creek, 2002.

	Little Granite Creek, 2002	
Parameter	HS sampler	Bedload traps
constant	-1.50	-3.55
c-coefficient	0.0316	2.81E-04
d-exponent	2.60	7.35
s_y	0.50	0.44
r^2	0.53	0.84
n	21	52
$CF_{(Ferg)}$	1.92	1.69
$CF_{(Duan)}$		
p-value	<<0.05	<<0.05

C) Compute the *c*-coefficient as 10^{constant} (or e^{constant} when using natural logarithms).

D) Compute the bias correction factor after Ferguson (1986, 1987) (CF_{Ferg}) from the standard error of the *y*-estimate (s_y) using Eq. 6. If s_y exceeds 0.5, compute the Duan (1983) smearing estimate (CF_{Duan}) instead using the residuals (Eq. 7).

E) Compute the *p*-value to evaluate the statistical significance of the regression.

3) Plotting fitted functions

Add the fitted regression functions to the plotted data (Figure 23). Check that the regression fits the data.

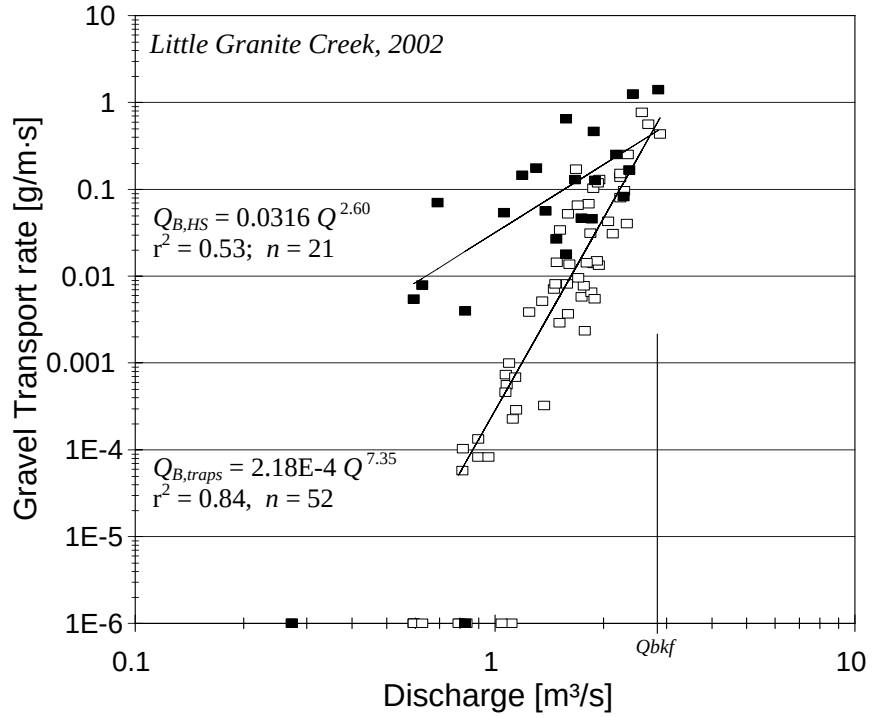

Figure 23: Relationships of gravel bedload transport and discharge for HS sampler and bedload traps and fitted rating curves. Measured zero-values are plotted along the x-axis.

4) Prediction of transport rates from fitted rating curves

A) Predict transport rates for each of the samplers for specified discharges from the fitted rating curves (Table 20).

B) Multiply transport predictions by CF_{Ferg} to account for the inherent underprediction of *y* from fitted power functions.

$$Q_{B,HS\ pred} = c\ Q^{d} \cdot CF$$

$$Q_{B,trap\ pred} = c\ Q^{d} \cdot CF.$$

For example, for the HS sampler, the rating curve predicted gravel transport rate at a discharge of $Q = 2.1$ m^3/s is

$$Q_{B,HS\ pred.} = 2.1^{2.60} \cdot 0.0316 \cdot 1.92 = 0.42$$

Table 20: Gravel transport rates predicted from the HS and bedload trap rating curves for specified discharges and log-transformations.

Discharge m^3/s	$Q_{B,HS\ pred}$ (g/m·s) CF_{Ferg} = 1.92	$Q_{B,traps\ pred}$ (g/m·s) CF_{Ferg} = 1.60	log($Q_{B,HS\ pred}$)	log($Q_{B,traps\ pred}$)
0.6	0.0161	1.11E-05	-1.79	-4.95
0.9	0.0461	0.000219	-1.34	-3.66
1.2	0.0974	0.00181	-1.01	-2.74
1.5	0.174	0.00934	-0.759	-2.03
1.8	0.280	0.0356	-0.553	-1.45
2.1	0.418	0.111	-0.379	-0.956
2.4	0.591	0.295	-0.228	-0.530
2.65	0.765	0.611	-0.116	-0.214
2.9	0.967	1.185	-0.0146	0.074

5. Computation of inter-sampler transport relationship

A) Regress data pairs of predicted $Q_{B\ traps}$ *vs*. predicted $Q_{B,HS}$ using a power function for specified discharges (i.e., linear regression of log-transformed predicted transport rates $Q_{B,trap\ pred}$ *vs*. $Q_{B,HS\ pred}$).

B) Compute the *a*-coefficient as 10 ^{constant} (or e ^{constant} when using natural logarithms).

For the Example computation, the regression parameters *a* and *b* of the inter-sampler transport relationship $Q_{B,HS,\ adj.} = a\ Q_{B,HS}{}^{b}$ are:

a = 10^0.115 = 1.30;
b = 2.82

6. Plotting the inter-sampler transport relationship

Plot the predicted transport rates for bedload traps and the HS sampler (Table 20) against each other in log-log space in a 1:1 plot (Figure 24). The line connecting the data points (i.e., the fitted power function) is the inter-sampler transport relationship $Q_{B,HS,\,adj.} = a\,Q_{B,HS}^{\,b}$.

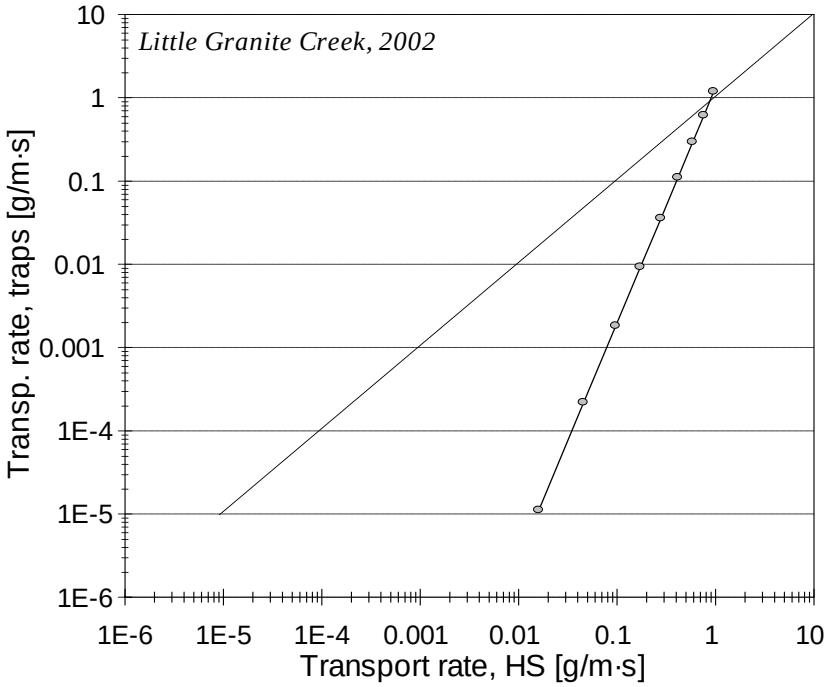

Figure 24: Inter-sampler transport relationship computed from rating curve approach.

7. Computation of intersection with 1:1 line

The transport rate at which $Q_{B,HS\,adj.}$ (x) equals $Q_{B,traps}$ (y) can be computed from the intersection of $Q_{B,HS\,adj.}$ with the 1:1 line as

$$x = a^{1/(1-b)} = 1.30^{(1/1-2.82)} = 0.87 \text{ g/m·s}$$

8. Use inter-sampler transport relationship to adjust HS transport rates

The computed inter-sampler transport relationship $Q_{B,HS,\,adj.} = a\,Q_{B,HS}^{\,b}$ serves as the HS adjustment function that may be applied to either individually measured HS gravel transport rates $Q_{B,HS}$ or to the HS transport relationship predicted from discharge $Q_{B,HS} = CF \cdot c\,Q^{d}$ to yield the HS adjustment function

$$Q_{B,HS,\,adj.} = a\,Q_{B,HS}^{\,b} = a\,(CF \cdot c\,Q^{d})^{b}$$

For example, at a discharge of $Q = 2.1$ m^3/s at Little Granite Creek, 2002, the adjusted HS gravel transport rate is

$$Q_{B,HS\,adj.} = 1.30\,(1.92 \cdot 0.0316 \cdot 2.1^{2.60})^{2.82} = 1.30\,(0.418 \text{ g/m·s})^{2.82} = 0.111 \text{ g/m·s}.$$

Note that the regressed data stem from predicted functions (i.e., the gravel bedload rating curves for the two samplers). The data points making up the inter-sampler transport relationship therefore have no scatter ($r^2 = 1$; s_y and p approach 0). Consequently, when predicting an adjusted HS transport rates ($Q_{B,HS\ adj.}$) from the inter-sampler transport relationship $a\ Q_{B,HS}{}^{b}$ multiplication by a bias correction factor *CF* is not necessary.

2. Paired data approach

The paired data approach is used when gravel transport rates collected concurrently or immediately after one another with a HS and a non-HS sampler (such as bedload traps) are available. A large sample size (>20 or 30) and a wide range of transport rates are typically necessary for the computation of a satisfactory inter-sampler transport relationship.

1) Data compilation

Compile data pairs (Table 21). Set a limit of an allowable difference in time or discharge between data collected with both samplers.

Table 21: Data pairs of gravel transport rates collected almost concurrently with bedload traps and the HS sampler at Little Granite Creek, 2002.

Bedload traps				Helley-Smith sampler		
$Q_{B,\ traps}$ (g/m·s)	Time	Q (m^3/s)	Date	Time	Q (m^3/s)	$Q_{B,HS}$ (g/m·s)
1E-06	15:22	0.27	May 9	17:54	0.27	1E-6
1E-06	14:44	0.60	May 15	15:43	0.63	0.00790
1E-06	11:21	0.63	May 16	13:58	0.60	0.00547
1E-06	11:05	0.84	May 18	12:01	0.83	1E-6
1E-06	16:34	1.11	May 18	17:36	1.19	0.146
1E-06	11:19	1.04	May 19	12:20	1.06	0.0536
0.00578	17:05	1.74	May 19	16:21	1.58	0.652
0.0967	16:00	2.29	May 20	16:58	2.28	0.0825
0.0307*	15:56	1.86	May 21	15:50	1.86	0.0457
0.0000575	15:25	0.81	May 25	16:13	0.83	0.00398
0.00273*	19:40	1.29	May 28	20:17	1.30	0.176
0.103	20:17	1.88	May 29	20:14	1.88	0.463
0.253	17:10	2.34	May 30	17:59	2.42	1.257
1.66*	19:05	2.95	May 31	18:29	2.84	1.41
0.152	19:36	2.23	June 1	18:24	2.17	0.252
0.0207*	14:51	1.63	June 3	15:34	1.67	0.129
0.0145	14:45	1.49	June 4	15:37	1.48	0.0268
0.00433*	13:31	1.38	June 5	14:27	1.38	0.0567
0.0525	18:41	1.60	June 5	17:50	1.58	0.0179
0.0217*	16:55	1.78	June 6	16:26	1.74	0.0467
0.113*	19:20	1.92	June 6	18:44	1.90	0.127

* 10-minute samples; gray shading indicates samples included in the paired data approach.

2. Plotting data pairs

Plot data pairs of transport rates measured with bedload traps *vs*. those measured with the HS sampler in a 1:1 plot in log-log space (Figure 25).

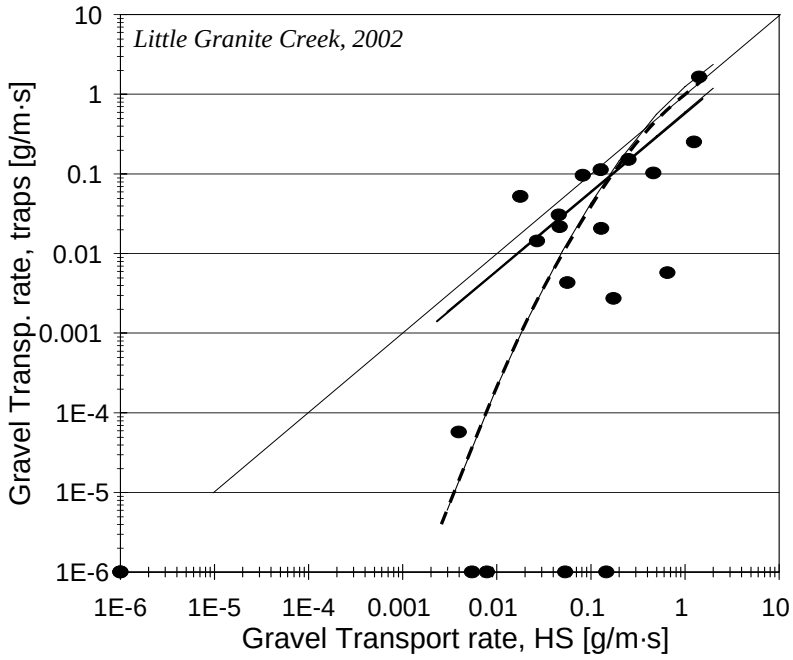

Figure 25: Bedload trap and HS gravel transport rates plotted *vs*. each other in a 1:1 plot. Also included are the two inter-sampler transport relationships: a fitted power function (solid line) and a guided 2nd order polynomial function (dashed line).

3. Regression analysis

A) Fit a power function regression to transport rates measured with bedload traps and the HS sampler (i.e., a linear regression of log-transformed measured data) to obtain the inter-sampler transport relationship. Zero-values are assigned a value one order of magnitude lower that the lowest transport rate collected by a sampler (the assigned value was 1E-6 for the example stream) Zero values (i.e., the assigned small transport rate) should be plotted, and they may be included in the analysis at the user's discretion.

B) Print a regression table (Table 22).

C) Compute the *a*-coefficient as 10^{constant} (or e^{constant} when using natural logarithms).

D) Because the standard error of the *y*-estimate s_y likely exceeds 0.5 which overpredicts the Ferguson (1986, 1987) bias correction factor CF_{Ferg}, compute instead the Duan (1983) smearing estimate (CF_{Duan}) from the residuals of the fitted power function (Eq. 7).

E) Compute the *p*-value to evaluate the statistical significance of the regression.

Table 22: Parameters of a power function regression and a 2nd order polynomial function fitted to the inter-sampler transport relationship of gravel transport rates collected with bedload traps and the HS sampler at Little Granite Cr. 2002 using the paired data approach.

Power function		2nd order polynomial function	
Parameters	Values	Parameters	Values
constant	-0.633	*A*	-0.4242
a-coefficient	0.233	*B*	1.0398
s_y	0.80*	*c*	-0.1
$CF_{(Ferg)}$	5.39*		
$CF_{(Duan)}$	2.58		
r^2	0.45		
n	15		
b-exponent	0.993		
p-values	0.00588		

* values too high; do not use.

4. Computation of inter-sampler transport relationship

A) Compute the inter-sampler transport relationship that serves as the HS adjustment function using the regression parameters *a* and *b*.

B) Multiply result by CF_{Duan} to account for the inherent underprediction of *y*-values from *x* in power functions fitted to scattered data sets.

$$Q_{B,HS,\,adj.} = Q_{B,trap} = a\, Q_{B,HS}^{\,b} \cdot CF_{Duan}$$

with

$a = 10^{-0.633} = 0.233$;
$b = 0.993$
$CF_{Duan} = 2.58$

5. Plotting the inter-sampler transport relationship

Add the graphed fitted inter-sampler transport relationship to the plotted data pairs (Figure 25).

6. Determining intersection point with 1:1 line

The point at which the inter-sampler transport relationships intersects the 1:1 line indicates the transport rate at which HS and bedload traps measurements are identical. The intersection point can be computed from

$$x = CF \cdot a^{1/(1-b)} = 2.58 \cdot 0.233^{(1/1-0.993)} = 1.1\text{ E-}90$$

There is no intersection for the inter-sampler transport relationship computed for Little Granit Creek within the range of commonly observed transport rates; the inter-sampler transport relationship runs nearly parallel to the 1:1 line.

7. Fitting a curvilinear function if necessary

A) Visually evaluate whether the inter-sampler transport relationship obtained from the fitted power function represents the plotted data. If not, consider fitting a curvilinear function such as a 2nd order polynomial function with the general form

$$y = a \cdot x^2 + b \cdot x + c$$

to log-transformed HS transport rates[7], thus $x = \log(Q_{B,HS})$.

B) Consider that a 2nd order polynomial function may need guiding to fit the data trend, particularly when the data set is relatively small and does not include a sufficient number of data points within the range of low to moderate transport rates. Several options are available for guiding the fit. The user may:

1) add a data point to the lower end of the data range and enter that data point multiple times if needed;
2) add a data point at the upper end of the data range and enter it several times if needed;
3) set the *y*-intercept.

To improve the fit for low data points from Little Granite Creek, 2002, two of the data pairs where $Q_{B,traps}$ = 1E-6 (see gray-shaded data in Table 21) that were not included in fitting the power function were included in the polynomial curve fitting. At the upper end of the data range a data pair ($\log(Q_{B,traps}) = \log 1$; $\log(Q_{B,HS}) = \log 1.0$) was added, and the *y*-intercept *c* was set to a value of log(-0.1). The parameters of the polynomial function for Little Granite Creek 2002 are a = -0.4242, b = 1.0398, and c = -0.1 (Table 22). Note that the parameters *a* and *b* obtained from the 2nd order polynomial fit are not the same as the power function *a*-coefficient and *b*-exponents.

8. Computation of inter-sampler transport relationship from 2nd order polynomial function

A) To compute an inter-sampler transport relationship from a 2nd order polynomial function, the parameters *a*, *b*, and *c* need to be applied to specified log-transformed values of *x* ($\log(Q_{B,HS})$) to compute

$$\log(Q_{B,HS\ adj.}) = a \cdot \log(Q_{B.HS})^2 + b \log(Q_{B.HS}) + c$$

The antilog of the result provides the adjusted HS transport rate

$$10\text{^}\log(Q_{B,HS\ adj.}) = Q_{B,HS\ adj.}$$

Computations need to be repeated for all HS transport rates for which adjustment is desired.

B) Intersection points with the 1:1 line are less important for polynomial inter-sampler transport relationships because the fitted polynomial functions tend to approach the 1:1 line asymptotically.

[7] The Excel function "fit trendline" may be used for this purpose. When guiding the fit, it may be useful to plot log-transformed data.

C) An estimated bias correction factor *CF* may be applied when using a polynomial function for the inter-sampler transport relationship. Values of 0.5 - 0.8 CF_{Duan} that should be within the range of >1 to <3 are suggested.

For the example of Little Granite Creek, 2002, the adjusted HS transport rate for a measured gravel transport rate of e.g., 0.02 g/m·s is computed as

$$Q_{B,HS,\,adj.} = 0.8\ CF_{Duan} \cdot 10\text{^}[\log(Q_{B,HS\,adj.}) = -0.4242 \cdot \log(Q_{B.HS})^2 + 1.0398 \log(Q_{B.HS}) + -0.1]$$

$$= 0.8\ CF_{Duan} \cdot 10\text{^}[-1.224 -1.767 - 0.1]$$

$$= 2.06 \cdot 10\text{^}[-3.091]$$

$$= 0.00167\ \text{g/m·s}$$

3. Prediction from bedmaterial and measured HS gravel transport rating curve

If measurements with a sampler other than the HS are not available, an adjustment function can be selected based on the parameters of the measured HS gravel transport relationship. It is assumed that data from the HS sampler extend over the range of flows commonly observed for the study stream.

1) Categorizing the study stream

Determine whether the study stream falls into the category of "red" or "blue" streams depending on the conditions listed in Table 23. Parameters printed in bold should be given highest consideration and values in gray the lowest for the categorization.

Table 23: Bedmaterial characteristics and parameters of the HS gravel transport relationship that determine the stream group and the respective inter-sampler relationships for the paired data approach.

Bedload conditions measured with HS sampler:	Streams in "red" group	Stream in "blue" group
Exponent of bedload rating curve	< 3.4*	> 3.4*
Coefficient of bedload rating curve	< 0.094	> 0.094
Exponent of flow competence curve	> 0.91*	< 0.91*
Coefficient of flow competence curve	< 9.7	> 9.7
Bedload D_{max} at 50% Q_{bkf}	**< 13 mm**	**> 13 mm**
Gravel transport rate at 50% Q_{bkf}	**< 0.15 g/m·s**	**> 0.15 g/m·s**
Bedload D_{max} at gravel transp. rate of 1 g/m·s	< 18 mm	> 18 mm

* Values from parameters printed in gray did not result from a statistically significant relationship.

The coefficients of the gravel bedload rating curve and the flow competence curve

$$Q_{B,HS} = 0.032\ Q^{2.60}$$

$$D_{max,HS} = 7.46\ Q^{0.35}$$

suggest a "red" stream group, while the exponent of the flow competence curve suggests a "blue" stream. The bedload D_{max} and transport rate measured at 50% Q_{bkf} are 8.4 mm and 0.078 g/m·s, while the bedload D_{max} measured at $Q_{B,HS}$ = 1 g/m·s is 11.8 mm. These two parameters should be given most weight, and they suggest that Little Granite Creek, 2002, falls in to the "red" stream group.

2) Applying the appropriate adjustment function for the HS sampler

Almost all of the criteria examined classified Little Granite Creek (2002) as a "red" stream. The adjustment function $Q_{B,HS\ adj} = a\ Q^{b}$ for "red" streams is

$$Q_{B,HS\ adj} = 0.532\ Q_{B\ HS}^{1.58}$$

and needs to be applied to the measured HS gravel transport relationship $Q_{B,HS} = c\ Q^{d}$ which for Little Granite Creek is

$$Q_{B,HS} = 0.0316\ Q^{2.60}$$

to yield the adjusted HS gravel transport rating relationship $Q_{B,HS\ adj} = a\ (c\ Q^{d})^{b}$ that for Little Granite Creek is

$$Q_{B,HS\ adj} = 0.532\ (0.0316\ Q^{2.60})^{1.58}$$

For streams categorized as "blue", the HS adjustment function is

$$Q_{B,HS\ adj} = 0.0235\ Q_{B\ HS}^{2.10}$$

For streams that appear to fall near the middle of red and blue streams, the user might take the geometric mean value obtained from applying the "red" and the "blue" adjustment functions to a measured HS transport rate.

C. Data tables

Time = Central time of sampling (mid point between start and stop of sampling time)
Q = Discharge (m^3/s)
$Q_{Bi\ traps}$ = Fractional Bedload Transport Rates, all traps (g/m·s)
$Q_{B,\ traps}$ = Total Gravel Transport Rates, all traps (g/m·s)
D_{max} = Sieve size class of largest collected bedload particle (mm)

Cherry Creek, OR, May and June 1999, bedload traps

Date	Time	Q	$Q_{B,\ traps}$ 4 – 64 mm	D_{max}
		(m^3/s)	(g/m·s)	(mm)
May 12	12:17	1.50	0	
May 12	13:52	1.51	1.40E-05	4
May 20	12:49	2.20	0.001813	8
May 24	12:04	3.85	0.024149	22.4
May 24	15:37	4.07	0.207165	45
May 25	12:46	4.47	0.695056	45
May 25	16:38	4.41	0.472336	32
May 26	11:56	4.12	0.598179	45
May 26	15:45	4.24	0.262162	32
May 27	11:28	4.18	0.393019	32
May 27	13:35	3.96	0.301449	32
June 7	13:19	2.32	0.000337	8
June 7	14:35	2.28	1.11E-05	4
June 9	12:22	1.97	0.000341	5.6
June 9	13:29	1.95	0.000185	4
June 11	10:34	2.16	0.000039	4
June 11	13:29	2.16	0	
June 11	13:29	2.12	6.60E-05	5.6
June 11	13:29	2.12	0	
June 18	11:42	3.03	0.014518	16
June 18	15:29	2.78	0.009506	8

Cherry Creek, May and June 1999, Helley-Smith samples

Date	Time	Q	$Q_{B\,HS}$ 4 – 64 mm	D_{max}
		(m^3/s)	(g/m·s)	(mm)
May 12	12:25	1.50	0.2135	11.2
May 12	14:02	1.51	0.0214	8
May 20	12:42	2.20	0.0138	4
May 20	13:37	2.20	0.0049	5.6
May 24	15:40	4.12	0.2549	11.2
May 25	12:25	4.50	0.9856	16
May 26	12:06	4.21	0.1558	11.2
May 26	15:56	4.24	0.2947	11.2
May 27	11:19	4.18	1.2636	22.4
May 27	13:40	3.96	1.6427	32
June 7	13:13	2.36	0.0057	5.6
June 7	14:02	2.32	0.1014	11.2
June 9	12:24	1.97	0.0787	11.2
June 9	13:29	1.95	0.0085	8
June 11	10:43	2.16	0.0131	8
June 11	11:51	2.16	0.1472	16
June 11	13:14	2.12	0.0015	4
June11	14:19	2.12	0.0127	8
June 18	11:47	3.08	0.5130	11.2
June 18	12:57	2.99	0.1055	11.2
June 18	15:28	2.85	0.4868	22.4

East Dallas Creek, May and June 2007, bedload traps

Date	Time	Q	$Q_{B,\ traps}$ 4 – 64 mm	D_{max}
		(m^3/s)	(g/m·s)	(mm)
May 3	15:06	0.53	0	
May 9	14:39	0.33	0	
May 9	18:00	0.34	0	
May 10	13:36	0.33	0	
May 10	15:56	0.34	0	
May 10	18:00	0.35	0	
May 11	17:27	0.40	0	
May 12	12:38	0.44	0	
May 12	15:31	0.45	0	
May 14	14:04	0.68	0.0007322	8.0
May 14	15:10	0.70	0.0016146	8.0
May 14	16:17	0.72	0.0011238	8.0
May 14	17:56	0.75	0.0027698	8.0
May 15	12:08	0.78	0.001637	8.0
May 15	13:24	0.79	0.0015238	8.0
May 15	14:41	0.79	0.0014907	8.0
May 15	15:51	0.82	0.0028389	8.0
May 15	16:58	0.87	0.0024873	11.3
May 15	18:09	0.89	0.0036156	11.3
May 17	11:50	0.79	0.0002284	5.6
May 17	13:05	0.79	0.0009091	5.6
May 17	14:20	0.79	0.0009441	11.3
May 17	15:20	0.79	0.0004449	5.6
May 17	16:18	0.79	0.0003639	5.6
May 17	17:17	0.79	0.0006564	8.0
May 19	11:56	0.86	0.0008212	8.0
May 19	12:57	0.86	0.0007562	5.6
May 19	13:56	0.86	0.0007829	5.6
May 19	14:56	0.88	0.0020036	8.0
May 19	15:56	0.97	0.0026986	8.0
May 19	16:56	1.02	0.0042112	8.0
May 19	17:58	1.03	0.00556	11.3
May 19	18:58	1.04	0.0055154	11.3
May 20	12:12	1.06	0.0057123	11.3
May 20	13:26	1.08	0.0047079	11.3
May 20	14:40	1.11	0.0145497	11.3
May 20	15:40	1.09	0.0133107	8.0
May 20	16:41	1.11	0.009325	8.0
May 20	17:41	1.11	0.0105365	11.3
May 20	18:40	1.11	0.0200509	8.0

Date	Time	Q	$Q_{B,\ traps}$ 4 – 64 mm	D_{max}
		(m^3/s)	(g/m·s)	(mm)
May 21	12:16	1.10	0.0023999	8.0
May 21	13:17	1.09	0.0037742	11.3
May 21	14:17	1.09	0.006335	16.0
May 21	15:17	1.10	0.0075309	11.3
May 21	16:18	1.11	0.0129758	11.3
May 21	17:19	1.11	0.0116095	16.0
May 21	18:19	1.16	0.0096276	11.3
May 24	14:53	0.86	0.0017242	8.0
May 24	15:58	0.86	0.0024042	11.3
May 24	16:59	0.86	0.0018385	8.0
May 24	18:01	0.86	0.0014956	8.0
May 25	11:53	0.78	0.0004969	5.6
May 25	12:56	0.79	0.0017054	8.0
May 25	14:00	0.78	0.0007428	5.6
May 25	15:03	0.77	0.0015535	11.3
May 25	16:06	0.76	0.000631	8.0
May 25	17:06	0.76	0.0006306	11.3
May 26	11:38	0.74	0.0002925	8.0
May 26	12:37	0.73	0.001237	8.0
May 26	13:38	0.73	0.0009453	8.0
May 26	14:41	0.73	0.000756	8.0
May 26	15:47	0.73	0.00067	11.3
May 29	12:02	1.05	0.0006926	8.0
May 29	13:02	1.05	0.0019999	16.0
May 29	14:04	1.05	0.0044618	8.0
May 29	15:03	1.06	0.0059677	11.3
May 29	16:04	1.07	0.0067372	11.3
May 29	17:05	1.09	0.0043194	11.3
May 30	12:09	1.08	0.003003	11.3
May 30	13:08	1.06	0.0028578	11.3
May 30	14:09	1.07	0.0073563	11.3
May 30	15:09	1.09	0.0043233	11.3
May 30	16:08	1.14	0.0049058	11.3
May 30	17:08	1.20	0.0138925	16.0
May 30	18:08	1.23	0.0128013	11.3
May 31	12:18	1.27	0.0106981	11.3
May 31	13:19	1.28	0.0145043	16.0
May 31	14:19	1.29	0.0216543	11.3
May 31	15:19	1.34	0.0327271	16.0
May 31	16:19	1.41	0.0282924	11.3
May 31	17:19	1.48	0.0288767	22.6

Date	Time	Q	$Q_{B,\ traps}$ 4 – 64 mm	D_{max}
		(m^3/s)	(g/m·s)	(mm)
May 31	18:21	1.53	0.0292188	11.3
May 31	19:21	1.56	0.0660094	16.0
June 1	11:59	1.63	0.0191316	11.3
June 1	13:00	1.63	0.0437138	16.0
June 1	14:01	1.63	0.0495472	16.0
June 1	15:02	1.66	0.0737532	16.0
June 1	16:03	1.71	0.1028313	16.0
June 1	17:04	1.81	0.1849609	16.0
June 1	18:06	1.86	0.1130675	32.0
June 1	19:05	1.90	0.1602192	22.6
June 2	12:15	1.95	0.0914691	16.0
June 2	13:15	1.94	0.2086881	16.0
June 2	14:18	1.97	0.2762846	22.6
June 2	15:17	1.98	0.2489274	22.6
June 2	16:18	2.11	0.511799	32.0
June 2	17:20	2.22	1.1459382	45.0
June 2	18:58	2.32	1.4082488	32.0
June 2	19:22	2.33	2.9455234	45.0
June 3	12:20	2.14	0.9808347	45.0
June 3	13:17	2.12	0.7084541	22.6
June 3	15:31	2.16	0.5854594	32.0
June 3	16:32	2.18	1.1287996	45.0
June 3	17:33	2.26	3.7659156	45.0
June 4	12:38	2.12	0.3310781	22.6
June 4	13:39	2.10	0.438143	22.6
June 4	14:39	2.08	0.345996	32.0
June 4	15:39	2.08	0.4605854	22.6
June 4	16:43	2.06	0.6294873	45.0
June 4	17:48	2.07	0.4153059	32.0
June 5	12:02	2.03	0.3172452	22.6
June 5	13:02	2.04	0.7781837	22.6
June 5	14:02	2.05	0.9234684	32.0
June 5	15:03	2.10	0.6013334	22.6
June 5	16:02	2.16	0.5847846	22.6
June 5	17:01	2.22	1.2893027	32.0
June 5	18:01	2.28	1.4447717	32.0
June 5	19:02	2.35	1.2973961	32.0
June 5	20:02	2.40	1.6275827	32.0
June 6	12:14	2.31	0.7850425	45.0
June 6	14:44	2.26	0.3089275	45.0
June 6	15:45	2.23	0.465448	32.0

Date	Time	Q	$Q_{B,\ traps}$ 4 – 64 mm	D_{max}
		(m^3/s)	(g/m·s)	(mm)
June 6	16:47	2.21	0.3382736	32.0
June 6	17:49	2.16	0.2521886	32.0
June 7	13:43	1.77	1.3577909	22.6
June 7	14:50	1.73	1.0792451	22.6
June 7	15:56	1.73	0.5377632	22.6
June 7	16:56	1.70	3.2997147	32.0
June 8	16:45	1.44	0.3674659	22.6
June 8	17:47	1.49	1.7493586	32.0
June 8	18:47	1.53	3.1465703	32.0
June 10	12:45	2.17	6.0390568	22.6
June 10	14:32	2.20	2.392673	45.0
June 10	15:19	2.22	1.9117372	32.0
June 10	15:48	2.24	5.6802385	64.0
June 11	11:26	2.76	8.9035243	45.0
June 11	13:18	2.73	12.105054	45.0
June 11	14:14	2.70	6.2235313	45.0
June 11	15:39	2.66	10.368195	45.0
June 11	16:13	2.67	8.9902864	45.0
June 13	11:30	2.21	0.3786963	22.6
June 13	12:32	2.21	1.1604304	45.0
June 13	15:52	2.19	5.8982614	45.0
June 13	16:15	2.20	10.717403	45.0
June 14	12:34	2.30	14.880883	32.0
June 14	15:57	2.37	10.142837	32.0
June 14	18:35	2.59	16.37302	45.0
June 15	12:16	2.71	8.844647	45.0
June 15	17:11	3.11	61.0389	45.0
June 16	12:58	3.44	16.3528	45.0
June 16	14:56	3.49	4.95697	32.0
June 16	15:10	3.49	5.65275	45.0
June 16	16:26	3.52	18.1688	45.0
June 16	17:12	3.55	10.9979	45.0
June 16	17:26	3.57	5.82899	64.0
June 17	13:36	3.32	3.60872	45.0
June 17	15:12	3.42	4.02045	45.0
June 17	15:45	3.49	16.9790	45.0
June 17	16:15	3.55	5.66976	64.0
June 17	17:35	3.92	20.1593	64.0
June 17	18:35	4.17	20.3260	45.0
June 18	14:11	3.48	13.8126	45.0
June 18	15:23	3.47	8.07285	64.0

Date	Time	Q	$Q_{B,\ traps}$ 4 – 64 mm	D_{max}
		(m^3/s)	(g/m·s)	(mm)
June 18	16:43	3.61	58.1703	64.0
June 18	17:08	3.61	130.854	64.0
June 20	13:56	3.42	15.0726	64.0
June 20	15:16	3.44	18.9801	45.0
June 20	18:34	3.78	39.7645	45.0
June 20	19:27	3.86	27.7277	64.0

East Dallas Creek, Helley-Smith samples, May and June 2007

Date	Time	Q	$Q_{B\,HS}$ 4 – 64 mm	D_{max}
		(m^3/s)	(g/m·s)	(mm)
May 3	17:25	0.50	0.1837	11.3
May 9	11:17	0.32	0.0117	5.6
May 10	11:11	0.32	0.0547	8
May 10	19:20	0.34	0.0335	11.3
May 11	13:23	0.35	0.0933	8
May 11	19:25	0.43	0.0542	8
May 12	11:16	0.44	0.0350	5.6
May 14	13:01	0.67	0.2377	11.3
May 14	19:49	0.79	0.5891	22.6
May 15	10:49	0.76	0.5220	22.6
May 15	19:25	0.89	0.1801	11.3
May 17	10:16	0.80	0.8122	22.6
May 17	18:37	0.81	0.8472	22.6
May 19	10:50	0.86	0.3842	11.3
May 19	20:17	1.04	0.6591	11.3
May 20	11:06	1.06	1.3138	32
May 20	19:55	1.13	0.1487	8
May 21	11:11	1.11	0.0838	11.3
May 21	19:48	1.18	0.8552	16
May 24	13:47	0.85	0.1320	16
May 24	19:15	0.84	0.4447	22.6
May 25	10:44	0.78	0.3230	22.6
May 25	18:20	0.76	0.7101	22.6
May 26	10:34	0.74	0.3456	22.6
May 26	17:29	0.73	0.0583	8
May 29	10:18	1.06	0.8034	16
May 29	18:38	1.09	0.8815	32
May 30	10:59	1.09	0.6255	16
May 30	19:26	1.27	0.5752	11.3
May 31	11:12	1.29	0.6088	16
May 31	20:27	1.57	0.2741	16
June 1	10:50	1.63	0.7553	16
June 1	21:02	1.96	1.2212	11.3
June 2	10:58	1.96	1.1913	22.6
June 2	20:57	2.44	4.8702	32
June 3	11:02	2.18	2.4708	32
June 3	18:45	2.26	7.8631	32
June 4	11:09	2.16	1.1702	16
June 4	19:03	2.09	5.2574	45
June 5	10:57	2.06	3.3180	32
June 5	21:08	2.45	5.5045	45

Date	Time	Q	$Q_{B\,HS}$ 4 – 64 mm	D_{max}
		(m^3/s)	(g/m·s)	(mm)
June 6	11:02	2.50	8.1678	32
June 6	19:05	2.20	3.0650	32
June 7	12:30	1.81	7.5970	32
June 7	18:54	1.65	10.924	22.6
June 8	15:33	1.40	5.3004	16
June 8	19:46	1.54	8.6483	32
June 10	11:47	2.17	7.9024	22.6
June 10	16:37	2.32	18.788	22.6
June 11	10:32	2.76	34.361	45
June 11	17:05	2.65	9.606	22.6
June 13	10:08	2.21	2.8434	22.6
June 13	17:30	2.21	49.590	45
June 14	11:11	2.32	99.516	32
June 14	19:35	2.72	12.746	32
June 15	12:07	2.70	48.272	32
June 16	12:12	2.93	41.449	32

East St. Louis Creek, bedload traps, May to July 2003

Date	Time	Q	$Q_{B,\ traps}$ 4 – 64 mm	D_{max}
		(m^3/s)	(g/m·s)	(mm)
May 30	13:27	0.801	0.175057	32
May 30	14:26	0.848	0.686412	32
May 30	15:30	0.889	0.837128	32
May 30	16:30	0.901	1.177065	45
May 30	18:36	0.901	0.763306	22.4
May 31	11:55	0.782	0.045635	32
May 31	12:56	0.823	0.036326	16
May 31	14:06	0.910	0.577494	32
May 31	15:02	0.989	1.023730	32
May 31	16:51	1.063	0.869915	32
May 31	17:30	1.071	0.984289	32
May 31	19:02	1.043	1.171875	45
May 31	19:21	1.041	1.869204	45
June 1	10:03	0.943	0.128637	45
June 1	10:50	0.941	0.220191	45
June 2	10:56	0.780	0.106006	32
June 2	11:58	0.779	0.035550	16
June 2	13:01	0.796	0.101559	22.4
June 2	14:00	0.826	0.337246	32
June 2	15:00	0.872	1.011652	32
June 2	15:54	0.904	2.842542	32
June 2	16:57	0.919	2.604593	45
June 2	18:47	0.931	0.785344	64
June 3	11:34	0.742	0.035369	32
June 3	12:38	0.743	0.012784	16
June 3	13:41	0.758	0.032828	22.4
June 3	14:46	0.783	0.060938	22.4
June 3	15:52	0.808	0.154280	32
June 3	17:01	0.824	0.279287	32
June 3	18:06	0.830	0.182011	22.4
June 4	10:36	0.681	0.026380	22.4
June 4	12:24	0.679	0.025432	22.4
June 4	13:37	0.689	0.009935	16
June 4	14:48	0.706	0.024265	32
June 4	15:55	0.716	0.013877	22.4
June 4	17:00	0.723	0.008430	16
June 5	09:39	0.622	0.011363	22.4
June 5	10:46	0.616	0.010727	22.4
June 7	19:25	0.508	0.002955	11.2
June 8	10:33	0.456	0.000290	5.6

Date	Time	Q	$Q_{B,\ traps}$ 4 – 64 mm	D_{max}
		(m^3/s)	(g/m·s)	(mm)
June 8	11:38	0.454	0.000598	8
June 8	12:56	0.459	0.000599	8
June 8	14:12	0.480	0.001996	16
June 8	15:18	0.502	0.007231	16
June 8	16:27	0.523	0.016832	16
June 8	17:34	0.542	0.007608	11.2
June 8	18:39	0.546	0.010301	11.2
June 9	13:02	0.478	0.009700	11.2
June 9	14:09	0.513	0.009117	16
June 9	15:16	0.544	0.013689	16
June 9	16:22	0.569	0.064545	22.4
June 9	17:28	0.592	0.015949	11.2
June 9	18:33	0.595	0.025036	22.4
June 10	11:56	0.534	0.009265	16
June 10	13:02	0.562	0.010079	16
June 10	14:07	0.611	0.030491	16
June 10	15:11	0.659	0.064788	22.4
June 10	16:18	0.676	0.044055	16
June 10	17:23	0.670	0.054766	22.4
June 10	18:28	0.661	0.033322	22.4
June 11	11:53	0.573	0.001945	8
June 11	12:58	0.596	0.002808	11.2
June 11	14:02	0.629	0.009041	22.4
June 11	15:07	0.678	0.029987	22.4
June 11	16:11	0.723	0.050899	22.4
June 11	17:17	0.744	0.131845	32
June 11	18:22	0.742	0.069745	32
June 11	19:27	0.731	0.060146	22.4
June 12	12:08	0.595	0.002047	11.2
June 12	13:14	0.604	0.003725	11.2
June 12	14:23	0.621	0.015875	22.4
June 12	15:28	0.633	0.002960	11.2
June 12	16:32	0.645	0.013774	22.4
June 12	17:37	0.655	0.005216	11.2
June 13	11:47	0.586	0.010188	22.4
June 13	12:56	0.591	0.002225	8
June 13	14:03	0.593	0.003032	16
June 13	15:06	0.596	0.000821	8
June 13	16:09	0.601	0.004046	16
June 13	18:50	0.611	0.003250	16
June 14	09:53	0.559	0.001392	8

Date	Time	Q	$Q_{B,\ traps}$ 4 – 64 mm	D_{max}
		(m^3/s)	(g/m·s)	(mm)
June 15	14:07	0.633	0.014016	16
June 15	15:12	0.663	0.013066	22.4
June 15	16:17	0.681	0.020163	22.4
June 15	17:23	0.681	0.024221	22.4
June 15	18:27	0.691	0.027614	22.4
June 15	19:31	0.701	0.026388	22.4
June 16	12:35	0.613	0.002876	8
June 16	13:42	0.616	0.012686	22.4
June 16	14:47	0.614	0.008954	22.4
June 16	15:49	0.616	0.009377	16
June 16	16:54	0.623	0.025533	32
June 16	18:00	0.636	0.015514	22.4
June 16	19:04	0.640	0.004898	8
June 17	11:43	0.572	0.005071	8
June 17	12:47	0.588	0.003289	11.2
June 17	13:49	0.608	0.008827	16
June 17	14:56	0.637	0.019407	22.4
June 17	16:02	0.657	0.026581	22.4
June 17	17:07	0.659	0.043424	22.4
June 17	18:13	0.654	0.027223	16
June 17	19:18	0.648	0.019410	16
June 18	12:13	0.575	0.005370	11.2
June 18	13:22	0.582	0.003009	8
June 18	14:29	0.595	0.006748	16
June 18	15:33	0.611	0.007327	11.2
June 18	16:39	0.628	0.022359	22.4
June 18	17:46	0.640	0.009613	16
June 18	18:51	0.643	0.034105	22.4
June 19	11:10	0.575	0.005198	16
June 19	13:26	0.582	0.006387	16
June 19	14:46	0.590	0.002714	11.2
June 19	17:30	0.606	0.007734	16
June 20	13:17	0.572	0.003970	11.2
June 20	14:24	0.579	0.002032	8
June 20	15:28	0.590	0.009519	22.4
June 20	17:47	0.595	0.004042	11.2
June 21	12:28	0.543	0.001024	8
June 21	14:04	0.562	0.002154	8
June 21	15:09	0.585	0.016354	32
June 21	16:14	0.601	0.006976	16
June 21	17:21	0.608	0.013178	16

Date	Time	Q	$Q_{B,\ traps}$ 4 – 64 mm	D_{max}
		(m^3/s)	(g/m·s)	(mm)
June 21	18:28	0.608	0.011778	16
June 22	10:52	0.538	0.001249	8
June 22	13:27	0.543	0.000799	8
July 3	13:25	0.346	0.000031	4
July 3	15:06	0.346	0.000059	4
July 3	16:12	0.346	0.001305	11.2
July 3	17:18	0.347	0.000690	8
July 3	18:27	0.352	0.000334	5.6
July 4	15:02	0.328	0.000114	2.8
July 4	10:43	0.337	0	2.8
July 4	11:54	0.333	0	2.8

East St. Louis Creek, May to July 2003, Helley-Smith samplers

Date	Time	Q	$Q_{B\,HS}$ 4 – 64 mm	D_{max}
		(m^3/s)	(g/m·s)	(mm)
May 30	17:39	0.908	3.0512	22.6
May 31	15:45	1.037	6.2286	22.6
May 31	18:11	1.059	7.7975	45
June 2	17:50	0.929	0.9952	16
June 3	10:18	0.748	0.8093	11.3
June 3	18:53	0.832	2.0113	32
June 4	11:29	0.679	0.6383	16
June 4	17:46	0.721	1.0230	22.6
June 5	11:37	0.614	0.5001	16
June 8	09:31	0.456	0.1750	16
June 8	19:26	0.543	0.5200	16
June 9	09:59	0.456	0.2903	16
June 9	19:25	0.593	0.3599	16
June 10	09:36	0.499	0.2157	11.3
June 10	19:16	0.653	0.4593	11.3
June 11	11:05	0.566	0.3162	8
June 11	20:20	0.715	1.7627	22.6
June 12	10:00	0.591	0.3500	11.3
June 13	09:39	0.587	0.5369	16
June 13	16:56	0.606	0.6393	16
June 14	08:57	0.561	0.3589	11.3
June 15	13:21	0.612	0.9335	22.6
June 15	20:18	0.698	1.1920	16
June 16	10:51	0.599	0.5776	11.3
June 16	19:53	0.640	0.5796	11.3
June 17	09:46	0.566	0.3997	11.3
June 17	20:06	0.643	1.1006	22.6
June 18	11:07	0.572	0.3191	16
June 18	19:43	0.640	0.4573	16
June 19	12:33	0.577	0.3271	11.3
June 19	19:46	0.619	0.3838	16
June 20	09:31	0.553	0.3867	11.3
June 20	19:49	0.598	0.2098	8
June 21	13:13	0.543	0.3629	16
June 21	19:20	0.603	0.6422	16
June 22	12:30	0.531	0.0974	11.3
July 3	14:13	0.346	0.0557	8
July 3	19:18	0.355	0.0875	8
July 4	09:44	0.337	0.1362	11.3
July 4	17:48	0.328	0.0318	5.6

East St. Louis Creek, May and June 2001, bedload traps

Date	Time	Q	$Q_{B,\ traps}$ 4 – 64 mm	D_{max}
		(m^3/s)	(g/m·s)	(mm)
May 16	16:00	0.194	0	
May 16	17:32	0.242	0	
May 22	14:30	0.189	0	
May 22	16:12	0.197	0	
May 23	11:29	0.179	0	
May 23	13:10	0.184	0	
May 23	14:45	0.199	2.746E-05	4
May 23	16:15	0.232	0	
May 24	13:15	0.200	0	
May 24	14:48	0.212	0	
May 24	16:25	0.227	8.777E-05	4
May 24	18:05	0.243	0	
May 24	19:36	0.254	0	
May 31	14:03	0.331	0.0002408	4
May 31	15:35	0.355	0.0005147	5.6
May 31	17:07	0.382	0.0010796	5.6
May 31	18:40	0.401	0.0016103	8
June 1	12:09	0.324	0.0003286	5.6
June 1	13:41	0.358	0.0010721	8
June 1	15:13	0.419	0.0058902	8
June 1	16:46	0.479	0.0150107	8
June 1	18:21	0.505	0.055562	11.2
June 1	19:54	0.505	0.0572851	11.2
June 2	10:36	0.379	0.0007056	5.6
June 2	12:16	0.385	0.0004006	5.6
June 2	13:53	0.425	0.0017579	8
June 2	15:28	0.473	0.0056868	11.2
June 2	17:03	0.496	0.0085603	11.2
June 2	18:39	0.519	0.0088685	16
June 2	20:14	0.528	0.0414671	11.2
June 3	10:37	0.411	0.0014916	8
June 3	12:10	0.414	0.0011613	8
June 3	13:53	0.425	0.0033717	11.2
June 4	12:06	0.391	0.0003333	5.6
June 4	13:45	0.386	0.0018198	11.2
June 4	15:17	0.389	0.0012045	5.6
June 4	16:49	0.398	0.0027106	11.2
June 4	18:29	0.405	0.0014336	5.6
June 5	10:10	0.350	0.0010388	5.6
June 5	05:31	0.348	0.0013276	8

Date	Time	Q	$Q_{B,\ traps}$ 4 – 64 mm	D_{max}
		(m^3/s)	(g/m·s)	(mm)
June 6	14:55	0.414	0.0033908	8
June 6	16:28	0.461	0.0148712	11.2
June 6	18:00	0.481	0.0184284	11.2
June 6	19:29	0.488	0.0198118	11.2
June 7	10:23	0.379	0.0012114	8
June 7	12:09	0.384	0.0035036	8
June 7	13:38	0.413	0.0025846	8
June 7	15:10	0.443	0.0075493	11.2
June 7	16:50	0.477	0.0115176	8
June 7	18:23	0.505	0.023105	11.2
June 7	19:57	0.508	0.0240305	11.2
June 8	10:32	0.400	0.0028831	11.2
June 8	12:06	0.405	0.0011409	5.6
June 8	13:38	0.420	0.0025819	8
June 8	15:11	0.456	0.0044074	11.2
June 8	16:45	0.485	0.0068805	11.2
June 8	18:19	0.496	0.0136237	11.2
June 8	19:51	0.498	0.0127155	11.2
June 9	11:42	0.409	0.0011262	8
June 9	13:14	0.419	0.0011373	5.6
June 9	14:45	0.430	0.00179	8
June 9	16:45	0.435	0.0015505	11.2
June 9	18:58	0.450	0.0034931	8
June 10	10:41	0.395	0.001348	8
June 10	12:21	0.399	5.104E-05	4
June 10	13:56	0.415	0.00063	8
June 10	15:29	0.447	0.0046886	11.2
June 10	17:02	0.462	0.0092575	11.2
June 11	12:57	0.401	0.0023012	11.2
June 11	14:54	0.429	0.0044031	8
June 11	16:31	0.451	0.0093011	11.2
June 11	18:17	0.454	0.0079941	11.2
June 11	19:55	0.456	0.0082938	11.2
June 12	09:10	0.393	0.002073	8
June 12	11:19	0.395	0.0016667	8
June 12	12:54	0.395	0.001295	8
June 12	15:26	0.407	0.0016561	8
June 12	16:57	0.409	0.0011483	5.6
June 12	18:28	0.409	0.003362	11.2
June 13	10:01	0.379	0.0003171	5.6
June 15	12:28	0.311	0.0003089	5.6

Date	Time	Q	$Q_{B,\ traps}$ 4 – 64 mm	D_{max}
		(m^3/s)	(g/m·s)	(mm)
June 15	14:05	0.331	0.0001553	5.6
June 15	15:44	0.339	0.000209	5.6
June 15	17:18	0.333	0.0002387	5.6
June 15	18:49	0.324	4.951E-05	4
June 15	20:22	0.317	0.0001686	5.6
June 16	10:13	0.282	0	
June 16	11:47	0.281	9.68E-05	4
June 16	13:23	0.279	7.969E-05	5.6
June 16	14:58	0.284	0	
June 16	16:34	0.292	0.0002002	5.6
June 16	18:08	0.294	0.0001755	5.6
June 17	10:15	0.272	0	
June 17	11:53	0.270	0	

East St. Louis Creek, May and June 2001, Helley-Smith sampler

Date	Time	Q	$Q_{B\,HS}$ 4 – 64 mm	D_{max}
		(m^3/s)	(g/m·s)	(mm)
May 22	15:20	0.193	0	2.8
May 22	17:00	0.198	0	2.8
May 23	10:45	0.179	0	2.8
May 23	12:15	0.179	0.0101	5.6
May 23	14:00	0.190	0	2.8
May 23	15:32	0.214	0	2
May 23	16:57	0.249	0	2.8
May 24	14:05	0.211	0.0091	4
May 24	15:32	0.223	0	2
May 24	17:10	0.235	0	2
May 24	18:48	0.249	0.0013	4
May 31	14:45	0.340	0.0328	8
May 31	16:18	0.367	0.0513	8
May 31	17:50	0.391	0.1430	11.2
May 31	19:20	0.409	0.2412	16
June 1	12:53	0.336	0.1520	16
June 1	14:25	0.382	0.1818	11.2
June 1	15:55	0.448	0.0377	5.6
June 1	17:30	0.499	0.2873	8
June 1	19:05	0.505	0.0995	5.6
June 1	20:40	0.505	0.1405	8
June 2	11:20	0.377	0.0403	8
June 2	13:00	0.395	0.0012	4
June 2	14:36	0.450	0.0203	8
June 2	16:13	0.486	0.2418	11.2
June 2	17:48	0.508	0	2.8
June 2	19:21	0.525	0.0100	4
June 2	21:00	0.531	0.1789	16
June 3	11:20	0.409	0.3243	11.2
June 3	12:55	0.409	0.1869	11.2
June 3	14:36	0.442	0.7036	22.4
June 4	12:50	0.389	0.0100	5.6
June 4	14:28	0.386	0.0013	4
June 4	16:00	0.394	0.0382	8
June 4	17:36	0.400	0.0601	5.6
June 4	19:14	0.409	0.2960	11.2
June 5	10:54	0.350	0.0498	8
June 5	12:00	0.346	0.0036	4
June 6	15:38	0.442	0.3372	11.2
June 6	17:12	0.474	0.7347	11.2
June 6	18:41	0.486	0.2333	11.2

Date	Time	Q	$Q_{B\,HS}$ 4 – 64 mm	D_{max}
		(m^3/s)	(g/m·s)	(mm)
June 6	20:13	0.491	0.3722	11.2
June 7	11:07	0.377	0.2402	8
June 7	12:53	0.393	0.0174	5.6
June 7	14:21	0.433	0.1160	5.6
June 7	16:01	0.458	0.0896	8
June 7	17:33	0.490	0.3846	11.2
June 7	19:07	0.508	0.4230	11.2
June 7	20:40	0.505	0.0527	5.6
June 8	11:17	0.400	0.1349	8
June 8	12:48	0.409	0.3814	11.2
June 8	14:17	0.435	0.0835	8
June 8	15:56	0.473	0.3150	11.2
June 8	17:27	0.491	0.1696	11.2
June 8	19:03	0.500	0.3673	11.2
June 8	20:36	0.495	0.1542	11.2
June 9	12:26	0.409	0.0796	8
June 9	13:58	0.428	0.0276	5.6
June 9	15:30	0.432	0.1536	8
June 9	18:01	0.447	0.0828	8
June 9	19:42	0.452	0.1645	11.2
June 10	11:27	0.395	0.0383	5.6
June 10	13:06	0.404	0.0578	5.6
June 10	14:39	0.429	0.0423	5.6
June 10	16:12	0.456	0.0943	11.2
June 10	17:46	0.469	0.0226	5.6
June 11	13:58	0.411	0.1592	8
June 11	15:39	0.440	0.1423	11.2
June 11	17:16	0.453	0.0228	5.6
June 11	19:02	0.456	0.2171	11.2
June 11	20:41	0.456	0.2130	8
June 12	09:55	0.392	0.1199	8
June 12	12:04	0.395	0.0987	11.2
June 12	13:38	0.395	0.0260	5.6
June 12	16:10	0.409	0.1000	11.2
June 12	17:40	0.409	0.0151	5.6
June 12	19:12	0.409	0.0077	5.6
June 13	10:45	0.381	0.0259	5.6
June 15	13:15	0.319	0	2.8
June 15	14:39	0.338	0.0129	4
June 15	16:29	0.337	0.0610	4
June 15	18:01	0.329	0.0168	4
June 15	19:33	0.320	0.0203	5.6

Date	Time	Q	$Q_{B\,HS}$ 4 – 64 mm	D_{max}
		(m^3/s)	(g/m·s)	(mm)
June 16	10:57	0.282	0.0073	5.6
June 16	12:33	0.279	0.0066	4
June 16	14:08	0.280	0.0156	4
June 16	15:43	0.288	0.0017	4
June 16	17:18	0.294	0.0004	4
June 16	18:50	0.294	0.0152	5.6
June 17	11:00	0.271	0.0081	4
June 17	12:39	0.270	0.0044	4

Halfmoon Creek, May and June 2004, bedload traps

Date	Time	Q	$Q_{B,\ traps}$ 4 – 64 mm	D_{max}
		(m^3/s)	(g/m·s)	(mm)
May 4	11:21	0.584	0	1.0
May 4	12:30	0.578	0	1.0
May 4	16:13	0.587	0	1.0
May 4	18:01	0.648	0	1.0
May 5	10:57	0.758	0	1.0
May 5	14:19	0.732	0	1.0
May 5	17:37	0.871	0	1.0
May 6	11:03	0.994	0	1.0
May 6	16:50	1.073	0.0002037	11.3
May 7	10:52	1.238	2.543E-05	4.0
May 7	13:36	1.181	1.312E-05	4.0
May 7	14:49	1.180	0	1.0
May 7	15:59	1.224	0.000024	4.0
May 7	17:08	1.340	0.000182	8.0
May 7	19:01	1.617	0.001219	11.3
May 8	10:52	1.468	0.000662	11.3
May 8	12:47	1.441	0.000725	11.3
May 8	14:39	1.405	0.000157	8.0
May 8	15:50	1.446	0.000254	8.0
May 8	16:59	1.547	0.000102	5.6
May 8	18:07	1.753	0.000024	4.0
May 9	10:46	1.608	0.000113	5.6
May 9	11:47	1.568	0.000283	8.0
May 9	14:22	1.497	0.000114	5.6
May 9	15:25	1.528	0.000066	5.6
May 9	16:35	1.610	0.000148	5.6
May 9	17:43	1.769	0.000554	5.6
May 9	19:30	2.039	0.000502	8.0
May 10	11:02	1.600	0.000219	5.6
May 10	12:54	1.545	0.000143	5.6
May 10	14:26	1.522	0.000108	5.6
May 10	15:57	1.584	0.000096	4.0
May 10	16:58	1.744	0.000190	8.0
May 10	17:53	1.950	0.001900	11.3
May 10	19:39	2.306	0.001590	11.3
May 11	15:54	1.741	0.000513	8.0
May 11	16:54	1.852	0.000261	5.6
May 11	17:55	1.965	0.001025	11.3
May 11	19:58	2.106	0.000880	8.0
May 14	12:39	1.034	0.000016	4.0

Date	Time	Q	$Q_{B,\ traps}$ 4 – 64 mm	D_{max}
		(m^3/s)	(g/m·s)	(mm)
May 14	13:50	1.047	0	1.0
May 14	15:11	1.015	0	1.0
May 14	16:28	0.954	0	1.0
May 15	11:53	0.845	0	1.0
May 15	13:22	0.844	0	1.0
May 15	15:48	0.821	0	1.0
May 17	15:26	0.937	0	1.0
May 17	16:25	0.945	0	1.0
May 18	11:19	1.024	0	1.0
May 18	13:33	1.029	0	1.0
May 18	15:45	1.046	0	1.0
May 18	16:46	1.120	0	1.0
May 18	17:45	1.282	0.000042	5.6
May 18	18:44	1.496	0.000108	8.0
May 18	19:44	1.710	0.003426	16.0
May 19	11:45	1.427	0.008885	32.0
May 19	13:35	1.414	0.000022	4.0
May 19	15:23	1.440	0	1.0
May 19	16:22	1.595	0.000562	11.3
May 19	17:22	1.933	0.0021015	16.0
May 19	18:21	2.348	0.0033236	11.3
May 19	20:12	2.890	0.0099668	22.6
May 20	12:23	1.820	0.0001333	5.6
May 20	14:21	1.844	5.502E-05	5.6
May 20	16:15	1.957	0.0001067	5.6
May 20	17:18	2.261	0.0011904	11.3
May 20	18:12	2.574	0.0003169	8.0
May 20	20:00	2.997	0.0034585	16.0
May 21	12:35	1.834	0.0005128	5.6
May 21	14:04	1.834	0.0006406	11.3
May 21	15:33	1.898	0.0005952	11.3
May 21	16:33	2.067	0.0025236	16.0
May 21	17:32	2.274	0.0020727	8.0
May 21	19:34	2.752	0.0040336	16.0
May 22	12:40	1.894	0.0017099	16.0
May 22	14:13	1.880	0.0007281	11.3
May 22	15:47	1.890	0.0008323	8.0
May 22	16:48	1.950	0.0063056	22.6
May 22	17:47	2.013	0.0004149	8.0
May 22	19:41	2.107	0.0044536	16.0
May 23	12:29	1.616	5.918E-05	4.0

Date	Time	Q	$Q_{B,\ traps}$ 4 – 64 mm	D_{max}
		(m^3/s)	(g/m·s)	(mm)
May 23	14:18	1.600	0.0001288	8.0
May 23	16:07	1.625	1.783E-05	4.0
May 23	17:09	1.632	5.92E-05	5.6
May 24	13:25	1.488	0.000267	16.0
May 26	16:24	1.460	7.37E-05	5.6
May 26	17:24	1.529	6.557E-05	5.6
May 27	11:44	1.503	8.866E-05	4.0
May 27	13:45	1.488	5.952E-05	8.0
May 27	15:47	1.512	4.74E-05	5.6
May 27	16:47	1.604	2.168E-05	4.0
May 27	17:48	1.711	0.0001736	5.6
May 28	11:42	1.629	9.942E-05	5.6
May 28	13:43	1.615	6.876E-05	5.6
May 28	15:44	1.648	2.19E-05	4.0
May 28	16:44	1.803	0.0001863	8.0
May 28	17:44	2.057	0.0002095	5.6
May 28	18:44	2.339	0.0006286	5.6
May 29	08:40	2.260	0.0006555	8.0
May 29	09:40	2.186	0.0035371	16.0
May 29	13:54	1.981	0.0007973	11.3
May 29	16:19	1.904	0.0002324	5.6
May 31	12:51	1.291	0.0001003	5.6
May 31	14:25	1.339	0.0020539	22.6
May 31	15:59	1.364	3.808E-05	4.0
May 31	16:59	1.391	0.0003313	11.3
May 31	17:58	1.429	0	1.0
June 1	11:49	1.185	5.437E-05	5.6
June 1	13:53	1.187	0	1.0
June 1	15:57	1.174	0	1.0
June 1	16:58	1.185	0	1.0
June 1	18:02	1.210	0	1.0
June 3	11:01	1.434	3.81E-05	4.0
June 3	13:43	1.434	0.0007745	16.0
June 3	16:23	1.445	1.749E-05	4.0
June 3	17:23	1.473	0.0006633	11.3
June 3	18:23	1.500	2.233E-05	4.0
June 3	19:23	1.540	0.0004148	8.0
June 4	10:02	1.572	0.0001171	5.6
June 4	11:02	1.566	0.0018899	16.0
June 4	13:36	1.565	0.000131	11.3
June 4	16:10	1.643	0.0026835	16.0

Date	Time	Q	$Q_{B,\ traps}$ 4 – 64 mm	D_{max}
		(m^3/s)	(g/m·s)	(mm)
June 4	17:10	1.846	0.0012798	11.3
June 4	18:10	2.087	0.0011138	11.3
June 4	19:10	2.283	0.0040692	16.0
June 4	20:10	2.421	0.0020244	16.0
June 5	11:20	1.911	0.0021806	11.3
June 5	12:20	1.882	0.0009949	11.3
June 5	14:12	1.950	0.0007506	11.3
June 5	16:03	2.198	0.0054293	11.3
June 5	17:02	2.585	0.0035467	16.0
June 5	18:00	3.024	0.0085007	16.0
June 5	18:59	3.500	0.0088401	22.6
June 5	19:54	3.893	0.0166029	16.0
June 6	11:26	2.580	0.0149858	16.0
June 6	12:26	2.528	0.0240367	22.6
June 6	14:04	2.608	0.0175738	22.6
June 6	15:41	2.913	0.0256349	22.6
June 6	16:42	3.318	0.0270914	16.0
June 6	17:38	3.744	0.0542754	16.0
June 6	18:30	4.152	0.1075489	32.0
June 6	19:16	4.496	0.1331787	22.6
June 7	12:10	3.028	0.0157291	16.0
June 7	13:12	2.968	0.0304039	22.6
June 7	14:14	2.995	0.0182162	16.0
June 7	15:15	3.163	0.0442489	22.6
June 7	16:15	3.427	0.1912015	32.0
June 7	17:13	3.787	0.1493928	32.0
June 7	18:02	4.194	0.2288555	22.6
June 7	18:49	4.497	0.5458968	32.0
June 7	19:41	4.727	1.0284763	32.0
June 8	11:11	3.191	0.1872565	22.6
June 8	12:24	3.093	0.2114495	32.0
June 8	14:08	3.081	0.0596092	22.6
June 8	15:51	3.251	0.1197847	32.0
June 8	16:52	3.537	0.1762885	32.0
June 8	17:52	3.830	0.2268859	22.6
June 8	18:55	4.070	0.462856	32.0
June 9	11:17	2.967	0.020469	32.0
June 9	12:18	2.945	0.0059765	16.0
June 9	14:02	2.982	0.0426261	22.6
June 9	15:49	3.095	0.0831272	22.6
June 9	16:56	3.258	0.0806028	32.0

Date	Time	Q	$Q_{B,\ traps}$ 4 – 64 mm	D_{max}
		(m^3/s)	(g/m·s)	(mm)
June 9	18:04	3.461	0.0911206	22.6
June 9	19:09	3.680	0.1084489	32.0
June 10	11:06	2.889	0.0049539	16.0
June 10	12:06	2.833	0.0055564	22.6
June 10	13:46	2.770	0.0048086	22.6
June 10	15:24	2.750	0.0056082	22.6
June 10	16:26	2.750	0.0059209	16.0
June 10	17:28	2.750	0.0039813	11.3
June 10	18:26	2.764	0.003576	11.3
June 11	14:14	2.210	0.0105146	22.6
June 15	16:39	2.184	0.0100509	16.0
June 15	17:39	2.270	0.0145539	16.0
June 15	18:39	2.334	0.0151749	22.6

Halfmoon Creek, May and June 2004, Helley-Smith samplers

Date	Time	Q	$Q_{B\,HS}$ 4 – 64 mm	D_{max}
		(m^3/s)	(g/m·s)	(mm)
May 4	13:38	0.578	0	2
May 4	19:33	0.689	0.0016	4
May 5	12:06	0.742	0.0146	5.6
May 5	19:25	1.023	0.0032	5.6
May 6	12:00	0.980	0.0217	8
May 6	18:25	1.249	0.0819	8
May 7	11:52	1.236	0.0651	11.3
May 7	18:05	1.532	0.0732	8
May 8	11:50	1.496	2.6479	45
May 8	19:25	1.943	0.5542	16
May 9	13:20	1.524	0.1045	11.3
May 9	18:39	1.975	0.4478	16
May 10	12:01	1.651	0.1118	8
May 10	18:48	2.216	0.3015	16
May 11	14:39	1.651	0.1656	11.3
May 11	18:55	2.133	0.0666	11.3
May 14	11:21	1.028	0.0744	11.3
May 14	17:29	0.922	0.0189	5.6
May 15	10:52	0.830	0.0389	5.6
May 15	17:36	0.819	0.0142	5.6
May 17	14:22	0.922	0.0263	8
May 18	10:09	1.038	0.0096	5.6
May 19	10:23	1.445	0.0550	11.3
May 19	19:20	2.756	0.1804	11.3
May 20	10:38	1.885	0.2375	16
May 20	19:03	2.882	1.8282	22.6
May 21	11:09	1.919	0.4768	16
May 21	18:32	2.631	0.0776	8
May 22	11:23	1.933	0.1294	11.3
May 22	18:47	2.165	0.2487	22.6
May 23	11:17	1.606	0.0584	11.3
May 23	18:09	1.666	0.0806	8
May 24	10:54	1.495	0.0863	11.3
May 26	15:08	1.452	0.0492	11.3
May 27	10:47	1.525	1.1089	32
May 27	18:50	1.816	0.0944	11.3
May 28	10:38	1.651	0.1480	11.3
May 28	20:15	2.719	0.6169	16
May 29	11:20	2.050	0.0530	8
May 31	11:43	1.265	0.0213	8
June 1	10:47	1.171	0.0104	5.6

Date	Time	Q	$Q_{B\,HS}$ 4 – 64 mm	D_{max}
		(m^3/s)	(g/m·s)	(mm)
June 3	09:58	1.445	0.0258	8
June 5	10:17	1.957	0.4461	22.6
June 6	10:08	2.621	0.1367	11.3
June 6	20:40	4.502	1.9790	32
June 7	10:37	3.086	2.5984	32
June 8	20:40	4.161	5.6471	45
June 9	20:55	3.769	2.9946	22.6
June 10	20:30	2.722	0.4404	16
June 15	20:10	2.480	0.4646	11.3

Hayden Creek, April to June, 2005, bedload traps

Date	Time	Q	$Q_{B,\ traps}$ 4 – 64 mm	D_{max}
		(m^3/s)	(g/m·s)	(mm)
April 27	13:02	0.390	0	
April 28	10:39	0.392	0	
April 28	12:13	0.390	0	
April 30	16:37	0.317	0.000013	4
May 4	16:36	0.324	0	
May 4	17:48	0.327	0.000149	8
May 5	11:15	0.337	0	
May 5	12:36	0.328	0	
May 5	14:00	0.336	0	
May 5	16:04	0.345	0	
May 6	11:55	0.436	0	
May 6	13:12	0.442	0	
May 6	17:22	0.542	0	
May 9	11:10	0.542	0.000128	5.6
May 9	12:14	0.546	0.000107	5.6
May 9	18:44	0.567	0.000261	8
May 10	10:32	0.663	0.000026	4
May 10	11:33	0.663	0.000644	5.6
May 10	12:33	0.662	0.000739	11.3
May 10	13:33	0.657	0.001006	8
May 10	14:34	0.659	0.000818	8
May 10	15:35	0.662	0.000986	11.3
May 10	17:31	0.691	0.001666	16
May 14	12:23	0.662	0.000134	5.6
May 14	13:24	0.654	0.000248	5.6
May 14	14:24	0.658	0.000705	11.3
May 14	15:24	0.661	0.000099	4
May 15	12:31	0.678	0	
May 15	13:33	0.679	0.000029	4
May 15	14:33	0.683	0.000059	4
May 15	15:32	0.683	0	
May 15	16:32	0.679	0.000021	4
May 16	13:12	0.757	0.000206	8
May 16	14:12	0.760	0.000080	5.6
May 16	15:12	0.765	0.000019	4
May 16	16:12	0.780	0.000316	8
May 16	17:12	0.802	0.000273	8
May 16	18:11	0.821	0.000066	4
May 17	10:05	1.164	0.021231	16
May 17	11:05	1.147	0.043062	16

Date	Time	Q	$Q_{B,\ traps}$ 4 – 64 mm	D_{max}
		(m^3/s)	(g/m·s)	(mm)
May 17	12:05	1.144	0.064955	22.6
May 17	13:05	1.133	0.033812	16
May 17	14:05	1.132	0.037043	22.6
May 17	15:05	1.117	0.033522	16
May 17	16:06	1.143	0.016864	16
May 17	17:05	1.145	0.033074	22.6
May 18	10:17	1.170	0.010911	16
May 18	11:17	1.155	0.016583	16
May 18	13:27	1.134	0.012523	22.6
May 18	15:37	1.147	0.034039	22.6
May 18	16:38	1.149	0.012836	16
May 18	17:40	1.169	0.012926	16
May 19	10:31	1.344	0.060558	32
May 19	11:32	1.334	0.011819	16
May 19	12:36	1.320	0.017179	22.6
May 19	13:39	1.342	0.029402	32
May 19	14:39	1.366	0.019022	16
May 19	15:40	1.388	0.021900	16
May 19	16:41	1.440	0.025821	16
May 19	17:40	1.498	0.068250	22.6
May 19	18:37	1.593	0.137056	32
May 19	19:16	1.635	0.104050	22.6
May 20	10:16	1.520	0.148813	22.6
May 20	11:23	1.463	0.257195	32
May 20	12:31	1.442	0.247326	22.6
May 20	13:36	1.446	0.191896	32
May 20	14:38	1.448	0.209685	32
May 20	17:38	1.524	0.130614	22.6
May 20	18:41	1.583	0.276041	32
May 21	10:37	1.798	0.343968	32
May 21	11:38	1.792	0.348951	45
May 21	12:38	1.802	0.160203	32
May 21	13:37	1.770	0.295668	32
May 21	14:41	1.818	0.499981	45
May 21	16:27	1.978	0.988975	45
May 21	17:07	2.085	1.501734	45
May 21	17:38	2.206	5.689891	45
May 21	18:52	2.499	19.05790	64
May 21	19:41	2.580	16.95861	64
May 22	11:34	2.075	0.588132	22.6
May 22	12:06	2.100	0.661036	32

Date	Time	Q	$Q_{B,\ traps}$ 4 – 64 mm	D_{max}
		(m^3/s)	(g/m·s)	(mm)
May 22	12:54	2.101	0.670980	32
May 22	15:02	2.140	1.012654	32
May 22	15:44	2.182	1.011514	45
May 22	17:25	2.351	5.075833	45
May 22	18:14	2.515	5.217394	64
May 22	19:12	2.745	5.606453	64
May 22	19:56	2.856	3.076023	64
May 23	11:35	2.439	1.883309	45
May 23	13:05	2.370	2.299692	64
May 23	14:23	2.500	3.040953	64
May 23	15:05	2.607	2.640360	45
May 23	16:12	2.633	2.626850	64
May 23	17:11	2.630	4.324902	64
May 23	18:29	2.765	13.31949	64
May 23	19:16	2.990	11.45183	64
May 24	11:00	2.437	3.116277	45
May 24	12:17	2.380	3.570883	64
May 24	13:46	2.322	2.124372	45
May 24	14:44	2.477	2.824924	64
May 24	15:17	2.440	5.630600	45
May 24	16:28	2.495	7.726509	64
May 24	17:22	2.520	7.880259	45
May 24	18:26	2.810	10.53074	64
May 24	19:29	2.695	24.45251	64
May 25	11:30	2.329	0.435245	45
May 25	12:39	2.340	1.814095	45
May 25	13:38	2.224	2.173333	64
May 25	14:37	2.259	2.955895	45
May 25	15:41	2.384	2.487853	45
May 25	16:28	2.560	4.229307	64
May 25	17:01	2.656	2.562026	45
May 25	18:11	2.823	5.080207	64
May 25	19:00	2.966	8.484988	64
May 26	11:35	2.309	2.402184	90
May 26	12:30	2.200	1.193629	45
May 26	13:30	2.085	1.839228	45
May 26	14:30	2.123	2.030916	45
May 26	15:30	2.240	2.136377	45
May 26	16:30	2.230	2.203414	64
May 26	17:29	2.249	2.705968	45
May 27	12:33	1.980	0.244120	45

Date	Time	Q	$Q_{B,\ traps}$ 4 – 64 mm	D_{max}
		(m^3/s)	(g/m·s)	(mm)
May 27	13:41	1.891	0.282036	32
May 27	14:41	1.894	0.625050	32
May 27	15:40	1.916	0.687925	45
May 27	16:41	1.949	0.503840	45
May 27	17:40	1.941	0.942796	32
May 27	18:38	1.935	0.583623	45
May 28	11:52	1.961	0.112312	22.6
May 28	14:12	1.960	0.169851	32
May 28	15:12	2.013	0.129177	32
May 28	16:09	2.109	0.172574	32
May 28	17:21	2.201	0.684145	45
May 28	18:33	2.340	1.049426	90
May 29	11:49	2.299	0.036205	22.6
May 29	12:49	2.229	0.041922	32
May 29	13:49	2.193	0.089684	32
May 29	14:56	2.200	0.132418	22.6
May 29	16:01	2.254	0.153272	22.6
May 29	17:07	2.253	0.144384	32
May 29	18:14	2.276	0.247603	32
May 29	19:18	2.276	0.250650	32
June 1	16:36	1.588	0.001834	8
June 1	17:38	1.615	0.001750	8
June 1	18:36	1.655	0.002988	11.3
June 2	11:32	1.661	0.003342	11.3
June 2	12:32	1.630	0.002903	11.3
June 2	13:38	1.604	0.003662	16
June 2	14:42	1.599	0.006894	16
June 2	15:42	1.606	0.012706	22.6
June 2	16:42	1.644	0.007172	11.3
June 2	17:43	1.654	0.005509	11.3
June 3	13:06	1.507	0.005047	16
June 3	14:36	1.470	0.009122	22.6
June 3	16:23	1.471	0.014783	32
June 3	17:50	1.486	0.003385	16
June 4	13:39	1.332	0.003935	11.3
June 4	15:09	1.321	0.001160	11.3
June 4	16:49	1.321	0.001078	11.3
June 4	18:20	1.322	0.001164	11.3
June 5	12:03	1.200	0.003328	16
June 5	13:09	1.196	0.000757	8
June 5	14:11	1.185	0.000245	5.6

Date	Time	Q	$Q_{B,\ traps}$ 4 – 64 mm	D_{max}
		(m^3/s)	(g/m·s)	(mm)
June 5	15:16	1.178	0.000209	8
June 5	16:17	1.185	0.000229	8
June 5	17:16	1.197	0.000182	5.6
June 5	18:15	1.214	0.000273	5.6
June 6	12:07	1.354	0.000681	8
June 6	13:38	1.286	0.001828	16
June 6	15:31	1.287	0.000733	8
June 6	16:56	1.349	0.000503	8
June 6	18:00	1.363	0.000922	11.3
June 8	13:06	1.254	0.001700	11.3
June 8	14:38	1.241	0.000237	8
June 8	16:15	1.265	0.000609	8
June 8	17:22	1.291	0.000391	5.6
June 11	12:47	1.060	0.000405	8
June 11	13:48	1.056	0.000139	4
June 11	14:47	1.048	0.000303	8
June 11	15:49	1.053	0.000123	5.6
June 11	16:52	1.073	0.000263	8
June 11	17:54	1.089	0.000438	8
June 11	18:56	1.109	0.000404	8
June 12	13:31	1.164	0.000603	11.3
June 12	14:34	1.130	0	
June 12	16:01	1.129	0.000216	8
June 12	17:36	1.127	0.000029	5.6
June 13	13:37	1.036	0.000118	4
June 13	15:07	1.021	0	
June 13	17:11	1.016	0.000007	4
June 14	13:11	1.008	0.000059	4
June 14	14:12	1.004	0.000013	4

Hayden Creek, April to June, 2005, Helley-Smith samples

Date	Time	Q	$Q_{B\,HS}$ 4 – 64 mm	D_{max}
		(m^3/s)	(g/m·s)	(mm)
April 28	13:45	0.383	0.1307	8
April 30	15:46	0.319	0.0598	5.6
May 4	15:33	0.312	0.1622	11.3
May 5	10:15	0.341	0.1067	11.3
May 6	11:08	0.432	0.1118	11.3
May 9	09:58	0.537	0.0418	8
May 10	09:43	0.664	0.0900	8
May 14	11:34	0.666	0.2160	11.3
May 15	11:45	0.685	0.2322	16
May 16	11:52	0.754	0.3033	8
May 17	18:08	1.155	0.7727	16
May 18	18:48	1.207	0.6422	22.6
May 19	20:30	1.794	2.4061	45
May 20	16:20	1.492	1.7656	32
May 22	10:23	2.105	15.739	64
May 24	09:56	2.302	7.1024	32
May 25	10:03	2.547	2.6741	32
May 26	10:05	2.423	3.2421	22.6
May 27	10:18	2.169	4.3016	45
May 28	10:41	2.027	2.0885	22.6
May 30	10:50	2.021	1.5280	16
June 2	09:05	1.671	0.3690	22.6
June 3	11:13	1.539	1.1069	22.6
June 4	11:53	1.382	0.7400	16
June 5	10:22	1.234	0.1224	8
June 6	10:00	1.228	0.5809	16
June 8	11:15	1.298	0.2965	16
June 11	10:44	1.056	0.0927	11.3
June 12	11:37	1.140	0.2969	16
June 13	11:51	1.054	0.4055	22.6
June 14	11:26	1.013	0.3426	16

Little Granite Creek, May and June 2002, Bedload traps

Date	Time	Q	$Q_{B,\ traps}$ 4 – 64 mm	D_{max}
		(m^3/s)	(g/m·s)	(mm)
May 9	15:22	0.272	0	
May 15	13:27	0.596	0	
May 15	13:54	0.596	0	
May 15	14:44	0.596	0	
May 16	11:21	0.627	0	
May 18	11:05	0.836	0	
May 18	16:34	1.112	0	
May 19	11:19	1.043	0	
May 19	13:45	1.147	0.0002873	5.6
May 19	15:17	1.372	0.0003242	5.6
May 19	17:05	1.740	0.0057808	11.2
May 19	17:38	1.854	0.0065569	11.2
May 19	18:11	1.877	0.0140027	22.4
May 20	12:55	1.778	0.0023507	5.6
May 20	13:47	1.945	0.013415	16
May 20	14:54	2.131	0.0307982	11.2
May 20	16:00	2.286	0.0966596	22.4
May 21	13:27	1.924	0.0150159	11.2
May 21	16:49	1.797	0.0142546	16
May 21	17:26	1.769	0.0077374	11.2
May 23	14:21	1.078	0.0005599	5.6
May 23	15:29	1.070	0.0004609	5.6
May 23	16:33	1.074	0.0007313	5.6
May 23	17:46	1.095	0.0009992	11.2
May 24	13:45	0.900	0.0001332	4
May 24	15:16	0.899	8.262E-05	4
May 25	13:56	0.799	0	
May 25	15:25	0.811	5.745E-05	4
May 26	14:29	0.793	0	
May 26	15:35	0.816	0.0001028	5.6
May 28	11:42	0.960	8.289E-05	4
May 28	16:30	1.123	0.0002281	4
May 28	18:04	1.245	0.003867	11.2
May 29	14:24	1.511	0.0028946	5.6
May 29	16:01	1.823	0.0683941	22.4
May 29	17:50	1.954	0.129557	22.4
May 29	20:17	1.879	0.1032226	32
May 30	13:37	1.892	0.0054771	11.2
May 30	15:23	2.065	0.042811	16
May 30	17:10	2.342	0.2531673	22.4

Date	Time	Q	$Q_{B,\ traps}$ 4 – 64 mm	D_{max}
		(m^3/s)	(g/m·s)	(mm)
May 30	20:58	2.562	0.7739191	32
May 31	14:06	2.324	0.0405511	22.4
May 31	16:36	2.670	0.5635877	45
May 31	20:57	2.881	0.4348708	32
June 1	14:35	2.233	0.0802994	22.4
June 1	16:26	2.231	0.1379474	22.4
June 1	19:36	2.235	0.151956	32
June 3	11:50	1.596	0.0036908	11.2
June 3	14:04	1.610	0.0137807	11.2
June 3	17:28	1.699	0.0659694	16
June 3	19:44	1.680	0.1710815	16
June 4	12:31	1.458	0.0071262	22.4
June 4	14:45	1.487	0.0144648	11.2
June 4	17:58	1.517	0.0339895	16
June 5	12:44	1.354	0.0051386	11.2
June 5	16:17	1.473	0.0081372	11.2
June 5	18:41	1.598	0.0525299	22.4
June 6	14:58	1.586	0.0080966	11.2
June 6	17:50	1.845	0.0312536	16
June 6	20:18	1.931	0.1190096	32
June 7	20:52	1.703	0.0095795	11.2
June 9	12:51	1.140	0.0006882	5.6

Little Granite Creek, May and June, 2002, Helley-Smith sampler

Date	Time	Q	$Q_{B\,HS}$ 4 – 64 mm	D_{max}
		(m^3/s)	(g/m·s)	(mm)
May 9	17:54	0.272	0	2
May 15	15:43	0.627	0.0079	5.6
May 16	13:58	0.596	0.0055	4
May 17	12:52	0.693	0.0705	11.2
May 18	12:01	0.828	0	
May 18	17:36	1.192	0.1458	8
May 19	12:20	1.060	0.0536	16
May 19	16:21	1.576	0.6520	45
May 20	16:58	2.282	0.0825	5.6
May 20	20:53	2.364	0.1670	11.2
May 21	15:50	1.862	0.0457	5.6
May 25	16:13	0.828	0.0040	5.6
May 28	20:17	1.304	0.1760	8
May 29	20:14	1.882	0.4633	8
May 30	17:59	2.422	1.2567	16
May 31	18:29	2.840	1.4127	16
June 1	18:24	2.171	0.2515	8
June 3	15:34	1.669	0.1292	8
June 4	15:37	1.481	0.0268	5.6
June 5	14:27	1.384	0.0567	8
June 5	17:50	1.579	0.0179	5.6
June 6	16:26	1.741	0.0467	5.6
June 6	18:44	1.900	0.1273	8

Little Granite Creek, May to June, 1999, bedload traps

Date	Time	Q	$Q_{B,\ traps}$ 4 – 64 mm	D_{max}
		(m^3/s)	(g/m·s)	(mm)
May 21	11:35	3.455	5.493E-05	5.6
May 21	12:58	3.540	0	
May 21	14:25	3.625	0.000628	11.2
May 21	15:59	4.106	0.0031291	22.4
May 21	17:20	4.248	0.0001953	5.6
May 21	19:04	4.191	0.0352135	11.2
May 22	13:01	4.106	0.001139	11.2
May 22	17:35	4.955	0.0075118	16
May 24	11:35	5.040	0.0015134	11.2
May 24	13:26	5.239	0.4615349	32
May 24	15:53	6.654	2.2178424	64
May 25	11:10	6.513	10.338474	64
May 25	12:48	6.485	0.9342657	64
May 26	09:37	6.145	9.8871292	64
May 26	11:43	6.116	12.665421	90
May 26	13:22	6.371	4.2479281	64
May 27	09:48	6.938	8.8942897	64
May 28	10:45	6.371	15.822528	64
May 28	13:11	6.371	20.237784	64
May 28	15:33	6.683	16.826401	90
May 30	13:05	6.513	1.447266	45
June 1	10:47	4.955	0.4452143	45
June 1	12:44	4.870	0.3390384	45
June 1	14:35	4.955	0.5482411	45
June 1	16:11	5.154	0.5538199	45
June 2	10:31	4.672	0.1041748	32
June 2	12:21	4.587	0.1004512	22.4
June 2	13:43	4.672	0.1460974	45
June 2	15:38	5.012	0.2696919	32
June 3	09:57	7.419	42.713128	64
June 3	11:40	6.853	9.5702562	90
June 3	13:32	7.023	2.5008397	64
June 3	14:56	7.164	7.2504865	90
June 4	13:30	6.173	2.1530287	64
June 4	15:49	6.173	2.7485767	64
June 9	10:12	4.870	0.1012226	32
June 9	12:01	4.814	0.6918159	64
June 9	13:53	4.814	0.1947762	45
June 9	15:49	4.955	0.0676705	32
June 10	10:24	4.644	0.0163219	16

Date	Time	Q	$Q_{B,\ traps}$ 4 – 64 mm	D_{max}
		(m^3/s)	(g/m·s)	(mm)
June 10	12:10	4.672	0.0593393	32
June 10	14:25	4.672	0.1114619	45
June 10	16:01	4.899	0.2180624	45
June 11	10:02	4.701	0.0888873	32
June 11	11:37	4.672	0.1003987	22.4
June 11	13:46	4.757	0.227734	45
June 11	15:19	4.927	0.3124368	45
June 12	10:54	4.814	0.0752589	32
June 12	12:33	4.814	0.1997555	32
June 12	14:07	4.842	0.6274927	64
June 12	15:43	4.899	0.5279673	32
June 14	14:08	5.210	0.1833138	32
June 14	15:45	5.663	0.4081287	32
June 14	17:23	5.607	2.5042145	90
June 14	18:44	5.947	2.0387847	64
July 24		1.065	0	0
July 24		1.039	0	0
July 24		1.017	0	0

Little Granite Creek, May and June 1999, Helley-Smith sampler

Date	Time	Q	$Q_{B\,HS}$ 4 – 64 mm	D_{max}
		(m^3/s)	(g/m·s)	(mm)
May 21	15:42	3.964	0.0975	11.2
May 21	18:57	4.219	0.3208	11.2
May 22	13:16	4.134	0.0200	5.6
May 22	17:30	4.955	0.3126	8
May 24	11:40	4.870	0.4338	22.4
May 24	13:22	5.154	3.3282	45
May 24	15:49	6.711	7.9004	45
May 25	13:24	6.456	11.194	45
May 30	14:21	6.541	3.3638	32
June 1	10:35	4.955	3.7356	22.4
June 1	12:27	4.870	1.0845	22.4
June 1	14:29	4.955	1.1732	11.2
June 1	16:08	5.182	1.7759	32
June 2	10:25	4.672	0.4034	22.4
June 2	12:18	4.616	1.3026	16
June 2	14:07	4.672	1.7777	16
June 2	15:52	5.040	0.3415	16
June 3	10:53	7.136	7.1948	45
June 3	13:44	7.023	6.2816	32
June 3	15:18	7.249	5.4893	45
June 4	13:32	6.173	4.4048	22.4
June 4	15:53	6.201	8.1243	32
June 9	10:10	4.870	0.4897	16
June 9	11:58	4.814	0.2904	16
June 9	13:46	4.814	0.2521	16
June 9	15:43	4.955	0.3032	16
June 10	10:19	4.644	0.4071	22.4
June 10	12:05	4.672	0.5395	22.4
June 10	14:19	4.757	0.7224	32
June 10	15:56	4.870	0.7212	22.4
June 11	09:57	4.729	0.3463	11.2
June 11	11:35	4.672	0.1756	11.2
June 11	13:40	4.757	0.2412	16
June 11	15:18	4.899	0.5249	22.4
June 12	10:49	4.814	0.1628	11.2
June 12	12:27	4.814	0.3092	16
June 12	14:00	4.870	0.5778	22.4
June 12	15:39	4.899	0.5547	16
June 14	14:00	5.210	0.6270	22.4
June 14	15:47	5.663	1.1264	16
June 14	17:17	5.607	1.1945	32

Date	Time	Q	$Q_{B\,HS}$ 4 – 64 mm	D_{max}
		(m^3/s)	(g/m·s)	(mm)
June 14	18:57	5.975	0.7692	16
July 24		1.065	0.0085	4

St. Louis Creek, June 1998, bedload traps

Date	Time	Q	$Q_{B,\ traps}$ 4 – 64 mm	D_{max}
		(m^3/s)	(g/m·s)	(mm)
June 19	13:40	1.073	0.0002474	8
June 19	20:00	1.628	0	
June 22	19:25	2.004	0.000188	5.6
June 22	20:29	2.146	0.004967	16
June 23	11:00	1.744	0.000459	5.6
June 23	12:06	1.744	0.000297	5.6
June 23	15:31	1.857	0.000028	4
June 23	16:48	2.198	0.000376	5.6
June 23	18:01	2.284	0.001616	16
June 23	19:17	2.318	0.001223	11.2
June 23	20:25	2.318	0.001256	11.2
June 23	20:56	2.318	0.011717	11.2
June 24	10:40	1.875	0.000166	5.6
June 24	11:56	1.857	0.000208	8
June 24	15:23	1.913	0.000035	4
June 24	16:27	2.075	0.000150	4
June 24	17:27	2.129	0.000762	5.6
June 24	20:03	2.129	0.000149	5.6
June 24	21:03	2.110	0.000165	8
June 24	21:32	2.075	0.001224	8
June 25	16:36	2.300	0.002796	8
June 25	17:36	2.351	0.001634	5.6
June 25	18:56	2.402	0.001235	11.2
June 25	20:35	2.385	0.003492	16
June 25	21:34	2.318	0.005339	11.2
June 26	10:01	2.040	0.000293	5.6
June 26	14:23	2.180	0.000051	8
June 26	15:25	2.385	0.000715	5.6
June 26	16:28	2.367	0.001472	11.2
June 26	17:36	2.565	0.005435	11.2
June 26	18:33	2.582	0.002955	11.2
June 26	19:42	2.565	0.004478	16
June 29	19:01	2.582	0.005044	11.2
June 29	20:20	2.582	0.006086	11.2
June 30	11:21	2.351	0.006843	16
June 30	13:41	2.418	0.002504	11.2
June 30	15:00	2.335	0.001645	11.2
June 30	16:00	2.500	0.002224	11.2
June 30	17:11	2.550	0.019500	16
June 30	18:02	2.582	0.003410	8

Date	Time	Q	$Q_{B,\ traps}$ 4 – 64 mm	D_{max}
		(m^3/s)	(g/m·s)	(mm)
June 30	19:03	2.565	0.002886	11.2
June 30	20:15	2.546	0.003760	11.2

St. Louis Creek, June 1998, Helley-Smith sampler

Date	Time	Q	$Q_{B\,HS}$ 4 – 64 mm	D_{max}
		(m^3/s)	(g/m·s)	(mm)
June 19	12:05	1.073	0.1261	8
June 19	19:35	1.628	0.6451	11.2
June 22	19:04	2.040	0.4578	16
June 22	20:55	2.110	0.6003	16
June 23	10:19	1.744	0.0236	5.6
June 23	16:02	2.146	0.1156	11.2
June 23	14:19	2.318	0.1827	16
June 24	09:53	1.894	0.0498	8
June 24	11:34	1.820	0.0704	8
June 24	20:41	2.110	0.0256	8
June 25	16:14	2.318	0.3905	16
June 26	09:28	2.040	0.0017	4
June 26	16:10	2.550	0.0245	8
June 26	19:23	2.582	0.1822	16
June 29	18:44	2.582	0.0810	11.2
June 30	14:43	2.451	0.0574	11.2
June 30	16:40	2.582	0.0481	8
June 30	19:54	2.517	0.0354	5.6

Hydrologic Analysis and Process-Based Modeling for the Upper Cache la Poudre Basin

Basic Information

Title:	Hydrologic Analysis and Process-Based Modeling for the Upper Cache la Poudre Basin
Project Number:	2008CO216B
Start Date:	3/1/2008
End Date:	2/28/2010
Funding Source:	104B
Congressional District:	
Research Category:	Not Applicable
Focus Category:	None, None, None
Descriptors:	
Principal Investigators:	Stephanie K Kampf

Publication

1. Kampf, Stephanie; Eric Richer, 2009, "Snowmelt Runoff in the Upper Cache la Poudre River Basin, Northern Colorado", pg 4-6 of Colorado Water Volume 26 issue 1.

Snowmelt Runoff in the Upper Cache la Poudre River Basin, Northern Colorado

by Stephanie Kampf, Assistant Professor, and
Eric Richer, M.S. Student, Watershed Science;
Department of Forest, Rangeland, and Watershed Stewardship

From its headwaters in Rocky Mountain National Park, the Cache la Poudre River travels approximately 80 miles down through the Poudre Canyon, eventually passing through Fort Collins and Greeley before reaching its confluence with the South Platte River (Figure 1). The basin covers an area of 1,890 square miles, with elevations ranging from over 13,000 feet above the headwaters to 4,600 feet at the outlet. The river has a long history of water use extending back to early settlements in the 1850s, and water is now used to support multiple agricultural, municipal, and industrial demands. In March 2008, we began a project funded by the Colorado Water Institute to explore runoff generation in the upper Cache la Poudre Basin and develop a model to predict flow in the basin under varying climate conditions. The objective of the first phase of this research is to determine which parts of the basin contribute runoff to the river during the snowmelt season.

Methods

To determine sources and timing of snowmelt runoff in the Cache la Poudre Basin, we compiled a hydrometric database combining climate and discharge data. This database includes point measurements of temperature and precipitation from National Climatic Data Center COOP stations, temperature and snow water equivalent from Natural Resources Conservation Service SNOTEL stations (Figure 1), and snow water equivalents from snow course surveys. These point measurements are located primarily in the highest elevations of the watershed. To estimate the spatial variability in precipitation and temperature, we used PRISM (Parameter-elevation Regressions on Independent Slopes Model; http://www.prismclimate.org), which predicts spatial distributions of precipitation and temperature at monthly time steps. To track the spatial distribution of snow in the basin, we compiled Snow-Covered Area (SCA) data from the Moderate Resolution Imaging Spectroradiometer (MODIS) satellite sensor. SCA data used in our analyses represent the 8-day maximum snow cover extent during each snowmelt season (late March to early June) from 2000-2006.

We compare time series and spatial patterns of these climate variables to discharge at the Canyon Mouth Gauge (Figure 1), which is the flow forecasting point for the Cache la Poudre. Because we are interested in sources and timing of snowmelt runoff in the basin, our analyses are conducted using 'naturalized' flow records in which the effects of diversions and impoundments have been removed. These naturalized flow rates are estimated using a basic accounting method: adding or subtracting diversions and changes in reservoir storage.

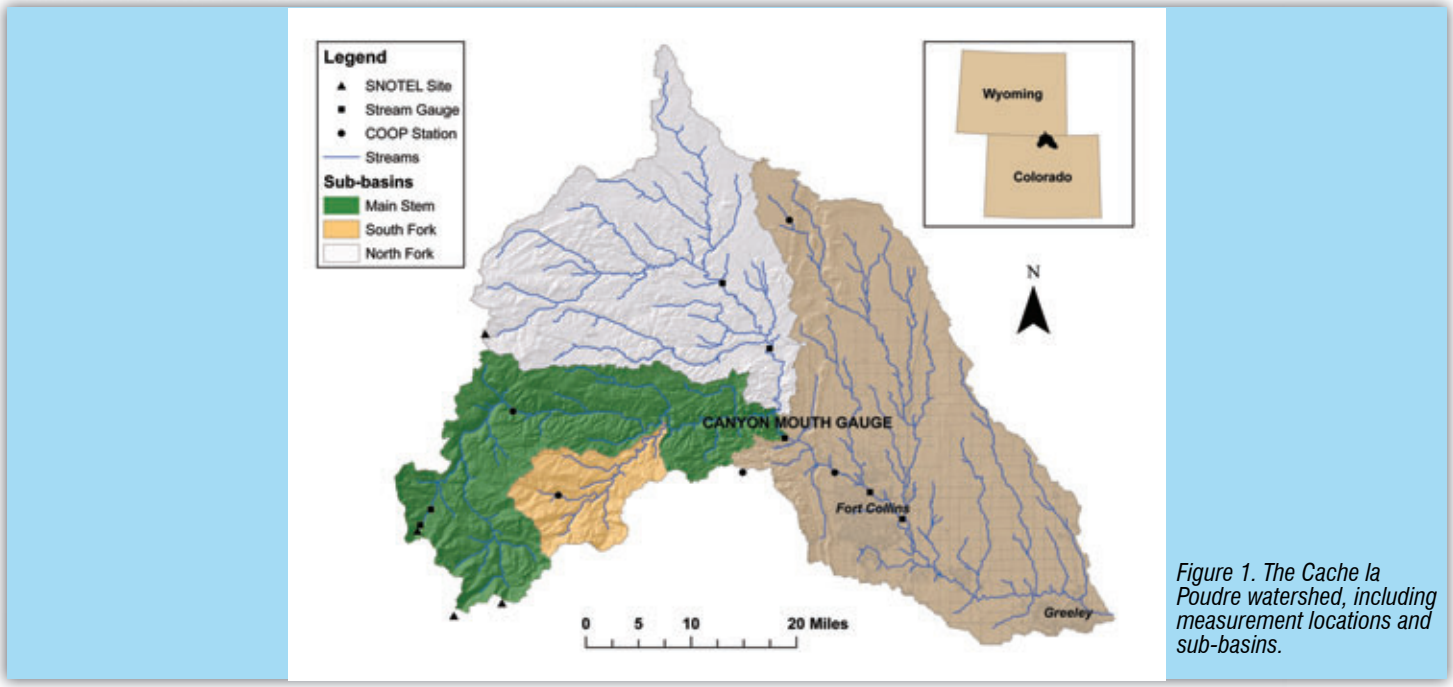

Figure 1. The Cache la Poudre watershed, including measurement locations and sub-basins.

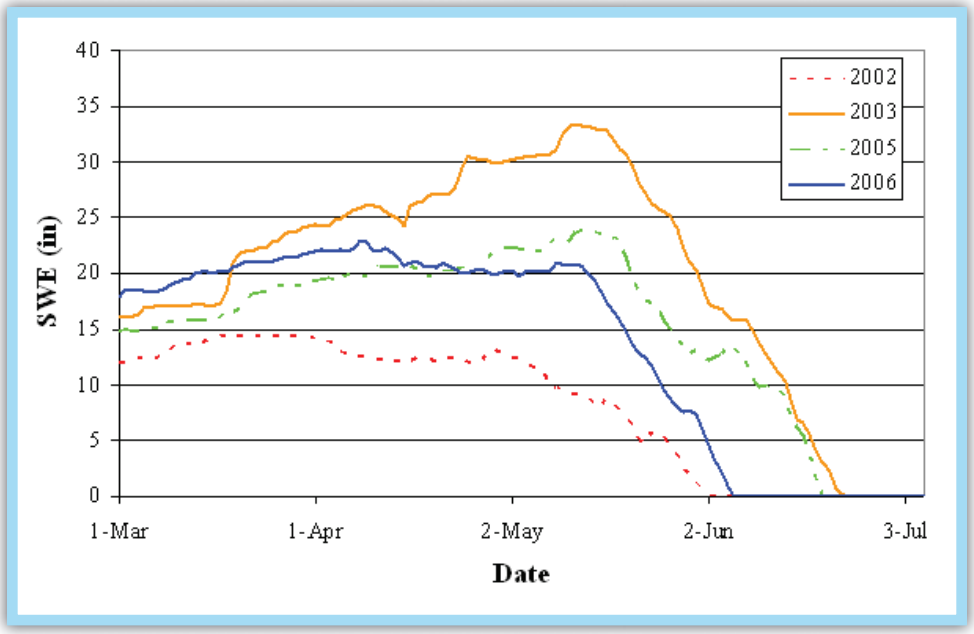

Figure 2. Spring-summer snow water equivalent at the Joe Wright SNOTEL site (10,120 feet). (Data source: Natural Resources Conservation Service)

Results

The upper Cache la Poudre Basin exhibits high spatial variability in temperature and precipitation. According to the PRISM model, average annual precipitation ranges from 13 inches at lower elevations to 53 inches near the headwaters, with a distinct increase in precipitation occurring above 10,000 feet. PRISM-derived average annual temperatures decrease from 50˚F at the lowest elevations to 25˚F at the headwaters. Temperature in the basin follows a seasonal cycle, with minimum temperatures in December and maximum temperatures in July. Average precipitation for the basin is lowest during the winter months and then increases during the spring, with maximum monthly average precipitation occurring in May.

Snow water equivalents measured at SNOTEL sites highlight the importance of spring precipitation. Figure 2 shows example snow water equivalent time series for the Joe Wright SNOTEL site (10,120 feet). During two of the years shown in Figure 2 (2003 and 2005), snow accumulation continued until mid-May. In all years, melt at this high-elevation site began in early to mid-May. In contrast, snow-covered area data show rapid snow melt over much of the basin area in late March (Figure 3), with the snow line gradually rising in elevation throughout the spring. Spring snow storms are evident in the snow cover data for all years except 2006. These spring storms caused abrupt rises in snow cover over the basin, but the additional snow cover typically melted within a week after each event.

These precipitation and snowmelt patterns affect the magnitude and timing of snowmelt runoff in the basin. River flow at the Canyon Mouth Gauge shows a gradual rise during early spring snowmelt, which begins from late March to late April (Figure 4). In most years, a gradual rise in discharge during early spring is followed by a rapid increase in discharge around mid-May. This rapid flow increase corresponds to the time when high elevation snowpack begins to melt (Figure 2). Peak flow occurs in late May to early June, and the river then recedes to baseflow conditions by mid-August.

Discussion

The spatial distribution of precipitation and temperature in the Cache la Poudre Basin implies a moisture surplus in the upper elevations of the basin and a moisture deficit in the lower elevation zones. Analyses of spring snow cover depletion and discharge data indicate that snow melt below around 8,000 feet does not typically result in increased river discharge. As the snow line rises above 8,000 feet, discharge begins to rise gradually, followed by a more rapid increase in flow as the snow line rises above around 9,500 feet elevation. Although each year exhibits a somewhat different relationship between snow cover depletion and discharge, the strong coupling between high elevation melt

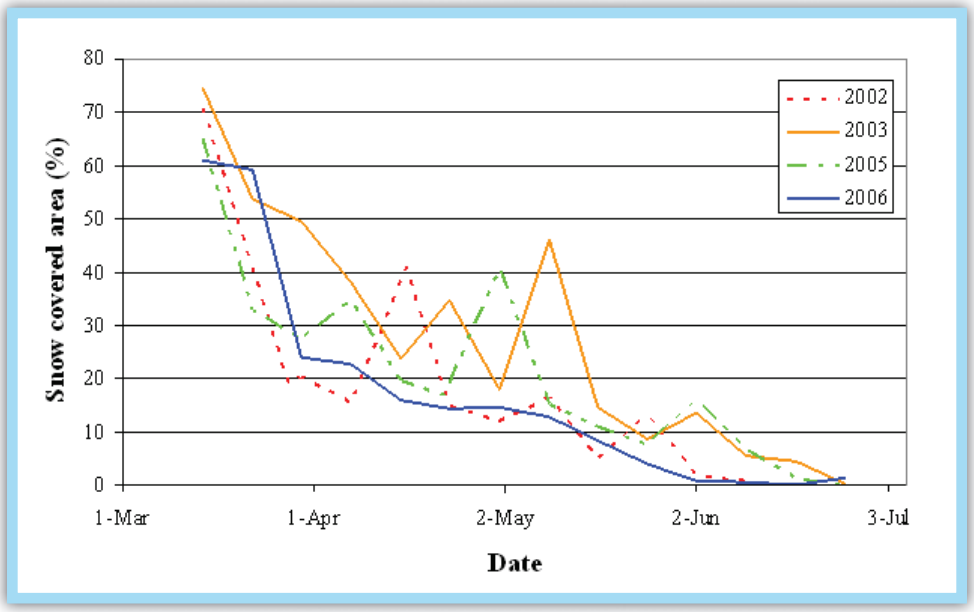

Figure 3. Spring-summer snow covered area depletion for the Cache la Poudre Basin. (Data source: MODIS 8-day composite snow cover, National Snow and Ice Data Center)

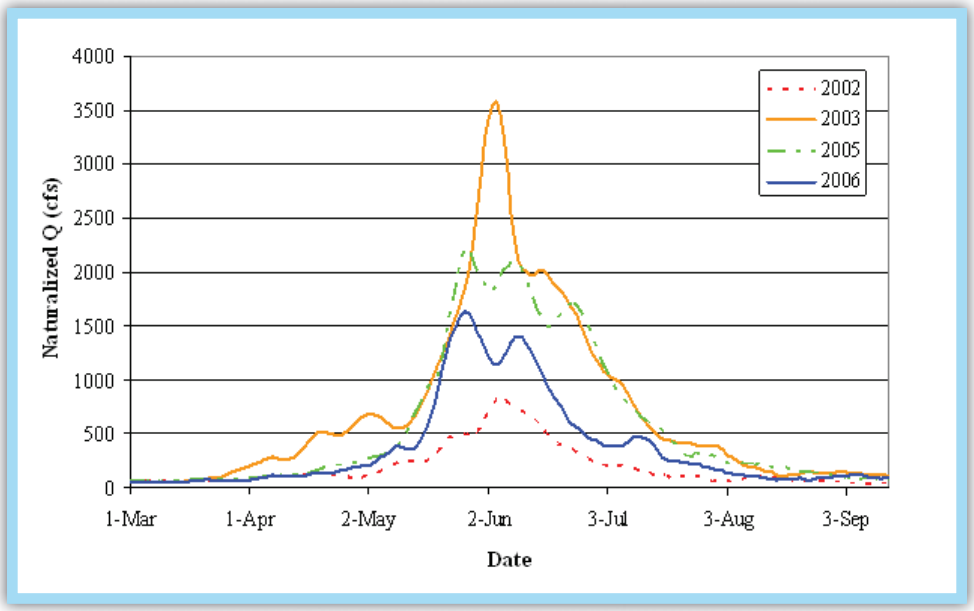

Figure 4. Naturalized discharge at the Cache la Poudre Canyon Mouth gauge. Discharge values represent a 7-day moving average. (Data sources: U.S. Geological Survey, Colorado Division of Water Resources, and water accounting by G. Varra)

and rapid increase in discharge suggests that high elevation zones contribute much of the snowmelt runoff to the river during high flows.

Under average conditions, the high-elevation moisture surplus is most significant in spring months, when precipitation is high but temperatures are still relatively low. Because precipitation in the basin is highest on average in the spring months, spring precipitation can contribute a significant portion of the annual water yield for the basin. The years 2005 and 2006 highlight the importance of spring conditions for river discharge. These years had similar high-elevation snow water equivalents on April 1 and May 1 (Figure 2), the dates when spring flow forecasts are issued, but the river flow was much higher in 2005 (Figure 4). During 2005, spring precipitation contributed to an increase in the high-elevation snowpack (Figure 2) and additional moisture input at lower elevations (Figure 3). With both high spring precipitation and cool spring temperatures, the 2005 snowpack persisted longer in the spring, and the river had a sustained high flow period lasting from mid-May through late June. In contrast, 2006 had low spring precipitation and warmer spring temperatures. The 2006 snowpack depleted rapidly throughout the basin (Figures 2 and 3), and the river had both lower peak flow and a shorter duration of high flows. With these warmer, drier spring conditions, the recession of the snowmelt hydrograph was already underway by mid-June.

Conclusions and Future Work

The timing and spatial distribution of precipitation in the Cache la Poudre Basin are both important controls on the amount of snowmelt runoff that occurs. Our preliminary results show that snowmelt from around 8,000-9,500 feet elevation tends to result in a gradual rise in Cache la Poudre river flow during April and early May. A rapid rise in the hydrograph occurs around mid-May, when the high elevation snowpack (above ~9,500 feet) begins to melt. Spring months have the highest average precipitation in this basin, and temperatures and precipitation during April and May can have a significant effect on river discharge.

MODIS snow cover data and the PRISM model have been useful for characterizing how and when different elevation zones in the basin contribute runoff to the Cache la Poudre during recent years (since 2000). We are working on quantifying these relationships and expanding the analysis to earlier years by using shape and timing characteristics of the hydrograph. Future work will incorporate snow cover, snow water equivalent, and temperature into a low-parameter model for predicting ensembles of snowmelt hydrographs under varying spring temperature and moisture conditions.

Acknowledgements

This project is funded by the Colorado Water Institute. We acknowledge the support and helpful contributions of Bill Fischer and Shawn Hoff from Cache la Poudre Water Users Association; Andy Pineda, Katie Melander, and Drew Linch of Northern Water; Tom Perkins and Mike Gillespie of the Natural Resources Conservation Service; and George Varra and Mark Simpson of the Colorado Division of Water Resources.

The Cache la Poudre River descends eastward in northwestern Colorado through Roosevelt National Forest in Poudre Canyon. (Image courtesy of Stephanie Kampf)

Hydrologic Analysis and Process-based Modeling for the Upper Cache la Poudre Basin, Year 2

Basic Information

Title:	Hydrologic Analysis and Process-based Modeling for the Upper Cache la Poudre Basin, Year 2
Project Number:	2009CO182B
Start Date:	3/1/2009
End Date:	2/28/2010
Funding Source:	104B
Congressional District:	4th
Research Category:	Not Applicable
Focus Category:	Hydrology, Water Quantity, None
Descriptors:	None
Principal Investigators:	Stephanie K Kampf

Publication

1. Kampf, Stephanie; Eric Richer, 2009, "Snowmelt Runoff in the Upper Cache la Poudre River Basin, Northern Colorado", pg 4-6 of Colorado Water, Volume 26 issue 1.

Snowmelt Runoff in the Upper Cache la Poudre River Basin, Northern Colorado

by Stephanie Kampf, Assistant Professor, and
Eric Richer, M.S. Student, Watershed Science;
Department of Forest, Rangeland, and Watershed Stewardship

From its headwaters in Rocky Mountain National Park, the Cache la Poudre River travels approximately 80 miles down through the Poudre Canyon, eventually passing through Fort Collins and Greeley before reaching its confluence with the South Platte River (Figure 1). The basin covers an area of 1,890 square miles, with elevations ranging from over 13,000 feet above the headwaters to 4,600 feet at the outlet. The river has a long history of water use extending back to early settlements in the 1850s, and water is now used to support multiple agricultural, municipal, and industrial demands. In March 2008, we began a project funded by the Colorado Water Institute to explore runoff generation in the upper Cache la Poudre Basin and develop a model to predict flow in the basin under varying climate conditions. The objective of the first phase of this research is to determine which parts of the basin contribute runoff to the river during the snowmelt season.

Methods

To determine sources and timing of snowmelt runoff in the Cache la Poudre Basin, we compiled a hydrometric database combining climate and discharge data. This database includes point measurements of temperature and precipitation from National Climatic Data Center COOP stations, temperature and snow water equivalent from Natural Resources Conservation Service SNOTEL stations (Figure 1), and snow water equivalents from snow course surveys. These point measurements are located primarily in the highest elevations of the watershed. To estimate the spatial variability in precipitation and temperature, we used PRISM (Parameter-elevation Regressions on Independent Slopes Model; http://www.prismclimate.org), which predicts spatial distributions of precipitation and temperature at monthly time steps. To track the spatial distribution of snow in the basin, we compiled Snow-Covered Area (SCA) data from the Moderate Resolution Imaging Spectroradiometer (MODIS) satellite sensor. SCA data used in our analyses represent the 8-day maximum snow cover extent during each snowmelt season (late March to early June) from 2000-2006.

We compare time series and spatial patterns of these climate variables to discharge at the Canyon Mouth Gauge (Figure 1), which is the flow forecasting point for the Cache la Poudre. Because we are interested in sources and timing of snowmelt runoff in the basin, our analyses are conducted using 'naturalized' flow records in which the effects of diversions and impoundments have been removed. These naturalized flow rates are estimated using a basic accounting method: adding or subtracting diversions and changes in reservoir storage.

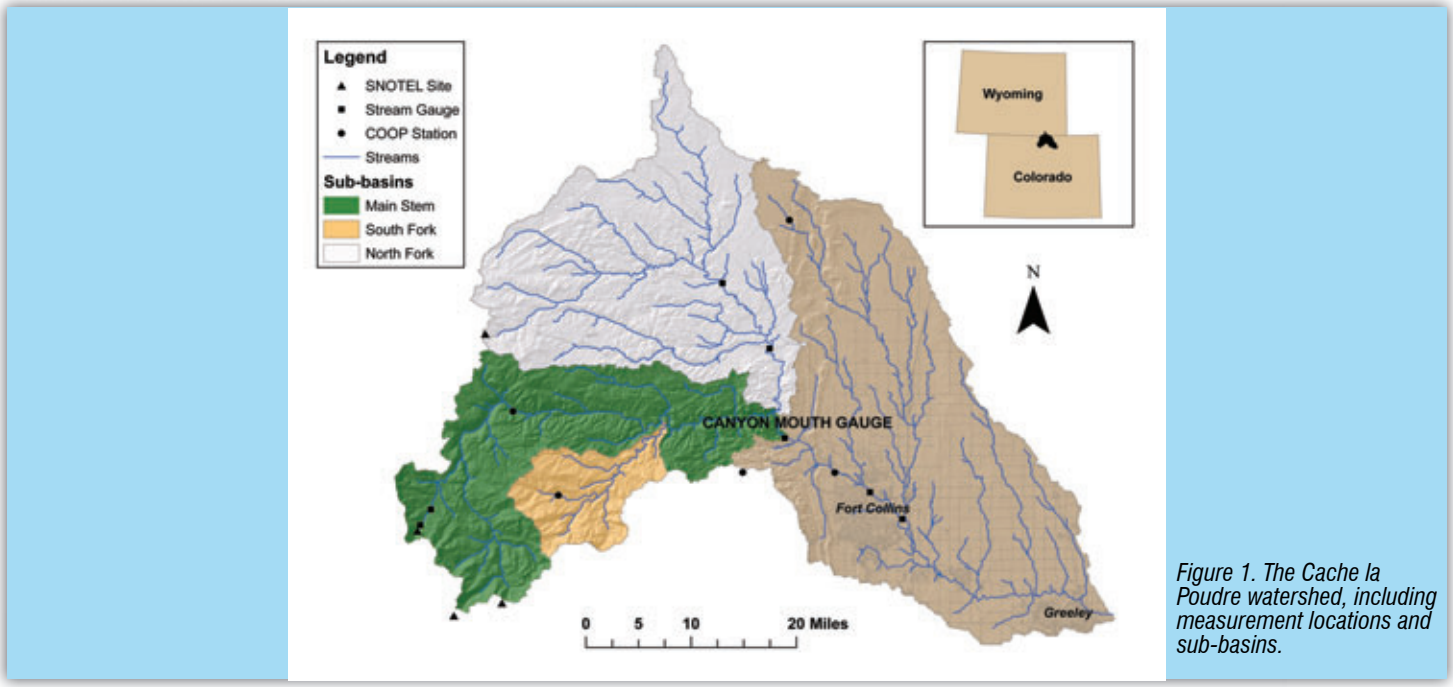

Figure 1. The Cache la Poudre watershed, including measurement locations and sub-basins.

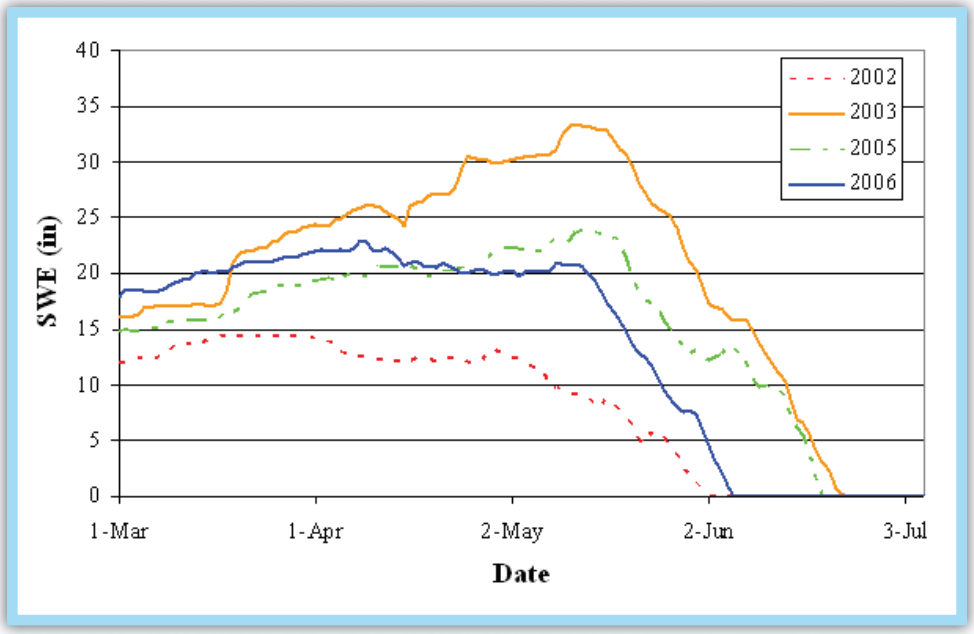

Figure 2. Spring-summer snow water equivalent at the Joe Wright SNOTEL site (10,120 feet). (Data source: Natural Resources Conservation Service)

Results

The upper Cache la Poudre Basin exhibits high spatial variability in temperature and precipitation. According to the PRISM model, average annual precipitation ranges from 13 inches at lower elevations to 53 inches near the headwaters, with a distinct increase in precipitation occurring above 10,000 feet. PRISM-derived average annual temperatures decrease from 50˚F at the lowest elevations to 25˚F at the headwaters. Temperature in the basin follows a seasonal cycle, with minimum temperatures in December and maximum temperatures in July. Average precipitation for the basin is lowest during the winter months and then increases during the spring, with maximum monthly average precipitation occurring in May.

Snow water equivalents measured at SNOTEL sites highlight the importance of spring precipitation. Figure 2 shows example snow water equivalent time series for the Joe Wright SNOTEL site (10,120 feet). During two of the years shown in Figure 2 (2003 and 2005), snow accumulation continued until mid-May. In all years, melt at this high-elevation site began in early to mid-May. In contrast, snow-covered area data show rapid snow melt over much of the basin area in late March (Figure 3), with the snow line gradually rising in elevation throughout the spring. Spring snow storms are evident in the snow cover data for all years except 2006. These spring storms caused abrupt rises in snow cover over the basin, but the additional snow cover typically melted within a week after each event.

These precipitation and snowmelt patterns affect the magnitude and timing of snowmelt runoff in the basin. River flow at the Canyon Mouth Gauge shows a gradual rise during early spring snowmelt, which begins from late March to late April (Figure 4). In most years, a gradual rise in discharge during early spring is followed by a rapid increase in discharge around mid-May. This rapid flow increase corresponds to the time when high elevation snowpack begins to melt (Figure 2). Peak flow occurs in late May to early June, and the river then recedes to baseflow conditions by mid-August.

Discussion

The spatial distribution of precipitation and temperature in the Cache la Poudre Basin implies a moisture surplus in the upper elevations of the basin and a moisture deficit in the lower elevation zones. Analyses of spring snow cover depletion and discharge data indicate that snow melt below around 8,000 feet does not typically result in increased river discharge. As the snow line rises above 8,000 feet, discharge begins to rise gradually, followed by a more rapid increase in flow as the snow line rises above around 9,500 feet elevation. Although each year exhibits a somewhat different relationship between snow cover depletion and discharge, the strong coupling between high elevation melt

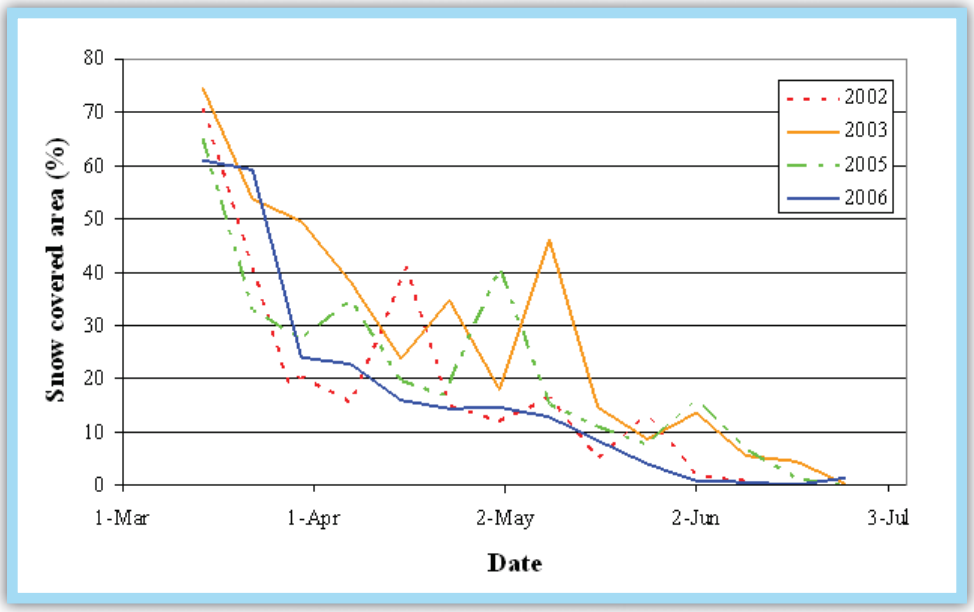

Figure 3. Spring-summer snow covered area depletion for the Cache la Poudre Basin. (Data source: MODIS 8-day composite snow cover, National Snow and Ice Data Center)

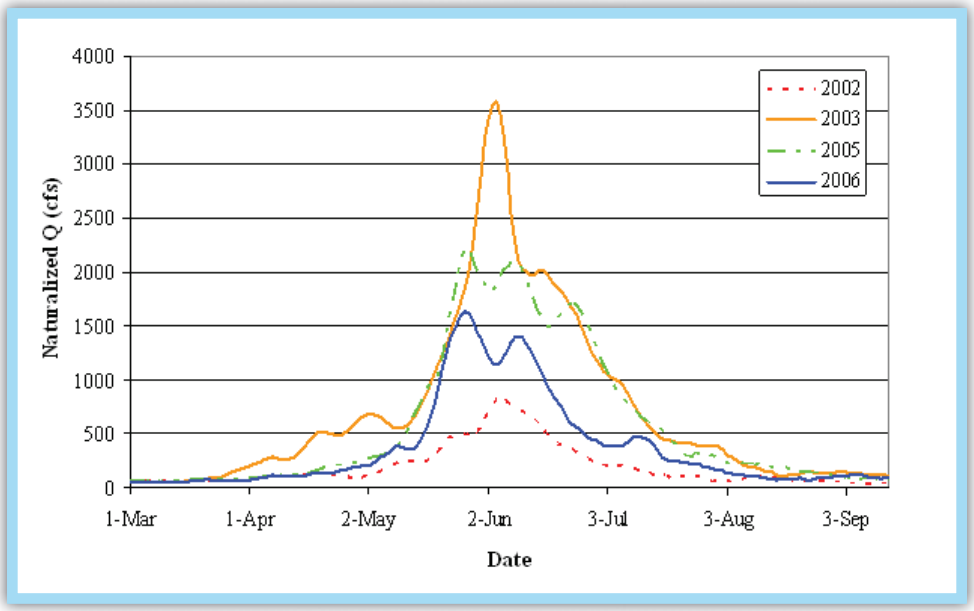

Figure 4. Naturalized discharge at the Cache la Poudre Canyon Mouth gauge. Discharge values represent a 7-day moving average. (Data sources: U.S. Geological Survey, Colorado Division of Water Resources, and water accounting by G. Varra)

and rapid increase in discharge suggests that high elevation zones contribute much of the snowmelt runoff to the river during high flows.

Under average conditions, the high-elevation moisture surplus is most significant in spring months, when precipitation is high but temperatures are still relatively low. Because precipitation in the basin is highest on average in the spring months, spring precipitation can contribute a significant portion of the annual water yield for the basin. The years 2005 and 2006 highlight the importance of spring conditions for river discharge. These years had similar high-elevation snow water equivalents on April 1 and May 1 (Figure 2), the dates when spring flow forecasts are issued, but the river flow was much higher in 2005 (Figure 4). During 2005, spring precipitation contributed to an increase in the high-elevation snowpack (Figure 2) and additional moisture input at lower elevations (Figure 3). With both high spring precipitation and cool spring temperatures, the 2005 snowpack persisted longer in the spring, and the river had a sustained high flow period lasting from mid-May through late June. In contrast, 2006 had low spring precipitation and warmer spring temperatures. The 2006 snowpack depleted rapidly throughout the basin (Figures 2 and 3), and the river had both lower peak flow and a shorter duration of high flows. With these warmer, drier spring conditions, the recession of the snowmelt hydrograph was already underway by mid-June.

Conclusions and Future Work

The timing and spatial distribution of precipitation in the Cache la Poudre Basin are both important controls on the amount of snowmelt runoff that occurs. Our preliminary results show that snowmelt from around 8,000-9,500 feet elevation tends to result in a gradual rise in Cache la Poudre river flow during April and early May. A rapid rise in the hydrograph occurs around mid-May, when the high elevation snowpack (above ~9,500 feet) begins to melt. Spring months have the highest average precipitation in this basin, and temperatures and precipitation during April and May can have a significant effect on river discharge.

MODIS snow cover data and the PRISM model have been useful for characterizing how and when different elevation zones in the basin contribute runoff to the Cache la Poudre during recent years (since 2000). We are working on quantifying these relationships and expanding the analysis to earlier years by using shape and timing characteristics of the hydrograph. Future work will incorporate snow cover, snow water equivalent, and temperature into a low-parameter model for predicting ensembles of snowmelt hydrographs under varying spring temperature and moisture conditions.

Acknowledgements

This project is funded by the Colorado Water Institute. We acknowledge the support and helpful contributions of Bill Fischer and Shawn Hoff from Cache la Poudre Water Users Association; Andy Pineda, Katie Melander, and Drew Linch of Northern Water; Tom Perkins and Mike Gillespie of the Natural Resources Conservation Service; and George Varra and Mark Simpson of the Colorado Division of Water Resources.

The Cache la Poudre River descends eastward in northwestern Colorado through Roosevelt National Forest in Poudre Canyon. (Image courtesy of Stephanie Kampf)

Development of Oilseed Crops for Biodiesel Production Under Colorado Limited Irrigation Conditions

Basic Information

Title:	Development of Oilseed Crops for Biodiesel Production Under Colorado Limited Irrigation Conditions
Project Number:	2009CO186B
Start Date:	3/1/2009
End Date:	2/28/2010
Funding Source:	104B
Congressional District:	4th
Research Category:	Not Applicable
Focus Category:	Agriculture, Irrigation, None
Descriptors:	None
Principal Investigators:	Jerry J Johnson

Publication

1. Johnson, Jerry; Jean-Nicolas Enjalbert, Joel Schneekloth, Alan Helm, Ravi Malhotra, Daren Coonrod, 2009, "Development of Oilseed Crops for Biodiesel Production Under Colorado Limited Irrigation Conditions", Completion Report 211, Colorado Water Institute, Colorado State University, Fort Collins, CO, 51 pages.

Development of Oilseed Crops for Biodiesel Production under Colorado Limited Irrigation Conditions

Jerry Johnson
Nicolas Enjalbert
Joel Schneekloth
Alan Helm
Ravi Malhotra
Daren Coonrod

April 2009

Completion Report No. 211

Colorado State University

Acknowledgements

The investigators are thankful for the support received from the Colorado Water Institute (CWI), without which most of the oilseed-for-biofuel research accomplishments during the past two years would not have been possible. Extension and training of students at all levels were also made possible by funding support from CWI. The authors extend a special thanks to CWI's director, Reagan Waskom, for his guidance and willingness to share in our triumphs and setbacks during the life of this project. As evidenced in this final report, our accomplishments have only been possible because we have worked seamlessly as a team, each author and investor depending on the knowledge, experience, and work of the other members of the team. No less important to the success of this project are the collaborating farmers, Colorado Agriculture Research Centers, USDA-ARS researchers, private companies, and state agencies that have conducted trials or supported oilseed research.

This report was financed in part by the U.S. Department of the Interior, Geological Survey, through the Colorado Water Institute. The views and conclusions contained in this document are those of the authors and should not be interpreted as necessarily representing the official policies, either expressed or implied, of the U.S. Government.

Additional copies of this report can be obtained from the Colorado Water Institute, E102 Engineering Building, Colorado State University, Fort Collins, CO 80523-1033 970-491-6308 or email: cwi@colostate.edu, or downloaded as a PDF file from http://www.cwi.colostate.edu.

Colorado State University

Extension

Development of Oilseed Crops for Biodiesel Production under Colorado Limited Irrigation Conditions

Final Report to the Colorado Water Institute

Jerry Johnson
Associate Professor
Extension Specialist

Nicolas Enjalbert
Graduate Research Assistant

Joel Schneekloth
Extension Water Resource Specialist

Alan Helm
Agronomy/Weed Management Specialist

Ravi Malhotra
Executive Director, iCast

Daren Coonrod
Plant Geneticist Cargill

Department of Soil and Crop Sciences
Colorado State University
Fort Collins, CO 80523

Table of Contents

Introduction

Since 2001, Colorado State University's Crops Testing Program, in collaboration with many other university and USDA ARS researchers, extension agents, farmers, private companies, and a non-profit organization, has undertaken oilseed-for-biofuel crop research and extension. The objective of this research is to test and adapt oilseed crop species (and varieties) to dryland, limited irrigation, and fully irrigated cropping systems prevalent in eastern Colorado, eastern Wyoming, western Kansas, and the Nebraska Panhandle. Regionally applied research has focused on agronomy trials, interaction with first-adopter farmers, weed control experiments, insect pest observations, crop water use experiments, and crop response to variable climatic conditions. This research has resulted in strong collegial relationships among researchers, farmers, private company representatives, and extension agents within the Great Plains area.

This research project is an integral contributor and benefactor of our overall efforts to provide cropping alternatives that are economically feasible and environmentally sustainable to eastern Colorado producers, specifically those with limited irrigation.

History of the Diesel Engine

During 1885, Rudolf Diesel set up his first shop-laboratory in Paris and began the 13-year ordeal of creating his distinctive engine. In 1893, he published a paper describing an engine with 'sparkless' combustion within a cylinder, named the internal combustion engine. Baron von Krupp and Machinenfabrik Augsburg Nurnberg Company in Germany supported Rudolf Diesel financially and provided engineers to work with him on the development of an engine designed to burn coal dust, because there were mountains of useless coal dust piled up in the Ruhr Valley. The first experimental engine was built in 1893and used high pressure air to blast the coal dust into the combustion chamber. The engine exploded and further developments of coal dust based fuel failed. However, a compression ignition engine that used oil, putatively peanut oil, as fuel was successful, and a number of manufacturers were licensed to build similar engines. In 1894, Diesel filed for a patent for his new invention, dubbed the diesel engine. Rudolf Diesel was almost killed by his engine when it exploded. However, the engine was the first to prove that fuel could be ignited without a spark. In 1896, Diesel demonstrated another model with the

theoretical efficiency of 75 percent, in contrast to the 10 percent efficiency of the steam engine. In 1898, Rudolf Diesel was granted his patent #608,845 for an "internal combustion engine" and in that same year, Busch installed a Rudolf Diesel-type engine in its brewery in St. Louis. That was the first engine of that kind in the United States.

Scope

This two-year project used field, greenhouse, and laboratory facilities to screen oilseed germplasm from around the world and to select oilseed cultivars adapted to Colorado's limited irrigation conditions and train a new crops specialist.

Objectives

1. To screen advanced lines of promising oilseed crop species (canola, camelina, soybean, sunflower) for adapted cultivars that could be grown by Colorado producers in the near future for biodiesel production and oilseed meal to feed northeast Colorado livestock.
2. To develop a research-based agronomic package of best management practices for oilseed production under limited irrigation conditions especially oriented toward weed control and water management.
3. To import and screen potentially new and underdeveloped oilseed crop species from temperate zones around the world.
4. To train a new crop agronomist/breeder to the PhD level. To train summer students and research associates in new crop research techniques and methodologies.
5. To determine the economic feasibility of oilseed crop production under limited irrigation conditions in light of dynamic interactions of variable yield, fuel costs, and input costs.

Definition and Conceptualization of Limited Irrigation in Colorado

"Limited irrigation occurs when water supplies are restricted in some way to the point that full evapotranspiration demands cannot be met" (Klocke et al., 2004). Full irrigation is the amount of water minus rainfall and stored soil moisture needed to achieve maximum crop yield. However, when irrigation water is insufficient to meet crop demand, limited irrigation management strategies should be considered (Norton et al., 2000).

There are two types of limited irrigation:

1. Supply: The amount of water available is fixed at any given time in the crop season and applied on a delivery schedule, not on crop demand. During high demand, the crop water requirements may not be met. The Fort Collins trials were conducted under this production environment (in addition to high pH and highly sodic soil conditions).
2. Capacity: The global water amount is limited in quantity but not in a fixed schedule, and crops can be irrigated on demand. However, it is important to choose the most critical stage when the water is to be applied. The other trials in the study were established under this water regime.

When addressing the definition of limited irrigation, the following question seems relevant: what is the goal of limited irrigation in the cropping system? Is it to homogenize the precipitation in a cropping system, or is it to decrease the amount of water use in an irrigated cropping system? In our experimentation, both situations are considered (Figure 1).

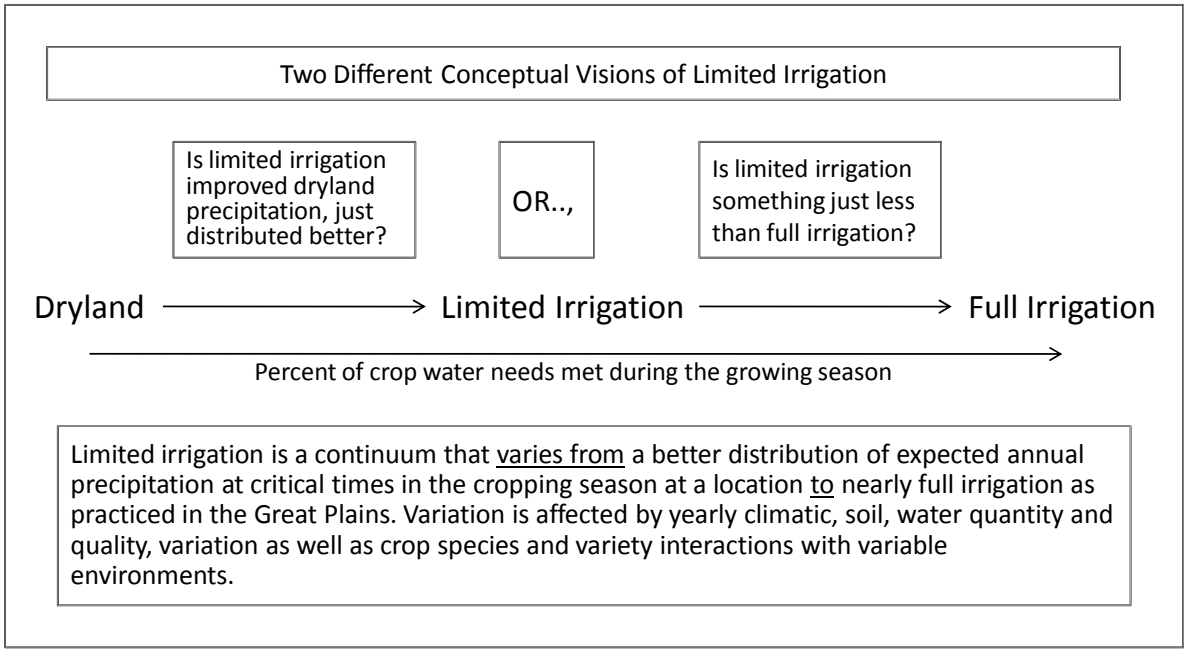

Figure 1: The two different conceptual visions of limited irrigation.

Crop response to limited irrigation can be determined by comparing the ETP with yield for four crop species (Fig 2). Based on data developed in 2006 at Akron, Colorado, camelina shows the highest potential for dryland production. Canola has a better response curve to irrigation and is

more suitable for limited and full irrigation than for dryland production. The best agronomic management practices for safflower are not developed enough to make any conclusions.

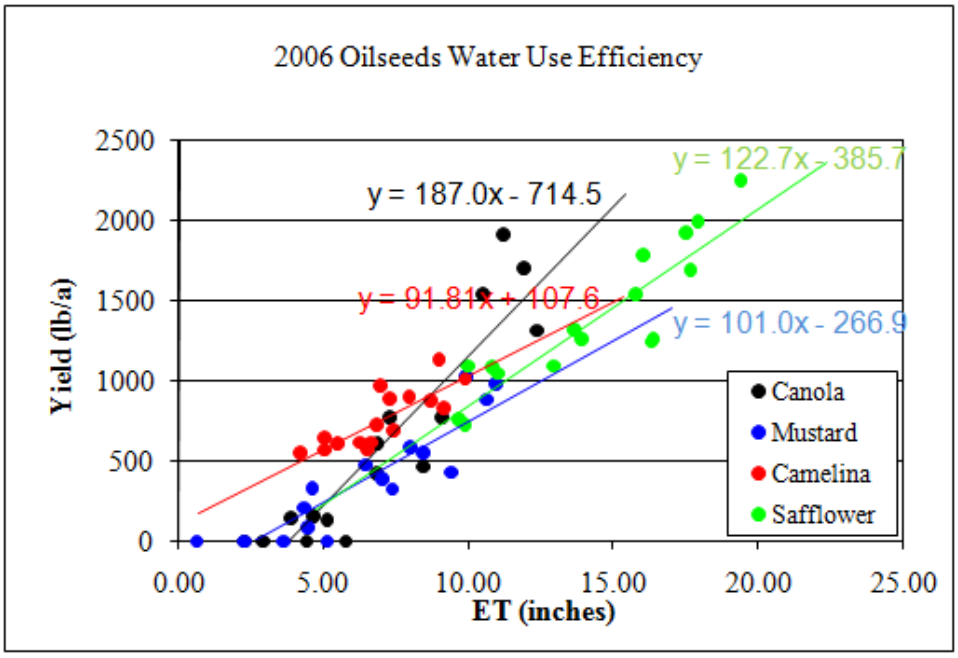

Figure 2: Comparison of oilseed species for water use efficiency (Akron, Colorado).

Project

Target Species Variety Performance Trials Results and Analyses

In 2007 and 2008, five target oilseed crops were studied: soybeans, safflower, sunflower, canola, and camelina. Performance trials were conducted at nine locations within Colorado: Fort Collins, Akron, Walsh, Dailey, Idalia, Yuma, Brandon, Julesburg, Yellow Jacket, and Rocky Ford. Oilseed crops were tested under three environmental conditions: dryland, limited irrigation, and full irrigation. Crop data included yield, percent grain moisture, plant height, and pod shattering. The oil profile was evaluated for canola, camelina, and safflower in 2007.

The five target oilseed crops being studied in three Colorado cropping systems are shown in Table 1. Sunflower, soybean, and safflower are summer annual broadleaf crops. Late fall harvest of sunflower eliminates the possibility of planting winter wheat the same year. Soybean is

primarily an irrigated crop. Sunflower is both a dryland and an irrigated crop. Safflower is primarily a dryland crop.

Winter canola and winter camelina can be either integrated into the dryland wheat-based cropping system or into an irrigated cropping system. Canola should be considered primarily as an irrigated crop, whereas camelina is competitive in both dryland and irrigated conditions.

Spring canola and camelina are opportunity crops that can be integrated into the dryland wheat rotations predominant in eastern Colorado, planted in early spring, harvested in July, and followed by wheat planting in September. Spring canola may be limited by high summer temperatures that reduce pollination and pod filling. Camelina is more drought tolerant and less sensitive to high temperature during pollination and pod filling.

Table 1: Cropping Systems for Adaptable Oilseed Crops in Colorado

	Month										
Crops	August	September	October to February	March	April	May	June	July	August	September	October
Soybean						Planting				Harvest	Harvest
Sunflower							Planting				Harvest
Safflower							Planting				Harvest
Winter Canola and Winter camelina		Planting						Harvest	Planted back to wheat		
Spring Camelina and Canola				Planting				Harvest	Planted back to wheat		

Results of 2007 and 2008 Crop Variety Performance Trials

In 2007, six variety performance trials of soybean, nine of sunflower, three of safflower, six of canola, and three of camelina were conducted. In 2008, one variety performance trial of soybean, four of sunflower, ten of canola, and eight of camelina were conducted. A total of 31 oilseed crop variety trials were conducted in nine eastern Colorado locations (Table 2) in 2007, and 23 were conducted in 2008, for a total of 54 oilseed trials over the two years of the project.

Table 2: Number of Trials by Irrigation Level and by Crop in 2007 and 2008

Water regime	Dryland		Limited Irrigation		Full irrigation	
	2007	2008	2007	2008	2007	2008
Soybean	1	0	4	0	1	1
Sunflower	4	2	2		2	2
Safflower	1	0	2	0	0	0
Canola (spring)	1	2	3	2	1	1
Canola (Winter)	1	1	2	2	3	2
Camelina (spring)	1	2	2	4	0	2
Total	9	7	15	8	7	8
Total Trials						54

Soybean

Soybean is a well-established oilseed crop currently grown on limited acreage in eastern Colorado. It has an established market and federal crop insurance. Soybean is a relatively good fit for irrigated cropping systems but is not suited for dryland production. Soybean variety trial maximum yields in eastern Colorado were 99 bu/ac in 2006 and 2007 (Table 3). Soybeans require 24 inches of water to produce maximum yields.

We believe that soybean is an underexploited crop in Colorado due to low input costs and lower water requirements than corn. Major seed companies are investing millions of dollars in soybean research, some of which benefits Colorado producers. Pest management and agronomics are well understood under Colorado conditions. Soybean has excellent emergence and stand establishment is not problematic. Soybean fits into an irrigated winter wheat rotation with wheat benefitting from symbiotically-fixed nitrogen from soybeans. Soybean processing into biofuel is straightforward and simply requires pressing the oil from the seed.

Soybean is the major oil source for current biodiesel production in the United States. The soybean oil profile is in accordance with the U.S. biodiesel standard (ASTM PS 121-99). It has a high level of oleic fatty acid, low level of saturated fatty acid, and medium polyunsaturated fatty acid content (24%), which also makes soybean oil a good source for straight vegetable oil (SVO). Soybean meal has high protein content and is the preferred and most consumed livestock protein feed additive, something of considerable interest to Colorado confined feeding operations. No specialized equipment is needed for soybean planting, cultivation, and harvest.

Limitations to soybean production in Colorado also exist. All soybean production, like most sunflower crops, must be transported out of state (usually to Goodland, Kansas) for crushing and processing. It is felt that the lack of a soybean crushing capacity in northeast Colorado is a major constraint to more widespread cultivation of soybeans in the state. Other constraints include above-average sensitivity to high pH, salty, and sodic soil conditions. Soybean crop residue after harvest is insignificant. Soybeans have low oil content in comparison to other oilseed crops (15-20%). Planting, irrigation, and harvest may overlap with other summer crops, creating a time constraint for some farmers. There is no state 'check-off' program in Colorado to support state crop improvement research. All soybean production in the United States, including Colorado, is potentially threatened by soybean rust.

Table 3: Soybean Trial Performance Summary

Location	Maturity	Water regime	Average	Max	Min	Oil
			lb/ac	lb/ac	lb/ac	gal/ac
Akron	Early	Dryland	684	1092	354	14
Fort Collins	Early	Limited Irrigation	1242	1818	654	25
Fort Collins	Medium	Limited Irrigation	1524	1998	924	30
Rocky Ford	Early	Limited Irrigation	2070	2934	1236	41
Rocky Ford	Medium	Limited Irrigation	2424	2694	2190	48
Yuma 2007	Late	Irrigated	4680	5964	4014	94
Yuma 2008	Late	Irrigated	3540	4320	3120	71

*Soybean oil content is estimated to be 18%.

Sunflower

Sunflower is a crop that has a long history in Colorado, but large acreages have been grown in Colorado only since the early-1990s due to local development and extension efforts by Golden Plains agronomist, Ron Meyer. Sunflower is adapted to both dryland and irrigated production. Crop variety trials conducted since the early 1990s show dryland oil sunflower yields from 1000-2000 lb/ac and irrigated yields in excess of 3000 lb/ac with oil content in seed as high as 47% (Table 4). High yields have been obtained under limited irrigation in northeast Colorado, where available water for irrigation is a serious production constraint for all crops. A well established market for the crop and a federal crop insurance program exist, and there is a premium for high oil content paid to sunflower producers. There is a good understanding of pest problems and

management in Colorado conditions, and sunflowers are better able to recover from hail damage than many other crops.

Sunflowers fit well into both conventional and no-till cropping systems. Colorado producers are adopting rotations, including a summer crop like sunflower, corn, or proso millet, while moving away from the traditional wheat-fallow rotation. Many high-yielding and high oil content sunflower hybrid varieties are available for producers who benefit from sunflower improvement conducted by many major crop seed companies and crop variety testing under Colorado conditions. Sunflowers are well suited to direct harvest with planting, tillage, and harvest equipment already owned by Colorado producers. Even prior to the recent release of herbicide-resistant sunflower hybrids, conventional chemical weed control packages existed that—albeit not perfect—were suitable for Colorado production. High protein sunflower meal is valuable to sunflower processing companies. In addition to the National Sunflower Association, which supports research and promotes sunflower products, the Colorado Sunflower Administrative Committee, our state 'check-off' organization created and funded by Colorado producers, supports applied research and promotion of Colorado produced sunflower products. Sunflower oil is the second most produced oilseed for biofuel in Europe.

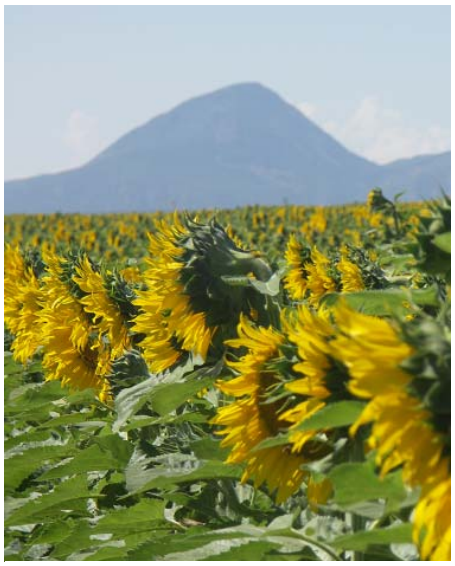

Figure 3: Sunflower field in Yellow Jacket, Colorado.

Some constraints to sunflower production should be mentioned. There have been some instances of yield reduction in the crops subsequent to sunflower due to extensive water and nutrient extraction by a good sunflower crop. Sunflowers have a history of poor emergence under dry planting conditions, resulting in poor stand establishment. Weed management in sunflower can be troublesome when dealing with late emerging weeds. Sunflower residue after harvest is not significant and does not stand up to high winds. Rodents, voles, ground squirrels, and birds can unearth newly planted sunflower seed, causing poor stand establishment in parts of fields. Bird damage can be severe before harvest, especially in areas where sunflowers are widely grown and have become targets

of local blackbird populations. When processing sunflower for biofuel, wax content from the oils needs to removed to avoid damage to engines. Although sunflower has good potential as a biofuel crop in Colorado, vegetable oil market prices have historically exceeded the value of the oil for biofuel. The Colorado company crushing sunflowers for oil is in Lamar, and the whole oil is exported out of Colorado for refining and retail sales. The majority of the Colorado sunflower crop produced in northeast Colorado must be transported to Goodland, Kansas, for crushing. A new facility will begin operations in 2009 in Dove Creek, Colorado.

Table 4: 2007 and 2008 Sunflower Trial Performance Summary

Location	Type	Water regime	Yield						Oil		
			Average		Max		Min				
			2007	2008	2007	2008	2007	2008	2007	2008	Average
			lb/ac	lb/ac	lb/ac	lb/ac	lb/ac	lb/ac	%	%	gal/ac
Brandon	Oil	Dryland	2005	1366	2445	1936	1611	953	38.7	40	89.9
Julesburg	Oil	Irrigated	2768		3474		2278		41.15	40	147.6
Idalia		Irrigated		2407		3620		1269		40	128.4

Safflower

Safflower is a potential oilseed crop for Colorado that is well suited to dryland production. There is a limited market established for safflower in the state meaning that producers interested in growing safflower should identify a market before planting the crop. There is no crop insurance available for safflower in Colorado, and there is no 'check-off' or grower organization that would support research and marketing of safflower. Being a relatively short-season crop, it fits well into crop rotations. It is also an aggressive scavenger for water and residual fertility. Safflower seed has relatively high oil content and is easily processed; it requires no special equipment for planting and is directly harvested. Emergence and stand establishment are typically not a problem in production of safflower.

Safflower production and use constraints outnumber the constraints for more widely produced crops like sunflower and soybean. There is not a varietal improvement program in the High Plains, and seed for planting can be hard to find. Weed management in safflower can be problematic due to the lack of herbicides labeled for broadleaf weed control. Hauling the harvested crop is an issue since the market is limited. The research knowledge base for safflower production in Colorado is scarce because there is no producer organization to promote this crop. Safflower's response to irrigation is not established but is being researched. Safflower can

present a fire hazard during harvest and leaves little residue. Safflower is another potential biofuel crop but, like sunflower, it competes directly with human consumption.

Safflower has an acceptable oil profile for SVO. Trial results in 2007 show yields up to 467 lbs/ac (Table 5). However, much higher yields have been achieved in different years with better crop management practices. Safflower oil content can approach 50% in some cultivars.

Table 5: Safflower Trial Variety Performance Summary

		Yield			Oil	
Location	Water regime	Average	Max	Min		
		lb/ac	lb/ac	lb/ac	%	gal/ac
Akron	Dryland	430	467	395	40	22.9
Fort Collins*	Limited irrigatior	221	301	182	40	11.8
Walsh	Dryland	208	250	148	40	11.1

*Grown under specific limited irrigation conditions in high pH and highly sodic soils.

Winter and Spring Canola

Canola is another potential irrigated biofuel crop in Colorado that could find a niche in limited irrigation rotations. There are both winter and spring canola varieties that can be planted in Colorado. Winter canola needs to be planted before the end of August to obtain plants that are developed enough to withstand low temperatures during winter. Late planted winter canola, especially north of I-70, has not been able to withstand winter freeze. Weed control is generally not a problem, because winter canola starts re-growth in early spring and competes well with weeds. Varieties from public and private sources have been screened in five different Colorado agro-climatic conditions through a collaborative research program with Kansas State University. Planting and harvest equipment are readily available, although canola is commonly swathed prior to threshing to allow uniform maturity of pods from the top to the bottom of the canopy and to avoid excessive shattering. Fall planted varieties present a grazing opportunity for livestock and can still yield well. Spring canola might be an attractive alternative crop under limited irrigation due to existence of high yielding roundup-ready cultivars from private seed companies. Peak water use for canola is at the end of May and early June, well before the peak water demands of summer crops (corn, alfalfa, and sunflower). Canola leaves relatively sturdy residue after harvest. Oil content in canola is relatively high (40-45%), and the seed is easily processed.

The meal byproduct is high in protein and is a valuable livestock feed, like soybean. Canola produces a high-quality fuel and has good potential for biofuel and meal production for use on the farm.

There are several downsides to canola production. Flea beetles that attack young canola seedlings must be controlled with chemical treatments. There is not a well established market, and there is no Colorado grower organization to promote production and research. Canola is not a good candidate for direct harvest and should be swathed and then picked up much the same as millet. Canola is sensitive to many of the herbicides used in other crops and in fallow periods such as atrazine, Ally, and others. Since there is not a well established market for canola in Colorado, hauling of the harvested product can be an issue.

Canola is small-seeded and needs to be shallow planted to obtain good stands. Deep seeding, or soil crusting, or planting into dry soil conditions can significantly reduce stands. Canola is sensitive to high temperatures during flowering, which may reduce yields. Lack of adequate soil moisture will reduce yields more than with camelina. Canola has a taproot system giving the crop access to deep water and nutrients (Downey et al., 1974). However, when grown in semiarid regions such as the High Plains, the canola roots require adequate subsoil moisture to sustain the crop during flowering and seed filling. Under managed irrigation, winter canola is capable of yielding more than 3,000 lbs/ac. Low crop prices and lack of an established market infrastructure for canola are significant obstacles to more widespread production in Colorado. With limited grower experience and the lack of insurance programs, production of canola has been limited.

Figure 4: 2008 oilseed harvest at Fort Collins, Colorado.

Winter and spring canola varieties are being screened to identify promising cultivars for Colorado's limited irrigation and dryland conditions. Trials conducted in 2007 and 2008 demonstrate yields of 800 lbs/ac under dryland, of 2,400 lbs/ac under limited irrigation, and up to 3724 lbs/ac under full irrigation (Table 6).

Table 6: 2007 and 2008 Canola Variety Trial Performance Summary

				Yield			Oil	
Location	Source	Year	Water regime	Average	Max	Min		
				Lbs/ac	Lbs/ac	Lbs/ac	%	gal/ac
Akron	Commercial	2007	Limited Irrigation	1891	2397	1458	40	101
	Commercial	2007	Full Irrigation	1837	2424	1205	40	98
	Cargill	2007	Limited Irrigation	1645	2900	831	40	88
	Cargill	2007	Dryland	401	807	343	40	21
	Blue Sun	2007	Limited Irrigation	1259	1777	1406	40	67
Fort Collins	Commercial	2007	Limited Irrigation	259	761	79	40	14
Fruita	National trial	2006-2007	Irrigated	2339	3621	872	40	125
Yello Jacket	National trial	2006-2007	Irrigated	651	1236	428	40	35
Rocky Ford	Commercial	2006-2007	irrigated	1750	3171	752	40	93
Rocky Ford	National trial	2007-2008	Irrigated	1816	2703	815	40	97
Fruita	National trial	2007-2008	Irrigated	2760	3724	2124	40	147
Walsh	National trial	2007-2008	dryland	602	1175	102	40	32
Akron winter canola	Blue Sun	2007-2008	Limited Irrigation	1172	1784	731	40	63
Akron winter canola	National trial	2007-2008	Limited Irrigation	1370	2236	828	40	73

Camelina

Camelina is an oilseed crop native to southeast Europe and southwest Asia. The plant has been known for about 4,000 years as a cultivated crop, but there has been relatively little research conducted on it worldwide. Camelina is a promising new oilseed crop that has become the

subject of widespread research in the last few years because it is not attacked by flea beetles, is more resistant to drought than other spring oilseed crops, and can be direct harvested. Camelina is a low input crop. It can be grown in both dryland and limited irrigation cropping systems. Water requirements for irrigated camelina are being investigated, but like canola, its peak water demand occurs early in the season when full summer crop water demands are low.

Camelina is an early maturing crop, planted in early April and harvested in mid-July. Although some production issues must be solved, camelina could become an excellent crop for the wheat-based, no-till cropping systems that dominate eastern Colorado. With sufficient spring precipitation, camelina can be planted in the spring following fall harvest of corn, sunflowers, or proso millet and can be harvested in time to allow for accumulation of late July to mid-September precipitation before planting wheat. Instead of harvesting two crops in three years, the current improved cropping system, by producing camelina in the spring it would be possible to harvest three crops in three years. Camelina's seed is extremely small, and seeding rates and seed costs are low. Fertilizer requirements of Camelina are low. Camelina does not respond well to nitrogen fertilizer application. Several private seed companies and universities have camelina improvement projects that are providing varieties for testing in Colorado. Winter camelina is more winter hardy than winter canola and can be planted later in the fall and still survive low winter temperatures. Camelina does not require any special planting equipment and can be direct harvested, which means that equipment is readily available for production. Insect pressure on camelina is almost non-existent. Camelina oil is high in Omega 3 fatty acids, and studies are currently underway to determine if real health benefits result from consumption of camelina oil. Under experimental conditions, camelina meal has been fed to livestock in Montana and Wyoming, and it appears to be wholly satisfactory.

Currently, there are significant production and marketing constraints for camelina. Understandably, the agronomics of camelina production are less well known than those of other crops. Due to small seed size, camelina must be planted shallow and pressed into the soil to have good seed-to-soil contact. Camelina can be planted in early spring; some claim that it can be seeded anytime during the winter or spring. Emergence is slow under cool spring soil temperatures, especially in variable soil moisture conditions. Unlike canola, camelina is not

attacked by flea beetles. Camelina's stand establishment and weed control are being investigated in the Great Plains and the Pacific Northwest. There is currently very little acreage of camelina being planted in Colorado, and there is no grower 'check-off' program to support research and production. Federal and state agencies are providing research funds that have helped address some basic water and fertilizer requirement issues and conduct variety trials. For several years, camelina producers were able to sell seed to Blue Sun Biodiesel, but seed prices were low and hauling to crushing facilities was an additional cost. Marketing needs to be fully investigated by producers before planting. Camelina is a small-seeded crop that may require adjustments to equipment to prevent loss during harvest and hauling. Camelina's meal is currently not legal for sale as livestock feed, although high omega 3 content in the oil and meal indicates that it might be more beneficial than other oilseed for human and livestock health.

Figure 5: Charlie Rife, a breeder from Blue Sun Biodiesel, inspects camelina trials.

Camelina's seed oil content ranges from 30% to 45%. Over 50% of its fatty acid, when cold pressed, is polyunsaturated. Alpha linolenic acid (omega 3) represents 30% to 45% of the total oil. Omega 3 fatty acid content has been shown to have beneficial effects on human health.

Trials conducted in 2007 and 2008 achieved dryland yields up to 1,138 lbs/ac under dryland conditions, up to 1,725 lbs/ac under limited irrigation, and up to 2386 lbs/ac under full irrigation (Table 7).

Table 7: Camelina Trial Performance Summary

Location	Source	Water regime	Yield						Oil*
			Average		Max		Min		
			2007 lb/ac	2008 lb/ac	2007 lb/ac	2008 lb/ac	2007 lb/ac	2008 lb/ac	Average gal/ac
Akron	Blue Sun/GPO/ MSU	Limited Irrigation	1243	1053	1725	1332	973	555	53.6
Akron	Blue Sun/GPO/ MSU	Dryland	789	-	1138	-	529	-	36.8
Fort Collins	Blue Sun/GPO/ MSU	Limited Irrigation	547	1159	839	1500	283	794	39.8
Yellow Jacket	Blue Sun/GPO/ MSU	Fully Irrigated	.	2002	.	2386	.	1739	93.4

*Camelina oil content is estimated to be 35%.

Oil Meal Quality

Camelina meal contains 40% to 45% crude protein and 10% fiber, which is similar to that of soybean. The glucosinolate content is close to zero (Korsrud et al., 1978; Lange et al, 1995), and camelina meal has 12% oil remaining after cold pressing with 5% of omega 3. A Montana study shows a higher level of omega-3 content in eggs as camelina meal content in feed increases. Up to 15% can be integrated into a balanced feed ration (Pilgeram et al., 2007). Budin et al. (1995) found that Camelina oil has 30% more antioxidant than other commercial edible oil, which could explain superior storage quality of raw camelina oil. Feed for beef containing camelina meal does not show significant difference for average daily gain nor feed efficiency (Pilgeram et al., 2007).

Fuel properties

The cloud point of camelina biodiesel is 4°C and the pour point is -8°C (Fröhlich et al., 2005), which is similar to other biodiesel feedstocks such as canola (Table 8).

Table 8: Low Temperature Properties of Blends of Camelina and Mineral Diesel Oil

Camelina ester %	Mineral diesel %	Cloud point °C	CFPP °C	Pour point °C
100	0	+3	-3	-4
80	20	+3	-7	-6
60	40	+3	-9	-9
40	60	+3	-11	-12
20	80	+3	-13	<-18
0	100	+3	-15	<-21

(Source: Fröhlich et al., 1998)
CFPP: Cold filter plug point

Camelina oil has a high iodine value: 155 mg I2/g Oil. The limit of the European standard is 120 mg I2/g Oil. This can be an issue for cold climates. A concern with a high iodine value is that unsaturated acids might polymerize in the engine and cause deterioration.

Oil Profile Analysis of the Targeted Crops

Different vegetable oils for fuel can be differentiated by their oxidative and cold flow properties. These two criteria are linked. Some vegetable oils have to be heated to ensure flow but warm temperatures increase the rate of fatty acid oxidation which adversely affects power.

Fatty acids that reduce the cold flow quality of SVO are palmitic (C16:0) and stearic acids (C18:0). The cloud point is correlated to the level of saturated fatty acid. The cloud point of vegetable oil ranges from 8C to -18C, with changes in saturated fat ranging from 23% to 3%. Table 9 provides the percentage of these fatty acids in three main crops of the study.

Table 9: Saturated Fatty Acid Profile Summary

Species Unit	Camelina %	Canola %	Safflower %
Palmitic (C16:0)	6	5	6
Stearic (C18:0)	2.5	2	2.5
Total saturated	11.5	8.5	10

There are no significance differences among these crops for saturated fatty acid content. These levels of saturated fatty acid are acceptable for SVO.

Polyunsaturated fatty acids improve cold flow properties but are more susceptible to oxidation. Bringe (2004) recommends no more than 24% polyunsaturated fatty acids in vegetable oil for dual use in the food and fuel industry. The level of polyunsaturated fatty acid (PUFA) has

another major impact. High levels of PUFA increase the amount of nitrogen oxides released into the atmosphere upon combustion (McCormick et al., 2001). Another important property of oil for fuel is ignition quality, which is measured by the cetane number (CN). High CN is desired to have the best ignition and combustion. The CN number increases with increased content of oleic acid in the oil.

Table 10: Oleic and Polyunsaturated Fatty Acid Profile

Species	Camelina	Canola	Safflower
Unit	%	%	%
Oleic (C18:1)	19	62	37
Linolenic (C18:3)	30	6	0.1
Total polyunsaturated	51	25	52

There are significant differences among crops regarding fatty acid content. Camelina has a very high level of linolenic acid and polyunsaturated fatty acid (Table 10). Crop improvement is needed to increase the oleic acid content of camelina. The ideal fuel oil profile is approximately 65% oleic acid, 22% linoleic fatty acid, 3% linolenic acid, and the lowest possible level of palmitic and stearic fatty acid (2%). The high level of polyunsaturated acid makes camelina one of the best crops known for human vegetable oil consumption.

Canola has an acceptable oil profile for fuel with a high level of oleic acid and medium level of polyunsaturated acids, which is the result of successful breeding programs.

Safflower's oil profile is similar to camelina's. However, high variation is noticed between safflower cultivars. Selection has reduced the level of polyunsaturated acid and increased the level of oleic acid. Oleic acid level varies from 14% to 70% and polyunsaturated fatty acids levels range from 18 to 75% (Table 11).

Table 11: Oil Profiles of the Targeted Crops Compared to Desired SVO Profile

Fatty Acid (Carbon saturation)	Palmitic (C16:0)	Stearic (C18:0)	Total saturated	Oleic (C18:1)	Linoleic (18:2)	Linolenic (C18:3)	Total polyunsaturated
unit	%	%	%	%	%	%	%
Ideal SVO Profile	<6	<5	<13	>50	±20	<5	<25
Soybean	5	2	10	65	18	2	22
Sunflower	5	2	8	75	8	2	12
Safflower	6	2.5	10	37	40	0.1	52
Canola	5	2	8.5	62	18	6	25
Camelina	6	2.5	11.5	19	20	30	51

Camelina Agronomy Trial

In 2008, two types of agronomy trials were conducted. The first trial examined the effect of seeding rates, variety, and nitrogen rate on camelina yield at multiple locations in a split plot factorial design (Table 12). The second study evaluated the impacts of different gypsum rates, varieties, and seeding rates on camelina yield in a sodic soil near Fort Collins (Table 13).

First trial:

1. Experimental design: split plot factorial
2. Nitrogen rates: Soil N, 60 lbs, 120 lbs
3. Seeding Rates: 2, 5, 8, 11 and 14 lbs/ac
4. Varieties: Cheyenne (Blue Sun) and Calena (Montana State University)
5. Location: Akron dryland and limited irrrigation, Yellow Jacket, Colorado

Only the Yellow Jacket trial was successful. In Akron, herbicide from previous years damaged the trial and no nitrogen was applied. Only the Yellow Jacket results are reported.

Table 12: 2008 Camelina Agronomy Trial Analysis of Variance

Effect	Num DF	Den DF	F Value	Pr > F
variety (var)	1	58	5.25	0.03
Seeding rate (sr)	4	58	2.41	0.06
var*sr	4	58	1.60	0.19
nitrogen	2	58	0.20	0.82
var*nitrogen	2	58	1.43	0.25
sr*nitrogen	8	58	1.48	0.18
var*sr*nitrogen	8	58	1.25	0.29

- Nitrogen was not was significant for yield (P value = 0.82)
- Seeding rate was weakly significant for yield (P value = 0.08)
- The seeding rate of 2 lbs/ac was significantly lower for yield than the other seeding rates

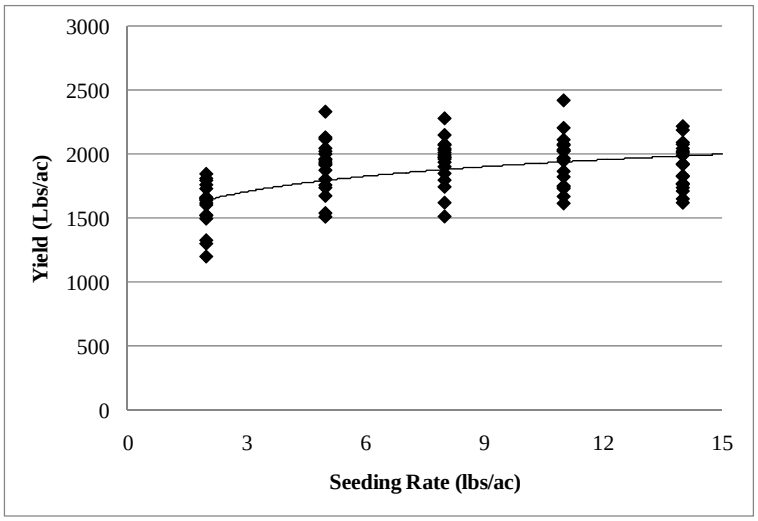

Figure 6: Non-linear regression of seeding rate by yield Averaged over all other factors at Yellow Jacket, Colorado, 2008.

In Fort Collins we are conducting trials in a specific environment with high sodium content. Crusting and high pH are the main issues. Gypsum could be a solution to fix and leach sodium down the soil profile.

Second Trial:

- Experimental design: split plot factorial
- Factors
    - Gypsum rates: 0, 1 and 2 t/ac
    - Seeding Rates: 2, 5, 8, 11 and 14 lbs/ac
    - Varieties: Cheyenne (Blue Sun) and Calena (Montana State University)

- Location: Fort Collins, limited irrrigation (total water: 11 inches) under one sodic soil: Medium high SAR: 7.5.

- No significant interaction between variety, seeding rate, and gypsum occurred.
- A positive yield response occurred with increasing gypsum rate with camelina. Plant height shows an increase with gypsum rate.
- All studied traits except height show a significance among seeding rates. Optimum yield appears to be at 5 lbs/ac. At this density, number of pods and number of branches are higher than at higher seeding rates. Figure 7 shows the high correlation between number of pods and number of branches.

Table 13: Statistical Analysis of Various Growth and Experimental Parameters for Camelina

	Average	Min	Max	P-Value		
Traits				Variety	Seeding-Rate	Gypsum
Primary Branches	1.9	1.2	3.8	0.53	0.0001	0.43
Total number of branches	4.1	1.7	7.6	0.86	>.0001	0.16
Pods Number	48.1	11.6	117.8	0.52	>.0001	0.22
Yield (lbs/ac)	610	282	999	0.11	0.002	0.35
Height (Inches)	21.72	19.33	25.33	0.15	0.08	0.63
Stand (plant/ac)	1419483	398000	2374000	0.75	>.0001	0.63

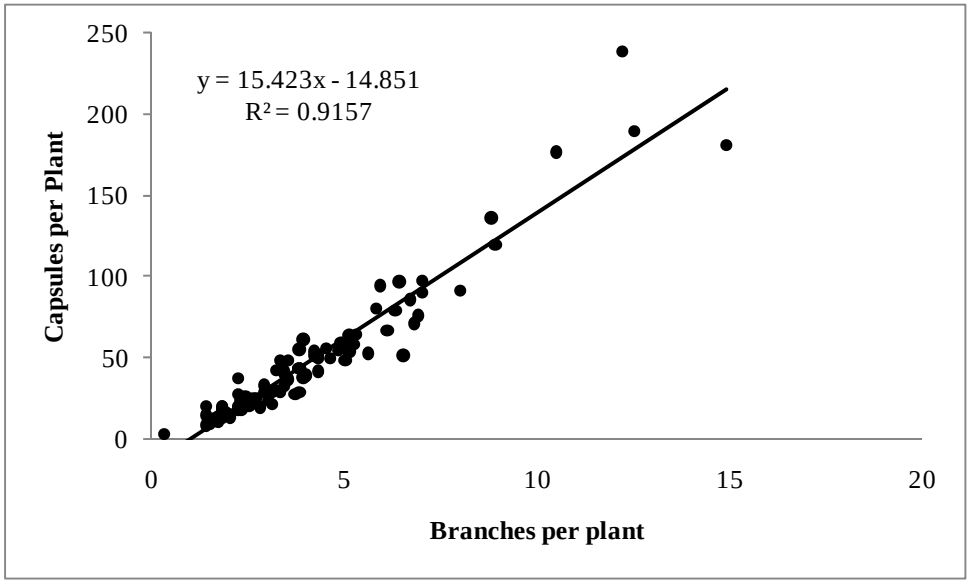

Figure 7: Correlation between branches per plant and capsules per plant in the seeding rate X gypsum rate trial.

Screening New Alternative Crops

The genetic study of camelina's drought resistance is based on a unique set of over 100 accessions from the European collection. Europe is the center of origin for camelina. The approach is simple, and water use efficiency is the main research objective. The collection is planted in the greenhouse and in the field under fully irrigated and dry conditions, and all growth and reproduction characteristics are measured. The first objective, which has already been met, is to determine if there is sufficient variation in drought response to justify further investigation, or if additional genetic material needs to be included in the set of accessions. After the first round of greenhouse/field observations, John McKay and Nicolas Enjalbert have identified accessions that show repeatable variation in response to drought both in the greenhouse and in the field. Correlations with growth and reproduction observations have given them some insight into which characteristics might be responsible for differential response to drought. This research should lead to identification of measurable traits that indicate improved water use efficiency, which can be used by breeders to identify drought resistant lines within their breeding populations. This research presents the base for future investigators to identify regions in the camelina genome responsible for the traits that confer drought resistance, and to provide oilseed physiologists the information necessary to better understand the mechanisms of drought resistance.

Camelina *sativa*

The Camelina *sativa* accessions in the tested collection have 16 countries of origin (Table 14).

Country of origin	# accessions
Czech Republic/Slovakia	1
Former Soviet Union	14
Belgium	2
Bulgaria	6
Germany	38
Italy	1
Kyrgyzstan	1
Poland	5
Romania	1
Russia	1
Spain	1
Sweden	1
Switzerland	1
Ukraine	1
unknown	26
Former Yugoslavia	1
Total	101

Table 14: Country of Origin of Camelina Accessions

Figure 8: Map of Europe showing countries of origin for camelina accessions.

Figure 8: Camelina experiment in the greenhouse.

Brassica *carinata* (Ethiopian mustard)

The Brassica *carinata* accessions in the tested collection have four countries of origin.

Table 15: Country of Origin of Ethiopian Mustard Accessions

Country of origin	# accessions
Ethiopia	33
Thailand	1
unknown	1
Zambia	4
Total	39

Figure 9: Brassica *carinata* experiment in the greenhouse.

Figure 10: A student works on the greenhouse experiment.

The Approach

Greenhouse Study

Two moisture treatments were applied: drought (60% of field capacity) and fully irrigated.

There were four replicates for each treatment.

Phenotypic measurement included height, number of pods, and seed weight.

Field Study

85 accessions of *Camelina sativa* were grown.

39 accessions of Brassica *carinata* were grown.

100 accessions of Brassica *juncea* were grown.

Two treatments: dryland and irrigated (flood irrigated three times).

Two replicates for each treatment.

Previous crop was alfalfa.

Planted by hand in one-meter rows.

Phenotypic measurements included height, date of flowering, number of pod, pods density, pod size, seed weight, number of seed per pods, number of branches, and biomass per plant.

Results and Analysis

Several field conditions affected plant emergence and growth. The seed bed was rough, and there was high clay content in the seed bed soil. Plant growth was suppressed and plant population was reduced by flooding caused by the tornado that struck the research station in June 2008.

Camelina sativa

There were significant differences among accessions for height and pod number in the greenhouse, as well as significant differences among accessions for seed weight in the field (Table 16).

Table 16: Summary of Camelina Performance in the Greenhouse and in the Field

	Greenhouse		Field		
	Height	Pods	Height	Seed wt	plt Biomass
	p-value	p-value	p-value	p-value	p-value
Accessions	0.0002	0.0013	0.0905	0.0018	0.1014
Treatment	<.0001	<.0001	<.0001	<.0001	<.0001
Interaction	0.99	0.27	0.16	0.0044	0.252
CV	16	41	47	79	53

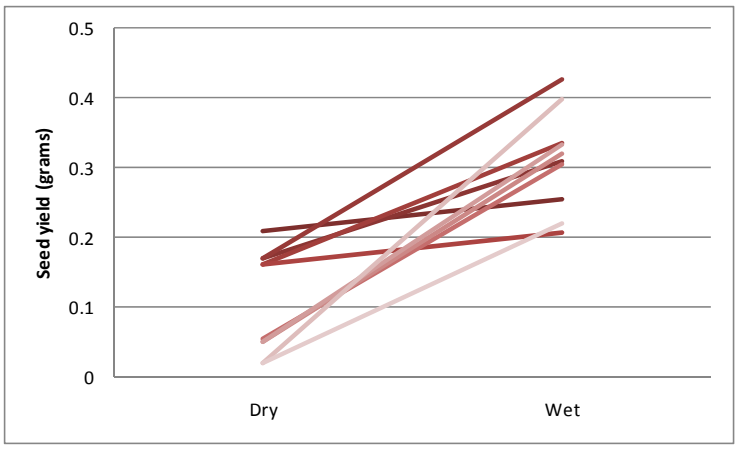

Figure 11: The interaction of accessions under wet and dry conditions for seed weight in the greenhouse.

All traits measured in the greenhouse were also measured in the field. Table 17 is the complete correlation table for these traits. Figure 13 is an example of one correlation showing that seed weight in the greenhouse is negatively correlated under dry conditions to seed weight from all accessions under well watered conditions (r = -0.36; P = 0.0099). This suggests that some accessions are better adapted to dry environments. These accessions are potential sources of genes for drought tolerance.

Table 17: Correlation of Traits in Field and Greenhouse-grown Plants

	heighGHD	Seedghd	podghd	heightghw	seedghw	podghw	heightfd	seedfd	biomassfd	heightfw	seedfw	biomassfw
heighGHD	1	0.20351	0.10886	0.64286	0.05818	0.11399	-0.03463	-0.00919	-0.01611	-0.08694	-0.1033	-0.07584
		0.1563	0.4517	<.0001	0.6882	0.4306	0.8133	0.9495	0.9116	0.5483	0.4753	0.6006
	50	50	50	50	50	50	49	50	50	50	50	50
Seedghd	0.20351	1	0.45218	-0.04652	-0.36171	0.03064	-0.25584	-0.14253	-0.21899	-0.24179	-0.21377	-0.25159
	0.1563		0.001	0.7484	0.0099	0.8327	0.076	0.3234	0.1265	0.0907	0.1361	0.078
	50	50	50	50	50	50	49	50	50	50	50	50
podghd	0.10886	0.45218	1	-0.05395	-0.28749	0.11883	-0.07708	-0.04315	-0.0905	-0.11927	-0.10529	-0.12568
	0.4517	0.001		0.7098	0.0429	0.4111	0.5986	0.7661	0.532	0.4094	0.4668	0.3845
	50	50	50	50	50	50	49	50	50	50	50	50
heightghw	0.64286	-0.04652	-0.05395	1	0.22733	0.33434	-0.10604	-0.16734	-0.1399	-0.30724	-0.30789	-0.29148
	<.0001	0.7484	0.7098		0.1124	0.0176	0.4684	0.2454	0.3325	0.03	0.0296	0.04
	50	50	50	50	50	50	49	50	50	50	50	50
seedghw	0.05818	-0.36171	-0.28749	0.22733	1	0.27548	0.0314	0.02137	-0.02397	0.00836	-0.07626	0.01545
	0.6882	0.0099	0.0429	0.1124		0.0528	0.8304	0.8829	0.8687	0.954	0.5987	0.9152
	50	50	50	50	50	50	49	50	50	50	50	50
podghw	0.11399	0.03064	0.11883	0.33434	0.27548	1	-0.17559	-0.35056	-0.24427	-0.21595	-0.23899	-0.25534
	0.4306	0.8327	0.4111	0.0176	0.0528		0.2275	0.0126	0.0873	0.132	0.0946	0.0735
	50	50	50	50	50	50	49	50	50	50	50	50
heightfd	-0.03463	-0.25584	-0.07708	-0.10604	0.0314	-0.17559	1	0.58265	0.95338	0.12442	0.15537	0.12334
	0.8133	0.076	0.5986	0.4684	0.8304	0.2275		<.0001	<.0001	0.3943	0.2864	0.3985
	49	49	49	49	49	49	49	49	49	49	49	49
seedfd	-0.00919	-0.14253	-0.04315	-0.16734	0.02137	-0.35056	0.58265	1	0.5809	0.12565	0.16767	0.1223
	0.9495	0.3234	0.7661	0.2454	0.8829	0.0126	<.0001		<.0001	0.3846	0.2445	0.3975
	50	50	50	50	50	50	49	50	50	50	50	50
biomassfd	-0.01611	-0.21899	-0.0905	-0.1399	-0.02397	-0.24427	0.95338	0.5809	1	0.14308	0.16778	0.14732
	0.9116	0.1265	0.532	0.3325	0.8687	0.0873	<.0001	<.0001		0.3215	0.2441	0.3073
	50	50	50	50	50	50	49	50	50	50	50	50
heightfw	-0.08694	-0.24179	-0.11927	-0.30724	0.00836	-0.21595	0.12442	0.12565	0.14308	1	0.92376	0.98827
	0.5483	0.0907	0.4094	0.03	0.954	0.132	0.3943	0.3846	0.3215		<.0001	<.0001
	50	50	50	50	50	50	49	50	50	50	50	50
seedfw	-0.1033	-0.21377	-0.10529	-0.30789	-0.07626	-0.23899	0.15537	0.16767	0.16778	0.92376	1	0.8853
	0.4753	0.1361	0.4668	0.0296	0.5987	0.0946	0.2864	0.2445	0.2441	<.0001		<.0001
	50	50	50	50	50	50	49	50	50	50	50	50
biomassfw	-0.07584	-0.25159	-0.12568	-0.29148	0.01545	-0.25534	0.12334	0.1223	0.14732	0.98827	0.8853	1
	0.6006	0.078	0.3845	0.04	0.9152	0.0735	0.3985	0.3975	0.3073	<.0001	<.0001	
	50	50	50	50	50	50	49	50	50	50	50	50

f: field; gh: Greenhouse; D: dry; W: wet.

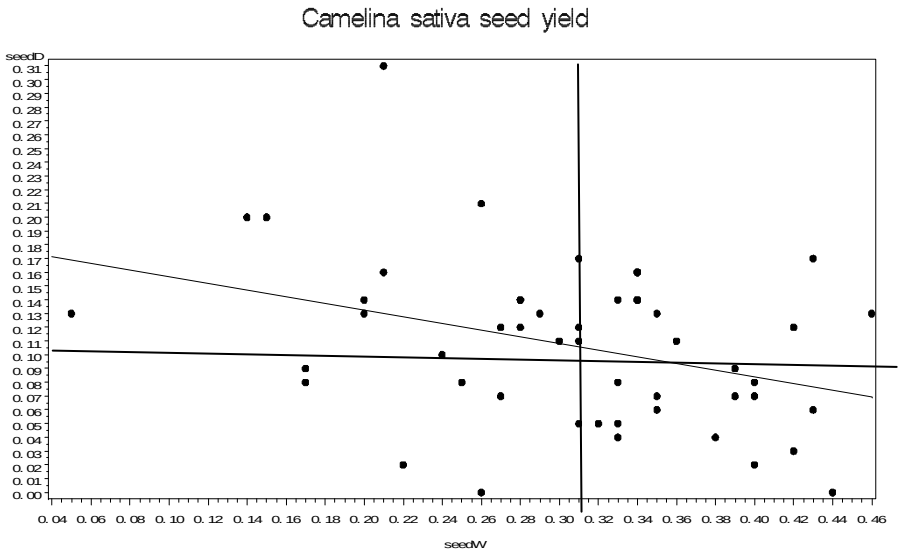

Figure 12: Example of a significant negative correlation in seed weight between wet and dry treatment in the greenhouse.

Depending on the origin of camelina accessions, their differences are significant. The Spanish camelina lines tend to do better under dry treatment in both environments. The origin of different accessions may explain some drought tolerance characteristics. For example, single accessions from Spain and Germany respond differently to wet vs. dry growing conditions. In both the greenhouse and the field, the accessions from Germany had higher seed weight than the accessions from Spain. However, the accession from Spain was equal or superior to accessions from Germany under dry conditions (Figures 14 and 16).

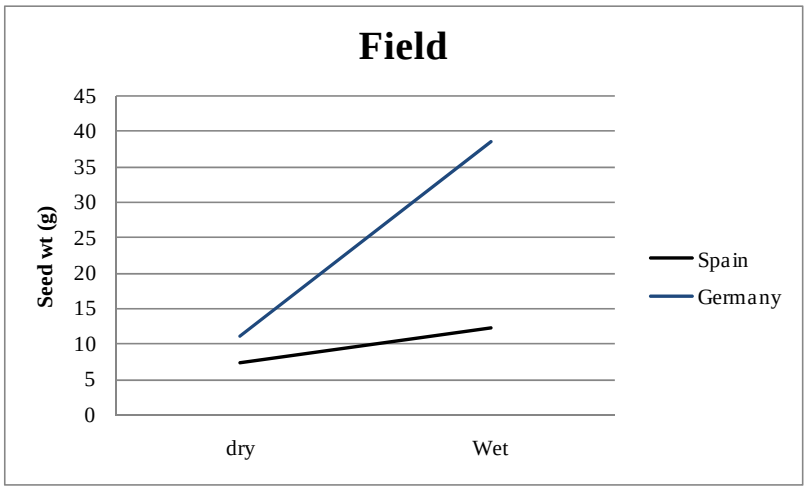

Figure 13: Reaction norm for seed weight per plant in the field between two accessions from different origins.

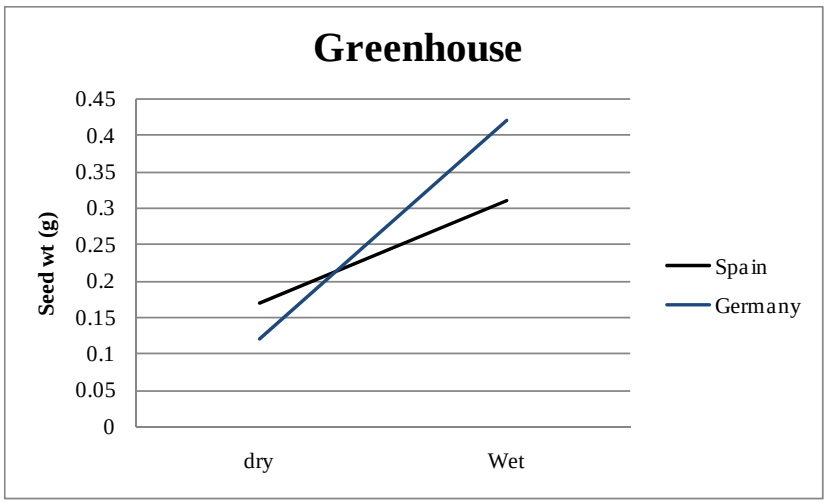

Figure 14: Reaction norm for seed weight per plant in the greenhouse between two accessions from different origins.

Brassica carinata

There were significant differences among accessions for height, seed weight, pod number, and plant biomass in the field (Table 18).

Table 18: Summary of *Brasica carinata* Screening Statistical Analysis

	Height	Seed wt	plt Biomass	Pods
	p-value	p-value	p-value	p-value
Accessions	<.0001	<.0001	0.1400	<.0001
Treatment	<.0001	<.0001	<.0001	<.0001
Interaction	0.0036	0.09	0.47	0.25
CV (%)	12	27	43	19

Flea beetle is one of the most damaging pests to canola. Notes were taken on all accessions. The flea beetle pressure was very high. Some *Brassica carinata* accessions did not have any flea beetles on them, and some were entirely infested. The evaluation was done on a scale from one to three:

- One: no damage
- Two: partially infested
- Three: entirely infested

The results show a strong correlation between dry and wet treatments, suggesting that the flea beetle tolerance is not dependent on water regime. Some accessions appear to be resistant to flea beetles. It could be attributed to the glucosinolate content in the plant, which inhibits insect feeding. Camelina was not affected by flea beetles.

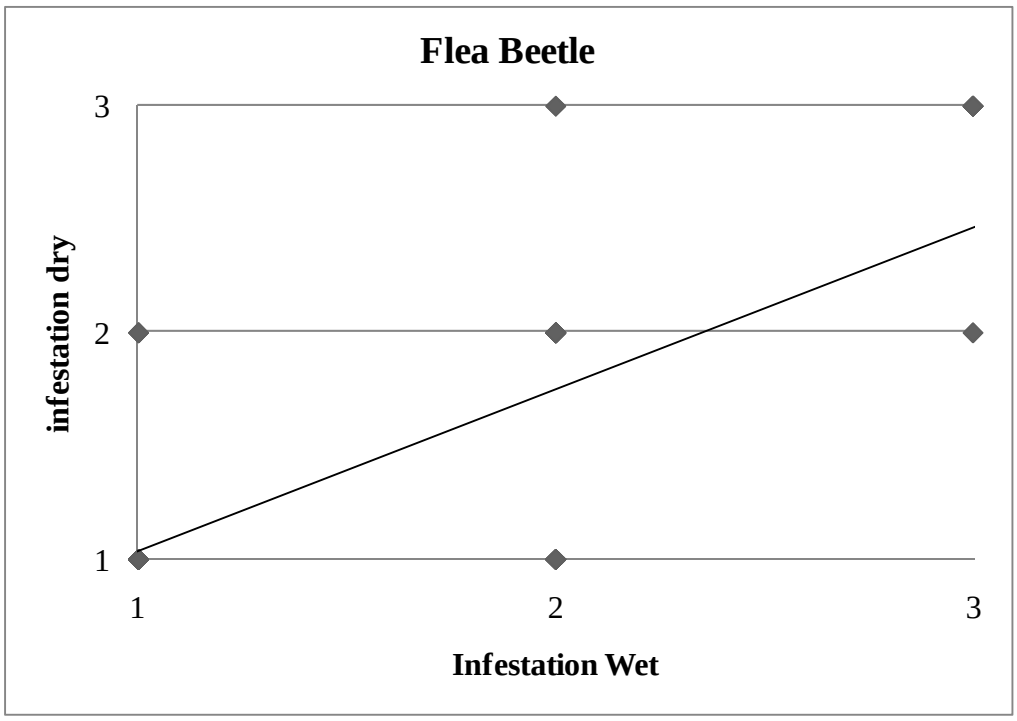

Figure 15: Significant positive correlation (r = 0.853) for flea beetle infestation of accessions between wet and dry treatments. (Infestation scale: one = no infestation; three = totally infested)

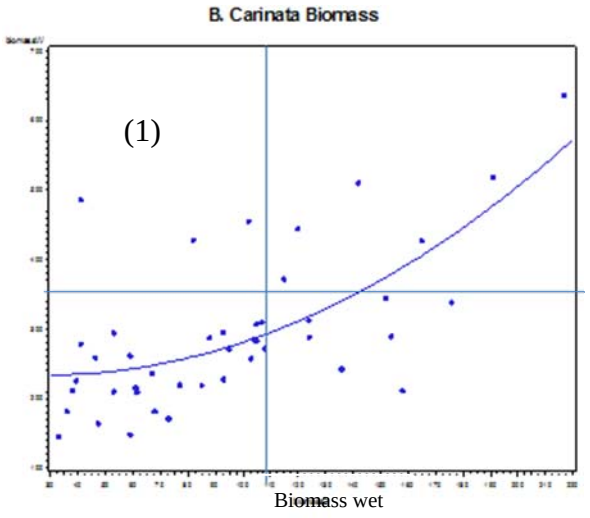

Figure 16: Significant positive correlation (r = 0.628) for biomass of accessions between wet and dry treatments. Presence of outliers (1) shows that some accessions do better under dry environments than other accessions.

Table 19: Correlation of Traits in Field-Grown *Brassica carinata*

	heightD	HeightW	biomasW	biomasD	seedW	seedD	podD	podW
heightD	1	0.23316	0.19738	0.25294	0.16641	0.12536	0.44935	0.22472
		0.1147	0.1937	0.0937	0.2636	0.4119	0.0015	0.1289
	47	47	45	45	47	45	47	47
HeightW	0.23316	1	0.53879	0.36023	0.33341	0.08989	0.3288	0.65001
	0.1147		0.0001	0.0139	0.0206	0.5524	0.0225	<.0001
	47	48	46	46	48	46	48	48
biomasW	0.19738	0.53879	1	0.62829	0.73085	0.11262	0.08611	0.0706
	0.1937	0.0001		<.0001	<.0001	0.4667	0.5694	0.641
	45	46	46	44	46	44	46	46
biomasD	0.25294	0.36023	0.62829	1	0.21302	0.37905	0.17958	-0.00553
	0.0937	0.0139	<.0001		0.1552	0.0094	0.2324	0.9709
	45	46	44	46	46	46	46	46
seedW	0.16641	0.33341	0.73085	0.21302	1	0.18996	0.09873	0.08807
	0.2636	0.0206	<.0001	0.1552		0.2061	0.5044	0.5517
	47	48	46	46	48	46	48	48
seedD	0.12536	0.08989	0.11262	0.37905	0.18996	1	0.10733	0.03764
	0.4119	0.5524	0.4667	0.0094	0.2061		0.4777	0.8039
	45	46	44	46	46	46	46	46
podD	0.44935	0.3288	0.08611	0.17958	0.09873	0.10733	1	0.48003
	0.0015	0.0225	0.5694	0.2324	0.5044	0.4777		0.0006
	47	48	46	46	48	46	48	48
podW	0.22472	0.65001	0.0706	-0.00553	0.08807	0.03764	0.48003	1
	0.1289	<.0001	0.641	0.9709	0.5517	0.8039	0.0006	
	47	48	46	46	48	46	48	48

W: irrigated; D: dryland

Many yield components of accessions show a positive correlation between dry (D) and wet (W) treatments.

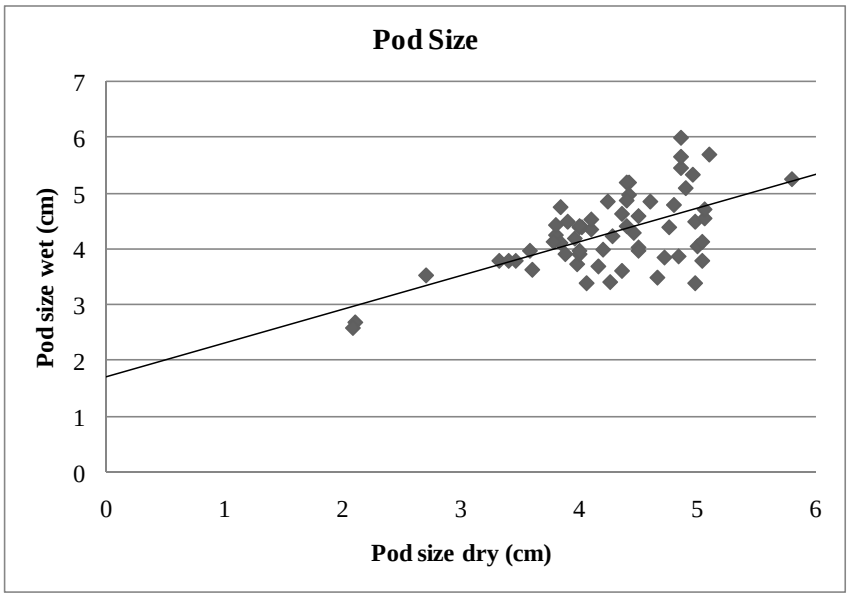

Figure 17: Significant positive correlation (r = 0.601) for pod size of accessions between wet and dry treatment.

We have found substantial variation among Camelina *sativa*, Brassica *carinata*, and Brassica *juncea* accessions in several traits of interest. These traits exhibit significant effects of genotype and treatment, as well as interactions between them, emphasizing the importance of local environment for the evaluation of lines for selection. Additional traits of importance will be evaluated in these accessions (such as oil content and profile, carbon isotope ratio, seed size, and protein content). In future years, a mapping population of camelina will be evaluated to localize genetic regions associated with these traits.

Economic Feasibility

The following economic feasibility study is designed to address three practical economic questions frequently asked about oilseed production for use as SVO on the farm. Oilseed crops in the Brassicacea family, like canola and camelina, are good rotation crops because they could fit into a wheat-based cropping system, and they can break some harmful pest cycles.

1. What is the break-even price per pound and yield that would make it economically feasible to produce oilseed under limited irrigation conditions, dryland and full irrigation?
2. What price per gallon of petroleum diesel vs. oilseed yield is feasible to grow your own fuel?
3. What is the break-even price per pound and diesel that would make it economically feasible to buy and crush oilseed for fuel without growing any crop?

Cropping systems options that include oilseed production for biofuel can be considered, but in the interest of answering these three questions as succinctly and clearly as possible our economic example is based on:

1. A limited irrigation system: three crops in three years and including winter wheat: corn/spring canola /winter wheat
2. A dryland system: three crops in three years and including winter wheat: corn/spring camelina/winter wheat

The rotation with spring canola allows the producer to harvest the oilseed in late July and plant winter wheat in the same year. Our limited irrigation cropping system production costs differ

from the costs of full irrigation by lower costs of nitrogen fertilizer and slightly lower irrigation costs. Moreover, the fixed cost per crop is lower in the spring oilseed/winter wheat rotation because there are three crops in three years, as opposed to three crops in four years. The operating costs and direct costs assumed for this example are provided in Table 17. The nitrogen cost is very volatile. The price used is $0.6/lb. Oilseed meal (approximately 2/3 of harvest weight) from crushed oilseed is currently worth approximately $0.15/lb and has been included in the net return calculations, based on the assumption that it could be sold locally or used on the farm.

Limited Irrigation Rotation

Price $/lb	Alternative Yield (lbs/acre)					
	1800	2000	2200	2400	2600	2800
0.1	-167	-147	-127	-107	-87	-67
0.12	-131	-107	-83	-59	-35	-11
0.14	-95	-67	-39	-11	17	45
0.16	-59	-27	5	37	69	101
0.18	-23	13	49	85	121	157
0.2	13	53	93	133	173	213
0.22	49	93	137	181	225	269
0.24	85	133	181	229	277	325
0.26	121	173	225	277	329	381
0.28	157	213	269	325	381	437

1. Limited Irrigated Spring Canola Break-Even Analysis – Per Acre Returns Over Total Direct Cost ($/acre) in Eastern Colorado.

Price $/lb	Alternative Diesel price($/gal)					
	2.5	2.8	3.1	3.4	3.7	4
0.1	246	276	306	336	366	396
0.12	202	232	262	292	322	352
0.14	158	188	218	248	278	308
0.16	114	144	174	204	234	264
0.18	70	100	130	160	190	220
0.2	26	56	86	116	146	176
0.22	-18	12	42	72	102	132
0.24	-62	-32	-2	28	58	88
0.26	-106	-76	-46	-16	14	44
0.28	-150	-120	-90	-60	-30	0

3. Limited Irrigated Spring Canola Break-Even Analysis – Per 2200 lbs Returns Over Total Cost Oilseed ($/lb) and Diesel Price ($/gal) in Eastern Colorado.

1. Producing canola under limited irrigation is profitable producing a positive net return of 49 $/ac
2. Producing seed and crushing is the most interesting option at current diesel price: 127 $/ac
3. Buying seed and crushing give a net return of $100 for every 2200 lbs crushed

Price $/gal	AlternativeYield (lbs/acre)					
	1800	2000	2200	2400	2600	2800
1.9	-33	2	37	71	106	141
2.2	-8	29	67	104	142	180
2.5	16	57	97	137	178	218
2.8	41	84	127	170	213	256
3.1	65	111	157	203	249	295
3.4	90	139	187	236	284	333
3.7	115	166	217	269	320	371
4	139	193	248	302	356	410

2. Limited Irrigated Spring Canola Break-Even Analysis – Per Acre Returns Over Total Direct Cost ($/acre) as a function of diesel price, in Eastern Colorado

Figure 18: Canola economic study under limited irrigation.

At average yield of 2,200 lbs/ac under limited irrigation (2007 average trial yield), the net return at the current market price ($0.18/lb) is estimated at $127/ac, if the seed is crushed on farm. At yields of 2,200 and 2,400 lbs/ac, the break-even points are estimated at $0.15 and $0.14, respectively. After several years of experimentation and experience in farmer's fields, we believe that average and sustainable limited irrigation canola yields of 2000-2400 lb/ac are realistically attainable. Even when the price of petroleum diesel is at $2.50/gallon and hypothetical yields of 1800 lb/ac, positive returns per acre would be expected for SVO production on the farm with canola, but not with camelina. At average yields of 2200 lb/ac and petroleum diesel at $2.50/gallon, net returns are expected to be $96/ac.

Dryland Rotation

Price $/lb	Alternative Yield (lbs/acre)					
	400	600	800	1000	1200	1400
0.1	-75	-55	-35	-15	5	25
0.12	-67	-43	-19	5	29	53
0.14	-59	-31	-3	25	53	81
0.16	-51	-19	13	45	77	109
0.18	-43	-7	29	65	101	137
0.2	-35	5	45	85	125	165
0.22	-27	17	61	105	149	193
0.24	-19	29	77	125	173	221
0.26	-11	41	93	145	197	249
0.28	-3	53	109	165	221	277

1. Dryland Spring Camelina Break-Even Analysis – Per Acre Returns Over Total Direct Cost ($/acre) in Eastern Colorado.

Price $/lb	Alternative Diesel price($/gal)					
	2.5	2.8	3.1	3.4	3.7	4
0.1	112.0	125.6	139.1	152.7	166.3	179.8
0.12	92.0	105.6	119.1	132.7	146.3	159.8
0.14	72.0	85.6	99.1	112.7	126.3	139.8
0.16	52.0	65.6	79.1	92.7	106.3	119.8
0.18	32.0	45.6	59.1	72.7	86.3	99.8
0.2	12.0	25.6	39.1	52.7	66.3	79.8
0.22	-8.0	5.6	19.1	32.7	46.3	59.8
0.24	-28.0	-14.4	-0.9	12.7	26.3	39.8
0.26	-48.0	-34.4	-20.9	-7.3	6.3	19.8
0.28	-68.0	-54.4	-40.9	-27.3	-13.7	-0.2

3. Dryland Spring Camelina Break-Even Analysis – Per 1000 lbs Returns Over Total Cost Oilseed ($/lb) and Diesel Price ($/gal) in Eastern Colorado.

1. Producing camelina under dryland is profitable. At 0.18 $/lbs and 1000 lbs/ac, the net return is 46 $/ac.
2. Producing seed and on farm crushing bring the biggest net return: 81.5 $/ac
3. Buying seed and crushing has an equivalent net return that to only producing seed, but safer.

Price $/gal	Alternative Yield (lbs/acre)					
	400	600	800	1000	1200	1400
1.9	-45	-10	24	59	94	129
2.2	-40	-2	35	73	111	148
2.5	-34	6	46	87	127	167
2.8	-29	14	57	100	144	187
3.1	-23	22	68	114	160	206
3.4	-18	31	79	128	176	225
3.7	-12	39	90	142	193	244
4	-7	47	101	155	209	263

2. Dryland Spring Camelina Break-Even Analysis – Per Acre Returns Over Total Direct Cost ($/acre) as a function of diesel price, in Eastern Colorado

Figure 19: Camelina economic study under dryland production.

At average yield of 1,000 lbs/ac under dryland (2007 average trial yield), the net return at the current market price ($0.18/lb) would be $81.5/ac if seed is crushed on farm. After several years of experimentation and experience in farmers' fields, we believe that average and sustainable dryland camelina yields of 800-1000 lb/ac are realistically attainable. Perhaps equally important is that on-farm production of biofuel (independence from foreign energy) would make Colorado's food and feed supply more secure without being affected by world affairs beyond local control. In addition, the carbon footprint of Colorado agriculture would be smaller.

Table 20: 2008 Estimated Production Costs and Returns – Limited Irrigation Spring Canola, Colorado

2008 Estimated Production Costs and Returns - Irrigated Spring Canola, Colorado

	Unit	Cost/unit	Quantity	**Cost/value per ac**	Cost per unit of production
Production	lbs.	0.11	3000	330	
Total Receipts				330	0.11
Direct Cost:					
Operating Preharvest					
Disc	Acre			2.66	0.006
Nitrogen	lbs.	0.60	120	72.00	0.164
Phosphate	lbs.	0.33	20	6.60	0.015
Potassium	lbs.	0.14	24	3.36	0.008
Sulfur	lbs.	0.21	10	2.10	0.005
Custom Fertilizer Appl	Acre			1.16	0.003
Seed	lbs.	7.00	5	35.00	0.080
Herbicide (Sonalan/treflan)	oz	0.40	24	9.60	0.022
Custom Herbicide Appl	Acre			1.55	0.004
Irrigation Energy	Acre			40.00	0.091
Irrigation Labor	hr.	10.00	1	10.00	0.023
Interest on Op.Cap	DOLS.				0.000
Total Preharvest:	DOLS.			184.03	0.419
Operating Harvest:					
Machinery Operating Cost/haul	bu.	0.24	50	12.00	0.004
Total Harvest				12.00	0.064
Total Operating Cost:				196.03	0.483
Property and Ownership Costs:					
Machinery replacement & Machinery Taxes & Insura	DOLS.			9.7	
General Farm Overhead	DOLS.			15	
Real Estate taxes	DOLS.			16	
Total Property and ownership costs:	DOLS.			40.7	
Total Direct Costs:				236.73	
Factor payment:				111.05	
Net Receipts - Factor Payments:				347.78	0.12
Net Return				-17.78	
Break-even to cover:	lbs			3,162	0.12

Table 21: 2008 Estimated Production Costs and Returns – Dryland Spring Camelina, Colorado

2008 Dryland Spring Camelina in Northeastern Colorado					
	Unit	Cost/unit	Quantity	**Cost/value per ac**	Cost per unit of production
Production	lbs.	0.15	1000	150	
Total Receipts				150	0.15
Direct Cost:					
Operating Preharvest					
Nitrogen	lbs.	0.6	40	24	0.0547
Phosphate	lbs.	0.33	0	0	0.0000
Potassium	lbs.	0.14	0	0	0.0000
Sulfur	lbs.	0.21	0	0	0.0000
Custom Fertilizer Appl	Acre			1.16	0.0026
Seed	lbs.	2	2.5	5	0.0114
Herbicide (Sonalan/treflan)	oz	0.4	24	9.6	0.0219
Custom Herbicide Appl	Acre			1.55	0.0035
Machinery Op. Costs	DOLS.			19.85	0.0452
Total Preharvest:	DOLS.			61.16	0.0942
Operating Harvest:					
Machinery Operating Cost	DOLS.			15.2	0.0152
Hauling	DOLS.			4	0.0040
Total Harvest				19.2	0.0641
Total Operating Cost:				80.36	0.1583
Net return				69.64	
Property and Ownership Costs*:					
Machinery replacement & Machinery Taxes & Insurance	DOLS.			18.0	
General Farm Overhead	DOLS.			6.6	
Real Estate taxes	DOLS.			1.2	
Total Property and ownership costs*:	DOLS.			35.0	
Total Direct Costs:				115.4	
Factor payment*: land at 4.00%				19.0	
Net Receipts - Factor Payments:				134.4	0.13
Net Return with fixe cost				15.6	
Break-even to cover:	lbs			1,222	0.13
*Fix costs established in a three years rotation with three crops.					

Benefits of SVO for Colorado

SVO has many benefits when compared to petro-diesel and other biofuels. It requires no refining, and it is not harmful to living organisms. As a renewable resource it provides a reliable income opportunity for many farming generations. The German Federal Water Act on the Classification of Substances Hazardous to Waters denotes SVO as NWG (non hazardous to water)[1]. Biodiesel, on the other hand, is slightly hazardous to water, while diesel and gasoline are rated as highest toxicity. A North American study of the toxicity of vegetable oil in freshwater has found no harmful SVO effects[2].

Figure 20: iCAST Engineering Project manager Micah Allen presents "How to Make Your Own Fuel" to a group of farmers.

As a fuel, SVO emits 40 to 60% less soot[3,4] than petro-diesel. It does not contain sulphur, and therefore does not cause acid rain[5]. In addition, carbon monoxide and particulate emissions are slightly lower. CO_2 emissions are also reduced by 80 to 96%[6,7] compared to petro-diesel when

[1] (*WGK (Wassergefährdungsklassen):The German Water hazard classes.* Available at http://www.folkecenter.dk/plant-oil/WGK_ENG.htm; http://www.folkecenter.dk/plant-oil/publications/vwvws.pdf)
[2] (http://www.epa.gov/oilspill/pdfs/Li-Lee-Cobanli-Wrenn-Venosa-Doe_FSS06.pdf)
[3] (http://home.clara.net/heureka/gaia/veggie-oil.htm).
[4] (http://www.biomatnet.org/secure/Fair/F484.htm)
[5] www.folkecenter.dk/plant-oil/publications/PPO-emissions.htm
[6] (http://www.folkecenter.dk/plant-oil/publications/energy_co2_balance.pdf)

locally produced and used for fuel. Finally, Polycyclic Aromatic Hydrocarbons (PAH) emissions are distinctly lower for all vegetable fuels, reducing risks of cancer[8] (Figure 22). SVO can contribute to an energy-independent Colorado agricultural system and can increase food and feed sector security. Gasoline has a 0.873[9] energy ratio (energy yield/energy input). If we include distribution and the value of canola meal, the energy ratio number for canola-based SVO is 5.45[10], while for sunflower-based SVO, it is 6.33[11] (Table 22).

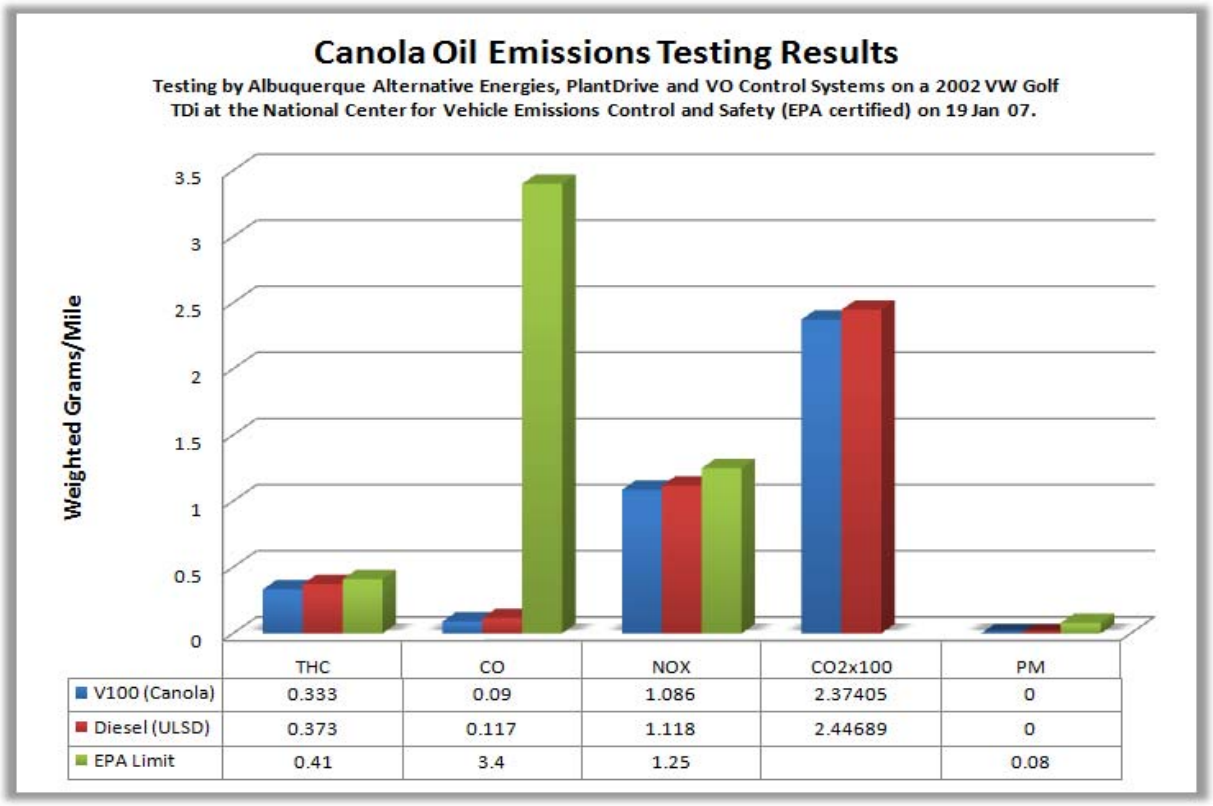

	THC	CO	NOX	CO2x100	PM
V100 (Canola)	0.333	0.09	1.086	2.37405	0
Diesel (ULSD)	0.373	0.117	1.118	2.44689	0
EPA Limit	0.41	3.4	1.25		0.08

Figure 21: Canola oil emissions testing results.

[7] Institut Français des Huiles Végétales Pure, ADEME 21/11/06
[8] http://www.biomatnet.org/secure/Fair/F484.htm

[9] Institut Français des Huiles Végétales Pure, ADEME 21/11/06
[10] http://www.valbiom.be/, Biomass certification
[11] ADVA 31

Table 22: Energy Ratio of Different Fuels Including SVO

	Regular Unleaded	Diesel	Biodiesel Canola	Biodiesel Sunflower	SVO Canola	SVO Sunflower
Ration energy produced / Non renewable energy used	0.873	0.917	2.99	3.16	**5.45**	**6.33**
Green house gas emissions (q eq. CO2 / kg)	3650	3390	888	745	**660**	**498**

Training

Figure 22: Shusong Zeng, a CSU post-doctoral researcher from China.

Figure 23 : CSU undergraduate student Tom Fitzgerald with Shusong Zeng.

Figure 24: Gaelle Berges, master's student from Ecole d'Ingenieur de Purpan in France.

Figure 25 : David Johnson and Blake Robinson, high school students Fort Collins.

Figure 26: CSU graduate student Jean-Nicolas Enjalbert.

Figure 27: A biodiesel adventure journalist from Japan.

Figure 28: A group of farmers at the Oilseed Field Day at Yellow Jacket, Colorado, summer 2008.

Figures and Tables

References

Budin, J.T., Breene, W.M., & Putnam D.H. (1995). Some compositional properties of Camelina (Camelina-sativa L Crantz) seeds and oils. *Journal of the American Oil Chemists Society, 72*, 309-315.

Downey, R.K., and Klassen A.J., Pawlowsk.Sh. (1974). Breeding quality improvements into Canadian Brassica oilseed crops. *Fette Seifen Anstrichmittel, 76*, 302-302.

Fröhlich, A., and Rice, B. (2005). Evaluation of Camelina sativa oil as a feedstock for biodiesel production. *Industrial Crops and Products, 21(1)*. 25-31.

Haas, M.J., Scott, K.M., Alleman, T.L., & McCormick R.L. (2001). Engine performance of biodiesel fuel prepared from soybean soapstock: A high quality renewable fuel produced from a waste feedstock. *Energy & Fuels, 15*, 1207-1212.

Klocke, N.L., Schneekloth, J.P., Melvin, S.R., Clark, R.T., & Payero, J.O. (2004). Field scale limited irrigation scenarios for water policy strategies. *Applied Engineering in Agriculture, 20,* 623-631.

Korsrud, G.O., Keith, M.O., & Bell, J.M. (1978). Comparison of nutritional value of Crambe and Camelina seed meals with egg and casein. *Canadian Journal of Animal Science, 58,* 493-499.

Lange, R., Schumann, W., Petrzika, M., Busch, H., & Marquard, R. (1995). Glucosinolates in linseed dodder. *Fett Wissenschaft Technologie-Fat Science Technology, 97,* 146-152.

Norton, N.A., Clark, R.T., & Schneekloth, J.P. (2000). Effects of alternative irrigation allocations on water use, net returns, and marginal user costs. *Journal of Agricultural and Resource Economics, 25,* 732-732.

Pilgeram, A.L., Sands, D.C., Boss, D., Dale, N., Wichman, D., Lamb, P., Lu, C., Barrows, R., Kirkpatrick, M., Thompson, B., & Johnson, D.L., (2007). Camelina sativa, A Montana Omega-3 and Fuel Crop. Issues in New Crops and New Uses.

Understanding the Hydrologic Factors Affecting the Growth of the nuisance diatom Didymosphenia Geminata in Rivers

Basic Information

Title:	Understanding the Hydrologic Factors Affecting the Growth of the nuisance diatom Didymosphenia Geminata in Rivers
Project Number:	2009CO201B
Start Date:	3/1/2009
End Date:	2/28/2010
Funding Source:	104B
Congressional District:	2
Research Category:	Water Quality
Focus Category:	Invasive Species, Hydrology, Water Quality
Descriptors:	None
Principal Investigators:	Diane Marie McKnight

Publication

1. Cullis, James, 2010, "Hydrologic Control of the Nuisance Diatom, Didymosphenia Geminata", pg 4-6 of Colorado Water, Volume 27 issue 3.

Hydrologic Control of the Nuisance Diatom, *Didymosphenia Geminata*

by James Cullis, PhD Candidate, Civil, Environmental and Architectural Engineering, University of Colorado at Boulder
Faculty Sponsor: Diane McKnight

In recent years, particularly since the 2002 drought, have you noticed your favorite mountain stream in Colorado becoming less pristine? Have you noticed a thick brown algal mat coating the streambed that looks horrible and snags your fly when you are fishing? In some places it is particularly troublesome, with mats 1-2 centimeters thick and long white streamers resembling wet toilet paper. Does it feel gritty like wet cotton wool? Chances are that your stream is another victim to an emerging nuisance algal species called *Didymosphenia geminata,* otherwise known as "didymo" or "rock snot."

An Emerging Nuisance Species

Traditionally, algal blooms in rivers and lakes can be associated with increased nutrient loading. This is often due to human impacts downstream of wastewater treatment plants or agricultural runoff. Not so with didymo. This type of diatom is uniquely adapted to grow in low-nutrient conditions typical of many otherwise unimpacted mountain streams. Didymo is not new to Colorado; this diatom has always been a part of the natural environment of mountain rivers in North America and northern Europe, and periodic blooms have been part of the natural cycle. In recent years, however, the tendency of this nuisance species to bloom and spread to new watersheds has increased. Most significantly, in 2004 it was first detected in streams in the South Island of New Zealand. The conditions in these streams were ideally suited to its growth, and it quickly spread to other watersheds and resulted in algal mats many centimeters thick. It now represents a significant threat to local economies and stream ecosystems in these areas.

James Cullis holds a rock covered with didymo in South Boulder Creek. (Courtesy of James Cullis)

Controlling Factors and Ecological Impacts

The invasion of streams in New Zealand sparked an interest in determining the factors contributing to the growth of this nuisance species. Studies have been conducted in New Zealand, the United Kingdom, Canada, and the United States. These studies have confirmed the tendency to bloom under low-nutrient conditions, specifically in streams with

These two photos of the stream bed in Boulder Creek show the impact of high-flow events in the spring of 2009, which resulted in significant removal of didymo coverage.

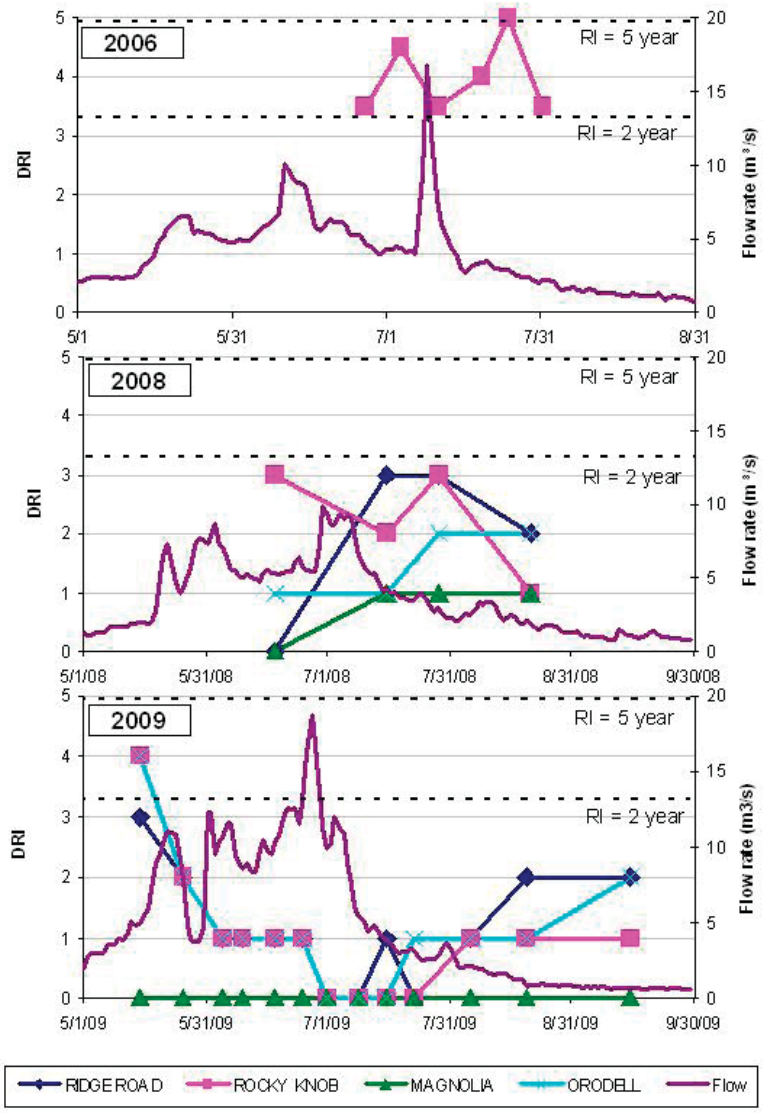

This graph shows observed didymo coverage, as measured by the Didymo Rating Index (DRI) at four study sites in Boulder Creek in relation to stream flow. Note that flows above 10m3/s result in a reduction in the coverage, but that the reduction depends on the time that the high flow occurs. The rate of recovery depends on the subsequent flows and can be rapid when high flows are not maintained.

a relatively high proportion of organic phosphorus in the total dissolved phosphate (TDP) concentration. Flow rate is also an important factor. High flows, and particularly the physical scouring and disturbance of the stream bed, are considered to be a primary control on didymo growth. The regulated flow regime downstream of dams and reservoirs provides a hot spot for growth. The thick algal mats have a significant impact on benthic macroinvertebrates, increasing the abundance of small worms and reducing the overall species diversity. It is unclear, however, what the resulting impact is on larger species such as fish.

Recreational users, such as fishermen, are one of the main contributors to the spread of this nuisance species. Individual cells can remain viable on the felt soles of wading boots for many days, facilitating the transport from one stream to another. This has resulted in a massive public awareness campaign in New Zealand, where felt-soled waders are now banned and wader wash stations have been established at popular fishing spots. There is mounting pressure in Canada, Alaska, and other parts of the United States to implement similar cleaning and disinfection control and to phase out the use of felt-soled waders.

Studies in Boulder Creek, Colorado

For the past several years, students at the University of Colorado at Boulder have been studying *D. geminata*. This species represents an excellent subject, as it is relatively easy to identify both in the field and under the microscope, is abundant in nearby streams, and can be used as the basis for discussions of stream ecosystems, human impacts, and watershed management. A particular area of ongoing research is to investigate the role of flood events, with the objective of determining the critical flow requirements necessary to remove the didymo mats from the streambed.

Preliminary data were collected during the summer of 2006, and further monitoring was conducted in Boulder Creek in 2008 and 2009. The primary metric for monitoring the growth of didymo was a qualitative Didymo Rating Index (DRI). The DRI takes into account the extent of the coverage and the thickness of the algal mat. It ranges from zero, representing no obvious signs of didymo growth, to a maximum of ten, representing 100% coverage and mats greater than 5 cm thick, as have been observed in New Zealand. The maximum for Boulder Creek was 100% coverage with a mat thickness of 1 to 2 cm, representing a 6 or 7 on the DRI scale. In addition to the DRI, physical samples from individual rocks were taken and analyzed in terms of the ash-free-dry-mass (AFDM), chlorophyll concentration, and didymo cell densities.

Determining the Critical Flow Requirements

The results of monitoring the growth of didymo at four study sites in Boulder Creek are shown in Figure 2. The coverage is measured in terms of the DRI on the left axis and is compared to the average daily flow rate on the right axis. The dashed lines represent the estimated 1 in 2-year and 1 in 5-year annual maximum flow, based on 100 years of flow records. The results show the importance of high flows in controlling the growth of didymo. In 2006 the spring melt was relatively low, but a heavy rainstorm produced a late-season flood, resulting in a significant reduction in the didymo coverage. 2008 was an average flow year with limited impact on the didymo coverage. In contrast, 2009 was

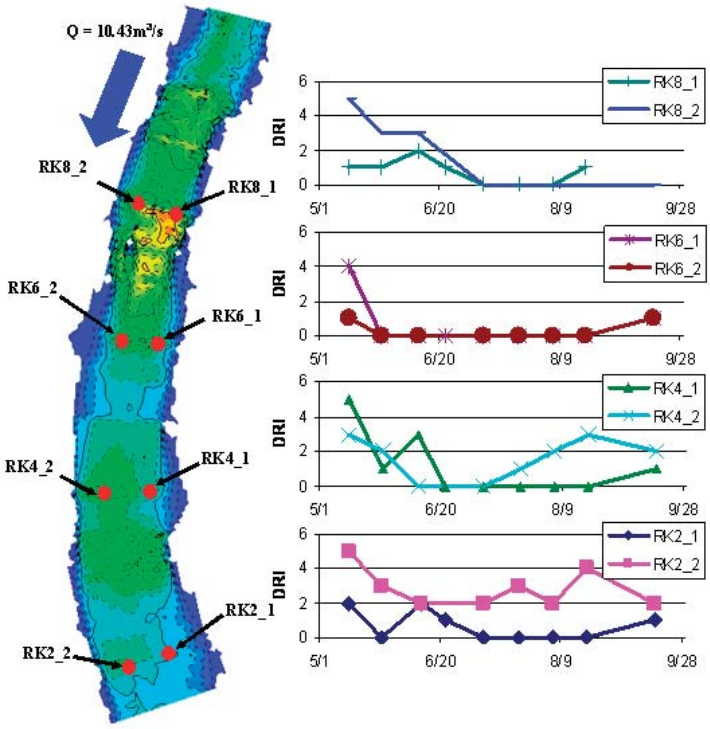

The figure on the left shows the spatial variation in bed shear stress at the maximum flow rate of 10.43m3/s for the Rocky Knob site. The yellow and orange areas indicate higher shear stress, and the red dots indicate the sampling locations. The figures on the right show the change in the Didymo Rating Index for each sample location. Note that for 2009, the maximum flow resulted in very high shear stress values and potential for bed disturbance over most of the study site. There is still, however, some difference in the impact at the different sampling locations

a very high flow year. The result was almost complete removal of didymo from the streambed at all study sites and limited recovery due to the sustained high flows.

The results indicate that a flow of 10m^3/s is a critical level for the removal of didymo in Boulder Creek, which is about the average annual maximum flow. Analysis of the average shear stress associated with this flow suggests that it is similar to the flow required to initiate significant bed disturbance. This supports the hypothesis that flows need to be high enough to result in the physical scouring of didymo due to bed disturbance rather than just elevated bed shear stress. It is unclear at this stage if these findings can be applied to other streams where didymo is a problem, and this should be a focus of future research using data from other locations and countries. Further studies to be conducted during the summer of 2010 will also determine the shear resistance of the didymo mats directly using flume experiments.

The Importance of Spatial Variation

One goal of the research being conducted in Boulder Creek is to quantify spatial variation within a stream habitat. During a flood event, shear stress is not evenly distributed across the stream bed. This results in spatial variations in the potential for bed disturbance and the removal of algae such as didymo. The resulting patchiness is considered important in maintaining the diversity of stream ecosystems. Spatial variation in the removal of didymo is being studied at the four study sites in Boulder Creek by developing a two-dimensional hydraulic model of each site. Preliminary results from the Rocky Knob site are shown in Figure 4, which illustrates the spatial variation in shear stress resulting from the maximum flow rate observed in 2009 of 10.43m^3/s. The result of this spatial variation in shear stress is apparent in the difference in the observed DRI at eight specific locations within the study site. By studying this spatial variation in shear stress and the impact on the removal of didymo, we hope to better determine the critical shear stress needed for removal.

Using Managed Flood Releases for Future Control

The overall objective of this study is to determine the critical flow requirements necessary to remove didymo in streams. This information will be useful in considering the potential to use managed flood releases from reservoirs to control future growth. This approach is already being used in New Zealand, where a number of flood releases have flushed the didymo out of impacted streams. In New Zealand, this approach is supported by an awareness of the negative impact of didymo on local economies and stream ecosystems, as well as the availability of spare water. In other parts of the world, such as Colorado, there is neither the level of awareness of the threat nor the availability of spare water. It is therefore important to not only better understand what the impact of didymo is in these areas, but also to improve our quantitative understanding of the magnitude, duration, and timing of flood events that would be most efficient in controlling future growth. The aim of this study is to provide this quantitative understanding that will enable water resources managers to consider the trade-offs between making flood releases with the objective of controlling didymo growth and considering the many other current and future demands on this precious resource.

Acknowledgements

Funding for this research is provided by the Colorado Water Institute, the Boulder Creek Critical Zone Observatory, the University of Colorado, the American Society of Civil Engineers, and the Aurecon Group.

For more information on the ecology and impact of *Didymosphenia geminata* and on what can be done to control the spread and future growth of this nuisance species, visit the Environmental Protection Agency web site at: http://www.epa.gov/region8/water/didymosphenia.

Developing Barriers to the Upstream Migration of New Zealand mudsnail (Potamopyrgus antipodarum) Phase III - Laboratory and Field Evaluations of Mudsnail Response to Copper-Based Materials Under Varied Water Quality Conditions

Basic Information

Title:	Developing Barriers to the Upstream Migration of New Zealand mudsnail (Potamopyrgus antipodarum) Phase III - Laboratory and Field Evaluations of Mudsnail Response to Copper-Based Materials Under Varied Water Quality Conditions
Project Number:	2009CO202B
Start Date:	3/1/2009
End Date:	2/28/2010
Funding Source:	104B
Congressional District:	4
Research Category:	Biological Sciences
Focus Category:	Invasive Species, Geochemical Processes, Ecology
Descriptors:	None
Principal Investigators:	Christopher A. Myrick

Publication

1. Hoyer, Scott, 2010, "Developing Barriers to the Upstream Migration of New Zealand mudsnail (Potamopyrgus antipodarum) Phase III - Laboratory and Field Evaluations of Mudsnail Response to Copper-Based Materials Under Varied Water Quality Conditions", pg 7-9 of Colorado Water, Volume 27 issue 3.

Developing Barriers to Prevent the Upstream Migration of the New Zealand Mudsnail

by Scott Hoyer, MS Candidate, Fish, Wildlife, and Conservation Biology, Colorado State University
Faculty Sponsor: Christopher Myrick

Waterways and aquaculture facilities throughout the western United States are at risk of invasion by the New Zealand mudsnail (*Potamopyrgus antipodarum*) (Figure 1). Originally endemic to New Zealand, mudsnails were first discovered in the United States in 1987 near Hagerman, Idaho, and have since spread to all the western states, excluding New Mexico. The mudsnail's high reproductive capacity allows them to reach extremely high densities in some situations (> 500,000 snails per square meter), leading to concerns that native aquatic communities and valuable sport fisheries could be negatively impacted. Several recreational fisheries have already suffered in California and Colorado by the closure of popular stretches of streams following mudsnail invasion. Additionally, several western aquaculture facilities have been invaded by mudsnails, resulting in revenue losses associated with the costs of facility disinfection to eradicate this organism and declines in fish produced for fisheries enhancement and restoration. The mudsnails' wide range of physiological tolerances and lack of effective native predators or competitors raises the possibility that it could spread to the majority of western waterways unless positive steps are taken to limit further invasion.

The New Zealand mudsnail is a small (< 6 mm at maturity) freshwater snail endemic to New Zealand that has rapidly spread across western North America. The snail's high reproductive potential, lack of natural predators, and broad environmental tolerance range have raised concerns about its potential impact on native aquatic communities and valuable sport fisheries. (Courtesy of Scott Hoyer)

This image shows a 21.5-cm diameter PVC arena that was used to evaluate the New Zealand mudsnails' response to various copper-based materials. (Courtesy of Scott Hoyer)

The New Zealand mudsnails' rapid and wide-ranging invasion across four continents over the last 150 years can partly be attributed to the ease in which it can be inadvertently spread by humans. Mudsnails are quite small (< 6 mm at maturity) and can survive long periods of desiccation, thus allowing them to "hitchhike" between waterways on gear such as boots, waders, and rafts. Management agencies are now working to eliminate this pathway by educating fisherman, biologists, and other recreational water users on the proper ways to disinfect gear. However, infested gear is not the only way in which mudsnails find their way into novel habitats; fish hatcheries are now being carefully monitored to ensure that their activities do not lead to further spread. Because an infested aquaculture facility could easily spread mudsnails through normal stocking, it is no surprise that facilities that are found to harbor mudsnails face harsh restrictions by management agencies. In some situations, a facility may be quarantined until all of the mudsnails have been eradicated, which can be very costly in terms of both time and money and may lead to bankruptcy for some small private operations.

To protect these operations, it is important to find ways of preventing invasion in the first place. Mudsnails find their way into hatcheries in several ways, including crawling upstream through effluent pipes that connect a facility to an infested waterway. To eliminate this pathway, we

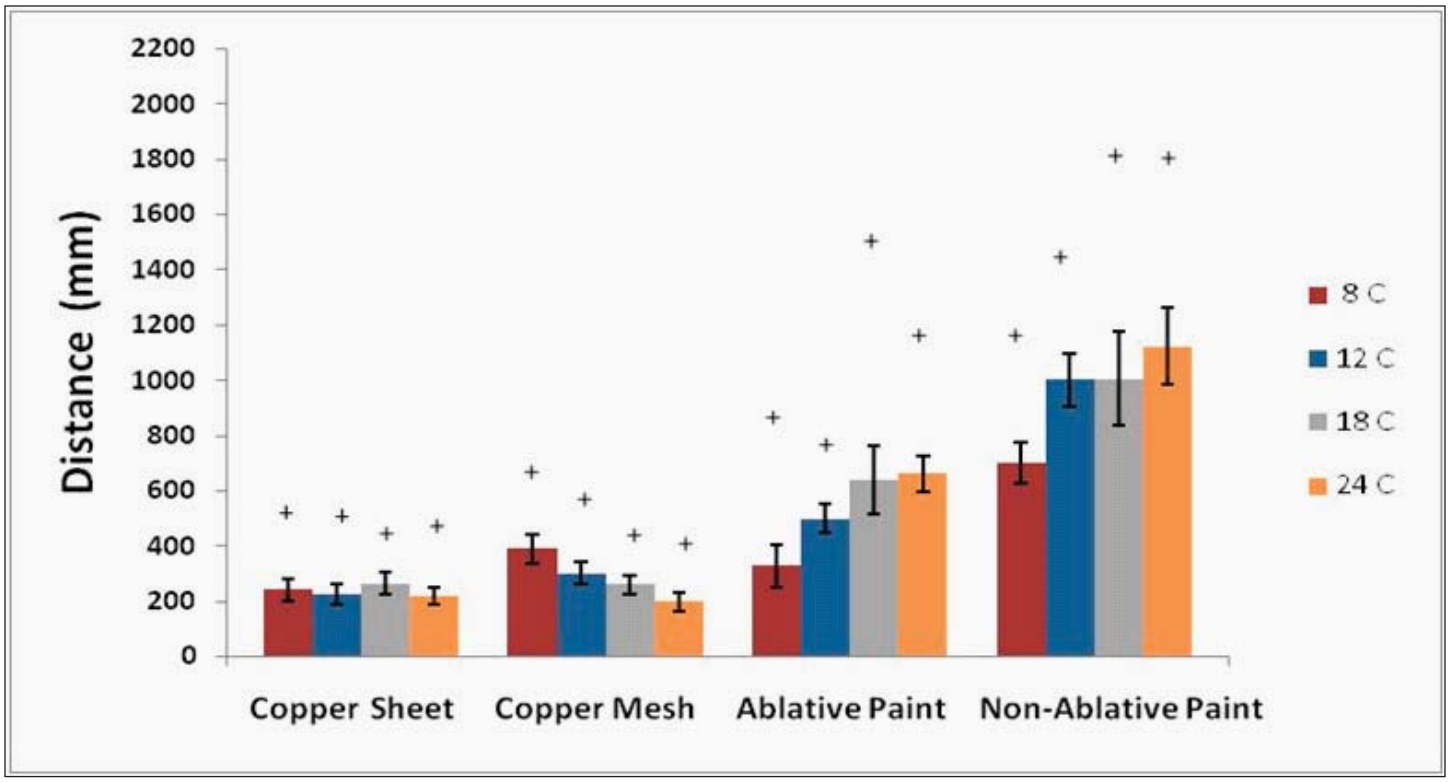

Average and maximum crawling distance of the New Zealand mudsnail on four copper-based substrates at various water temperatures. Averages are shown with standard error bars; + indicates the maximum distance traveled by any single snail within a treatment group.

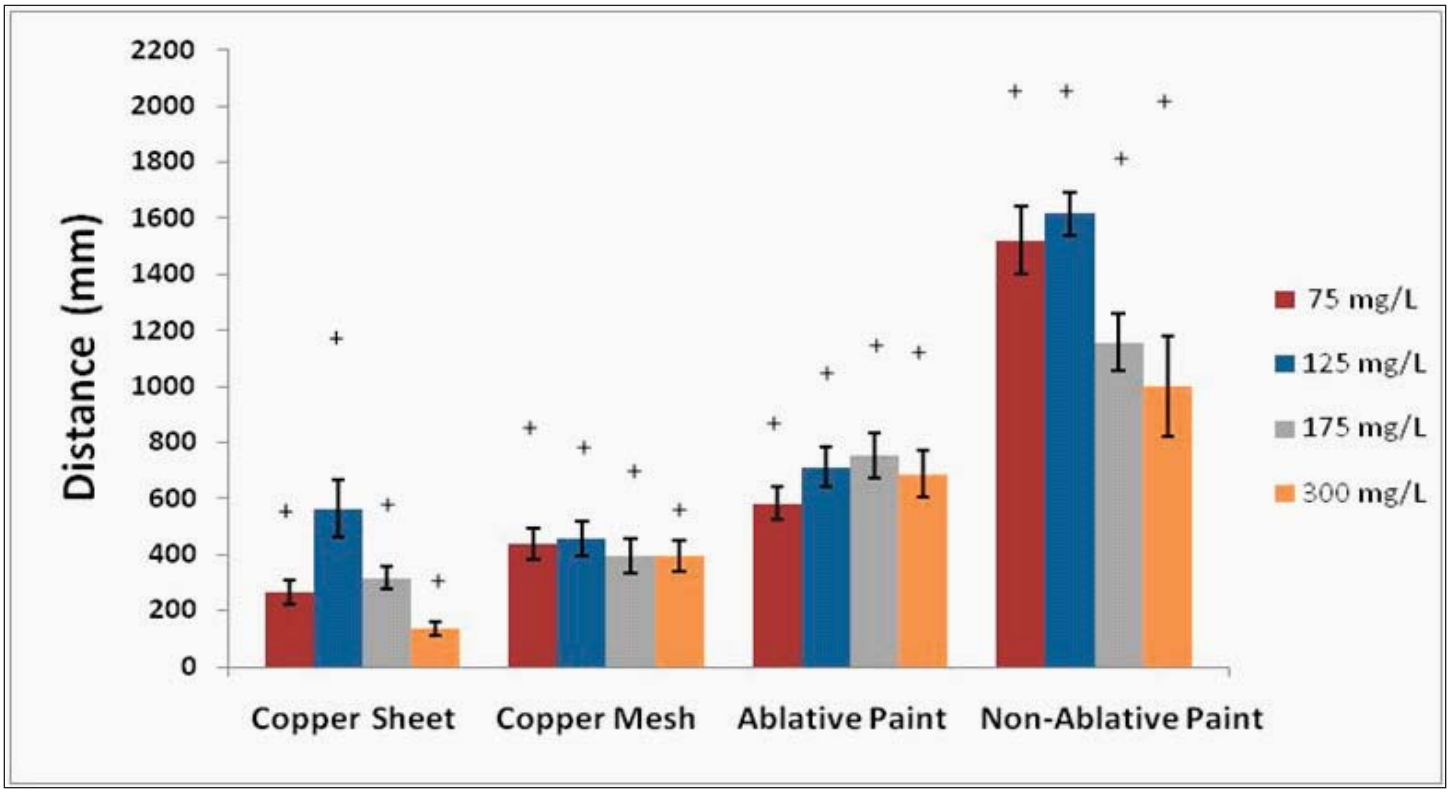

Average and maximum crawling distance of the New Zealand mudsnail on four copper-based substrates at various water hardness levels. Experiments were conducted at 18° C. Averages are shown with standard error bars; + indicates the maximum distance traveled by a single snail within each treatment group.

need to develop a barrier system for these pipes. One potential class of barriers is copper-based substrates such as copper sheeting or marine anti-fouling paints. Copper-based materials are commonly used to control mollusk colonization on boat hulls and other submerged structures, so there is some possibility that they could also be used in this application. To test this hypothesis, Dr. Christopher Myrick and Sarah Conlin conducted a pilot study in 2007-2008, in which they exposed mudsnails to several types of copper-based materials. When compared to movements on bare PVC control surfaces, Myrick and Conlin found that the mudsnails' crawling distance was up to 7 times less on the copper surfaces, suggesting that these materials could indeed function as a barrier to mudsnails.

Over the last several years, some at-risk hatcheries have installed these copper materials in their effluent pipes, and while in some situations they were successful, in others they were not. There could be several reasons for this difference in effectiveness, perhaps most notably—differences in the physical and chemical characteristics of each hatchery's water supply.

It is well known that copper toxicity (and perhaps barrier efficiency) is affected by several variables including water temperature, water hardness, pH, and organic carbon concentration. The purpose of my current research is to determine the conditions under which copper-based materials function best as barriers to New Zealand mudsnails. Below I describe the findings of the first two phases of this project, in which we attempt to determine how water temperature and water hardness affected the mudsnails' response to potential copper barrier materials.

To address these questions, we conducted two separate experiments to test the barrier efficiency of the following four copper-based compounds: copper sheeting (99.9% pure), copper mesh (99.0% pure), ablative anti-fouling paint (25% cuprous thiocyanate as the active ingredient), and non-ablative anti-fouling paint (39% cuprous oxide as the active ingredient). All experiments were conducted at the Colorado State University Foothills Fisheries Laboratory.

For the water temperature experiment, mudsnails collected from Boulder Creek (Boulder, CO) were acclimated to 8, 12, 18, or 24°C for a period of two weeks before the initiation of the experiment. This temperature range was chosen to cover most of the mudsnail's temperature tolerance range and the range of temperatures likely to be discharged from a hatchery. For the water hardness experiments, we acclimated the mudsnails to one of four hardness levels (75, 125, 175, or 300 mg/L as $CaCO_3$) for a period of two weeks at 18° C. Following the acclimation period, we conducted experiments in circular PVC arenas (Figure 2), in which we covered one-half of the surface with a copper substrate and left the other half bare to serve as a control. At the beginning of a trial, a single mudsnail was placed in the center of the arena, and its movements were recorded for a two hour period. We later analyzed and compared movements on each the copper surface types.

After analyzing the data from these two experiments, we found that crawling distances were reduced on the copper sheet and mesh in both experiments (Figures 3 and 4). The non-ablative paint did not seem to limit the snails' movements in either experiment, which strongly suggests that substance would not be an effective barrier. We also determined that water temperature did not have a strong effect on the barrier ability of the four copper-based materials, although we did notice an increase in movement with increased temperatures (Figure 3). This observation was expected considering that the metabolic and activity rates of most cold-blooded organisms increase with temperature. Finally, water hardness did affect mudsnail movements across the copper surfaces, with crawling distance being the greatest in the 125 mg/L water hardness group (Figure 4).

Conclusions and Future Work

In both experiments, copper sheet and copper mesh consistently reduced the crawling distance and velocity of the mudsnails, suggesting that these materials have the ability to function as effective mudsnail barriers across a broad range of temperatures and water hardness levels. In contrast, the non-ablative anti-fouling paint did not appear to limit the mudsnails' movement under any of the experimental conditions. Upon considering the amount of copper in each of these materials, it appears that in order for a copper-based substrate to function as an effective barrier, it must contain a high percentage of copper. Furthermore, the maximum crawling distances that we observed in these experiments suggest that barriers must be at least 1.5 meters in length to stop 100% of the mudsnails. This last point is very important, because it is crucial to ensure that not a single mudsnail gets into a hatchery since the mudsnails reproduce asexually (i.e., it only takes one snail to start an entirely new population).

In 2010 we will continue to evaluate the performance of these copper-based compounds by testing each of them in a variety of conditions. We are currently evaluating barrier efficiency across a range of pH values. We will also determine how water velocity and the buildup of organic biofouling affect the mudsnails' response to these materials. Finally, to reduce the negative effects of copper on non-target species, we will evaluate the amount of copper that is leached from the materials. By doing so, we can determine the optimal barrier length that will block mudsnails, while also preventing unnecessary harmful effects to nearby aquatic communities.

High Resolution Soil Moisture Retrieval in the Platte River Watersheds

Basic Information

Title:	High Resolution Soil Moisture Retrieval in the Platte River Watersheds
Project Number:	2009CO203B
Start Date:	3/1/2009
End Date:	2/28/2010
Funding Source:	104B
Congressional District:	1
Research Category:	Climate and Hydrologic Processes
Focus Category:	Climatological Processes, Hydrology, Water Quantity
Descriptors:	None
Principal Investigators:	Lynn E Johnson

Publication

1. Hsu, Chengmin;, 2010, "High-Resolution Soil Moisture Retrieval in the Platte River Watersheds", pg 26-29 Colorado Water, Volume 27 Issue 3.

High-Resolution Soil Moisture Retrieval in the Platte River Watersheds

by Chengmin Hsu, Ph.D. Candidate, Civil Engineering, University of Colorado Denver
Faculty Sponsor: Lynn E. Johnson

Research Question and Objective

Hydrological and other applications require soil moisture data at high spatial and temporal scales. Of the various methods to obtain soil moisture data, satellites hold promise of providing data at the appropriate scales. Currently, there are only two sources of operational global soil moisture data from satellites: (1) Advanced Microwave Scanning Radiometer (AMSR-E) aboard NASA's Aqua satellite, and (2) the Soil Moisture and Ocean Salinity (SMOS) satellite operated by the European Space Agency.

However, neither is a high-resolution product. The AMSR-E surface soil moisture product has a 25-km resolution, whereas SMOS can create only 50-km resolution products. Motivated by the urgent need for high-resolution soil moisture data, the purpose of this research is to develop an algorithm for disaggregating the 25-km AMSR-E daily soil moisture to a 250-m resolution product.

Study Site

The study site encompasses areas within the South and North Platte River watersheds and the Republican River watershed (Figure 1). The total study area is approximately 45,000 square kilometers. Most of the area is composed of open grassland and agriculture areas.

Data

Data used include: (1) X band (centered at 10.7 GHz) derived soil moisture from the AMSR-E sensor, (2) Moderate Resolution Imaging Spectroradiometer (MODIS) data, (3) data from the Soil Survey Geographic (SSURGO) database, (4) station data from the NRCS Soil Climate Analysis Network (SCAN), (5) wind speed measurements, (6) in-situ soil moisture data collected from the Automated Weather Data Network (AWDN) of the High Plains Regional Climate Center (HPRCC), and (7) Advanced Spaceborne Thermal Emission and Reflection Radiometer (ASTER) imagery collected over parts of Weld and Larimer Counties in Colorado.

The MODIS data used are version 5 MODIS/Terra and MODIS/Aqua 1-km resolution daily surface temperatures and MODIS/Terra 250-m resolution 16-day Enhanced Vegetation Index (EVI). The observations from the 16-day EVI product were cloud free and were used to generate fractional vegetation cover (Figure 3). Seven MODIS Version 5 surface temperature images with the least amount of cloud cover were acquired (July 13, 19, 20, 30, 31 and August 1 and 20, 2008). The ASTER image was captured on August 19, 2008. Land surface temperature was estimated from 90-m resolution L1B thermal radiances using the emissivity normalization method implemented in ENVI (ENvironment for Visualizing Images image processing software, http://www.ittvis.com/ProductServices/ENVI.aspx).

Disaggregation Algorithm

The soil moisture downscaling algorithm is composed of three sequential stages:

Stage 1: Downscaling of a 25-km resolution AMSR-E soil moisture to a 5-km resolution product. In this stage the basic concept is that the evaporation rate of the sub-pixel at 5-km resolution should be higher than the average evaporation of the pixel at 25-km resolution if the soil temperature of the sub-pixel is greater than that of theAMSR-E pixel. Thus, soil moisture of that sub-pixel will be drier than that in the 25-km resolution pixel.

Stage 2: Downscaling of 5-km resolution soil moisture to 1-km resolution soil moisture. In the second

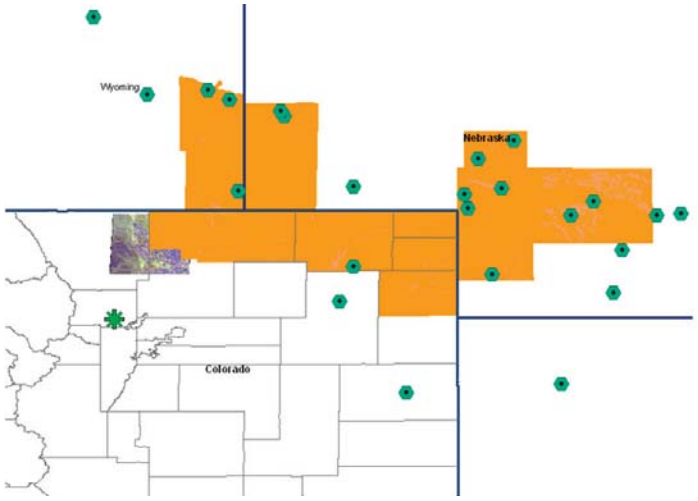

Figure 1: The study site (in orange) is located across Colorado, Nebraska and Wyoming, comprising the areas within the North and South Platte River Basin and the Republican River Basin. The malachite green points are Automated Weather Data Network (AWDN) stations from the High Plains Regional Climate Center (HPRCC).

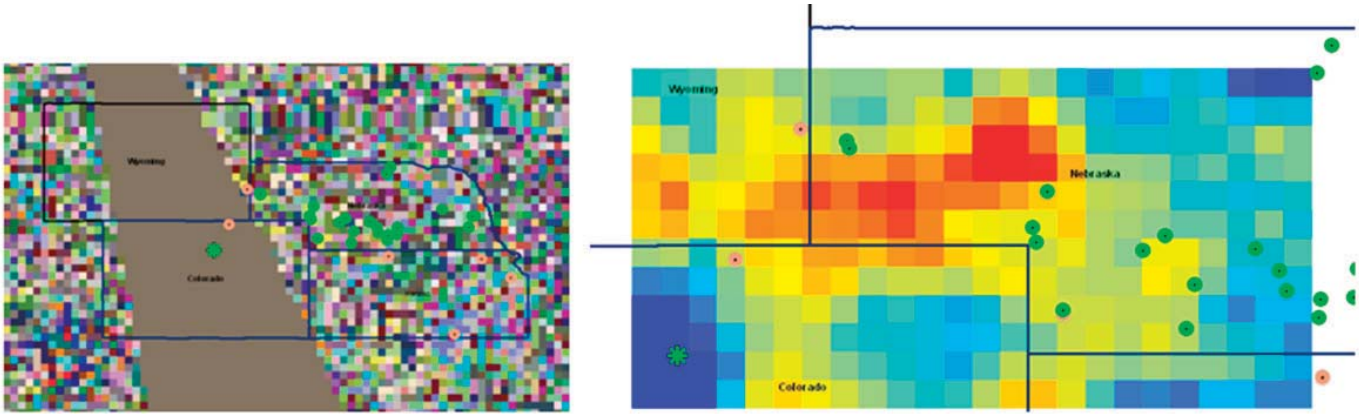

Figure 2: The graph on the left is the AMSR-E soil moisture imagery on July 20, 2008. It shows that a large area without data occupies the left edge of the study site. The graph on the right is the magnified interpolated soil moisture data, seen after using Krigirg interpolation method.

stage, the Percent Clay from SSURGO data and the fractional vegetation cover derived from EVI are used for downscaling. This operation's purpose is to account for the lower soil moisture sensitivity of the MODIS surface temperature and the poor capability of AMSR-E to differentiate soil and vegetation signals.

Stage 3: Downscaling of 1-km resolution soil moisture to a 250-m product. The method applied in this stage is similar to that in Stage 1 but uses ASTER derived surface temperature and Normalized Difference Vegetation Index (NDVI).

The equations below represent the philosophy used for the first stage of downscaling AMSR-E soil moisture using MODIS data. Notice that all equations are also appropriate for disaggregation using ASTER data in Stage 3. This brings together soil properties and the philosophy mentioned above. The downscaling relationship for the first stage can be represented by:

$$SM_{MODIS,\ 5km} = SM_{AMSR\text{-}E,\ 25km} + \theta c * SMD_{MODIS,5km}$$

with SMD as the MODIS-derived soil evaporative efficiency estimated based on the difference of soil temperatures between the 5-km resolution and its average within the AMSR-E pixel. The equation also integrates the lab findings of Komatsu (2003) by adding a downscaling coefficient, θc. θc is a semi-empirical parameter that depends on soil properties and boundary conditions of soil layers. In this research, the data extracted from the SSURGO database was used. SMD is assumed to be linear and can be defined as:

$$SMD_{MODIS,\ 5km} = \frac{T_{MODIS,\ 25km} - T_{MODIS,\ 5km}}{T_{MODIS,\ 25km} - T_{\ min,\ 1km}}$$

Here, $T_{MODIS,\ 5km}$ is the soil temperature at the 5-km resolution. It is derived by using MODIS derived EVI and surface temperature aggregated at the 5-km resolution. $T_{MODIS,\ 25km}$ is its average within the AMSR-E pixel, and $T_{min,\ 1km}$ is the minimum MODIS derived soil temperature at the 1-km resolution. The assumption for the minimum soil temperature is that it is equal to the minimum MODIS surface temperature. The soil temperature can be estimated by using a simple equation developed by Merlin et al. (2008). The equation can be defined as:

$$TMODIS,\ 5km\ = \frac{T_{surf,\ MODIS,\ 5km} - f_{v,\ MODIS,\ 5km} * T_{v,\ 5km}}{1 - f_{\ v,\ MODIS,\ 5km}}$$

Table 1: 5-km Resolution Soil Moisture Downscaling Validation

	Nunn Station		Johnson Farm Station	
Date	Observed Soil Moisture (%) at 5-cm depth	Estimated Soil Moisture (%) at 5-cm Depth	Observed Soil Moisture (%) at 5-cm depth	Estimated Soil Moisture (%) at 5-cm Depth
7/13/2008	0.113	0.119	0.072	0.091
7/19/2008	0.101	0.109	0.197	0.094
7/20/2008	0.100	0.110	0.105	0.095
7/30/2008	0.108	0.096	0.252	0.101
7/31/2008	0.105	0.101	0.153	0.106
8/1/2008	0.101	0.101	0.107	0.093
8/20/2008	0.320	0.112	0.235	0.089

with $T_{surf,MODIS,5km}$ as the MODIS-derived surface temperature, $T_{v,5km}$ as the vegetation temperature, and $f_{v,MODIS,\ 5km}$ as the fractional vegetation cover at the 5-km resolution. In this research, $T_{v,5km}$ was estimated to $T_{min,\ 1km}$. fv can be estimated using EVI directly. The coefficient θc, is calculated using von Karman wind turbulence models and SSURGO soil database. Detailed steps are described in a paper published by Komatsu (2003).

In Stage 2, a variable produced by multiplying the percent clay of SSURGO and f_v was used for downscaling. The equation is represented by:

$$SM_{1km} = SM_{5km} + 0.025 * \frac{f_v * P_{clay,\ 1km} - f_v * P_{clay,\ 5km}}{f_v * P_{clay,\ 5km}}$$

where "P_{clay}" is the percentage of clay extracted from SSURGO. The concept is that clayish soil can retain a large percentage of water, but it is not good for vegetation growth. The pixels that have high fractional vegetation cover and also a high percentage of clay must be wetter than the pixels that do not have them.

Results

The results of downscaling at the 5-km and 1-km resolutions are quite good in the dry phase, based on the comparison of observed and downscaled soil moisture (Table 1). One day's result of the downscaled 5-km resolution soil moisture is shown in Figure 4. However, in wet phases, downscaling results do not reflect the true soil moisture. For example, the in-situ soil moisture data on August 20, 2008, for the Nunn station is 0.32, while the downscaled soil moisture data for that specific pixel shows it as only 0.112. Further examination of the original AMSR-E soil moisture data finds that soil moisture in that specific pixel is only 0.104. This indicates that the AMSR-E sensor cannot capture the true soil moisture variability in wet phases.

The 5-km soil moisture data of July 13, 2008, was further downscaled to the 1-km resolution using the method depicted in the second stage (Figure 5). The derived soil moisture for the pixel where the Nunn station is located is 0.113, which is exactly the same as the soil moisture observed at the station. This is an encouraging sign for the second stage of downscaling. The 1-km resolution soil moisture data of July 13, 2008, was also downscaled to the 250-m resolution. But because the downscaling was based on the only available ASTER data of August 19, 2008, large amounts of error can be expected. Therefore, validation has not yet been executed.

Conclusion

The developed downscaling algorithm seems satisfactory, based on the limited analyses conducted. The problem of AMSR-E indicating soil moisture that is too dry compared to reality during the wet phase suggests that

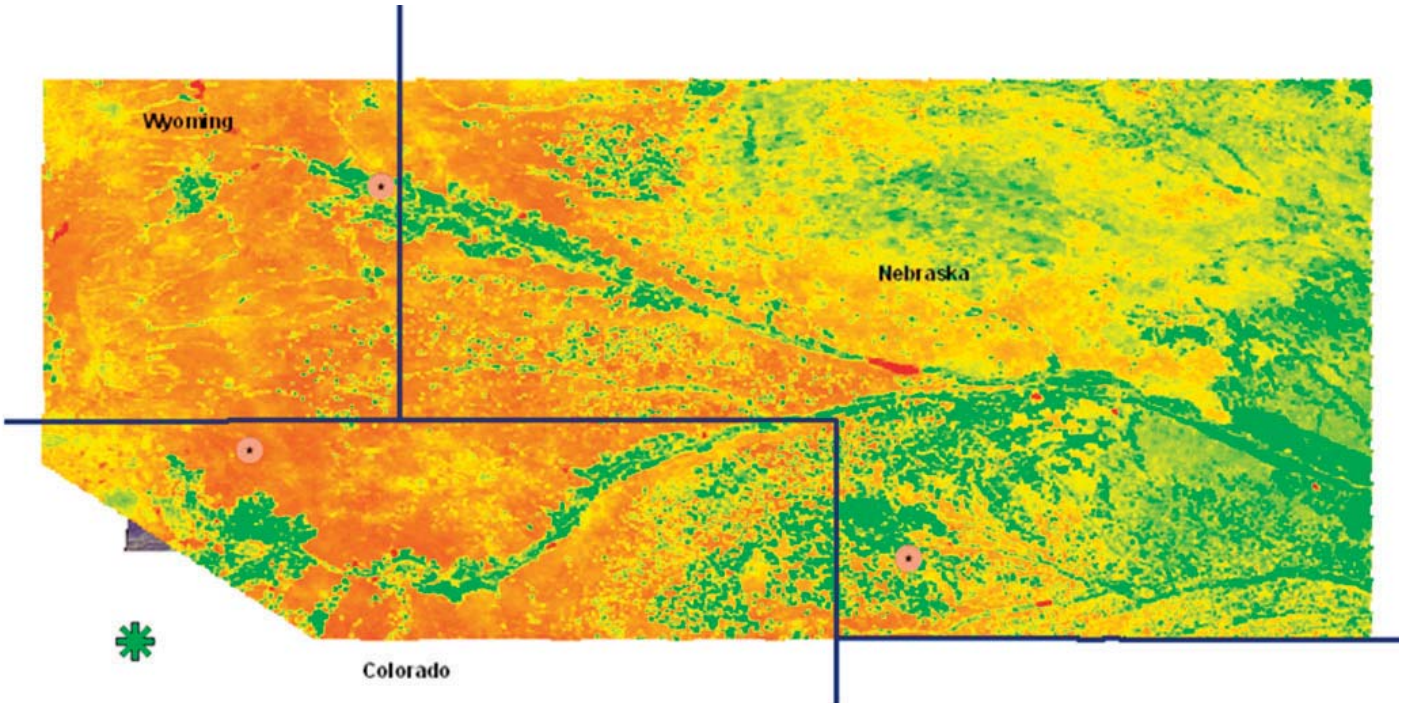

Figure 3: The EVI of the period between July 27, 2008 and August 11, 2008 represents the factional vegetation cover of that period of time. The greener the color is, the higher the percentage of vegetation cover.

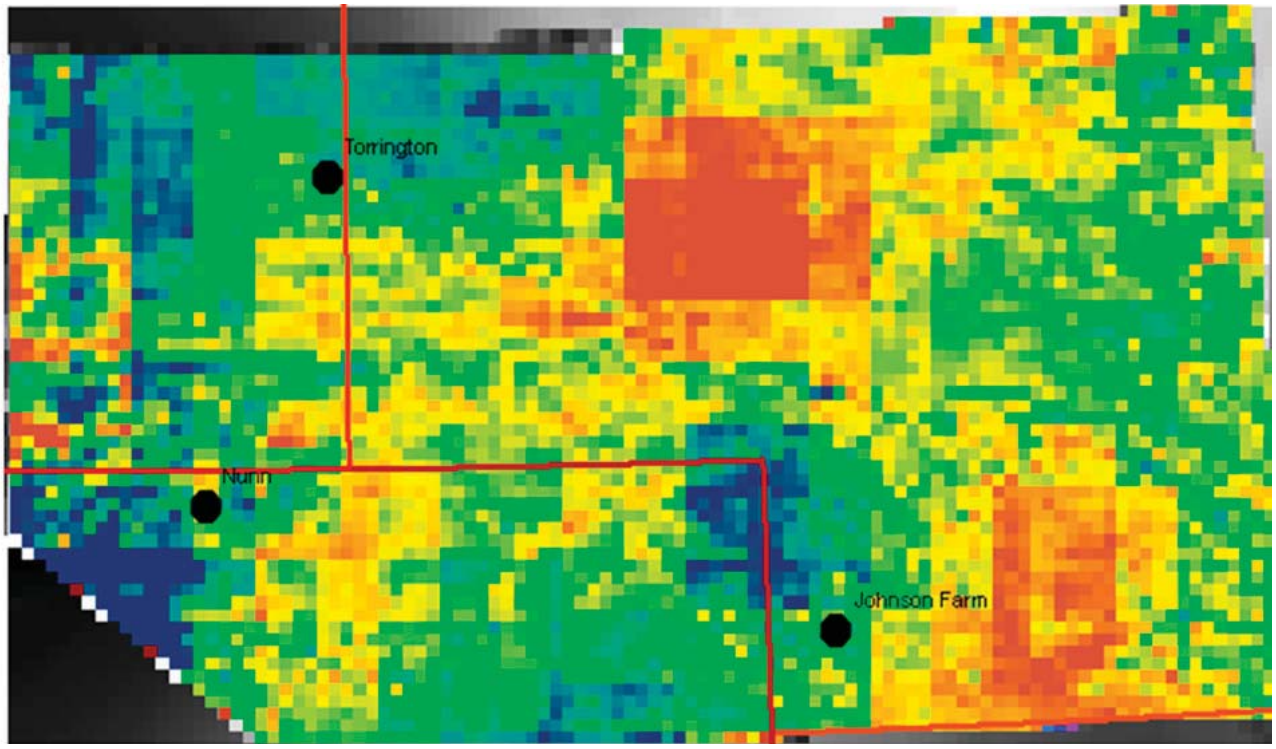

Figure 4: The downscaled 5-km resolution soil moisture data on August 1, 2008.

AMSR-E data are not adequate for downscaling. However, this deficiency can perhaps be overcome by integrating SMOS data, because the SMOS satellite equips sensors that can detect L-band energy ~~emitted from the Earth. Th~~is will reduce the problem of vegetation canopy forming an opaque layer that hinders the signal from the soil as detected by AMSR-E sensor. Another way to improve this downscaling model is to make adjustments to the second stage. In this research, a constant value of 0.025 was used. In fact, it can be shaped as a parameter integrating the dynamics of precipitation. Improvement of the second phase of the downscaling algorithm deserves additional attention.

References

Komatsu, T. S. (2003). Toward a robust phenomenological expression of evaporation efficiency for unsaturated soil surfaces. *Journal of Applied Meteorology* , *42*, 1330-1334.

Merlin, O., Walker, J. P., Chehbouni, A., & Kerr, Y. (2008). Toward deterministic downscaling of SMOS soil moisture using MODIS derived soil evaporative efficiency. *Remote Sensing of Environment* , *112*, 3935-3946.

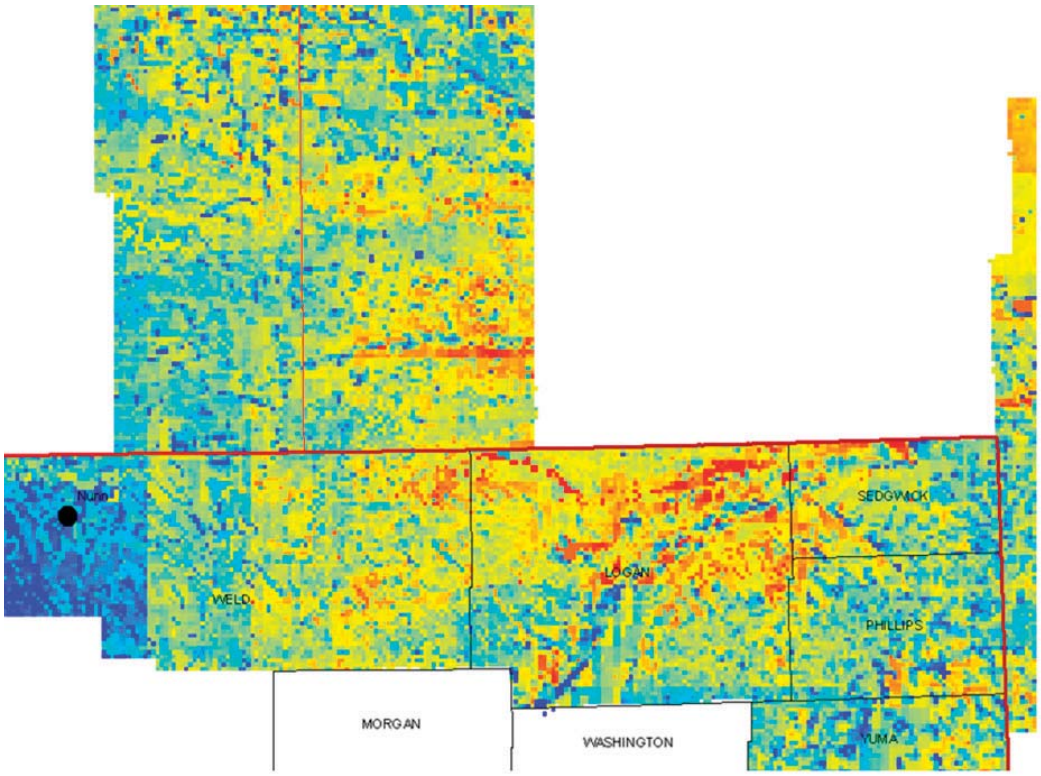

Figure 5: The downscaled 1-km resolution soil moisture data of July 13, 2008. The black spot in the left corner is the Nunn station of the Soil Climate Analysis Network.

Information Transfer Program Introduction

Requests from the Colorado legislature to facilitate and inform basin-level discussions of water resources and help develop an interbasin compact for water management purposes emphasized the role Colorado Water Institute plays in providing a nexus of information. Some major technology transfer efforts this year include:

- Provide training for Extension staff in various water basins to help facilitate discussions of water resources
- Encourage interaction and discussion of issues between water managers, policy makers, legislators, and researchers at Colorado Water Future one-day conference
- Publication of the bi-monthly newsletter which emphasizes water research, current water issues
- Posting of all previously published CWI reports to the web for easier access
- Working with land grant universities and water institutes in the intermountain West to connect university research with information needs of Western Water Council, Family Farm Alliance, and other stakeholder groups
- Work closely with the Colorado Water Congress, Colorado Foundation for Water Education, USDA-CSREES funded National Water Program to provide educational programs to address identified needs

Technology Transfer and Information Dissemination

Basic Information

Title:	Technology Transfer and Information Dissemination
Project Number:	2009CO184B
Start Date:	3/1/2009
End Date:	2/28/2010
Funding Source:	104B
Congressional District:	4th
Research Category:	Not Applicable
Focus Category:	None, None, None
Descriptors:	None
Principal Investigators:	Reagan M. Waskom

Publications

1. Colorado Water Newsletter, Volume 26 -Issue 2 (March/April 2009), Colorado Water Institute, Colorado State University, Fort Collins, Colorado, 40 pages.
2. Colorado Water Newsletter, Volume 26 -Issue 3 (May/June 2009), Colorado Water Institute, Colorado State University, Fort Collins, Colorado, 44 pages.
3. Colorado Water Newsletter, Volume 26 -Issue 4 (July/August 2009), Colorado Water Institute, Colorado State University, Fort Collins, Colorado, 40 pages.
4. Colorado Water Newsletter, Volume 26 -Issue 5 (September/October 2009), Colorado Water Institute, Colorado State University, Fort Collins, Colorado, 40 pages.
5. Colorado Water Newsletter, Volume 26 -Issue 6 (November/December 2009), Colorado Water Institute, Colorado State University, Fort Collins, Colorado, 40 pages.
6. Colorado Water Newsletter, Volume 27 -Issue 1 (January/February 2010), Colorado Water Institute, Colorado State University, Fort Collins, Colorado, 40 pages.
7. Brown, Jennifer, 2009, "Proceedings, South Platte Forum, 20th Annual, 1989 to 2029: A River of Odyssey, Information Series 108", Colorado Water Institute, Colorado State University, Fort Collins, Colorado, 36 pages.

Colorado Water Institute Activities

2009 Arkansas River Basin Water Forum

The 2009 Arkansas River Basin Water Forum will be held March 31-April 1 at CSU-Pueblo in the Occhiato University Center.

Registration is $55 for both days, $25 for one day, and no charge for students.
Please visit the Forum web site at http://www.arbwf.org or contact Dr. Perry E. Cabot at (719) 549-2045 for more information.

Purpose

The Forum has been a focal point for highlighting current water issues in the Arkansas River Basin and in Colorado since its inception in 1995. Planners, presenters, and attendees represent a wide variety of organizations, agencies, and public citizenry working on water resources issues in the basin.

Description

As Colorado charts a course for a new energy economy, the Forum theme this year is "Water to Fuel Our Future." Topics discussed will include water use for energy production, invasive species, and other watershed management topics of interest to the basin. Our keynote speaker this year will be Jennifer Gimbel, director of the Colorado Water Conservation Board.

Scholarships

The Forum sponsors are pleased to offer a $4000 scholarship to an outstanding graduate student. Applicants must currently be enrolled as a second-year graduate student in a field relating to water resources management (e.g., water law, limnology, hydrology, water resources engineering) at a university or college in the state of Colorado. Applicants must have attended high school within the Arkansas River Basin.

AGU Hydrology Days 2009
March 25–27, 2009

Hydrology Days, which has been held on the campus of Colorado State University each year since 1981, is a unique celebration of multi-disciplinary hydrologic science and its closely related disciplines. The Hydrology Days vision is to provide an annual forum for outstanding scientists, professionals, and students involved in basic and applied research on all aspects of water to share ideas, problems, analyses, and solutions. The Hydrology Days 2009 Award presentation will take place during the luncheon on Thursday, March 26, in the North Ballroom of the Lory Student Center. Professor George F. Pinder of the College of Engineering and Mathematical Sciences, University of Vermont, will present the award lecture.

For information regarding this event and registration please visit www.hydrologydays.colostate.edu.

WATER TABLES 2010

Save the date: Saturday, February 20, 2010

Location: Morgan Library
Colorado State University, Fort Collins

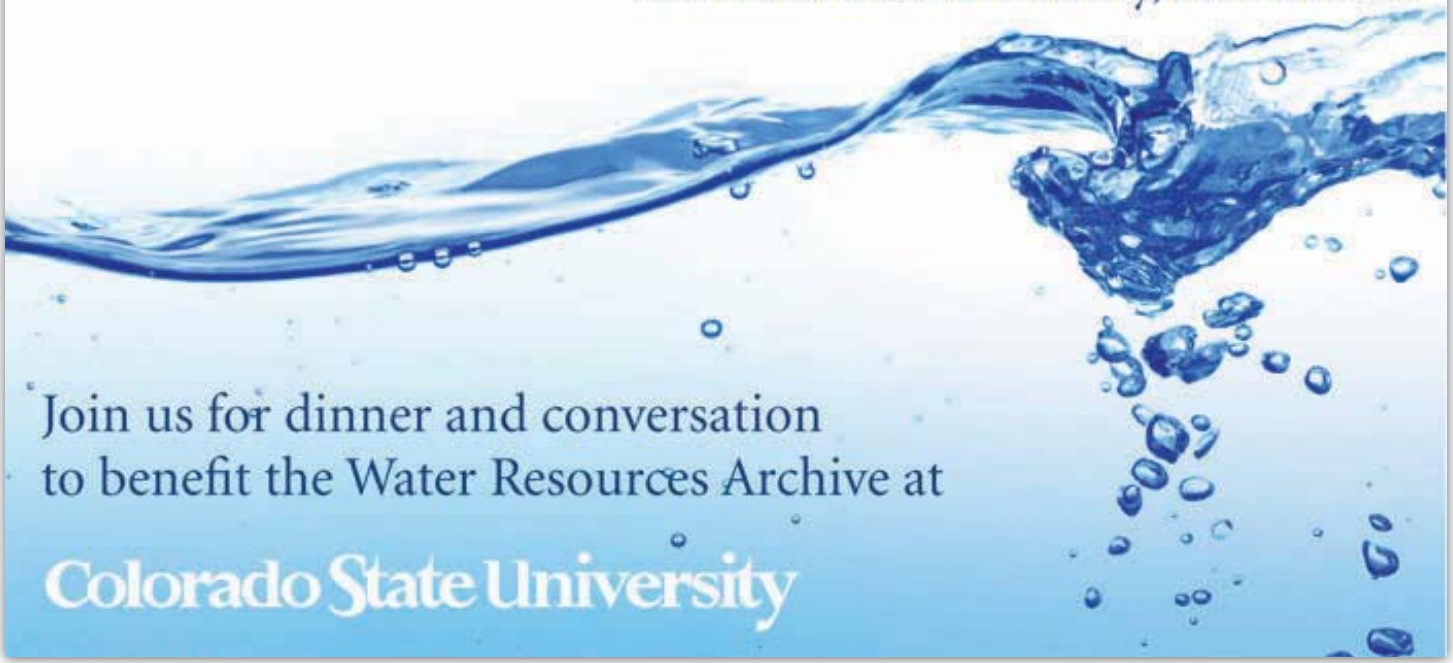

Join us for dinner and conversation
to benefit the Water Resources Archive at

Colorado State University

34th Annual Colorado Water Workshop
July 22–24, 2009

Theme and Keynote

On July 22-24, 2009, the Colorado Water Workshop will investigate non-consumptive water use in Colorado and the American West. The proceedings will offer a wide range of speakers, including well known biologists, ecologists, attorneys, elected officials, non-profit organizations, engineers, planners, historians, and interested members of the public. Drawing on their passion and expertise, we will address topics as diverse as climate change, the economic value of non-consumptive use, invasive plant and animal species, the law of the river, the ski industry, the right to float (or not), and many others. We are fortunate to have the current Superintendent of Grand Canyon National Park, Steve Martin, as our keynote speaker. Few people in the West have more knowledge of the challenges of balancing water use demands between consumptive and non-consumptive uses.

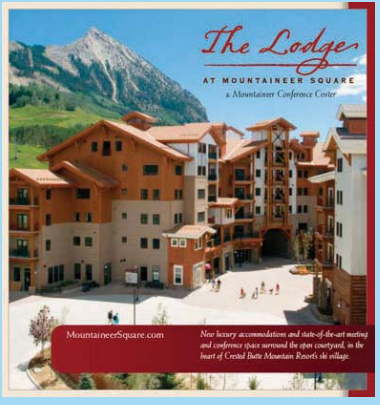

Venue and Lodging

This year we will be moving "up valley" to the Mountaineer Square Lodge in Mt. Crested Butte. Not only does this venue offer fine dining and plush accommodations, it also boasts ample conference and exhibitor space. We have negotiated a reduced room rate ($109 base rate) with Crested Butte Mountain Resort for a limited number of rooms. To reserve your room call 1-888-443-6715 and tell them you are with the Colorado Water Workshop. Reduced rate rooms are on a first call, first serve basis.

Additional Events

We have partnered with the Crested Butte Policy Forum, which has invited Colorado Supreme Court Justice Hobbs to offer the keynote address on the evening of July 22. We have also included an optional field trip to the Roaring Judy Fish Hatchery for the morning of July 23, and live music to coincide with our Banquet on July 23. For more information, registration forms, and exhibitor forms, visit www.western.edu/water.

World Water Day 2010
22 March 2010
Clean Water for a Healthy World

Colorado State University

COLORADO STATE UNIVERSITY PRESENTS WORLD WATER DAY
in conjunction with Hydrology Days

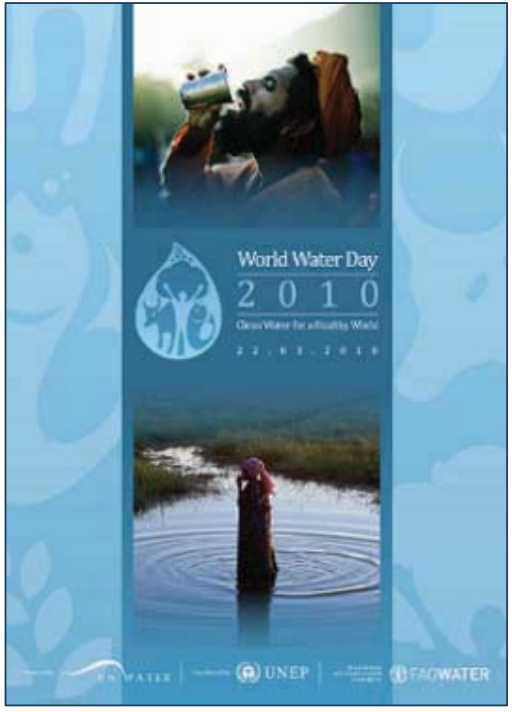

WHAT: **World Water Day**
WHEN: **Monday, March 22, 2010**
WHERE: **Lory Student Center, Fort Collins, CO**

KEYNOTE: **Dr. John Matthews**
Senior Program Officer of Freshwater Program,
World Wildlife Fund

CSU is hosting its first World Water Day event at the Lory Student Center on March 22, 2010. Activities include a World Water Day Fair, dignitary and keynote speakers, workshops, demonstrations, and community service projects. World Water Day at CSU will highlight local, regional, and global educational and outreach programs.

For more information about CSU World Water Day and Hydrology Days please visit the CSU World Water Day web site at www.globalwater.colostate.edu. To participate, please contact faith.sternlieb@colostate.edu.

The 2009 Ag Water Summit

by Reagan Waskom

The Colorado Agricultural Water Alliance (CAWA) sponsored its third Ag Water Summit on December 1, 2009, at the Jefferson County Fairgrounds. At a reception the previous evening, Governor Bill Ritter kicked off the Summit by stressing the importance of agriculture to Colorado's economic and cultural identity. Farm Bureau's vice president and current CAWA chairman Don Shawcroft opened the program by stating the mission of the Alliance and describing the history of irrigation development in Colorado. The Alliance is a group of agricultural organizations dedicated to preserving water and agriculture in Colorado.

Pat O'Toole, president of the Family Farm Alliance and rancher from the Little Snake River Valley north of Steamboat Springs, was the opening keynote speaker and set the tone for the Summit, stating that every state in the West has water conflict and that issues will only become more difficult with population growth and a changing climate—both will increase the pressure on agricultural water. O'Toole emphasized the importance of food production in the United States and stated that protecting working private lands in West is the key to preserving wildlife and the environment. The Family Farm Alliance proposes structural solutions to our water problems—more water storage is needed across the West.

A legislative panel moderated by Senate Ag Chair Mary Hodge included Rep. Sal Pace, Rep. Jerry Sonnenburg, Rep. Randy Fischer, Rep. Randy Baumgardner, Sen. Bruce Whitehead, and Sen. Gail Schwartz, all of whom discussed potential 2010 water legislation.

An agency panel moderated by commissioner of agriculture John Stulp addressed water agency priorities and issues. Dan McAulliffe discussed the CWCB's Colorado River Water Availability study and the need for stability in the construction fund. State engineer Dick Wolfe discussed the loss of irrigated lands and the increased implementation of sprinkler irrigation in Colorado. Alex Davis, Department of Natural Resources deputy director for water, indicated how vexing agricultural water problems are for water managers and expressed the desire to keep a productive agriculture in Colorado.

The remainder of the Ag Water Summit focused on potential solutions for Colorado agriculture. CSU professor Neil Hansen presented data on five years of limited irrigation trials in eastern Colorado. Water managers Eric Wilkinson of Northern Water and Mark Pifer of Aurora Water described their water projects. Todd Doherty discussed the CWCB's Alternative Water Transfer Methods grant program and methods being studied to share water between agriculture and municipalities. Jay Winner of the Lower Arkansas Valley Water Conservancy District focused on one of these projects—the SuperDitch. Greg Larson of the Republican River Water Conservancy District provided details on the $21 million 12-mile pipeline that will carry water to Nebraska to resolve the compact compliance dispute.

Finally, Chris Treese of the Colorado River District briefed participants on the proposals for new Wild and Scenic River designations, and Sen. Bruce Whitehead showed photos of the newest water project—the filling of Nighthorse Reservoir. In all, some 130 participants were thoroughly briefed on potential solutions and mechanisms to preserve water in agriculture. The Colorado Ag Water Alliance will continue to meet quarterly and may be contacted through Crystal Korrey at the Colorado Farm Bureau.

Pat O'Toole, president of the Family Farm Alliance, speaks at the 2009 Ag Water Summit.

20th Annual South Platte River Forum

by Laurie Schmidt, Colorado Water Institute

On October 21-22, 2009, 180 attendees gathered for the 20th annual South Platte Forum in Longmont, Colorado. With the theme *1989 to 2029: A River Odyssey*, the two-day meeting took a look back at the Forum's evolution over the past 20 years, as well as a look forward at water issues and challenges on the horizon.

Robert Ward, former director of the Colorado Water Institute, kicked off the meeting with a brief history of the Forum, noting the gradual change in the meeting's tone during its first five years. "In the first year, we were simply trying to get both sides in the same room, but by the fifth year—any subject was open for discussion," he said. Colorado State Senator Brandon Shaffer followed up with a discussion of challenges facing the state, including a skyrocketing state population that he said will triple water consumption rates by 2050. "We need to improve efficiency, increase conservation efforts, and plan for water storage projects," he said.

The meeting's first session focused on Colorado water law. Justice Gregory Hobbs provided a look back at Colorado Supreme Court water decisions, and Paul Frohardt, Colorado Water Quality Control Commission, examined changes in water quality policy. David Getches, dean of the University of Colorado Law School, discussed the unique challenges posed by the intersection of Colorado's growing population and hotter, drier climate conditions, saying that a combination of management, cooperation, and planning is essential to survival. "It is about scarcity, not business as usual," he said. "We may be entitled to it, but if nature doesn't provide it—it's not there."

Justice Gregory Hobbs (left), Diane Hoppe, and Jon Altenhofen catch up during the morning break at the 2009 South Platte Forum.

State climatologist Nolan Doesken, recipient of the 2009 Friends of the South Platte Award, and South Platte Forum coordinator Jennifer Brown at the 2009 South Platte Forum.

The final morning session, titled *Scenic Overlook*, included retrospective discussions by Jeris Danielson, a 20-year state engineer, and Alan Berryman, a 20-year division engineer. Max Dodson, retired assistant regional administrator for EPA Region 8, talked about "180-degree turns," including the dramatic "renaissance" of the South Platte River as an environment that provides resources for diverse interests. We face difficult challenges, such as population growth, climate change, new pollutants, and infrastructure deterioration, Dodson said, "but there will be continuing successes in improving and maintaining the aquatic environment."

During the lunch break, state climatologist Nolan Doesken was honored with the sixth annual Friends of the South Platte Award in recognition of his contributions to the South Platte River Basin and the South Platte Forum. Doesken was presented with a framed "South Platte Sunset" photo donated by Colorado photographer John Fielder. Following the award presentation, Denver Water manager Chips Barry gave the keynote address titled *From the DNR to Denver Water* and discussed how the Two Forks decision changed the culture and approach at Denver Water.

In an afternoon session titled *River Trippin',* the discussion turned to the subject of river conservation and native fish protection. Jay Skinner, wildlife manager with the Colorado Division of Wildlife (CDOW), provided an overview of the CDOW's efforts to assist the IBCC basin roundtables in prioritizing fish and wildlife values in the South Platte Basin. Next, Ryan Fitzpatrick, also of the CDOW, identified reasons for

> "It [water] is about scarcity, not business as usual. We may be entitled to it, but if nature doesn't provide it - it's not there."
>
> David Getches | Dean of University of Colorado Law School

declining fish populations: habitat alteration, non-native species, water quality, and changing flow regimes.

Linda Bassi, Colorado Water Conservation Board, gave an overview of the state's Instream Flow Program, focusing particularly on the challenges faced by the CWCB in implementing the program with its limited authority. "The CWCB cannot unilaterally reduce a decreed instream flow without water court approval," she said. The session concluded with a talk by Jeff Shoemaker on the Greenway Foundation's preservation and enhancement efforts on the South Platte and its tributaries during the past 35 years. "This is what can happen when a city or community gets together to right a wrong," he said.

The final session on Wednesday focused on Colorado climate, with Nolan Doesken reporting on the state of climate research 20 years ago—the foundations for automated weather networks were in place, and climatologists were beginning to use digital elevation model maps and GIS to map climate variables. "Back then, climate change was more an academic discussion than a topic to be taken seriously," he said. NOAA research meteorologist Martin Ralph concluded the session with a climatic look forward, focusing on the subject of atmospheric rivers, which are critical to the global water cycle and to the distribution of precipitation.

On Thursday, the Forum reconvened with Brian Werner quizzing the audience about events of 1989–the fall of the Berlin Wall, the San Francisco earthquake, the Broncos' Super Bowl bid, and the year's top song, "Don't Worry, Be Happy." Brighton vegetable farmer Robert Sakata reflected on how his family's farming business has changed as municipal growth has surrounded

Robert Ward (left), former director of the Colorado Water Institute, discusses the morning session with Andy Pineda, Northern Water, at the 20th Annual South Platte Forum.

the family's land. Sakata concluded with the certainty that farmers and municipalities are going to have to learn to cooperate for the sake of all involved.

CSU professor James Pritchett discussed his recent study on the impact of biofuel production on South Platte commodity and water prices and availability. His data show that the four Colorado ethanol plants have had little impact on water supplies or grain prices, as Colorado is a grain importing state and new ethanol plants are unlikely now due to market saturation. Other Thursday speakers included Joe Frank, manager of the Lower South Platte Water Conservancy District; Carol Ekarius of the Coalition for the Upper South Platte; Tom Cech of the Central Colorado Water Conservancy District; and Mark Waage and Melissa Elliot of Denver Water.

The 21st Annual South Platte Forum will be held on October 21-22, 2010. Stay tuned to www.southplatteforum.org and future issues of *Colorado Water* for details.

Colorado Water Congress 51st Annual Convention

by Laurie Schmidt, Colorado Water Institute

The 51st Annual Convention of the Colorado Water Congress was held on January 28-30, 2009, at the Hyatt Regency Denver Tech Center. With the theme "Water Buffaloes in the Mist: On Solid Ground in an Uncertain Time," the meeting kicked off with a legislative breakfast, during which Senator Jim Isgar and Representative Kathleen Curry reviewed water legislation for 2009.

Tim Storey, National Conference of State Legislatures, opened the general session by discussing national election trends, priorities, and budgets for state legislatures. He listed the top nine legislative issues for 2009 as state budget gaps, transportation and infrastructure, access to higher education, health costs and reform, energy alternatives, sentencing and corrections, home ownership, working families, and unemployment. State budget gaps on a national level are expected to reach $84 billion in 2010, he said. Pam Inmann followed Storey with a discussion of the strategic agenda for the Western Governors Association.

Thursday's luncheon keynote speaker was the Honorable Terrance Carroll, Speaker of the Colorado House of Representatives, who discussed "beginning with a vision" and entertained attendees with humorous anecdotes about his knowledge of water (or lack thereof) and his observations on water bills and the legislature. The afternoon general session included a presentation by Colorado pollster Floyd Ciruli, who presented the results of a survey titled "What Coloradans Think about Water."

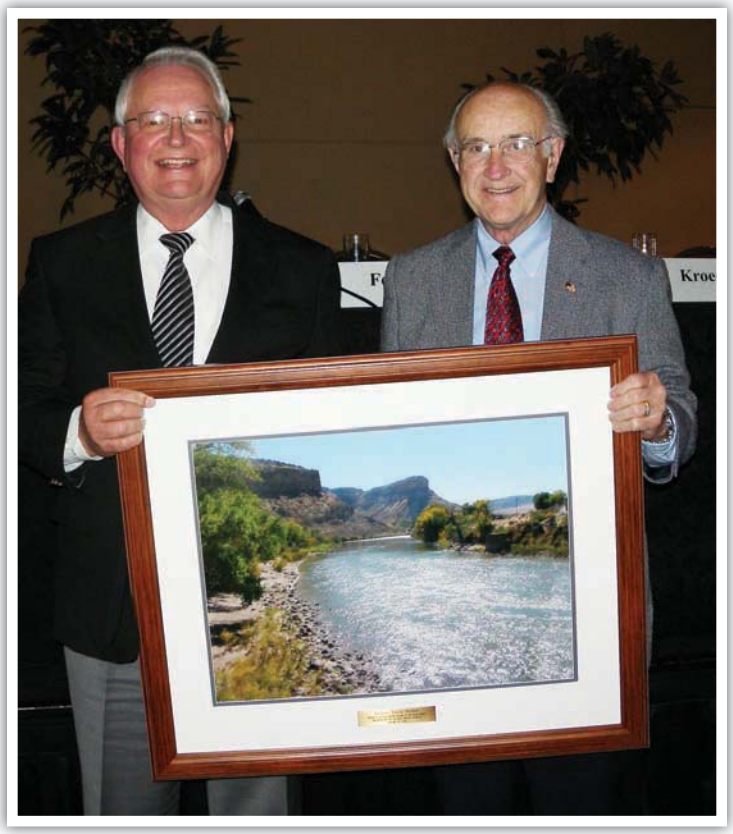

Don Ament (left) presents Tillie Bishop with the 2009 Wayne Aspinall Water Leader of the Year Award at the Colorado Water Congress 51st Annual Convention on January 30, 2009.

The general session on Friday morning featured talks by Rick Cables, Regional Forester with the U.S. Forest Service; Sally Wisely, Colorado State Director for the BLM; and Larry Walkoviak, Upper Colorado Regional Director for the Bureau of Reclamation. Cables focused on the importance of Colorado's forests to the future of the state's water. "The reach of the watersheds in our state is huge—143 counties in 10 states use a piece of Colorado's water," he said. Referring to Colorado's high country and forests as the "water towers of the West," Cables discussed the impacts of forested lands on water quality and quantity. Addressing the current mountain pine beetle outbreak, he highlighted the indirect impacts of dead trees, including blocked access to 3,500 miles of roads and power lines when the trees fall, and increased wildfire threat. "Denver Water can tell you—post-Hayman Fire—that the cost of dredging reservoirs after the fact (post-fire) is hugely expensive," he said. (Cables' talk can be read in its entirety in this issue of *Colorado Water*.)

Wisely discussed the value of partnerships and working together to create a sustainable future, saying "The bottom line of our (BLM) multi-use mission must be sustainability." Walkoviak reviewed priorities for the Upper Colorado region, including project maintenance, such as for the Animas La-Plata, and project completion. He also discussed the ongoing challenge of equalization efforts to keep a balance between Lake Powell and Lake Mead.

The conference wrapped up during Friday's luncheon with a keynote address by the Honorable Hank Brown, after which Tilman "Tillie" Bishop, former Mesa County commissioner and state lawmaker, was presented with the 2009 Wayne Aspinall Water Leader of the Year Award.

The 15th Annual Arkansas River Basin Water Forum (March 31-April 1, 2009)

by Perry Cabot, Extension Water Resources Specialist, Colorado State University

Every year, right around the time that the snowpack begins its slow surrender of water to the Arkansas River, Lake Pueblo, and finally the Southern Plains, the Arkansas River Basin Water Forum ("the Forum") commences. First held in 1995, the Forum was initiated to encourage dialogue among those with differing views on how the water of the Arkansas River should be managed.

About 170 stakeholders representing agricultural, municipal, commercial, industrial, and public interests attended this year's Forum, which was held at the CSU-Pueblo Occhiato University Center. The theme—*Water to Fuel our Future*—highlighted the important connection between water consumption and energy production in the Arkansas Basin.

Jennifer Gimbel, director of the Colorado Water Conservation Board, gave the Forum's keynote address, advancing a critical point. "When you are dealing with water, you are dealing with our future," Gimbel noted. "It's going to take choices, and it's going to take trade-offs." Indeed, as the Basin contends with demands for water to serve multiple and competing purposes, such "trade-offs" will require cool heads and compromising attitudes. More importantly, with the Colorado population expected to at least double by 2050, we must consider how to manage the river and its water under tighter constraints.

An ensuing panel discussion on the "Energy-Water Nexus" underscored this urgency. The Forum heard several perspectives on how water affects, and is affected by, renewable energy development, coalbed methane production, bioenergy cropping, and large-scale power generation. Rounding out the first day, the Forum also convened a panel on "Climate Risk and Drought Preparedness" to illustrate the importance of drought mitigation planning by both municipal and agricultural water users. This topic is worthy of regular emphasis in a region where water shortages force us to accept the variability and occasional harsh reality of our climate.

A "Fountain Creek Visioning" panel started off the Forum's second day. Rather than rehashing issues of problematic flooding and water quality, this panel focused on what basin residents can expect as the new Fountain Creek District assumes the responsibility of guiding restoration and enhancement projects for the stream system. Pueblo County Commissioner Jeff Chostner, along with the other panelists, took the audience through the long process that led to the new district's formation.

Invasive species also made the list of important panel topics. As a brief aside, the 1986 classic movie *Aliens* offers a humorous comparison to the tamarisk and zebra mussel saga that has found its way to parts of the basin. In one scene, after a merciless defeat by the territorial and ferocious aliens, Bill Paxton's character "Hudson" nervously declares, "Hey, maybe you haven't been keeping up on current events, but we just got our [rears] kicked, pal!" Okay, the situation admittedly isn't *that* bad, but we definitely have our fair share of unwanted guests here in the Arkansas Basin. The "Invasive Species" panelists highlighted some of the success stories in fighting this pressing problem.

Other activities included a panel that discussed the importance of Lake Pueblo Dam and Reservoir to both the local economy and the river flows. Pueblo City School students also entered pieces in an art contest that provided a number of paintings for participants to enjoy. Lastly, Carl Genova, a long-time board member of the Bessemer Ditch and Southeastern Colorado Water Conservancy District, was given the Bob Appel "Friend of the Arkansas" Award. Genova was recognized for his work on the winter water storage program.

Rio Grande Basin Tour, June 18-19, 2009

by Troy Lepper, Colorado State University Sociology Water Lab
Julie Kallenberger, Colorado Water Institute

For a number of water users, managers, state representatives, and academics, mid-summer in Colorado means it is time for the Colorado Foundation for Water Education's (CFWE) annual river basin tour. The CFWE's basin tours combine visits to basin sites with talks by expert speakers who focus on past, present, and future problems and solutions facing Colorado's river basins. The annual event serves not only as an educational opportunity for the state's water users and managers, but also as a fundraiser for the foundation's non-partisan educational work.

This year's tour took place on June 17-19 and visited the Rio Grande Basin. Located in south-central Colorado, the Rio Grande Basin is nestled between the Sangre de Cristo and San Juan Mountains and covers 7,700 square miles of land. Although its primary water use is agriculture, the basin is characterized by multiple uses, including recreation, wildlife preservation, and municipal use, that are all important to the successful and sustainable operation of the basin. This year's tour began on Wednesday, June 17, with two field trip options: (1) a whitewater rafting trip on the headwaters of the Rio Grande with speakers Brent Woodward (Colorado Division of Wildlife) and Dan Dallas (U.S. Forest Service), or (2) a walking tour of the historic Costilla County acequias hosted by former county commissioner Joe Gallegos. The day closed with a dinner and reception hosted by the Rio Grande Watershed Association of Conservation Districts *Teachers Workshop* at the Trincherra Ranch in Fort Garland. On Thursday, the tour officially started when the bus departed Alamosa for our first stop at the Native Aquatic Species Restoration Hatchery, where Steve Vandiver (Rio Grande Water Conservation District) and Dave Schnoor (Colorado Division of Wildlife) spoke about water management issues on the Rio Grande, as well as the challenges of protecting endangered species. The tour then turned west to the Rio Grande Reservoir, where Travis Smith (San Luis Valley Irrigation District), Dan Dallas, Tom Spezze (Colorado Division of Wildlife), and Kelly DiNatale (DiNatale Water Consultants, Inc.) spoke about the rehabilitation of the Rio Grande Reservoir and the potential for collaboration between multiple agencies and organizations for a multi-purpose reservoir project on the Rio Grande.

After lunch we boarded the bus for our next stop at the Rio Oxbow Ranch, which included a panel discussion focused on the Rio Grande restoration and conservation project. Rio de la Vista and Nancy Butler (Rio Grande Headwaters Land Trust), Mike Gibson (San Luis Valley Water Conservancy District), Dale Pizel and Greg Higel (Rio Grande Water Conservancy District), and Karla Shriver (Great Outdoors Colorado) discussed the in-progress efforts to preserve the natural flows of the Rio Grande for

Rio Grande Basin Tour attendees gather at Rio Oxbow Ranch near Creede, Colorado. (Courtesy of Colorado Foundation for Water Education)

Zeke Ward discusses floodplain reclamation and watershed protection with Rio Grande Basin Tour attendees in the Creede Mining District.

species protection, recreation, and conservation. After visiting the private Rio Oxbow Ranch, we travelled to Creede to look at the Willow Creek Reclamation Project, which is focused on improving water quality on Willow Creek following years of mining in Creede. At the base of the old mine, we were greeted by Zeke Ward and Kathleen Murphy (Willow Creek Reclamation Committee), who updated us on water quality improvements on Willow Creek. The evening ended with dinner and entertainment at the La Garita Ranch in South Fork. Evening speakers included Nicole Seltzer and Matt Cook (Colorado Foundation for Water Education), Mike Gibson, and Doug Shriver (Rio Grande Water Users Association) representing the Rio Grande Basin Roundtable, and Colorado State Senator Gail Schwartz, who gave the keynote address on a vision for sustainable water management for the San Luis Valley.

Day three began with speeches by Ray Wright (Rio Grande Water Conservation District) and Allen Davey (Davis Engineering Service, Inc.) on groundwater management issues in the San Luis Valley. The tour then headed to the Alamosa National Wildlife Refuge, where we heard from Clark Dirks (U.S. Fish and Wildlife Service) on preserving habitat and conserving water resources on the refuge. After touring the wildlife refuge we stopped at Entz Farm, where former Colorado State Senator Lewis Entz and his son Mike Entz spoke about the history of agricultural water in the Closed Basin and the viability of agriculture in the San Luis Valley. After a short stop at the Alamosa Photovoltaic Solar Plant, we headed to our final two stops of the tour. Following lunch at the Zapata Ranch in Mosca, Paul Robertson and John Sanderson (The Nature Conservancy) spoke on water management at the ranch and the non-consumptive water needs of the San Luis Valley. This stop was highlighted by a photo presentation of the Rio Grande River Basin by freelance photographer Michael Lewis (National Geographic). Finally, we boarded the buses one last time and headed to Colorado's newest national park: Great Sand Dunes National Park and Preserve. Here we were met by Art Hutchinson and Fred Bunch (National Park Service) who explained the importance of hydrology to the creation of the sand dunes and the park. We arrived back in Alamosa late Friday afternoon where we parted ways with our new and old friends and headed back to our various institutions and organizations.

The quality of the Rio Grande Basin Tour is a testament to the hard work and attention to detail by the staff of the Colorado Foundation for Water Education. Their continued efforts to provide Colorado water users and managers with educational opportunities helps focus management on the challenges related to sustainable water management in the 21st century. For more information about the CFWE, please visit www.cfwe.org.

Colorado Water Congress 2009 Summer Conference

The Colorado Water Congress (CWC) met on August 19-21, 2009, in Steamboat Springs for its annual summer conference. This year's theme was "A Change in the Financial Climate," reflecting the concerns about the state budget and the funding challenges facing water management agencies.

Two pre-conference forums were held: one that focused on how the state budget process works and a second for CWC members on developing better writing for advocacy skills. In addition, the Colorado Legislator's Interim Water Resources Review Committee met to discuss upcoming water legislation.

The conference kicked off on Thursday morning with about 200 CWC members in attendance. Congressman John Salazar opened the conference by describing federal water project funding that has been recently appropriated, including the Arkansas Valley Conduit and a number of much-needed rehabilitation projects around the state. He also read a tribute to former CWC Executive Director Dick MacRavey, noting many of Dick's accomplishments.

Congressman Salazar discussed the proposed Clean Water Restoration Act and the amendments being offered to limit jurisdiction. He remarked on the proposed Cap-and-Trade Bill, the need for clean coal technology, and the cost of the current proposals on household utility bills. The current health care debate is likely to capture most of the attention and energy for the next six months, he said.

A legislative panel discusses upcoming water legislation.

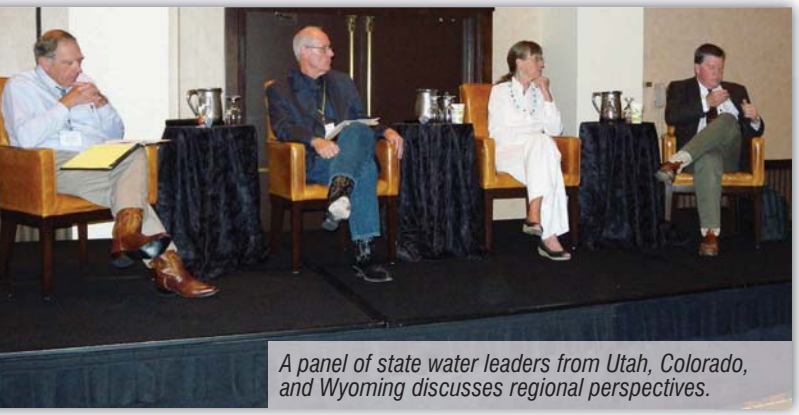

A panel of state water leaders from Utah, Colorado, and Wyoming discusses regional perspectives.

Attendees John McClow, Senator Bruce Whitehead, and Erin Light enjoy a break at the conference.

A panel of state legislators, including Rep. Kathleen Curry, Rep. Wes McKinnley, Rep. Randy Fischer, Sen. Al White, Sen. Grant Schwartz, Sen. Mary Hodge, Rep. Sal Pace, Rep. Jerry Sonnenberg, Rep. Randy Baumgardner, and new state Senator Bruce Whitehead reviewed last year's legislation and next year's budget and potential legislation. Their focus is on preserving the state's core mission while searching for long-term funding solutions.

Regional perspectives on water issues were provided by Pat Tyrrell, Wyoming State Engineer; Dennis Strong, director of the Utah Division of Water Resources; and Jennifer Gimbel, executive director of the Colorado Water Conservation Board. Although Utah has never built a state water project, it has recently directed work on two state water supply projects: one on the Bear River and one on the Colorado River. The State of Wyoming has one water project: the High Savery Project. In general, the three state governments are not in the business of water development, but they attempt to facilitate the development of water by other entities. All three state leaders expressed concern about meeting delivery obligations on the Colorado River and that additional development would further deplete the river, jeopardizing endangered species recovery.

Other program highlights included Harris Sherman, executive director of the Colorado Department of Natural Resources, who addressed the need for the water community to unify its voice and help address the state budget crisis as a whole, not just the funding shortages for water. John Fetcher, deceased director of the Upper Yampa Water Conservancy District was honored during a reception for CWC members and guests. The Colorado Water Congress Annual Winter Meeting will be held on January 27-29, 2010, in Denver. For further information on the CWC, visit www.cowatercongress.org.

Water Tables Raises $29,000 for Water Resources Archive

by Colorado State University Libraries staff

On February 21, 2009, more than 160 water experts and honored guests gathered to support the Water Resources Archive at Colorado State University Libraries. *Water Tables 2009: Compact Issues and Conflict Resolution* was a huge success, raising more than $29,000. The donation of Maury Albertson's papers to the Water Resources Archive was also announced.

Water engineers, ranchers, lawyers, professors, and students kicked off the event, now in its fourth year, with a reception at Morgan Library and tours of the Water Resources Archive. Dinner and a night of conversation were then hosted at the Lory Student Center ballroom at CSU. Thanks to the generosity of many individual and corporate sponsors, 25 graduate students were able to attend the event and interact with current leaders in the water industry.

The Archives featured two exhibits: one discussed the *Wyoming v. Colorado* court case of 1911, and the other featured highlights from the Maurice Albertson Papers. The first exhibit, *Headlines of History: Exploring the Evolution from Conflicts to Compacts*, contained original Supreme Court documents that led to a change in water law philosophy for Colorado's lead attorney on the case, Delph E. Carpenter. On display from the Delph Carpenter Papers were materials related to the case, which showed his efforts with the 11-year-long court battle and how he came to the conclusion that water compacts would better serve states and water users.

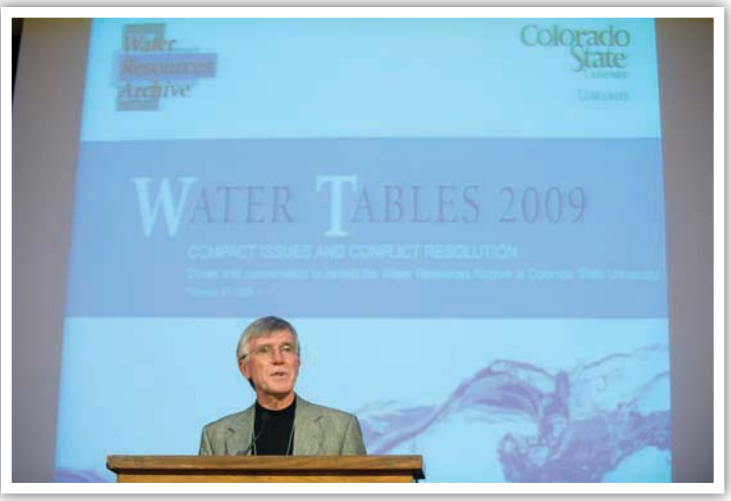

Robert Ward, former director of the Colorado Water Institute and CSU Faculty Emeritus, speaks to attendees at Water Tables 2009.

Ruth and Ken Wright look at an historic water document exhibit at Water Tables 2009.

The second exhibit, a table display of documents and artifacts from the Maurice Albertson Papers, reflected on the former CSU professor's achievements in teaching, research, and international development. Following a moment of silence for Albertson, who passed away in January at age 90, it was only fitting that his widow, Audrey Faulkner, discussed her husband's contribution to water resources at CSU and around the globe. While over 200 boxes had been donated by Albertson before he passed away, Faulkner assured head archivist Patty Rettig that many more boxes will be donated to the archive—a testament to Albertson's contribution to water resources research and education. Faulkner told guests how her husband's passion for water arose during the Great Depression when his father took him on tours of previously drought-ridden areas that were suddenly flooded. Her remarks about his life's dedication to water solutions in the West and throughout the world truly fit the evening's theme of conflict and compacts and were well received by all who attended.

At dinner, esteemed hosts at each table discussed past and current water conflict and compact issues, including topics related to climate, habitat, population, agriculture, law, and management. The hosts' expertise and insight made for lively, entertaining, and enlightening conversation. A tremendous success for both the CSU Libraries and the Water Resources Archive, Water Tables 2009 will provide the Archive with much needed funding for student assistants, supplies, and outreach activities. As a true testament to an enjoyable evening, guests left the event already anticipating Water Tables 2010.

34th Annual Colorado Water Workshop
July 22-24, 2009

by Laurie Schmidt, Colorado Water Institute

Members of the state's water community gathered at the Colorado Water Workshop on July 22-24 to investigate and discuss issues related to non-consumptive water use in Colorado. Due to renovations on the Western State College campus in Gunnison, the Workshop was held "up valley" in Mt. Crested Butte.

The meeting opened on Wednesday, July 22, with lunch and a welcome by new director Jerritt Frank, who provided a rationale for this year's theme. "We have become a nation of recreators," he said. "America used to know nature through labor; now we know nature through play." Lunch was followed by two afternoon sessions, the first of which focused on water and democracy in modern America. George Sibley, retired Western State College faculty member and former director of the Workshop, discussed the tradition of "hydraulic democracies" in the West. Justice Gregory Hobbs then provided an overview of the decision-making process in Colorado water court.

Taylor Hawes, director of the Natural Conservancy's Colorado River Program, began the second afternoon session, titled *Diverse Voices: Managing for Multiple Missions*, by explaining the Colorado River's "math" problem:

	30 million people
+	3.5-4 million acres of irrigated agriculture
+	non-consumptive needs
+	tribal settlements
+	Mexico
+	hydropower releases
=	**Deficit Spending**

This problem, she said, is compounded by the projected addition of 12-15 million more people by 2035, as well as by future climate variability.

Rick Cables of the U.S. Forest Service addressed managing forests for non-consumptive uses and "The New Water Project"—protecting forest headwaters while sustaining non-consumptive uses. Harris Sherman, executive director of the Colorado Department of Natural Resources, wrapped up the session with a discussion on how Colorado's economic future depends on the health of non-consumptive uses. "Companies often come here for the outdoor recreation opportunities that will attract employees," he said.

On Thursday morning, speakers during a session focused on environmental challenges included Angela Kantola, who provided an overview of the Upper Colorado River Endangered Fish Recovery Program and a status report on endangered fish in the Colorado and efforts to remove non-native fish species. Brad Taylor, a professor at Dartmouth College, discussed the nuisance blooms of *Didymosphenia geminata* (didymo) throughout western Colorado rivers that is particularly common below dams and reservoirs. Taylor's study on didymo's impacts to invertebrate populations showed a higher density of bugs where didymo is present. Finally, Mark Anderson of Glen Canyon National Recreation Area discussed efforts by the National Park Service to address the increasing threats posed by Zebra mussels to western waterways. Although Lake Mead was declared infested in 2007, the invasive species has—so far—been kept out of Lake Powell and Glen Canyon. Continued success, however, depends greatly on future funding. "With no suitable eradication options currently existing for most locations, prevention is the only hope," he said.

In a session on past, present, and future climate change, topics of discussion included impacts of reduced snowpack on Colorado's ski industry, by Matthew K. Reuer of Colorado College; effects of climate change on stream insects, by Bobbi Peckarsky of the University of Wisconsin; and hydroclimatic variability in the Upper Colorado River Basin, by Margaret Matter, Ph.D. candidate at Colorado State University.

Thursday afternoon included a lively discussion on the public's "right to float" on Colorado rivers. Attorney John Hill educated attendees on Colorado law regarding the issue, which holds that the public has no right to float through private property without the consent of the landowners. Attorney Lori Potter followed Hill with an overview of how other western states approach the "right to float" issue and posed the question of whether Colorado has laid the legal foundation necessary to support the public's right to float. The session concluded with a talk by Greg Felt, co-owner of a fly-fishing guide service on the Arkansas River, who asserted that lawmakers are not willing to stand for public access. "If an amendment were left up to Colorado voters, I believe it would pass because most people think it's the law already," he said.

On Thursday evening, a reception and dinner banquet were followed by a keynote address by Steve Martin, superintendent of Grand Canyon National Park. Martin, who has worked at Grand Canyon since 1973, discussed the recreation plan for the canyon, as well as the growing concerns about Glen Canyon Dam and its impacts on the canyon downstream. Speaking in terms of Grand Canyon's future, he said, "Change is going to be the constant."

The Workshop concluded on Friday morning with two sessions that focused on collaborative solutions and consensus. After lunch, director Jerritt Frank invited the Workshop Advisory Committee, speakers, and attendees to discuss themes and topics for next year's Workshop. Make plans to attend the 2010 Colorado Water Workshop, which will return to its regular venue on the Western State campus in Gunnison.

GRAD592
Interdisciplinary Water Resources Seminar

Fall 2009 Theme: **Environmental Protection and Water Management: Are They Compatible?**
Mondays at 4:00 PM, Clark A 206

The purpose of the 2009 Interdisciplinary Water Resources Seminar (GRAD 592) is to examine how the environment is protected as water supplies are developed and managed in Colorado. More specifically, the seminar will:

- Examine environmental laws, institutions and policies that affect water development
- Understand current approaches to environmental protection and water management
- Discuss the evolution of environmental protection and public participation in water management
- Examine current Colorado water case studies to understand the management of public water supply, growth, environmental mitigation, endangered species needs, water quality protection and other topics.

Aug. 24 **Organizational Meeting**—First Day of Class

Aug. 31 **Environmental History as a Tool in Water Resource Protection and Management**—Mark Fiege & Jared Orsi

Sept. 7 *Labor Day*—No class

Sept. 14 **US Department of Interior & Bureau of Reclamation's Role in Water & Environmental Management**—Bennet Raley

Sept. 21 **Conservation Priorities and Environmental Flow Quantification: Colorado's Non-Consumptive Needs Assessment**—John Sanderson

Sept. 28 **State's Role in Water Quality Protection & Management**—Steven Gunderson

Oct. 5 **Resolving Transboundary Environmental Issues**—Jennifer Pitt

Oct. 12 **Negotiating Better Environmental Governance in the Platte River Basin: Implementing the Endangered Species Act**—David Freeman

Oct. 19 **Holistic Management of the Colorado River System**—Taylor Hawes

Oct. 26 **Public Participation in Water Management - Case Study: Bear Creek Watershed**—Russ Clayshulte

Nov. 2 **Water Management & the Environment: Programs & Priorities for the Western Governors**—Tom Iseman

Nov. 9 **Legal Tools & Legal Constraints in Environmental Protection**—Melinda Kassen

Nov. 16 **35 Years of The Clean Water Act - Are We There Yet?**—Ayn Schmidt

Nov. 23 *Thanksgiving Break*—No class

Nov. 30 **Instream Flow Protection Program & Wild & Scenic Designations to protect Colorado Waters**—Ted Kowalski

Dec. 7 **Student Discussion & Participation**—Final Class

Dec. 14 *Final Exams*—No class

Presentations will be posted online each week if available. http://www.cwi.colostate.edu/grad592.asp

All interested faculty, students, and off-campus water professionals are encouraged to attend.
For more information, contact Reagan Waskom at reagan.waskom@colostate.edu or visit the CWI web site.

Spring 2010
Interdisciplinary Water Resources Seminar

Sponsored by: CSU Water Center, USDA-ARS, Civil and Environmental Engineering, and Forest, Rangeland, and Watershed Stewardship

Wednesdays from Noon to 1:00 PM

February 3 **LSC Room 228**	**Tim Scheibe**, Pacific Northwest National Laboratory, Hydrology Group **2010 Darcy Distinguished Lecture--Flow and Reactive Transport: From Pores to Porous Media to Aquifers**
February 10 LSC Room 210	**Faith Sternlieb**, Colorado Water Institute, CSU **Planning for CSU's first World Water Day Celebration**
February 17 **LSC Virginia Dale**	**Mark Williams**, Institute of Arctic and Alpine Research, CU **Potential Climate Impacts on the Hydrology of High Elevation Catchments, Colorado Front Range**
February 24 LSC Room 210	**Jim Ascough**, Agricultural Systems Research, USDA-ARS **Spatially Distributed Modeling using the Component-Based AgroEcoSystem Model**
March 3 LSC Room 210	**Dennis Harry**, Geosciences, CSU **Opportunities and Adventures in Hydrogeophysics**
March 10 LSC Room 210	**David Theobald**, Human Dimensions of Natural Resources, CSU **Assessing Threats to Colorado Watersheds**
March 17	**No Seminar** **Spring Break**
March 24	**No Seminar** **Hydrology Days (LSC Cherokee Park Room); www.hydrologydays.colostate.edu**
March 31 LSC Room 210	**Tom Sale**, Civil and Environmental Engineering, CSU **Emerging Concepts in Subsurface Contaminant Transport and Remediation**
April 7 LSC Room 210	**Tim Steele**, TDS Consulting **Clear Creek Long Range Planning**
April 14 **LSC Room 224**	**Thijs Kelleners**, Renewable Resources, University of Wyoming **Measurement and Modeling of Water Flow, Heat Transport, and Gaseous Exchange in Rangeland Soils**
April 21 LSC Room 210	**Domenico Bau**, Civil and Environmental Engineering, CSU **Anthropogenic Uplift of Venice by Seawater Injection into Deep Aquifers**
April 28 LSC Room 210	**Mike Coleman**, Civil and Environmental Engineering, CSU **Soil Moisture Estimation**
May 5 LSC Room 210	**Romano Foti**, Civil and Environmental Engineering, CSU **TBA**

* Room may be changed if needed. Check weekly announcements.

All interested faculty, students, and off-campus water professionals are encouraged to attend.
For more information, contact Reagan Waskom at reagan.waskom@colostate.edu or visit the CWI web site.

CSU Professor Honored by Interior Secretary Ken Salazar

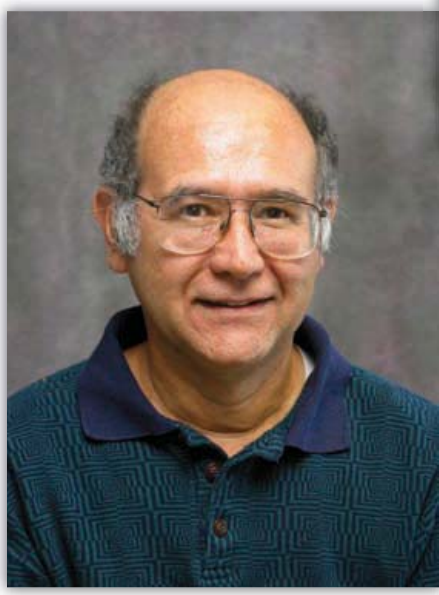

Interior Secretary Ken Salazar recently honored Jose 'Pepe' Salas, a Colorado State University civil and environmental engineering professor, with the U.S. Department of the Interior Partners in Conservation Award. Salas and his colleagues at three other universities received the award for helping to develop new operational guidelines for the Colorado River.

Honored with Salas were representatives of the University of Colorado, the University of Arizona, and the University of Nevada, Las Vegas. Together with the U.S. Bureau of Reclamation and a variety of other government agencies, Salas and his partners helped develop Colorado River Interim Guidelines, which has been praised as the most important agreement among the seven basin states since the original 1922 compact. States signing the agreement were Arizona, California, Colorado, Nevada, New Mexico, Utah, and Wyoming.

Salas has served as principal investigator on two projects funded by the U.S. Bureau of Reclamation in connection with the Colorado River Basin. His activities on these projects included:

- Using innovative record extension techniques for updating the data base of naturalized flows of the Colorado River system
- Developing new approaches for reconstructing streamflows of the Colorado River based on tree-ring indices
- Developing potential scenarios of streamflows that may occur in the Colorado in future years
- Characterizing multi-year droughts using simulation and mathematical techniques
- Testing the effects of stochastic streamflows on the operations of the Colorado River system, particularly the effects on reservoir levels and outflows of the two major lakes, Lake Powell and Lake Mead

**This article was adapted from a June 30, 2009, CSU news release.*

Upper Yampa Water Conservancy District John Fetcher Scholarship Awarded

The Upper Yampa Water Conservancy District (UYWCD) funds an annual scholarship named in honor of John Fetcher in support of CSU students preparing for careers in water-related fields. The scholarship program is administered by the CSU Water Center and provides financial assistance to committed and talented students who are pursuing water-related careers at CSU. The UYWCD $3,000 scholarship is open to any major at CSU. Criteria require the recipient to be a full-time student enrolled at CSU with a minimum GPA of 3.0. The scholarship duration is one year.

The UYWCD John Fetcher Scholarship recipient for the 2009-10 academic year is Luke Javernick. Luke is a senior in the Department of Civil and Environmental Engineering at Colorado State University and plans to pursue a master's degree in hydrology. He is currently the vice president of the CSU chapter of the American Society of Civil Engineers (ASCE), is a member of the American Concrete Institute, and is involved with Tau Beta Pi.

Luke's interest in engineering developed at an early age—while most five-year-olds were playing, he spent his days landscaping with his father. After many years of pursing an aviation career, Luke realized how much he missed the challenges and unique projects that landscaping offered. So he began researching his options and decided to study civil engineering, which he says has proven to be the best decision he ever made.

Luke is a nontraditional student and has been married to his wife, Tiffany, for over three years. Both Luke and Tiffany grew up in Canon City, Colorado, and they hope to stay in Colorado and raise a family. In the future, after developing a solid engineering foundation and passing the Principles and Practice of Engineering (PE) exam, Luke aspires to one day become a city or county engineer.

The CSU Water Center and Colorado Water Institute congratulate Luke and wish him success in his future academic studies and career. The ongoing support of CSU students by the UYWCD is acknowledged and greatly appreciated.

CSU Professor Receives NSF Award

Thomas Borch, assistant professor of environmental soil chemistry in the Department of Soil and Crop Sciences at Colorado State University, has received a Faculty Early Career Development (CAREER) Award from the National Science Foundation. The honor is considered one of the most prestigious for up-and-coming researchers in science and engineering.

Borch will use the nearly $500,000, five-year grant to investigate how climate change, and especially the projections of increased precipitation and flooding, may impact important biogeochemical cycles, such as those related to iron. Iron minerals are among the most important reactive solids in earth surface environments, acting as natural filters of inorganic contaminants and nutrients, sorbents for organic matter, and poising the redox potential of groundwater. Lack of biologically available iron in soils can also lead to iron deficiency anemia which is a major public health and financial problem in Central Asia, with primary impact on woman and children.

Iron minerals are responsible, in part, for stabilization of organic matter in soils. Consequently, any changes in iron chemistry may also result in changes in the atmospheric carbon dioxide concentration and the global climate. In high-elevation watersheds of the Rocky Mountains, more than 95% of spring snowmelt infiltrates through soils and moves along shallow groundwater flow paths before merging with stream water. In fact, one-sixth of the world's population depends on water released from seasonal snowpacks and glaciers, so an improved understanding of the soil processes that sustain the supply of clean water from mountain headwaters is critical to current and future human natural resource demands.

"This award will allow us to initiate a new important research area in environmental biogeochemistry at CSU; attract high-caliber postdoctoral researchers, graduate, and undergraduate students; and develop a set of new courses targeting undergraduate students interested in environmental biogeochemical processes from the molecular scale to field scale," said Borch.

Borch earned his doctorate degree in environmental soil chemistry from Montana State University and his Master of Science and Bachelor of Science degrees in environmental chemistry from the University of Copenhagen. He joined Colorado State University in 2005 to initiate a program in environmental soil chemistry.

This article adapted from a June 5, 2009, CSU news release.

CWI Announces Funded Student Projects

The Colorado Water Institute is pleased to announce the funding of six student projects this year. This program is intended to encourage and support graduate and undergraduate research in disciplines related to water resources and to assist Colorado institutions of higher education in developing student research expertise. The purpose of the funding is to help students initiate new research projects or to supplement existing student projects focused on water resources research. The FY09 funded projects and funding recipients are listed below:

James Cullis
Department of Civil, Environmental, & Architectural Engineering, University of Colorado

Faculty Sponsor: Diane McKnight

Understanding the Hydrologic Factors Affecting the Growth of the Nuisance Diatom *Didymosphenia Geminata* in Rivers

Didymosphenia geminata, also known as "didymo" or "rock snot," is a nuisance algal species that occurs in many mountain streams in the western U.S. It tends to produce large amounts of extracellular stalk material, and while it is not considered to be toxic, the growth of these large algal mats has a significant impact on the aesthetics of a stream and on the sustainability of stream ecosystems and water supply infrastructure. Not much is known about this species, as it has only become a significant problem in the past 10 to 15 years. This research will look specifically into the hydrologic factors affecting the growth of this nuisance species at a number of study sites in Boulder Creek, Colorado, with a particular focus on the role of flood-induced bed disturbance as a primary control of growth. The overarching research hypothesis is that high levels of shear stress and bed disturbance due to flood events are necessary to control the growth and bloom tendency of *D. geminata*, and that these levels can be provided through environmental flood releases from reservoirs to maintain functioning stream ecosystems and water supply systems.

Bear Creek Watershed Project

Kimberly Gortz-Reaves, College of Architecture and Planning, University of Colorado (Faculty Sponsor: Charlie Chase)

Bear Creek watershed encompasses four counties and more than eight cities and towns. The extent to which public and private land use managing agencies or organizations involved with the watershed offer "on-the-ground" projects for young people and community groups to participate in (e.g., habitat restoration, stream bank stabilization, or other watershed conservation projects) is unknown. Furthermore, there is no existing system to provide coordination for watershed-wide projects. The purpose of this research project is to identify stakeholders and potential partners operating in the Bear Creek watershed and their needs, resources, and capacities. The project will be facilitated by the Bear Creek Watershed Partnership (BCWP), which is aimed at connecting youth-based stewardship and leadership programs to opportunities offered by Bear Creek watershed stakeholders. To date, facilitating partners include City of Denver Parks and Recreation, University of Colorado at Denver, National Park Service RTCA, AmeriCorps, FrontRange Earth Force, and Groundwork Denver. To date, there has been limited program coordination among municipalities and other public and private agencies within the Bear Creek watershed. The objective is to contact agencies and associations, build a database of information based on conversations with contacts, create a stronger partnership effort, and develop a GIS-web based interactive map with the gathered information. The long-term goal is to create a forum in which partners will be able to share or coordinate their objectives, improve management strategies, and post stewardship projects for youth.

Jason F. Smith
Department of Horticulture and Landscape Architecture, CSU

Faculty Sponsor: James E. Klett

Impact of Limited Irrigation on the Health of Four Common Shrub Species

The shrub water study was started in 2005 in response to the 2002 drought to evaluate the actual water requirements of some commonly used landscape plants. Currently, most water use statements for landscape plants are based on personal opinions or observations, and few studies have evaluated the water use of landscape plants. This research involves determining the water use values for some common landscape shrubs from a replicated study. The research is continuing in 2009 and will evaluate the growth of Redosier dogwood, smooth hydrangea, Diablo ninebark, and arctic blue willow when subjected to four different amounts of irrigation (0%, 25%, 50%, and 100%), based on the evapotranspiration rate of Kentucky bluegrass. By the end of 2009, accurate water requirements for these four species will be determined after a season of collecting various types of data. If the study results show that these shrubs do well with 0% or 25% of the evapotranspiration rate of Kentucky bluegrass, then they would be well suited for planting in many Colorado landscapes that require little to no irrigation. However, if these shrubs are found to need 50% or 100%, then the use of these shrubs could be limited for landscape use in Colorado.

Potential Changes in Groundwater Acquisition by Native Phreatophytes in Response to Climate Change

Throughout western North America, arid regions are likely to experience changes in the timing and amount of precipitation as global surface temperatures increase. Altered rainfall and runoff patterns will exacerbate current stresses on water resources from growing human demands and could produce long-term changes in water availability for ecosystems, agriculture, and municipalities. In Colorado's arid San Luis Valley (SLV), competing water interests will be particularly sensitive to climate change. The SLV receives only 180-250 mm of precipitation annually; yet, a shallow unconfined aquifer recharged by snowmelt supports over 600,000 acres of irrigated agriculture, substantial water transfers out of the valley, and native rangeland for livestock grazing. The dominant native plants in the SLV are phreatophytes, plants that use groundwater. Evapotranspiration by phreatophyte communities accounts for more than one-third of the total annual groundwater consumption. Some SLV phreatophytes can also utilize predictable pulses of summer monsoon rain to reduce or supplement their groundwater use. Thus, changes in monsoon rainfall patterns may produce changes in groundwater acquisition of phreatophytes, which could have considerable effects on the SLV groundwater budget and regional agriculture. Our research investigates the response of four native phreatophytes to changes in growing season precipitation using a rainfall manipulation experiment. Our goal is to understand how plant community adjustment to climate change in the SLV would affect regional groundwater resources, and to incorporate this understanding into the Rio Grande Decision Support System groundwater management model.

Julie Kray
Department of Forest Rangeland and Watershed Stewardship, CSU

Faculty Sponsor: David J. Cooper

Chengmin Hsu
Department of Civil Engineering,
University of Colorado Denver

Faculty Sponsor: Lynn E. Johnson

High-Resolution Soil Moisture Retrieval in the Platte River Watersheds

An accurate estimate of soil moisture is necessary for various hydrometeorological, ecological, and biogeochemical modeling and applications. Unfortunately, continentally available soil moisture data (AMSR-E) are currently derived using passive remote sensing technology that has a very rough resolution (i.e., 25 km). This rough resolution character of the AMSR-E products makes them difficult to use for hydrological and ecological purposes at the watershed scale. In this project, I propose to: (1) improve and update the AMSR-E soil moisture products by assimilating the AMSR-E products into the NOAH land surface model, (2) downscale the coarse resolution soil moisture outcome to a higher resolution product (e.g., 240-meter resolution), and (3) validate the final product with the joint soil moisture observations obtained from NRCS Soil Climate Analysis Network (SCAN) and from soil moisture monitoring stations in Nebraska by the High Plains Regional Climate Center (HPRCC). The study area will include portions of the North and South Platte River Basins and a portion of the Republican River Basin. The work proposed in this project constitutes a first attempt to understand the spatial structure of brightness temperature and soil moisture images when applied at a higher resolution. It will also test the capability of the NOAH land surface model to generate high-resolution surface soil moisture. More importantly, the work will be a foundation for the future estimation of root-zone soil moisture.

Developing Barriers to the Upstream Migration of New Zealand Mudsnail (*Potamopyrgus antipodarum*); Phase II: Laboratory and Field Evaluations of Mudsnail Response to Copper-based Materials under Varied Water Quality Conditions

The objective of this research is to evaluate the ability of copper-based substrates to prevent the upstream spread of the invasive New Zealand mudsnail (*Potamopyrgus antipodarum*). Over the last 20 years, mudsnails have spread rapidly across the western U.S., prompting management agencies to close several streams and fish hatcheries. There is currently a need for effective methods to prevent further invasion into novel waterbodies. Preliminary research results suggest that several copper-based substrates may be useful in stopping the upstream spread of this organism. I am currently studying how physicochemical parameters, including pH, temperature, and water hardness, affect the mudsnail's response to the copper materials. We are hopeful that copper-based substrates can eventually be integrated into mudsnail management plans once the barrier ability of each of the materials has been evaluated.

Scott Hoyer
Department of Fish, Wildlife, and Conservation Biology, CSU

Faculty Sponsor: Christopher Myrick

Colorado Water Institute Reports

Estimating the Water Lost Due to Evaporative Upflux from Shallow Groundwater

by Jeffrey D. Niemann, Timothy K. Gates, Niklas U. Halberg, and Brandon M. Lehman
Department of Civil and Environmental Engineering, Colorado State University

Introduction

Many agricultural water systems in the western U.S. are facing extraordinary pressures that constrain water availability and use, and the Lower Arkansas River Valley (LARV) is no exception. In the face of such pressures, various strategies have been proposed to conserve water in agricultural systems like the LARV. One conservation strategy is the removal of invasive phreatophytes, such as tamarisk (salt cedar). Another proposed strategy is the application of polyacrylamides or polysaccharides to canals, which promote settling of clay particles out of canal water and reduce seepage losses. Improved irrigation practices, such as drip irrigation, have been suggested as another possible method for water conservation.

All of these conservation strategies aim—directly or indirectly—to reduce the amount of non-beneficial consumptive use in the system, which is mostly the evapotranspiration (ET) from uncultivated areas. The ET from uncultivated lands within the Arkansas Valley is likely a major component of the overall water balance, but much uncertainty persists regarding the magnitude of this loss and the effectiveness of proposed water conservation strategies at reducing this loss. A key source of uncertainty is the actual reduction of the non-beneficial consumptive use that would occur if the water table is lowered by a particular amount.

The overarching objective of this project is to quantify the controls on non-beneficial consumptive use of water from uncultivated lands in the LARV. In particular, we seek to determine: (1) the portion of total ET from uncultivated lands that comes from groundwater upflux, (2) the sensitivity of the non-beneficial ET to the water table depth, and (3) the role that vegetation and soil properties play in mediating the relationship between water table depth and upflux. A better understanding of the evaporative upflux from fallow fields and naturally vegetated lands in the Arkansas Valley will improve the assessment of water conservation strategies in the valley. It is also expected to benefit soil salinity and water quality assessments.

Approach

Our strategy has focused on making detailed measurements at three uncultivated field sites in the LARV. The field sites were selected to represent different topographic and land-use conditions found in the valley (Figure 1). One of these sites is a retired field north of the town of Swink and close to the Arkansas River. The field is no longer cropped because it lies in a conservation easement that aims to reduce agricultural losses from floods. Roughly one third of this site is vegetated by legacy alfalfa; the remainder has relatively natural grasses and forbs, but about half of this section is currently grazed. Because the site lies within the alluvial valley, it has very little topographic relief.

The second site is located southeast of the town of Manzanola and adjacent to the Rocky Ford Highline Canal. It is naturally vegetated and has some topographic relief because it lies at the edge of the alluvial valley. The third site, which is located south of the town of Rocky Ford between the Catlin Canal and Timpas Creek, is vegetated with grasses and forbs. It has little topographic relief, but it is situated several meters above the creek.

Both ET and vegetation greenness at the three field sites were estimated from remote-sensing data. The thermal

Figure 1. (a) Researcher downloading data from a raingage at the Swink field site, (b) Raingage and atmometer at the Manzanola field site, and (c) monitoring well at the Rocky Ford field site.

infrared and visible band information from the Landsat5 and LandSat7 satellites are used in an energy balance approach called ReSET to estimate ET in the LARV. These estimates were calibrated using weather station observations and are expected to have an accuracy of 10–20%. This approach provides ET estimates on a 30-meter grid each time a satellite passes over the site if cloud cover is not present. Both LandSat5 and LandSat7 pass over the sites every 16 days, but their timing is offset so that one of the satellites passes over the site every 8 days. LandSat5 is the preferred satellite for this project because LandSat7 covers changeable regions where data are unavailable. The remote sensing algorithm also produces the so-called normalized difference vegetation index (NDVI), which measures the greenness of the vegetation.

The three field sites were extensively instrumented to quantify potential influences on the variation of ET. At the Swink site, 39 wells were drilled on a 60-meter grid, 29 wells were drilled at the Manzanola site on an irregular 45-meter grid, and 17 wells were drilled at the Rocky Ford site on a 60-meter grid (the layout of the monitoring wells is shown in Figure 2). Automated water level loggers were placed at the base of most wells to continuously measure the water level above the sensor. One water level logger was also placed at the ground surface at each field site to measure variations in atmospheric pressure, which improves the accuracy of the water table estimates.

At each site, precipitation was measured using two tipping bucket gages, and reference crop ET was estimated using two atmometers. Reference crop ET also was computed using data from a CoAgMet weather station at Rocky Ford, which is located about 5 miles from the Swink site, 15 miles from the Manzanola site, and 6 miles from the Rocky Ford site. On cloud-free days that the satellite passed over, measurements were made in each field of potential explanatory variables. Spot measurements of water table depth were made at all wells, soil moisture was measured near all wells at 2-, 3-, and 4-foot depths, and soil salinity was estimated using a calibrated electromagnetic induction probe.

Key Results

The contribution of groundwater upflux to the total ET was estimated using a water balance approach. Water for the actual ET can be supplied by changes in soil water storage, precipitation events, and groundwater upflux. No significant lateral flow or runoff is expected due to the dry condition of the soil during the period of analysis. It is assumed that all precipitation became ET (i.e., groundwater recharge was negligible), and changes in soil water storage were found to be negligible over long time periods. Thus, the cumulative groundwater upflux for a period of time can be estimated as the cumulative ET minus the recorded precipitation depths. Figure 3 shows results from this analysis for two of the field sites for 4/1/2007 to 3/21/2008. On average, 2.4 millimeters per day (mm/day) of groundwater was lost to ET at the Swink site, and 2.0 mm/day was lost to ET at the Manzanola site during this period. Both the ET and the groundwater upflux rates are greater during the summer than in the winter. Total cumulative groundwater upflux is estimated to be 0.79 m and 0.68 m at the Swink and Manzanola sites, respectively. This suggests that about 75% and 70% of the total estimated ET was supplied by groundwater upflux at the Swink and Manzanola sites, respectively. These estimates suggest that the non-beneficial consumptive use of water is primarily supplied from upflux

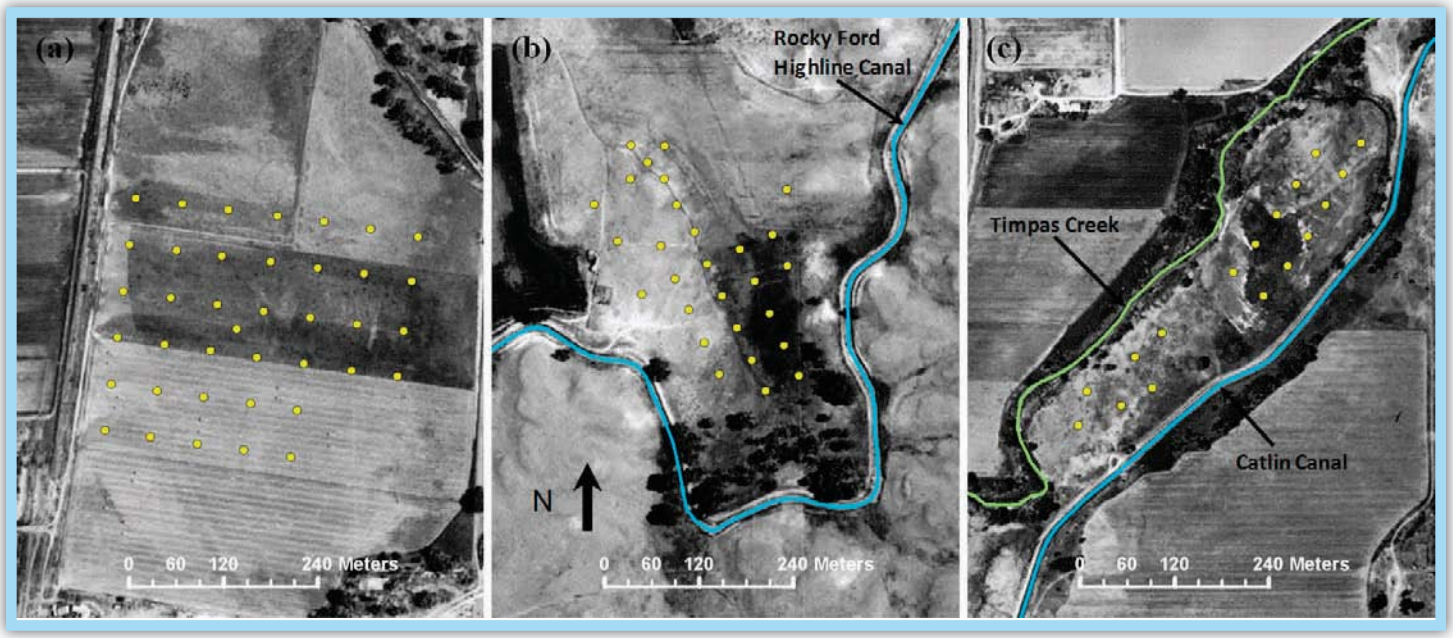

Figure 2. These views show the layout of monitoring wells at the (a) Swink, (b) Manzanola, and (c) Rocky Ford sites.

from the shallow water tables at both sites.

Figure 4 shows the temporal average ET rate plotted against the temporal average water table depth at each monitoring well for the Swink and Manzanola field sites. At the Swink site, the average ET rate does not clearly vary with the average water table depth. However, if the monitoring wells are divided according to their associated vegetation types (alfalfa, grass, and grazed grass), possible relationships are observed for the alfalfa and grass sections (not shown), but the number of wells in each group is small. For the Manzanola site, the range of water table depths is larger and the vegetation cover has fewer disturbances. At this site, the average ET rate approaches 5 mm/day when the water table is close to the surface and drops to roughly 4 mm/day when the water table reaches 2.5 meters in depth.

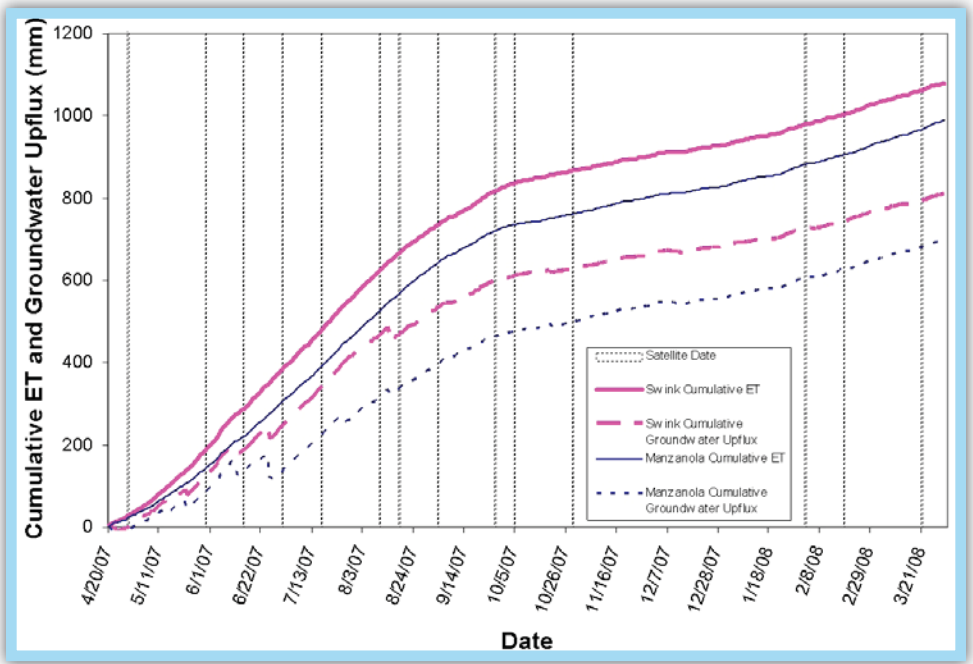

Figure 3. Estimated cumulative groundwater upflux in support of ET (mm) for the Swink and Manzanola field sites. Vertical lines indicate dates on which ET is estimated from remote sensing.

Key Conclusions

Although monitoring and data analysis are ongoing, these preliminary results demonstrate that groundwater upflux was the dominant contributor to ET at both the Swink and Manzanola sites during the period of analysis. This finding confirms that non-beneficial ET is closely linked to the presence of a shallow water table under the uncultivated lands in the LARV. More research is needed to determine the water savings that might be achieved by lowering the water table by a specified amount. In particular, the vegetation patterns observed in this study have likely adapted to the spatial variations in water table depth within these sites. If the water table is abruptly lowered, the vegetation would require a significant period of time to adapt to the new conditions, which would potentially alter the relationship between water table depth and non-beneficial ET.

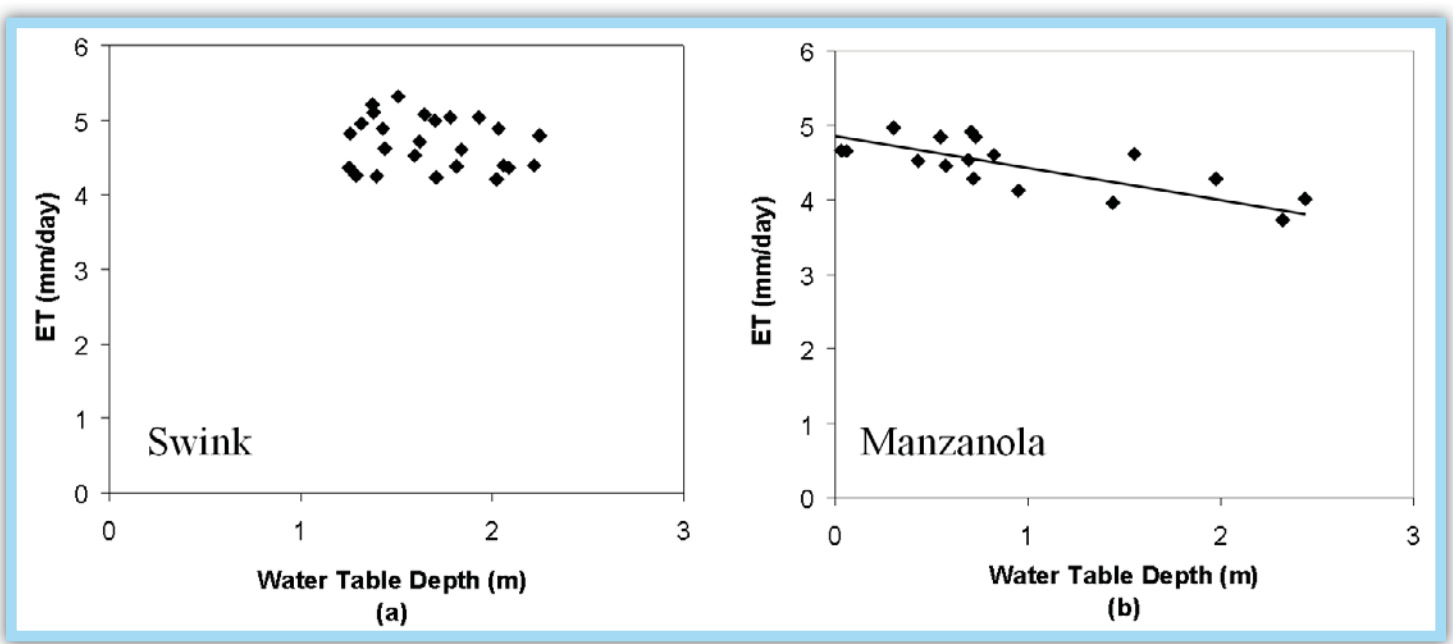

Figure 4. The average ET rate plotted against the average water table depth for 4/1/2007 to 3/21/2008 at each monitoring well at the (a) Swink and (b) Manzanola sites.

Progress on the Lysimeter Project at Rocky Ford

by Allan Andales, *Assistant Professor, Department of Soil and Crop Sciences, Colorado State University*

Accurate estimates of crop consumptive water use are needed to effectively manage irrigation in the Arkansas River Basin of Colorado and to maintain compliance with the Arkansas River compact with Kansas. Consumptive water use is normally defined as water that is lost from the crop root zone of the soil through the processes of soil surface evaporation and transpiration from crop leaves. The two processes occur simultaneously and are difficult to separate. Therefore, the term evapotranspiration (ET) is commonly used to refer to both processes.

The concept of "reference crop ET" was developed in the 1970s to represent the potential amount of ET from a standardized un-stressed crop, given adequate water and actual weather conditions at a particular location. Historically, alfalfa has been used as the reference crop in Colorado. The ET of other crops can then be estimated by multiplying reference crop ET by a crop coefficient (Kc). At any given point in the growing season, the Kc for a crop is simply the ratio of its ET over reference crop ET. The Kc can be thought of as the fraction of the reference crop ET that is used by the actual crop. Values of Kc typically range from 0.2 for young seedlings to 1.0 for crops at peak vegetative stage with canopies fully covering the ground.

The American Society of Civil Engineers (ASCE) standardized reference ET equation (from here on referred to as the ASCE standardized equation) has been approved by the U.S. Supreme Court as the method of determining reference crop ET for compact compliance. This equation calculates the daily or hourly alfalfa reference ET based on inputs of solar radiation, air temperature, wind speed, and humidity data that are usually available from weather stations. However, it has not been tested in the Arkansas Basin. Furthermore, localized crop coefficients that can be used to estimate the ET of crops grown in the area are not available. A validated ASCE standardized equation, along with locally derived crop coefficients, can be a widely applicable tool for irrigation management in the Arkansas River Basin of Colorado.

Figure 1. This image shows the retainer tank of the reference lysimeter after being set on the foundation. (Image courtesy of Lane Simmons)

An accurate way to measure alfalfa reference ET and the ET rates of other crops is to use a precision weighing lysimeter that directly measures ET based on changes in weight of an intact block of soil (monolith) containing an actively growing crop. By 2003, plans for building two weighing lysimeters in the Arkansas River Basin were in full swing, one to be used for measuring alfalfa reference ET and the other for measuring ET of other crops. In 2006, construction of the precision weighing lysimeter for measuring crop ET was completed at CSU's Arkansas Valley Research Center (AVRC) at Rocky Ford, Colorado. The monolith tank dimensions of the crop lysimeter are 10 feet wide by 10 feet long by 8 feet deep (3 m x 3 m x 2.4 m). By 2007, construction began on the reference lysimeter for measuring alfalfa reference ET. The monolith tank dimensions of the reference lysimeter are 5 feet wide x 5 feet long x 8 feet deep (1.5 m x 1.5 m x 2.4 m).

Completion of the Reference Lysimeter

The reference lysimeter monolith tank and retaining (outer) tank were constructed at the USDA-Agricultural Research Service workshop in Fort Collins, Colorado. Work began in 2007 and was completed in spring 2008. The monolith tank was then transported to the installation site at AVRC. On June 23, 2008, the tank was hydraulically pulled into the ground to fill the tank with an undisturbed block of soil (monolith). Excavation for the installation of the retainer tank proceeded shortly afterwards. The laying of the reinforced concrete foundation for the retainer tank was slightly delayed because of shallow groundwater at approximately 14 feet below the ground surface, but the retaining tank was eventually transported to the installation site and set on the foundation in September 2008 (Figure 1).

The weighing mechanism on which the monolith tank was to be set was assembled in December 2008. It consists of a mechanical lever scale-load cell combination that operates similar to a truck scale. The load cell output is in millivolt

Figure 2. In this photo, the soil monolith tank is being installed in the retainer tank of the reference lysimeter. The monolith tank was set on the weighing mechanism inside the retainer tank. The manhole (right of photo) allows access to the underground chamber that houses the weighing mechanism, drainage tanks, and data loggers. (Image courtesy of Lane Simmons)

Figure 3. This image shows calibration of the reference lysimeter weighing scale. Certified weights of varying size were placed on top of the monolith to derive the relationship between load cell output and monolith tank weight. (Image courtesy of Lane Simmons)

per volt. Changes in weight of the monolith tank (caused by evapotranspiration of water, for example) cause changes in the load cell output. The load cell output can thus be calibrated to give equivalent weights of the monolith tank. Partial backfilling of the excavated soil and painting of the retainer tank interior were also done in December. The soil monolith tank was set on the weighing scale on December 17, 2008 (Figure 2).

In February 2009, a steel "top hat" was installed to fit around the top of the monolith tank to prevent water from entering through the small clearance between the monolith and retaining tanks. A thin rubber sheet was applied along the top edge of the monolith tank and surrounding top hat edge to seal the small clearances between them without restricting the movement of the monolith tank. On March 24, 2009, the weighing scale was calibrated using certified weights (Figure 3).

Weather and soil sensors are currently being installed and will be connected to the data loggers mounted in the underground chamber of the retainer tank. Weather and soil heat flow data from the sensors will be used in the ASCE standardized equation. Oats will be planted on the reference lysimeter and surrounding field to keep them under a short-duration crop during the summer. The reference lysimeter and surrounding field will then be seeded to alfalfa in August 2009. They will be permanently cropped to alfalfa for making measurements of alfalfa reference ET each growing season.

Preliminary Comparison of ASCE Standardized Equation ET Estimates with Lysimeter Data for 2008

The 2008 growing season was the first full season of data collection from the crop lysimeter. The hourly alfalfa ET rates measured from the lysimeter throughout the season provided a basis for evaluating the accuracy of the ASCE standardized ET equation. Because the equation estimates ET from a tall reference crop that is assumed to be at a constant height of 20 inches (0.5 meter), similar to full cover alfalfa, lysimeter ET data taken before alfalfa achieved full cover, or a couple of weeks after cutting, could

Figure 4. This view of the crop lysimeter is looking to the east. The manhole for accessing the data logger, weighing mechanism, and drainage tanks is on the left; and micrometeorological (weather) sensors are mounted above the lysimeter.

not be compared with equation estimates. Hourly weather data measured by the sensors mounted directly above the monolith (Figure 4) were used in the hourly version of the ASCE standardized equation and included solar radiation, air temperature, wind speed at 2-meter height, vapor pressure (a measure of humidity), and heat flow at the soil surface.

June 7, 2008, (Figure 5) is an example of a day (early season) when hourly ET estimates from the ASCE standardized equation and hourly measurements from the lysimeter matched well throughout the day. Wind conditions were relatively calm, and humidity was relatively stable.

In contrast, June 2 (Figure 6) was also early in the season but had elevated afternoon temperatures, higher afternoon wind speeds, and a drop in humidity. There was a drop in solar radiation after 12:00 hours due to increased cloud cover, which was reflected in the drop in both the lysimeter and ASCE standardized ET rates. However, the ASCE standardized ET equation seemed to be overly sensitive to higher wind speed and decreased humidity that occurred after 14:00 hours. The equation over-predicted ET under these conditions.

Based on preliminary analysis of the 2008 data, the ASCE standardized equation generated alfalfa reference ET estimates that agreed well with lysimeter measurements when sensible heat advection (movement of warm air mass from another area) was not significant. The equation tended to over-estimate hourly ET rates when high wind speeds (> 5 m s-1) occurred with elevated air temperature and decreased humidity. On the other hand, the equation under-estimated mid-day alfalfa ET rates on some days late in the season (data not shown), possibly because of the assumed canopy height (0.5 m) being lower than the actual canopy height and/or soil water and leaf transpiration dynamics not being accounted for in the equation. Further analyses are needed to evaluate the accuracy of the ASCE standardized ET equation in estimating alfalfa reference ET for different conditions in the Arkansas River Basin.

Technical Meeting and Open House

On the morning of April 3, 2009, 14 individuals working directly with or having interest in the weighing lysimeters

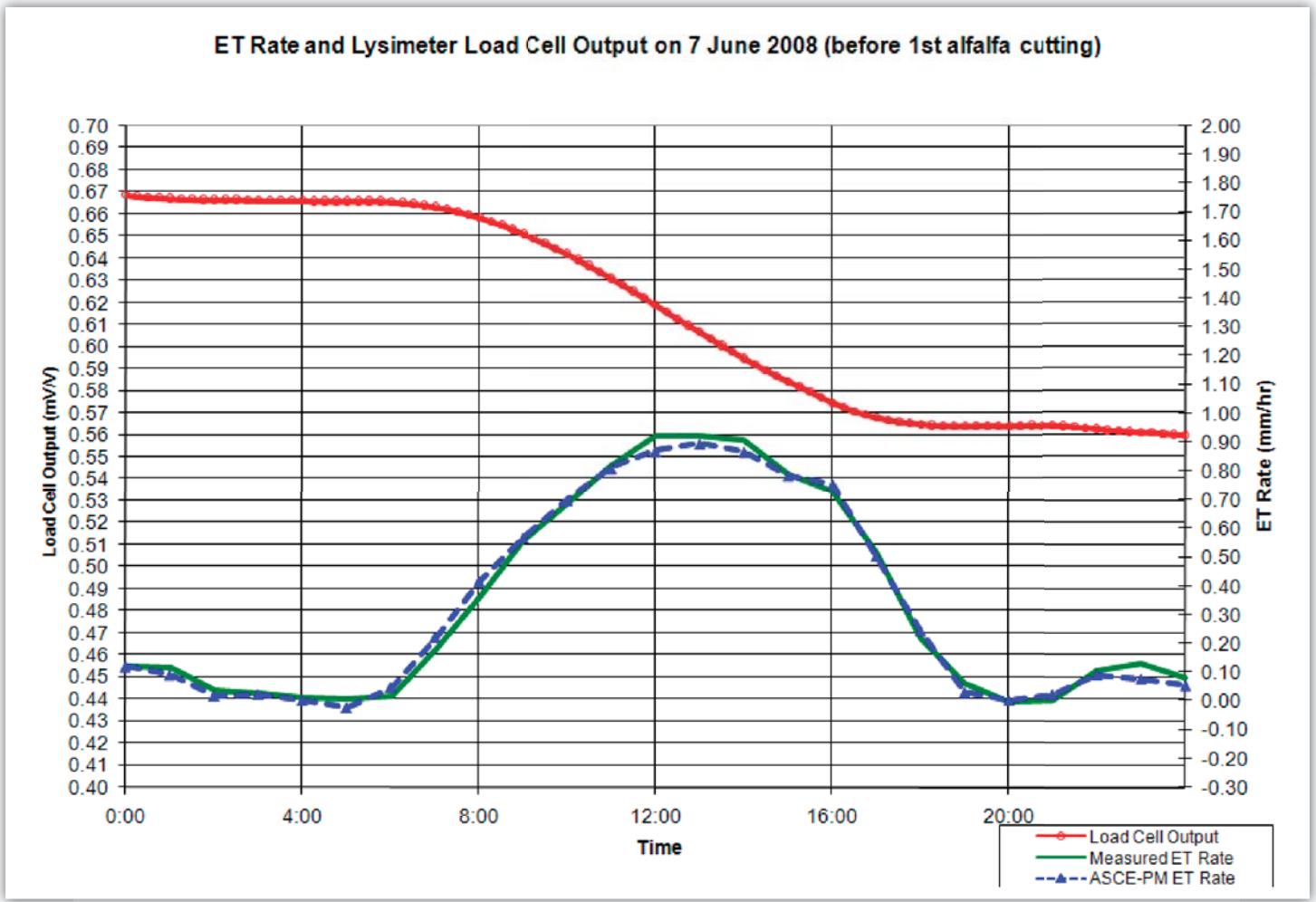

Figure 5. Example lysimeter load cell output (top line) and corresponding hourly ET rates measured by the lysimeter (solid line) and estimated by the ASCE standardized reference ET equation (dashed line).This example shows very good agreement between the ASCE standardized ET equation and lysimeter measurements.

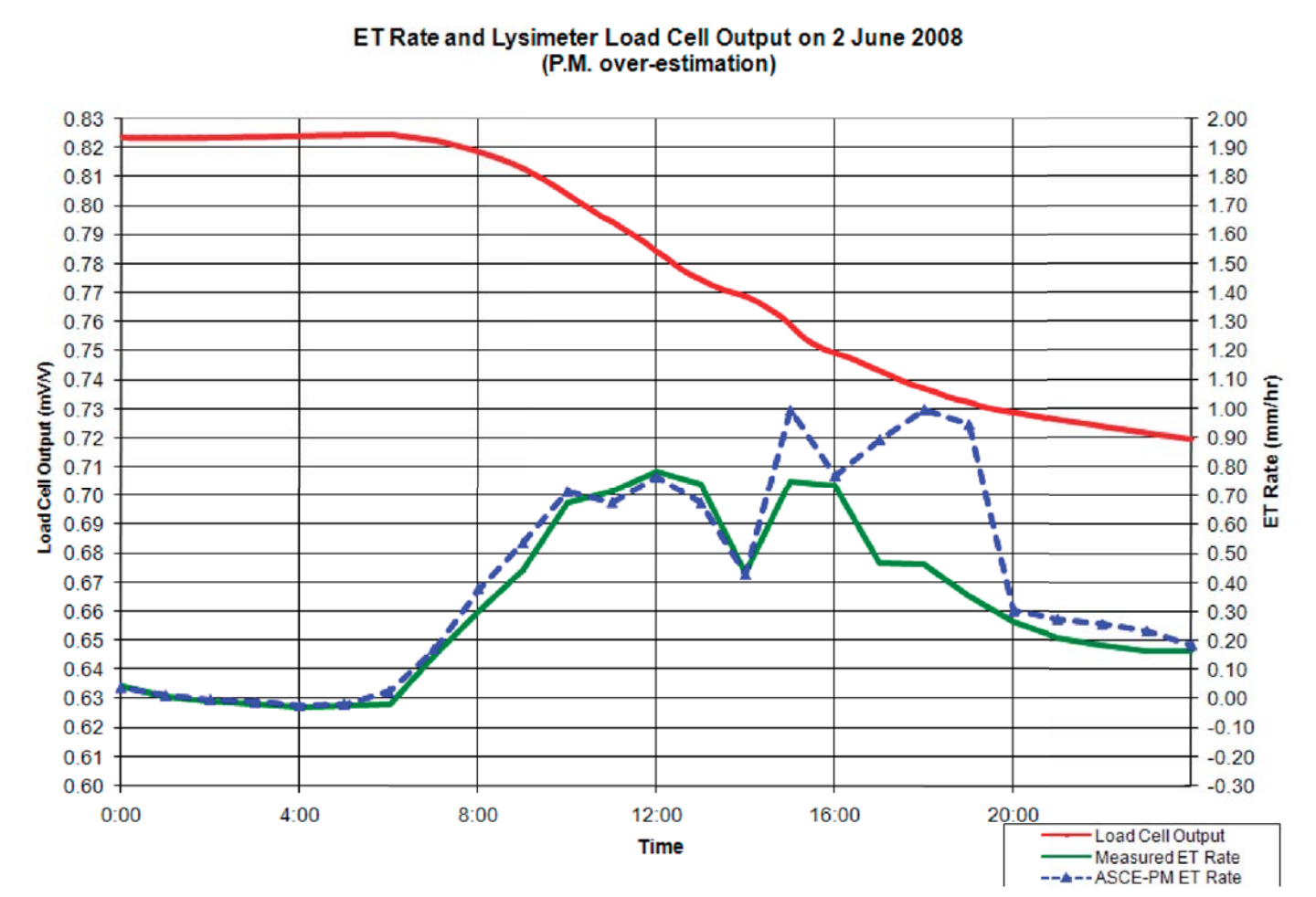

Figure 6. Example of over-estimation of afternoon hourly ET rates by the ASCE standardized reference ET equation (dashed line), compared to measured alfalfa ET from the lysimeter (solid line). In the afternoon of June 2, 2008, dry, warm wind originating from a nearby prairie blew from the southwest.

held a technical meeting. Representatives from CSU, Colorado Division of Water Resources, and USDA-Agricultural Research Service talked about the operation of the two lysimeters, preliminary analyses of 2008 data, and future data collection and management. In the afternoon, local producers, state personnel, and representatives of water conservancy districts were updated on the lysimeter construction and data collection. Attendees then visited the lysimeter site and were given the opportunity to view the underground chamber of the reference lysimeter that was nearing completion. Approximately 27 people attended the event.

Future Plans

The reference lysimeter will be permanently cropped to alfalfa to make measurements of alfalfa reference ET each growing season. The crop lysimeter will be cropped to alfalfa through 2011 to verify that the reference lysimeter is measuring similar alfalfa ET rates. Beginning in 2012, the crop lysimeter and surrounding field will be planted to corn and other major crops in the Arkansas Valley (wheat, sorghum, onions, etc.) to determine their crop coefficients. Simultaneous measurements of alfalfa reference ET from the reference lysimeter and crop ET from the crop lysimeter are needed to calculate crop coefficients. It will take at least two years per crop (planted in the crop lysimeter) to generate reliable crop coefficient values that cover the entire growing season.

Acknowledgements

The lysimeter project is a joint effort between the Colorado Water Conservation Board, Colorado Division of Water Resources (CDWR), Colorado Water Institute, and Colorado State University. Technical support has also been provided by USDA-Agricultural Research Service engineers and scientists in Fort Collins, Colorado, and Bushland, Texas. Lane Simmons, Michael Bartolo, and Abdel Berrada of CSU; and Dale Straw and Thomas Ley of CDWR contributed to the data collection described in this article.

Fulbright Scholarship Experience in Zambia, Africa

by Perry E. Cabot, Extension Water Resources Specialist, Colorado State University

Introduction

I don't know where the saying originated, but "the trouble with Africa," it goes, "is that it gets in your blood." That statement is even medically accurate in my case, given that I contracted malaria on my recent trip to Zambia. Illness aside, however, I would do it all over again, because what really gets in your blood is the beauty, enormity, and innocence of what has been referred to as this "forgotten continent."

So, on April 20 of this year, my wife Leah and I embarked on the two-day journey that would culminate in our relocation to Lusaka, Zambia, for five months. The main purpose of this trip was for me to teach and conduct research at the University of Zambia (UNZA) under the auspices of the Fulbright Scholarship Program. As the largest city in the country, the capital of Lusaka is intimidating, to say the least. With slightly over three million residents, it is about 15 times more populated than Pueblo, Colorado, where my wife and I live.

We quickly secured housing across the highway from the university that the locals call "Un-Za," and I prepared for my first day of the semester that was scheduled to start April 26. Upon first meeting with my faculty collaborator, Prof. Elijah Phiri in the Department of Soil Science, I was disheartened to learn that the semester had been delayed, and his best guess was that it would be another two months before classes would resume. Such delays were apparently common at UNZA, resulting from a confluence of student strikes, lecturer strikes, and financial obstacles. Be that as it may, my Fulbright schedule was less fluid, so Prof. Phiri inquired as to whether I could prepare an interim series of lectures on Geographic Information Systems (GIS) for their upper-level undergraduates. That was the moment when I recalled the singular advice I had gotten from other Fulbrighters in developing countries. Future Fulbrighters, take heed … ***Be flexible***.

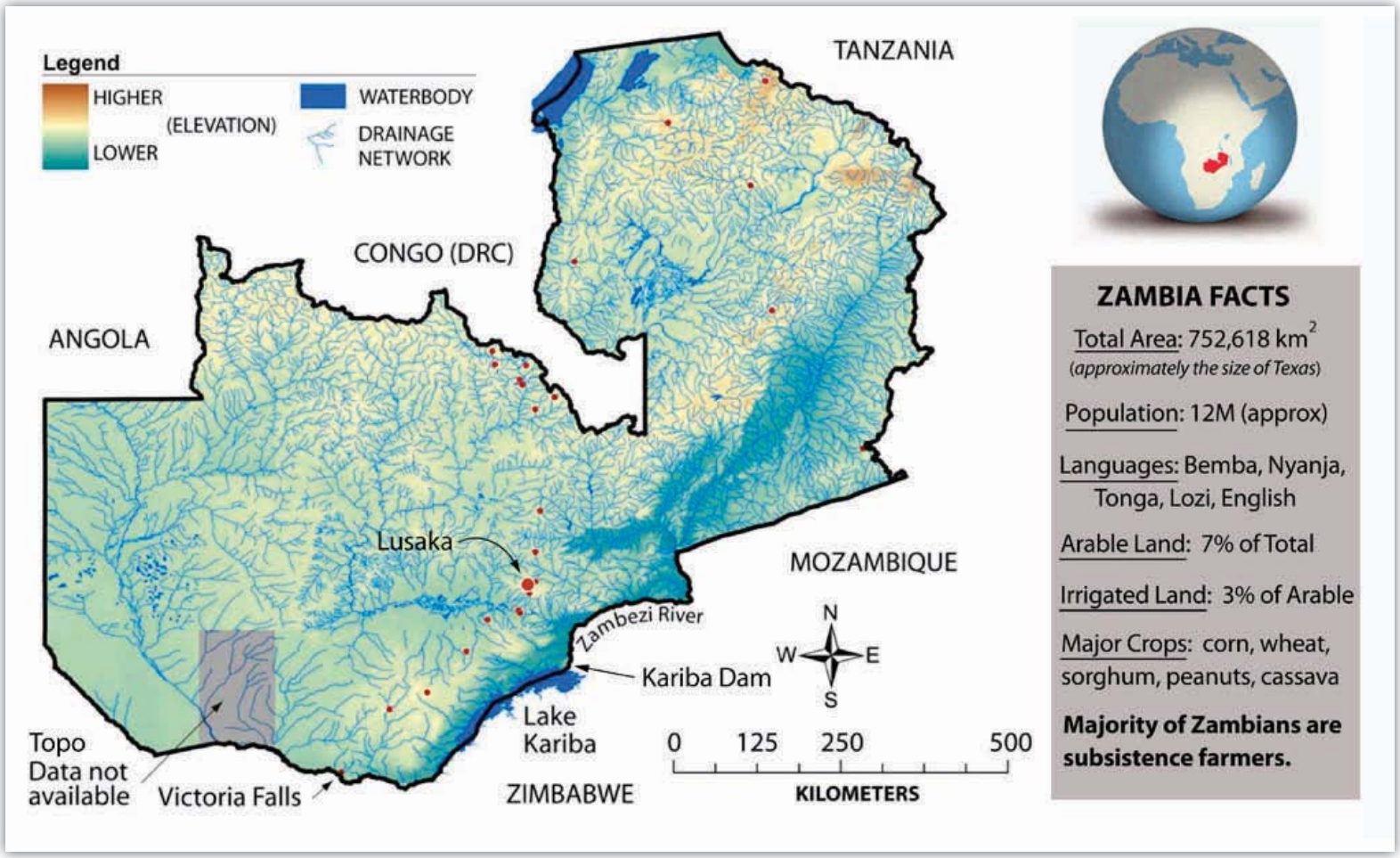

"There Should Not Even Be a Door on Your Office."

I attribute the above quote to a good colleague I made during my stay at UNZA. Prof. Obed Lungu jokingly noted that there seemed to be such a steady stream of students to my office that the door was completely unnecessary. True—I found the students so eager to learn GIS that they seemed disappointed when the lab sessions concluded, and many even pestered me for extracurricular work. Considering that I was already teaching an extracurricular interim session, I found their expanded requests absolutely remarkable. For the next six weeks, it was all I could do to stay ahead of their unquenchable interest.

Hydrology students from UNZA take their first trip to Kariba Dam. Back row (from left): Nkanga Hantambu, Joel Kashinge, Webster Mwale, Dominic Balengu, Chindi Kapembwa. Middle row (from left): Mukuka Mwansa, Kenny Mweemba, John Kachingwe. Front row (from left): Mwilile Simwanza, Prudence Kauzi, Benny Kabwela, Elijah Kabwe, Stanley Haabowa. (Courtesy of Perry Cabot)

Since my original Fulbright proposal included a component related to GIS, I packed several copies of *Getting to Know ArcGIS* published by the Environmental Systems Research Institute (ESRI). Complete with 180-day trial versions of ArcGIS 9.3, these books were invaluable to me as I forged ahead setting up a temporary computer lab using laptops that some of the students were willing to offer up to our cause. For their final class project, I assigned the student teams the task of digitizing David Livingstone's journeys throughout southern Africa between 1840 and 1870. At the suggestion of the department, each of the 32 students who participated in the course was awarded a certificate attesting to their newly acquired skills, which I evaluated through a series of assignments, tests, and individual assessments. In a country where employment is increasingly scarce and opportunities for advancement are minimal, one student remarked as he held the certificate, "Wow. This is going to help me get a job." Understated as it may seem, I couldn't have asked for a kinder validation of my efforts.

Once the semester finally started, I aimed to fulfill my lecturing responsibility to the Fulbright Program by teaching their standard course in agricultural hydraulics and hydrology. This proved to be slightly more difficult than it would seem, given that students at UNZA can barely cover the costs of their own subsistence and tuition, let alone purchase the books and lecture notes that are standard for American students. Needless to say, the man they called "the duplicator" (he who guarded the copy machine) and I became fast friends. As a reward for their hard work, I navigated a maze of bureaucratic permits to take my students on a trip of Kariba Dam, from which Zambia derives the majority of its electricity. Unfortunately, because of power-sharing arrangements with other countries as far away as South Africa, the dam is now operating at its maximum capacity (1320 MW), and load-shedding became a frequent occurrence during the last two months of my stay. Regular blackouts were a stark reminder of the increasing demand for power in a region that is eager to industrialize and achieve the comforts we are afforded in much of the Northern Hemisphere.

Agricultural Advancement in Zambia

I would describe Fulbrighters—in developing countries at least—as the academic equivalent of a "smart bomb." You simply have to get in country first and once there, you target the opportunities where you can have the greatest impact. In accord with this principle, I devoted most of my time to teaching. However, I also wanted to learn as much as possible about Zambian agricultural practices, in hopes that such a knowledge base would lay the groundwork for future collaboration. The most fruitful of my ventures along these lines were the regular trips I made to various agricultural research stations in and around the Lusaka Province, where I was based. Golden Valley Agricultural Research Trust (GART) is as fine an example of a research station as you could expect in the heart of Africa, directed capably by Dr. Stephen Muliokela who oversees all manner of conservation farming, livestock development, and HIV and AIDS mitigation research at the 1300-acre operation.

Aside from certain unfortunate political impediments, Zambian agricultural advancement is hindered by a problem that is strangely familiar to Colorado, except not as one might assume. We might expect that African countries suffer from water shortages, and by and large this fact is true, but not Zambia. Although rainfall varies across the country, annual precipitation rates on the order of 800 mm (31.5 inches) should be a boon to agricultural

Between his teaching schedules, Perry Cabot was able to visit Victoria Falls, taking in this wonder of the natural world from the passenger seat of a microlight aircraft. (Courtesy of Batoka Sky Adventures; Livingstone, Zambia)

development. At commercial scales, even mechanized irrigation is being practiced. Nevertheless, most agricultural operations in Zambia still experience water shortages, just like Colorado. This is because, unlike in our home state, there has been little to no investment in the infrastructure required to store and transport water, even at local scales. With electricity and fuel also at a premium, even pumping from the abundant aquifer situated in the limestone and dolomite layers of the Katanga system is a costly undertaking. Aside from these power constraints, the supply lines of seed, fertilizer, and agri-chemicals are also too unpredictable to allow for stable farming commerce to develop. Consequently, many Zambians are reliant on imported food, despite the abundance of resources surrounding them.

Parting Thoughts

Having little to compare with, aside from my previous experience in Rwanda and the extremes that are broadcast about Africa in the popular media, I can only offer a few generalized observations about Zambia. First, Zambians proudly refer to their country as "the real Africa." Given the abundant macro fauna and stunning landscapes, I would agree with this characterization. I would only add that its "realness" is also reflected in its efforts at modernization, which are becoming more common throughout Africa.

Secondly, I was humbly surprised at the quality of research facilities and laboratories, both on campus and at facilities I visited outside Lusaka. Truth be told, projects move at a slower pace there, but their faculty and staff were engaged in research ventures such as variety trials and drip irrigation, just as you would find at any Land-grant university in the United States.

Finally, I cannot imagine how the students could have demonstrated a greater level of enthusiasm for contact with the world beyond Zambia, even in Lusaka. In my short time there, I had already visited more locations than most of my students combined. In a sense, I would say their eagerness reflected a refreshing trust that many of them felt towards the developed world. Even from their faraway vantage point, they seem to know that their best hopes for the future are still linked to the goodwill of industrialized nations.

USGS Summer Intern Program

None.

Student Support					
Category	**Section 104 Base Grant**	**Section 104 NCGP Award**	**NIWR-USGS Internship**	**Supplemental Awards**	**Total**
Undergraduate	9	0	0	0	9
Masters	9	1	0	0	10
Ph.D.	3	0	0	0	3
Post-Doc.	0	0	0	0	0
Total	21	1	0	0	22

Notable Awards and Achievements

- Upper Yampa Water Conservancy District Scholarship
- CSU Professor Honored by Interior Secretary Ken Salazar
- CSU Professor Receives Prestigious NSF Award
- "Walking Through the Water Year"
- CWI Announces Funded FY09 Student Projects

Awards

Upper Yampa Water Conservancy District Scholarship Awarded to CSU Student

The Upper Yampa Water Conservancy District (UYWCD) funds an annual scholarship in support of CSU students preparing for careers in water-related fields. The scholarship program is administered by the CSU Water Center and provides financial assistance to committed and talented students who are pursuing water-related careers at CSU. The UYWCD $3,000 scholarship is open to any major at CSU. Criteria require the recipient to be a full-time student enrolled at CSU with a minimum GPA of 3.0. Financial need may be considered, and preference is given to students from the Yampa Valley area. The scholarship duration is one year.

The Upper Yampa Water Conservancy District Scholarship recipient for the spring semester of 2009 is Michael Macklin. A senior majoring in political science with an interdisciplinary study in water resources, Mike was born in La Junta, Colorado, and raised in Springfield, Colorado. For the past four years, while attending Colorado State University, he has worked at the Colorado State 4-H Office, where he has helped coordinate state and national 4-H youth development events. His studies in water resources and political science led him to Lincoln University in Lincoln, New Zealand, for a semester of study in natural resource and water economics during the spring of 2008. Mike has been active in Alpha Gamma Rho, an agriculturally based fraternity, and has served as an ASCSU Senator for the College of Agriculture for two years. Following graduation, Mike plans to pursue a law degree with an emphasis on water law in the fall of 2009. Mike's love for small towns and rural America has driven his passion to protect the farmers and ranchers of rural America.

The CSU Water Center and Colorado Water Institute congratulate Mike and wish him success in his future academic studies and career. The ongoing support of CSU students by the UYWCD is acknowledged and

greatly appreciated.

CSU Professor Honored by Interior Secretary Ken Salazar

U.S. Interior Secretary Ken Salazar recently honored Jose 'Pepe' Salas, a Colorado State University civil and environmental engineering professor, with the U.S. Department of the Interior Partners in Conservation Award. Salas and his colleagues at three other universities received the award for developing new operational guidelines for the Colorado River.

Honored with Salas were representatives of the University of Colorado, the University of Arizona, and the University of Nevada, Las Vegas. Together with the U.S. Bureau of Reclamation and a variety of other government agencies, Salas and his partners helped develop Colorado River Interim Guidelines, which has been praised as the most important agreement among the seven basin states since the original 1922 compact. States signing the agreement were Arizona, California, Colorado, Nevada, New Mexico, Utah, and Wyoming.

Salas has served as principal investigator on two projects funded by the U.S. Bureau of Reclamation in connection with the Colorado River Basin. His activities on these projects included:

- Using innovative record extension techniques for updating the data base of naturalized flows of the Colorado River system
- Developing new approaches for reconstructing streamflows of the Colorado River based on tree-ring indices
- Developing potential scenarios of streamflows that may occur in the Colorado in future years
- Characterizing multi-year droughts using simulation and mathematical techniques
- Testing the effects of stochastic streamflows on the operations of the Colorado River system, particularly the effects on reservoir levels and outflows of the two major lakes, Lake Powell and Lake Mead

*This article was adapted from a June 30, 2009, CSU news release.

CSU Professor Receives Prestigious NSF Award

Thomas Borch, assistant professor of environmental soil chemistry in the Department of Soil and Crop Sciences at Colorado State University, has received a Faculty Early Career Development (CAREER) Award from the National Science Foundation. The honor is considered one of the most prestigious for up-and-coming researchers in science and engineering.

Borch will use the nearly $500,000, five-year grant to investigate how climate change, and especially the projections of increased precipitation and flooding, may impact important biogeochemical cycles, such as those related to iron. Iron minerals are among the most important reactive solids in earth surface environments, acting as natural filters of inorganic contaminants and nutrients, sorbents for organic matter, and poising the redox potential of groundwater. Lack of biologically available iron in soils can also lead to iron deficiency anemia which is a major public health and financial problem in Central Asia, with primary impact on woman and children.

Iron minerals are responsible, in part, for stabilization of organic matter in soils. Consequently, any changes in iron chemistry may also result in changes in the atmospheric carbon dioxide concentration and the global climate. In high-elevation watersheds of the Rocky Mountains, more than 95% of spring snowmelt infiltrates through soils and moves along shallow groundwater flow paths before merging with stream water. In fact, one-sixth of the world's population depends on water released from seasonal snowpacks and glaciers, so an improved understanding of the soil processes that sustain the supply of clean water from mountain headwaters is critical to current and future human natural resource demands.

"This award will allow us to initiate a new important research area in environmental biogeochemistry at CSU; attract high-caliber postdoctoral researchers, graduate, and undergraduate students; and develop a set of new courses targeting undergraduate students interested in environmental biogeochemical processes from the molecular scale to field scale," said Borch.

Borch earned his doctorate degree in environmental soil chemistry from Montana State University and his Master of Science and Bachelor of Science degrees in environmental chemistry from the University of Copenhagen. He joined Colorado State University in 2005 to initiate a program in environmental soil chemistry.

*This article was adapted from a June 5, 2009, CSU news release.

Acheivements

"Walking Through the Water Year"

"Walking Through the Water Year" is a water education initiative introduced a few years ago by the Colorado Climate Center at Colorado State University in collaboration with several organizations involved in water monitoring, climate, and education. After getting off to a slow start, WTTWY is about to take its first steps. A pilot project currently being planned could begin this fall. This effort will be funded by the U.S. Bureau or Reclamation in partnership with the Poudre School District in northern Larimer County. Media broadcasts distributed to classrooms, local cable TV, and via Internet streaming video will creatively show how the progression of storms and weather patterns throughout the year delivers water to the region. Students from the school district and interns from CSU will produce these broadcasts with the help of local weather and water experts.Colorado's water managers, planners, forecasters, and water users traditionally track water resources using the water year calendar that begins October 1 and ends September 30. The beginning of the Water Year coincides with the start of the snow accumulation season in the Colorado high country. It includes the dynamic spring snowmelt period, when the mountain snowpack relinquishes water to tumbling rivers and streams. The year ends with the completion of the summer growing season and irrigation season. Each year follows a common seasonal cycle, but the number, size, intensity, location, and timing of rain and snow storms dictates the amount of water available to Colorado each year. This is modulated by the sequences of warm and cold weather along with variations in wind, sunshine, and humidity that influence evaporation and transpiration.

Water experts, accustomed to tracking weather conditions through the water year, learn through years of experience the intimate connections between weather and water. There is tension and drama each year as weather patterns unfold and our water story is told. Walking Through the Water Year will strive to capture this excitement to bring a greater awareness and appreciation for our limited water resources.

For more information about Walking Through the Water Year or to find out how you or your organization can get involved, please contact:
Nolan Doesken
Colorado Climate Center
Department of Atmospheric Science
Colorado State University
(970) 491-3690
nolan@atmos.colostate.edu

CWI Announces Funded FY09 Student Projects

The Colorado Water Institute is pleased to announce the funding of six student projects this year. This program is intended to encourage and support graduate and undergraduate research in disciplines related to water resources and to assist Colorado institutions of higher education in developing student research expertise. The purpose of the funding is to help students initiate new research projects or to supplement existing student projects focused on water resources research. The FY09 funded projects and funding recipients are listed below:

- **Understanding the Hydrologic Factors Affecting the Growth of the Nuisance Diatom *Didymosphenia Geminata* in Rivers**

James Cullis, Department of Civil, Environmental, & Architectural Engineering, University of Colorado
Faculty Sponsor: Diane McKnight

Didymosphenia geminata, also known as "didymo" or "rock snot," is a nuisance algal species that occurs in many mountain streams in the western U.S. It tends to produce large amounts of extracellular stalk material, and while it is not considered to be toxic, the growth of these large algal mats has a significant impact on the aesthetics of a stream and on the sustainability of stream ecosystems and water supply infrastructure. Not much is known about this species, as it has only become a significant problem in the past 10 to 15 years. This research will look specifically into the hydrologic factors affecting the growth of this nuisance species at a number of study sites in Boulder Creek, Colorado, with a particular focus on the role of flood-induced bed disturbance as a primary control of growth. The overarching research hypothesis is that high levels of shear stress and bed disturbance due to flood events are necessary to control the growth and bloom tendency of *D. geminata*, and that these levels can be provided through environmental flood releases from reservoirs to maintain functioning stream ecosystems and water supply systems.

- **Bear Creek Watershed Project**
  Kimberly Gortz-Reaves, College of Architecture and Planning, University of Colorado
  Faculty Sponsor: Charlie Chase

  Bear Creek Watershed encompasses four counties and more than eight cities and towns. The extent to which public and private land use managing agencies or organizations involved with the watershed offer "on-the-ground" projects for young people and community groups to participate in (e.g., habitat restoration, stream bank stabilization, or other watershed conservation projects) is unknown. Furthermore, there is no existing system to provide coordination for watershed-wide projects. The purpose of this research project is to identify stakeholders and potential partners operating in the Bear Creek watershed and their needs, resources, and capacities. The project will be facilitated by the Bear Creek Watershed Partnership (BCWP), which is aimed at connecting youth-based stewardship and leadership programs to opportunities offered by Bear Creek watershed stakeholders. To date, facilitating partners include City of Denver Parks and Recreation, University of Colorado at Denver, National Park Service RTCA, AmeriCorps, FrontRange Earth Force, and Groundwork Denver. To date, there has been limited program coordination among municipalities and other public and private agencies within the Bear Creek watershed. The objective is to contact agencies and associations, build a database of information based on conversations with contacts, create a stronger partnership effort, and develop a GIS-web based interactive map with the gathered information. The long-term goal is to create a forum in which partners will be able to share or coordinate their objectives, improve management strategies, and post stewardship projects for youth.

- **Developing Barriers to the Upstream Migration of New Zealand Mudsnail (*Potamopyrgus antipodarum*); Phase II: Laboratory and Field Evaluations of Mudsnail Response to Copper-based Materials under Varied Water Quality Conditions**
  Scott Hoyer, Department of Fish, Wildlife, and Conservation Biology, CSU
  Faculty Sponsor: Christopher Myrick

  The objective of this research is to evaluate the ability of copper-based substrates to prevent the upstream spread of the invasive New Zealand mudsnail (*Potamopyrgus antipodarum*). Over the last 20 years, mudsnails have spread rapidly across the western U.S., prompting management agencies to close several streams and fish hatcheries. There is currently a need for effective methods to prevent further invasion into novel waterbodies. Preliminary research results suggest that several copper-based substrates may be useful in stopping the upstream spread of this organism. I am currently studying how physicochemical parameters, including pH, temperature, and water hardness, affect the mudsnail's response to the copper materials. We are hopeful that copper-based substrates can eventually be integrated into mudsnail management plans once the barrier ability of each of the materials has been evaluated.

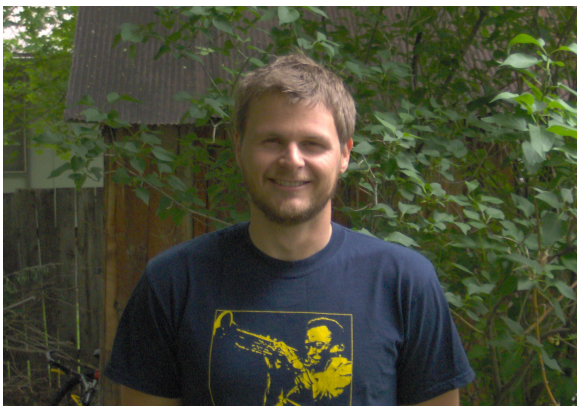

- **High-Resolution Soil Moisture Retrieval in the Platte River Watersheds**
  Chengmin Hsu, Department of Civil Engineering, University of Colorado Denver
  Faculty Sponsor: Lynn E. Johnson

  An accurate estimate of soil moisture is necessary for various hydrometeorological, ecological, and biogeochemical modeling and applications. Unfortunately, continentally available soil moisture data (AMSR-E) are currently derived using passive remote sensing technology and has a very rough resolution (i.e., 25 km). This rough resolution character of the AMSR-E products makes them difficult to use for hydrological and ecological purposes at the watershed scale. In this project, I propose to: (1) improve and update the AMSR-E soil moisture products by assimilating the AMSR-E products into the NOAH land surface model, (2) downscale the coarse resolution soil moisture outcome to a higher resolution product (e.g., 240-meter resolution), and (3) validate the final product with the joint soil moisture observations obtained from NRCS Soil Climate Analysis Network (SCAN) and from soil moisture monitoring stations in Nebraska by the High Plains Regional Climate Center (HPRCC). The study area will include portions of the North and South Platte River Basins and a portion of the Republican River Basin. The work proposed in this project constitutes a first attempt to understand the spatial structure of brightness temperature and soil moisture images when applied at a higher resolution. It will also test the capability of the NOAH land surface model to generate high-resolution surface soil moisture. More importantly, the work will be a foundation for the future estimation of root-zone soil moisture.

- **Potential Changes in Groundwater Acquisition by Native Phreatophytes in Response to Climate Change**
  Julie Kray, Department of Forest Rangeland and Watershed Stewardship, CSU
  Faculty Sponsor: David J. Cooper

  Throughout western North America, arid regions are likely to experience changes in the timing and amount of precipitation as global surface temperatures increase. Altered rainfall and runoff patterns will exacerbate current stresses on water resources from growing human demands and could produce long-term changes in water availability for ecosystems, agriculture, and municipalities. In Colorado's arid San Luis Valley (SLV), competing water interests will be particularly sensitive to climate change. The SLV receives only 180-250 mm of precipitation annually; yet, a shallow unconfined aquifer recharged by snowmelt supports over 600,000 acres of irrigated agriculture, substantial water transfers out of the valley, and native rangeland for livestock grazing. The dominant native plants in the SLV are phreatophytes, plants that use groundwater. Evapotranspiration by phreatophyte communities accounts for more than one-third of the total annual groundwater consumption. Some SLV phreatophytes can also utilize predictable pulses of summer monsoon rain to reduce or supplement their groundwater use. Thus, changes in monsoon rainfall patterns may produce changes in groundwater acquisition of phreatophytes, which could have considerable effects on the SLV groundwater budget and regional agriculture. Our research investigates the response of four native phreatophytes to changes in growing season precipitation using a rainfall manipulation experiment. Our goal is to understand how plant community adjustment to climate change in the SLV would affect regional groundwater resources, and to incorporate this understanding into the Rio Grande Decision Support System groundwater management model.

- **Impact of Limited Irrigation on the Health of Four Common Shrub Species**
  Jason F. Smith, Department of Horticulture and Landscape Architecture, CSU
  Faculty Sponsor: James E. Klett

  The shrub water study was started in 2005 in response to the 2002 drought to evaluate the actual water requirements of some commonly used landscape plants. Currently, most water use statements for landscape plants are based on personal opinions or observations, and few studies have evaluated the water use of landscape plants. This research involves determining the water use values for some common landscape shrubs from a replicated study. The research is continuing in 2009 and will evaluate the growth of Redosier dogwood, smooth hydrangea, Diablo ninebark, and arctic blue willow when subjected to four different amounts of irrigation (0%, 25%, 50%, and 100%), based on the evapotranspiration rate of Kentucky bluegrass. By the end of 2009, accurate water requirements for these four species will be determined after a season of collecting various types of data. If the study results show that these shrubs do well with 0% or 25% of the evapotranspiration rate of Kentucky bluegrass, then they would be well suited for planting in many Colorado landscapes that require little to no irrigation. However, if these shrubs are found to need 50% or 100%, then the use of these shrubs could be limited for landscape use in Colorado.

Publications from Prior Years

1. 2005CO118G ("Development of Characterization Approaches and a Management Tool for the Groundwater-Surface Water System in the Vicinity of Sutherland Reservoir and Gerald Gentlemen Station, Lincoln County, Nebraska") - Water Resources Research Institute Reports - Poeter, Eileen; Clint P. Carney, 2010, "Development of Characterization Approaches and a Management Tool for the Ground Water-Surface Water System in the Vicinity of Sutherland Reservoir and Gerald Gentlemen Station Lincoln County, Nebraska", Completion Report 212, Colorado Water Institute, Colorado State University, Fort Collins, Colorado, 46 pages.